DISS. ETH NO. 30355

Mathematical Analysis of Dispersive and Damped Materials and Applications

A thesis submitted to attain the degree of

DOCTOR OF SCIENCES
(Dr. sc. ETH Zurich)

presented by

Konstantinos Alexopoulos

MASt. Mathematics, University of Cambridge

born on 12.07.1999

accepted on the recommendation of
Prof. Dr. Habib Ammari, examiner
Prof. Dr. Pierre Millien, co-examiner

2024

Abstract

Dispersion and damping are two characteristics of wave propagation which are present when different types of waves propagate through a variety of materials in nature. Materials with such aspects have multiple applications because of their useful electromagnetic properties. Apart from the electromagnetic setting, dispersive and damped systems have also applications in other fields, such as acoustics and elasticity. Nevertheless, understanding the effect that dispersion and damping have on the particle interactions and the material properties is a challenging task.

In this thesis, we study the spectral properties of dispersive and damped materials. By varying the material parameters and modifying both dispersion and damping, we obtain results on the dependence of the spectrum of these materials on these characteristics. Then, considering periodic media and exploiting the underlying symmetries, we show the existence of strongly localised waves on an interface. This aspect is a key element in the design of wave guiding and control devices.

We will also consider a specific example of dispersive materials called halide perovskites. Halide perovskites have high absorption coefficient and also they are cheap and easy to manufacture. Thus, they make excellent choices for making electromagnetic devices. We will use asymptotic techniques to study the resonance problem associated to halide perovskites in the two and three dimensional setting. We will study systems of finitely many halide perovskite resonators in the subwavelength regime and provide analytic expressions for their resonances. Finally, we will provide an optimal way to design surfaces of subwavelength halide perovskite resonators for the detection of frequencies lying in the visible light spectrum.

Résumé

La dispersion et l'amortissement sont deux caractéristiques de la propagation des ondes qui sont présents pendant la propagation des differents types d'ondes à travers une variété de matériaux dans la nature. Les matériaux présentant de tels aspects ont des applications varieés grâce à leurs propriétés électromagnétiques. En dehors du cadre électromagnétique, l'étude de la dispersion et de l'amortissement a des applications dans d'autres domaines, comme l'acoustique et l'élasticité. Néanmoins, comprendre l'effet de la dispersion et de l'amortissement aux interactions des particules et aux propriétés des matériaux est une tâche difficile.

Dans cette thèse, nous étudions les propriétés spectrales des matériaux dispersifs et amortis. En variant les paramètres des matériaux et en modifiant la dispersion et l'amortissement, nous obtenons des résultats sur la dépendance du spectre de ces matériaux à ces caractéristiques. Ensuite, en considérant des milieux périodiques et en exploitant les symétries sous-jacentes, nous montrons l'existence d'ondes fortement localisées sur une interface. Cet aspect est un élément clé dans la conception des dispositifs de guidage et de contrôle des ondes.

Nous considérerons également un exemple spécifique des matériaux dispersifs, appelés pérovskites halogénures. Les pérovskites halogénures ont un coefficient d'absorption élevé et ils sont pas chers et faciles à fabriquer. Ces caractéristiques les rendent un choix excellent pour fabriquer des appareils électromagnétiques. Nous allons utiliser des techniques asymptotiques pour étudier le problème de résonance associé aux pérovskites halogénures aux dimensions deux et trois. Nous allons étudier des systèmes d'un nombre fini de résonateurs pérovskites halogénures dans le régime sous-longueur d'onde et donner des expressions analytiques décrivant les résonances. Enfin, nous présenterons une manière optimale de créer des surfaces de résonateurs de pérovskites halogénures de sous-longueurs d'onde pour la détection de fréquences dans le spectre visible de la lumière.

Acknowledgements

I would like to express my deep gratitude to my supervisor, Professor Habib Ammari, for his guidance and invaluable advice during my doctoral studies. His enthusiasm, his generosity and the inspiring discussions with him have been a constant source of motivation for me.

I would also like to express my gratitude to Bryn Davies for the time he invested in our collaboration. Our enjoyable discussions have provided me with important insights in our research and have nurtured my mathematical curiosity. Working with him has been a great experience and has resulted in some exciting projects [3, 5, 4, 6].

In addition, I would like to thank my colleagues in Habib's group for our conversations and for the productive and supportive environment.

In particular, I would like to thank my office mate, Thea Kosche, for her willingness to discuss ideas and for sharing an office with me for the past three years.

Finally, I would like to thank my parents for their constant support during my studies.

Contents

Introduction

Photonic crystals: dispersion and damping

Dispersion and damping are two phenomena present in optical nanostrusctures, such as photonic crystals, which have many applications. The term was first used after the seminal work carried in [74, 39]. Photonic crystals are optical nanostructures with non-constant refractive index. This affects the propagation of light in the structure. They are constituted by regularly repeating regions of varying refractive index. Light waves may propagate through this structure or propagation may be disallowed, because of amplitude decay and reflection of energy, depending on their wavelength.

The dielectric permittivity and the magnetic permeability of these structures are the material characteristics which explain how the light is impacted while propagating inside them. In this work, we will assume that the magnetic permeability is constant and we will study the effect of the permittivity. The dispersive nature of the system appears in the dielectric permittivity in the form of a dependence on the frequency of the wave propagation.

Much of the existing theory [9] treats the case where these permittivity functions are non-dispersive inside the particles of the crystals. However, when working at certain electromagnetic frequencies, which often include the visible spectrum, it is important to take into account the oscillatory behaviour of the free electrons in the material. This behaviour leads to resonances at characteristic frequencies and gives photonic crystals a highly dispersive character. This is manifested in the permittivity since we observe a highly non-linear dependence on the frequency with which the light propagates in the system. Quite often, we also observe the existence of damping in the system, appearing in the form of a non-zero imaginary part of the dielectric permittivity. This is translated into increase or loss of energy in the system during the light propagation. We aim to understand the effect of dispersion and damping on the light propagation and extend the existing theory to such settings.

In general, photonic crystals present interesting and useful wave propagation properties. Even very simple photonic crystals, such as those composed of periodically alternating layers of non-dispersive materials, can display exotic dispersive properties. As a result, they are able to support band gaps: ranges of frequencies that are unable to propagate through the material [65]. These band gaps are the fundamental building blocks for the many different wave guides and wave control devices that

have been conceived. Notable examples include flat lenses [58], invisibility cloaks [54], rainbow trapping filters [68] and topological waveguides [43].

From a mathematical point of view, we will see how dispersion and damping affect the spectral structure of these materials. In particular, by studying periodic one-dimensional systems we will obtain the dispersion relation characterising each material. This expression describes the behaviour of the spectral band and gaps of the materials. By varying the material parameters and adding dispersion and damping to the system, we observe how the spectrum of the photonic crystal is affected. We will generalise this result to multi-dimensional systems by providing the equivalent analytic expressions for the resonance problem. For these settings, we will work on a particular example of photonic crystals called halide perovskites.

Subwavelength regime

It is expected that the impact that small particles have on waves propagating through the surrounding medium is minimal. This is even more evident in the *subwavelength regime*, i.e. when the particle's size is significantly smaller than the wavelength of the incident wave. This phenomenon complicates the study of wave propagation in these settings. Working in the subwavelength regime means working at very low frequencies. This implies that the material no longer behaves like a homogeneous material and hence, the conventional homogenisation techniques cannot be applied. However, there exist particles which interact strongly with their environment, even in the subwavelength regime, leading to pronounced scattering and resonance at subwavelength frequencies, called *subwavelength resonators*. This property makes them ideal candidates for the creation of a variety of material structures, called *metamaterials*. It has been shown that they display extraordinary properties absent in common materials [12].

Photonic crystals, and in particular halide perovskites, belong to the category of metamaterials with strong interaction with incident waves via their high absorption coefficient. This helps in detecting frequencies in the complete visible light spectrum. Thus, they have a crucial role in the creation of microscopic devices, which detect visible light in the subwavelength regime, i.e. devices that can be even a few nanometres. This has further implications, as their small size makes them quite light, cheap and also very efficient.

We will study the resonance problem associated to halide perovskites in the two and three dimensional settings in the subwavelength regime. By adapting the asymptotic techniques and taking advantage of the spectrum of the integral operators used, we are able to obtain expressions for the resonances. In addition, we will study systems with more than one particles and show the presence of hybridisation, i.e. the separation of resonances as the number of particles increases due to inter-particle interactions. With numerical experiments, using examples of halide perovskites and their associated material parameters, we show that for small particles, at subwavelength

scales, the resonances detected are indeed in the visible light spectrum. Finally, exploiting these expressions, we propose a mechanism for designing subwavelength surfaces of halide perovskite particles which can detect light waves with frequencies lying in the visible spectrum.

Halide perovskites

Halide perovskites are crystals, composed of crystalline lattices which have octahedral shapes and contain atoms of heavier halides, such as chlorine, bromine and iodine [2]. They have excellent optical and electronic properties, which combined with the fact that they are cheap and easy to manufacture puts them at the center of interest for the next generation of electromagnetic devices [38, 52, 64].

A particular benefit of halide perovskites is that their high absorption coefficient enables microscopic devices (measuring only a few hundred nanometres) to absorb the complete visible spectrum. Thus, we are able to design very small devices that are lightweight and compact while also being low cost and efficient. Research is ongoing to develop perovskites capable of fulfilling their theoretical capabilities for use in applications such as optical sensors [36], solar cells [64] and light-emitting diodes [72].

The dielectric permittivity of halide perovskites has been shown to depend heavily on excitonic transitions, leading to a permittivity that has symmetric poles in the lower complex plane [52]. In particular, if we denote the dielectric permittivity by ε, in terms of the frequency ω and wavenumber k, it is given by [52]

$$\varepsilon(\omega, k) = \varepsilon_0 + \frac{\omega_p^2}{\omega_{exc}^2 - \omega^2 + \hbar\omega_{exc}k^2\mu_{exc}^{-1} - i\gamma\omega},$$

where ω_{exc} is the frequency of the excitonic transition, ω_p is the strength of the dipole oscillator, γ is the damping factor, μ_{exc} is related to the non-local response and ε_0 is the background dielectric constant. This expression captures the highly non-linear dispersive character of the material. We refer to [52] for the values of these constants for different halide perovskites at room temperature.

Another essential attribute of the halide perovskites is that their first resonance is magnetic, as observed in [52]. The existing mathematical work focuses on the regime of the electric field. This renders the mathematical analysis of such materials quite complicated since the various asymptotic techniques that can be used often fail to account either for the dispersive part or for the difference between the electric and the magnetic resonances.

Wave localisation and topological protection

Materials with electromagnetic properties are being studied under the form of periodic media. When it comes to designing surfaces with beneficial optical properties, the number of nanoparticles used tends to be extremely large. The existing theory in such settings shows that these structures converge to periodic ones. An important application is the design of wave guiding and control devices. By combining different periodic materials, we can create interfaces and edges on which the propagating waves are localised. The existence of strongly localised waves in periodic media is one of the foundations of modern wave physics. Such modes allow for waves of specific frequencies to be strongly localised at desired locations.

In reality, the construction of perfect periodic media is complicated. Imperfections can be easily introduced to the system, either by small changes to the material parameters or by structural modifications such as breaking the symmetry of the particle positions. An important characteristic of the localised waves is their stability profile once these so called "imperfections" are introduced to the material. This is called *topological protection* [43]. This field of research was inspired by ideas related to the famous quantum Hall effect [44] and was successfully translated to classical wave systems around 15 years ago [73]. This theory uses topological indices associated to the underlying periodic structures [19] to predict the existence of localised waves at interfaces and edges of the material. Further, the invariant nature of topological indices means we can expect that such modes experience enhanced robustness with respect to imperfections. Given how desirable a priori robustness properties are for being able to confidently manufacture functional devices, topological waveguides have emerged as an important sub-field of wave physics [59].

The mathematical theory developed around the topological protection usually considers one-dimensional systems since the fundamental mechanism requires an interface or edge to be introduced in just one axis of periodicity. In addition, it is mostly focused on non-dispersive systems since they provide great insight in physical settings, such as microwaves and perfect conductors. Exploiting the symmetric characteristics of the periodic structures, we are able to extend these results to dispersive systems. Viewing the damped systems as small perturbations of the undamped regime, we prove similar results for materials with damping.

1. Dispersion, damping and spectrum

1.1. Introduction

The material characteristics of photonic crystals gives them a variety of wave properties. From non-dispersive to highly dispersive and damped structures, the spectral properties of these materials are quite exotic. Several different models exist to describe this behaviour. Most models are variants of the Lorentz oscillator model, whereby electrons are modelled as damped harmonic oscillators due to electrostatic attractions with nuclei [51]. A popular special case of this is the Drude model, in which case the restoring force is neglected (to reflect the fact that most electrons in metals are not bound to any specific nucleus, so lack a natural frequency of oscillation). Many other variants of these models exist, for instance by adding or removing damping from the various models, *cf.* [61] or [49], and by taking linear combinations of the different models, as in [62].

A key feature that unites dispersive permittivity models is the existence of singularities in the permittivity. The position of these poles in the complex plane, which correspond to resonances, are one of the crucial properties that determines how a metal interacts with an electromagnetic wave. In conventional Lorentz models the poles appear in the lower complex plane [51]. The imaginary part of the singular frequency is determined by the magnitude of the damping, and the singularities accordingly fall on the real line if the damping is set to zero. In the Drude model, the removal of the restorative force causes the singularities to fall at the origin and on the negative imaginary axis.

A particularly important example of photonic crystals, that is central to our motivation, are halide perovskites. They have excellent optical and electronic properties and are cheap and easy to manufacture at scale [52]. As a result, they are being used in many applications, including optical sensors [36], solar cells [64] and light-emitting diodes [72].

There are a range of methods that can be used to capture the spectra of photonic crystals. For one-dimensional systems, explicit solutions typically exist and transfer matrices are particularly convenient. These were used for Drude materials in [63] and for undamped Lorentz materials in [49], for example. In multiple dimensions, studies often resort to numerical simulation (for instance with finite elements). A valuable approximation strategy is a multi-scale asymptotic method known as high-frequency homogenisation [28], which can be extended to approximate the dispersion curves in dispersive media [67].

In this chapter, we will study photonic crystals composed of metals with permittivity inspired by that of halide perovskites, in the sense that it has symmetric poles in the lower complex plane. After setting out the Floquet-Bloch formulation of the periodic problem in Section 1.2, we will study the one-dimensional periodic Helmholtz problem in Section 1.3. We retrieve the dispersion relation which characterises the halide perovskite system and show how its properties depend on the characteristics of the dispersive permittivity (namely, being real or being complex and having poles either on or below the real axis). Finally, in Section 1.4, we use integral methods and asymptotic analysis in order to obtain the dispersion relation for the two- and three-dimensional cases, showing how to extend our analysis to multi-dimensional photonic crystals. This is a product of the work carried in [4].

1.2. Problem setting

In this section, we present the mathematical setting associated to the Drude-Lorentz model. After applying the Floquet-Bloch theory, we obtain the quasiperiodic problem and provide the main definitions which describe the spectrum of the photonic crystal.

1.2.1. Initial Helmholtz formulation

Let us consider $N \in \mathbb{N}$ particles $D_1, D_2, \dots, D_N$ which together occupy a bounded domain $\Omega \subset \mathbb{R}^d$, for $d \in \{1, 2, 3\}$. The collection of particles Ω will be the repeating unit of the periodic photonic crystal. We suppose that the permittivity of the particles is given by a Drude–Lorentz-type model,

$$\varepsilon(\omega) = \varepsilon_0 + \frac{\alpha}{1 - \beta\omega^2 - i\gamma\omega}, \tag{1.1}$$

where ε_0 denotes the background dielectric constant and α, β, γ are positive constants. α describes the strength of the interactions, β determines the natural resonant frequency and γ is the damping factor. This is motivated by the measured permittivity of halide perovskites, as reported in [52]. We choose to use this expression as a canonical model for dispersive materials whose permittivities have singularities in the complex frequency space. Notice that (1.1) is singular at two complex values of ω. These are given by

$$\omega_{\pm}^{*} = \frac{1}{2\beta}\Big(- i\gamma \pm \sqrt{4\beta - \gamma^2}\Big). \tag{1.2}$$

By varying the parameters α, β and γ, we can force these singularities to lie in the lower half of the complex plane ($\gamma > 0$), on the real line ($\gamma = 0$) or to vanish completely ($\beta = \gamma = 0$). We will make use of this property when trying to interpret the dispersion diagrams in the following analysis. We suppose that the particles are surrounded by a non-dispersive medium with permittivity ε_0. We assume that the

particles are non-magnetic, meaning that the magnetic permeability μ_0 is constant on all of $\mathbb{R}^d$.

We consider the Helmholtz equation as a model for the propagation of time-harmonic waves with frequency ω. This is a reasonable model for the scattering of transverse magnetic polarised light (see *e.g.* [55, Remark 2.1] for a discussion). The wavenumber in the background $\mathbb{R}^d \setminus \overline{\Omega}$ is given by $k_0 := \omega\varepsilon_0\mu_0$ and we will use k to denote the wavenumber within Ω. Let us note here that, from now on, we will suppress the dependence of k_0 and k on ω for brevity. We then consider the system of equations

$$\begin{cases} \Delta u + \omega^2\varepsilon(\omega)\mu_0 u = 0 & \text{in } \Omega, \\ \Delta u + k_0^2 u = 0 & \text{in } \mathbb{R}^d \setminus \overline{\Omega}, \\ u|_+ - u|_- = 0 & \text{on } \partial\Omega, \\ \frac{\partial u}{\partial \nu}|_+ - \frac{\partial u}{\partial \nu}|_- = 0 & \text{on } \partial\Omega, \\ u(x) - u_{in}(x) & \text{satisfies an outgoing radiation condition as } |x| \to \infty, \end{cases} \tag{1.3}$$

where u_{in} is the incident wave, assumed to satisfy $(\Delta + k_0^2)u_{in} = 0$, and the appropriate outgoing radiation condition depends on the dimension of the problem and of the periodic lattice.

1.2.2. Periodic formulation

We will assume that the collection of N particles is repeated in a periodic lattice Λ. We suppose that the lattice has dimension d_l, in the sense that there are lattice vectors $l_1, \ldots, l_{d_l} \in \mathbb{R}^d$ which generate Λ according to

$$\Lambda := \{m_1 l_1 + \cdots + m_{d_l} l_{d_l} \mid m_i \in \mathbb{Z}\}. \tag{1.4}$$

The fundamental domain of the lattice Λ is the set $Y \in \mathbb{R}^d$ given by

$$Y := \{c_1 l_1 + \cdots + c_{d_l} l_{d_l} \mid 0 \leq c_1, \ldots, c_{d_l} \leq 1\}. \tag{1.5}$$

The dual lattice of Λ, denoted by Λ^*, is generated by the vectors $\alpha_1, \ldots, \alpha_{d_l}$ satisfying $\alpha_i \cdot l_j = 2\pi\delta_{ij}$ for $i, j = 1, \ldots, d_l$. Finally, the *Brillouin zone* Y^* is defined by

$$Y^* := (\mathbb{R}^{d_l} \times \{\mathbf{0}\})/\Lambda^*, \tag{1.6}$$

where $\mathbf{0}$ is the zero vector in $\mathbb{R}^{d-d_l}$. The Brillouin zone Y^* is the space that the reduced unit cell of reciprocal space.

The periodic structure, denoted by $\mathcal{D}$, is given by

$$\mathcal{D} = \bigcup_{i=1}^{N} \left(\bigcup_{m \in \Lambda} D_i + m \right).$$

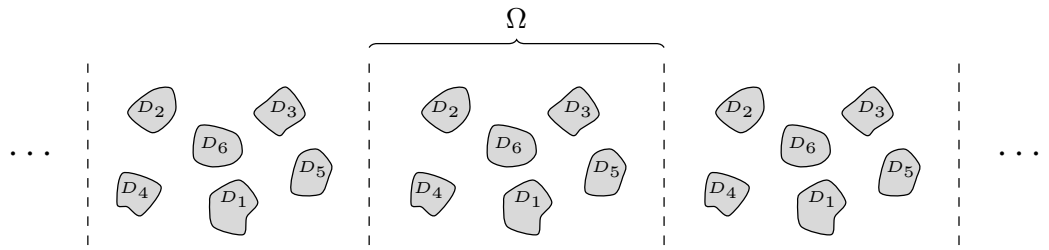

Figure 1.1.: A periodic array of halide perovskite particles. Here, we have six particles $D_1, \ldots, D_6$ repeated periodically in one dimension. Each of them has the halide perovskite permittivity $\varepsilon(\omega)$ defined by (1.1).

Hence, the problem we wish to study is the following:

$$\begin{cases} \Delta u + \omega^2 \varepsilon(\omega)\mu_0 u = 0 & \text{in } \mathcal{D}, \\ \Delta u + k_0^2 u = 0 & \text{in } \mathbb{R}^d \setminus \overline{D}, \\ u|_+ - u|_- = 0 & \text{on } \partial\mathcal{D}, \\ \frac{\partial u}{\partial \nu}|_+ - \frac{\partial u}{\partial \nu}|_- = 0 & \text{on } \partial\mathcal{D}, \\ u(x_l, x_0) & \text{satisfies the outgoing radiation condition as } |x_0| \to \infty. \end{cases} \tag{1.7}$$

1.2.3. Floquet-Bloch theory

In order to study the problem (1.7), we will make use of Floquet-Bloch theory [46]. Let us first give certain definitions which will help with the analysis of the problem.

Definition 1.2.1. *A function $f(x) \in L^2(\mathbb{R}^d)$ is said to be κ-quasiperiodic, with quasiperiodicity $\kappa \in Y^*$, if $e^{-i\kappa\cdot x} f(x)$ is Λ-periodic.*

Definition 1.2.2 (Floquet transform)**.** *Let $f \in L^2(\mathbb{R}^d)$. The Floquet transform of f is defined as*

$$\mathcal{F}[f](x,\kappa) := \sum_{m\in\Lambda} f(x-m)e^{-i\kappa\cdot x}, \quad x \in \mathbb{R}^d,\ \kappa \in Y^*.$$

We have that $\mathcal{F}[f]$ is κ-quasiperiodic in x and periodic in κ. The Floquet transform is an invertible map $\mathcal{F} : L^2(\mathbb{R}^d) \to L^2(Y \times Y^*)$, with inverse given by

$$\mathcal{F}^{-1}[g](x) = \frac{1}{|Y_l^*|}\int_{Y^*} g(x,\kappa)\mathrm{d}\kappa, \quad x \in \mathbb{R}^d,$$

where $g(x,\kappa)$ is extended quasiperiodically for x outside of the unit cell Y.

Let us define $u^\kappa(x) := \mathcal{F}[u](x,\kappa)$. Then, applying the Floquet transform to (1.7), we obtain the following system:

$$\begin{cases} \Delta u^\kappa + \omega^2 \varepsilon(\omega)\mu_0 u^\kappa = 0 & \text{in } \mathcal{D}, \\ \Delta u^\kappa + k_0^2 u^\kappa = 0 & \text{in } \mathbb{R}^d \setminus \overline{D}, \\ u^\kappa|_+ - u^\kappa|_- = 0 & \text{on } \partial\mathcal{D}, \\ \frac{\partial u^\kappa}{\partial \nu}|_+ - \frac{\partial u^\kappa}{\partial \nu}|_- = 0 & \text{on } \partial\mathcal{D}, \\ u^\kappa(x_d, x_0) & \text{is } \kappa\text{-quasiperiodic in } x_d, \\ u^\kappa(x_d, x_0) & \text{satisfies the } \kappa\text{-quasiperiodic radiation condition as } |x_0| \to \infty. \end{cases} \tag{1.8}$$

The solutions to (1.8) typically take the form of a countable collection of spectral bands, each of which depends continuously on the Bloch parameter κ. The goal of our analysis is to identify and explain the gaps between the spectral band. At frequencies within these band gaps, waves do not propagate in the material and their amplitude decays exponentially. As a result, they are the starting point for building waveguides and other wave control devices.

For real-valued permittivities, it is straightforward to define band gaps as the intervals between the real-valued bands.

Definition 1.2.3 (Band gap for real permittivities). *A frequency $\omega \in \mathbb{R}$ is said to be in a band gap of the periodic structure $\mathcal{D}$ if it is such that* (1.8) *does not admit a non-trivial solution for any $\kappa \in \mathbb{R}$.*

We are interested in materials for which the permittivity takes complex values, corresponding to the introduction of damping to the model. In which case, we elect to keep the frequency $\omega \in \mathbb{R}$ as a real number but allow the Bloch parameter κ to take complex values. In which case, the imaginary part of κ describes the rate at which the waves amplitude decays. It should be noted that it is also quite common to do the opposite by forcing κ to be real and allowing ω to be complex valued, as in [11, 67] for example.

In the real-valued case, it is clear that κ belongs to the Brillouin zone Y^* (which has the topology of a torus, due to the periodicity in κ). When κ is complex valued, its real part still lives in Y^* but its imaginary part can take arbitrary values. Thus, κ lives in a subset of the complex plane that is isomorphic to $Y^* \times \mathbb{R}$. This can be thought of as a "generalised" Brillouin zone; this idea has been used to describe the spectral convergence of non-Hermitian systems in [7].

In our setting, which is a damped model that is characterised by a complex permittivity, we have that $\kappa \in \mathbb{C}$ and it is less clear how to define a band gap. Intuitively, a band gap is a range of frequencies at which the damping is particularly large. Hence, we provide a modified definition for the notion of a band gap for complex permittivities in terms of local maxima of the amplitude decay.

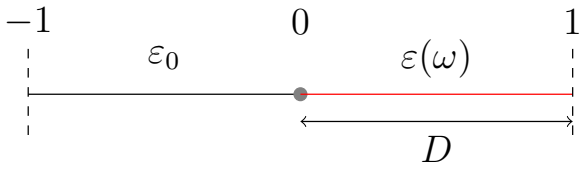

Figure 1.2.: The one-dimensional setting. The periodically repeated cell is of length 2. Here the interval $[-1, 0)$ is the background and the interval $[0, 1)$ is the particle.

Definition 1.2.4 (Band gap for complex permittivities)**.** *We define a band gap for complex permittivities to be the set of frequencies $\omega \in \mathbb{R}$ for which (1.8) admits a non-trivial solution with quasiperiodicity $\kappa \in \mathbb{C}$ and $|\Im(\kappa)|$ is at a local maximum.*

We will first study the problem in the one-dimensional setting. In one dimension, the problem is easier to manipulate and we are able to retrieve explicit expressions. Hence, we can get a variety of results concerning the characteristics of the quasiperiodic system. In particular, our main goal is to obtain the dispersion relation, an expression which relates the quasiperiodicities $\kappa \in \mathbb{C}$ with the frequencies $\omega \in \mathbb{R}$, and study its properties. Then, in Section 1.4 we will provide an analysis for higher dimensional systems and we will give the equivalent relation.

1.3. One dimension

Let us first treat the Helmholtz problem (1.8) in the one-dimensional case. We will work on the interval $[-1, 1]$, with $[-1, 0)$ denoting the background and $[0, 1)$ the particle. A schematic depiction of this is given in Figure 1.2. Hence, the problem reads as follows:

$$\frac{\mathrm{d}^2 u}{\mathrm{d}x^2} + \mu_0 \omega^2 \varepsilon(x, \omega) u(x) = 0, \tag{1.9}$$

on the domain $[-1, 1]$, where

$$\varepsilon(x, \omega) := \begin{cases} \varepsilon_0, & x \in [-1, 0) \quad \text{(background)}, \\ \varepsilon(\omega), & x \in [0, 1] \quad \text{(particle)}, \end{cases} \tag{1.10}$$

with the boundary conditions

$$u(1) = e^{2i\kappa} u(-1) \quad \text{and} \quad \frac{\mathrm{d}u}{\mathrm{d}x}(1) = e^{2i\kappa} \frac{\mathrm{d}u}{\mathrm{d}x}(-1). \tag{1.11}$$

1.3.1. Dispersion relation

We will now retrieve an expression for the solution to (1.9). Let us define the quantities

$$\sigma_0 := \omega\sqrt{\varepsilon_0\mu_0}, \quad \text{and} \quad \sigma_c := \omega\sqrt{\varepsilon(\omega)\mu_0}. \tag{1.12}$$

For many of the results that follow, the crucial quantity will be the contrast between the material inside the particles and the background medium. With this in mind, we introduce the frequency-dependent contrast ρ as

$$\rho(\omega) := \frac{\sigma_c}{\sigma_0} = \sqrt{\frac{\varepsilon(\omega)}{\varepsilon_0}}. \tag{1.13}$$

Then, the following expression holds for the solution to (1.9).

Lemma 1.3.1. *Let u denote a solution to* (1.9)*. Then, u is given by*

$$u(x) = \begin{cases} \mathcal{A}\rho\sin\Big(\sigma_0 x\Big) + \mathcal{B}\cos\Big(\sigma_0 x\Big), & x \in [-1,0), \\ \mathcal{A}\sin\Big(\sigma_c x\Big) + \mathcal{B}\cos\Big(\sigma_c x\Big), & x \in [0,1], \end{cases} \tag{1.14}$$

where $\mathcal{A}, \mathcal{B} \in \mathbb{C}$ are two constants.

Proof. We know that a solution to (1.9) must be given by

$$u(x) = \begin{cases} \mathcal{A}_1\sin\Big(\omega\sqrt{\varepsilon_0\mu_0}x\Big) + \mathcal{B}_1\cos\Big(\omega\sqrt{\varepsilon_0\mu_0}x\Big), & x \in [-1,0), \\ \mathcal{A}_2\sin\Big(\omega\sqrt{\varepsilon(\omega)\mu_0}x\Big) + \mathcal{B}_2\cos\Big(\omega\sqrt{\varepsilon(\omega)\mu_0}x\Big), & x \in [0,1], \end{cases} \tag{1.15}$$

where $\mathcal{A}_1, \mathcal{A}_2, \mathcal{B}_1, \mathcal{B}_2 \in \mathbb{C}$ are constants to be defined. This, also, gives

$$\frac{\mathrm{d}u}{\mathrm{d}x}(x) = \mathcal{A}_1\omega\sqrt{\varepsilon_0\mu_0}\cos\Big(\omega\sqrt{\varepsilon_0\mu_0}x\Big) - \mathcal{B}_1\omega\sqrt{\varepsilon_0\mu_0}\sin\Big(\omega\sqrt{\varepsilon_0\mu_0}x\Big),$$

for $x \in [-1,0)$, and

$$\frac{\mathrm{d}u}{\mathrm{d}x}(x) = \mathcal{A}_2\omega\sqrt{\varepsilon(\omega)\mu_0}\cos\Big(\omega\sqrt{\varepsilon(\omega)\mu_0}x\Big) - \mathcal{B}_2\omega\sqrt{\varepsilon(\omega)\mu_0}\sin\Big(\omega\sqrt{\varepsilon(\omega)\mu_0}x\Big),$$

for $x \in [0,1]$. Now, from the boundary transmission conditions in (1.7), we require

$$\lim_{x\to 0^-} u(x) = \lim_{x\to 0^+} u(x) \qquad \text{and} \qquad \lim_{x\to 0^-} \frac{\mathrm{d}u}{\mathrm{d}x}(x) = \lim_{x\to 0^+} \frac{\mathrm{d}u}{\mathrm{d}x}(x).$$

These conditions mean we must have that $\mathcal{B}_1 = \mathcal{B}_2$ and $\mathcal{A}_1 = \sqrt{\varepsilon(\omega)/\varepsilon_0}\mathcal{A}_2 = \rho(\omega)\mathcal{A}$, which gives the desired result. □

Using the boundary conditions (1.11), we can obtain the dispersion relation for the one-dimensional problem. This is a well-known result, that first appeared in a quantum-mechanical setting [45] and has since been shown to describe a range of periodic classical wave systems also [1, 57]. We include a brief proof, for completeness.

Theorem 1.3.2 (Dispersion relation). *Let u denote the solution to* (1.9) *along with the boundary conditions* (1.11). *Then, for u to be non-trivial, the quasiperiodicities $\kappa \in \mathbb{C}$ satisfies the dispersion relation*

$$\cos(2\kappa) = \cos(\sigma_0)\cos(\rho\sigma_0) - \frac{1+\rho^2}{2\rho}\sin(\sigma_0)\sin(\rho\sigma_0). \tag{1.16}$$

Proof. From Lemma 1.3.1, we have that u is given by (1.14). Then, using (1.11), we have

$$\begin{cases} \Big[\sin(\sigma_c) + e^{2i\kappa}\rho\sin(\sigma_0)\Big]\mathcal{A} + \Big[\cos(\sigma_c) - e^{2i\kappa}\cos(\sigma_0)\Big]\mathcal{B} = 0, \\ \Big[\sigma_c\cos(\sigma_c) - e^{2i\kappa}\rho\sigma_0\cos(\sigma_0)\Big]\mathcal{A} - \Big[\sigma_c\sin(\sigma_c) + e^{2i\kappa}\sigma_0\sin(\sigma_0)\Big]\mathcal{B} = 0. \end{cases} \tag{1.17}$$

We observe that for (1.9) to have a non-zero solution, it should hold

$$\begin{aligned} \Big[\sin(\sigma_c) + e^{2i\kappa}\rho\sin(\sigma_0)\Big] \cdot \Big[\sigma_c\sin(\sigma_c) + e^{2i\kappa}\sigma_0\sin(\sigma_0)\Big] + \\ + \Big[\cos(\sigma_c) - e^{2i\kappa}\cos(\sigma_0)\Big] \cdot \Big[\sigma_c\cos(\sigma_c) - e^{2i\kappa}\rho\sigma_0\cos(\sigma_0)\Big] = 0, \end{aligned}$$

which gives

$$\sqrt{\varepsilon(\omega)}e^{4i\kappa} + \left[\frac{\varepsilon_0+\varepsilon(\omega)}{\sqrt{\varepsilon_0}}\sin(\sigma_0)\sin(\sigma_c) - 2\sqrt{\varepsilon(\omega)}\cos(\sigma_0)\cos(\sigma_c)\right]e^{2i\kappa} + \sqrt{\varepsilon(\omega)} = 0. \tag{1.18}$$

Making some algebraic rearrangements, we observe that

$$2\sqrt{\frac{\varepsilon(\omega)}{\varepsilon_0}}\Big[\cos(\sigma_0)\cos(\sigma_c) - \cos(2\kappa)\Big] - \frac{\varepsilon_0+\varepsilon(\omega)}{\varepsilon_0}\sin(\sigma_0)\sin(\sigma_c) = 0. \tag{1.19}$$

Finally, making the substitutions $\sigma_c = \rho\sigma_0$ and $\sqrt{\varepsilon(\omega)} = \rho\sqrt{\varepsilon_0}$, we obtain the desired result. □

The dispersion relation (1.16) can be used to plot the dispersion curves. For a given frequency ω, $\rho(\omega)$ can be calculated to yield the right-hand side of (1.16), which can subsequently be solved to find κ. This is shown in Figure 1.3. Since $\epsilon(\omega)$ is complex valued, κ will generally take complex values. We plot only the absolute values of both the real and imaginary parts; as we will see below, this is sufficient to characterise the full dispersion relation. Notice also that $\Re(\kappa) \in Y^* = [-\pi/2, \pi/2)$.

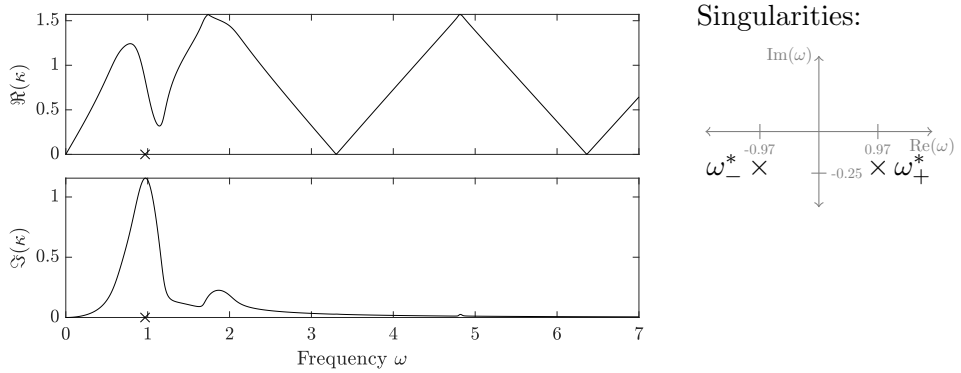

Figure 1.3.: The dispersion relation of the halide perovskite photonic crystal. We model a material with permittivity given by (1.1) with $\alpha = 1$, $\beta = 1$ and $\gamma = 0.5$. The frequency ω is chosen to be real and the Bloch parameter κ allowed to take complex values. The permittivity is singular at two points, which are in the lower complex plane and are symmetric about the imaginary axis, as indicated in the sketch on the right and (the real parts) by the crosses on the frequency axes of the plots.

1.3.2. Properties of the dispersion relation

The dispersion relation (1.16) describes the behaviour of the periodic system and reveals the relationship between the quasiperiodicities $\kappa \in \mathbb{C}$, the frequencies $\omega \in \mathbb{R}$ and the permittivity $\varepsilon(\omega)$ of the material. We can use it to derive some simple results about the dispersion curves. The first thing to understand is the symmetries of the dispersion curves.

Lemma 1.3.3 (Opposite quasiperiodicities)**.** *Let $\kappa \in \mathbb{C}$ be a complex quasiperiodicity satisfying the dispersion relation* (1.16) *for a given frequency $\omega \in \mathbb{R}$. Then, the opposite quasiperiodicity, i.e. $-\kappa$, satisfies the same dispersion relation.*

Proof. We just have to use that $\cos(\cdot)$ is an even function. Then, if $\kappa \in \mathbb{C}$ is such that (1.16) holds, from the fact that $\cos(-2\kappa) = \cos(2\kappa)$, we get that $-\kappa \in \mathbb{C}$ also satisfies (1.16). This concludes the proof. □

It is with Lemma 1.3.3 in mind that we are able to plot only the absolute values of the imaginary parts in Figure 1.3 and the subsequent figures.

1.3.2.1. Real and imaginary parts

In the analysis that will follow, it will be useful to be able to describe the behaviour of the real and imaginary part of the quasiaperiodicity with respect to the permittivity. In particular, we will decompose both the quasiperiodicity κ and ρ into real and

imaginary parts, and we will derive this dependence from the dispersion relation. Since $\kappa \in \mathbb{C}$ and $\rho \in \mathbb{C}$, let

$$\kappa = \kappa_1 + i\kappa_2 \quad \text{and} \quad \rho = \rho_1 + i\rho_2, \tag{1.20}$$

with $\kappa_1, \kappa_2, \rho_1, \rho_2 \in \mathbb{R}$. We will also define $\mathscr{L}_1$ and $\mathscr{L}_2$, which depend on $\omega \in \mathbb{R}$, as follows:

$$\begin{aligned}\mathscr{L}_1(\omega) :=& \cos(\sigma_0)\cos(\sigma_0\rho_1)\cosh(\sigma_0\rho_2) - \\ &- \frac{\sin(\sigma_0)}{2(\rho_1^2+\rho_2^2)}\Big[\rho_1(1+\rho_1^2+\rho_2^2)\sin(\sigma_0\rho_1)\cosh(\sigma_0\rho_2) - \\ &- \rho_2(\rho_2^2 - 1 + \rho_1^2)\cos(\sigma_0\rho_1)\sinh(\sigma_0\rho_2)\Big],\end{aligned} \tag{1.21}$$

and

$$\begin{aligned}\mathscr{L}_2(\omega) :=& \cos(\sigma_0)\sin(\sigma_0\rho_1)\sinh(\sigma_0\rho_2) + \\ &+ \frac{\sin(\sigma_0)}{2(\rho_1^2+\rho_2^2)}\Big[\rho_2(\rho_2^2 - 1 + \rho_1^2)\sin(\sigma_0\rho_1)\cosh(\sigma_0\rho_2) + \\ &+ \rho_1(1+\rho_1^2+\rho_2^2)\cos(\sigma_0\rho_1)\sinh(\sigma_0\rho_2)\Big],\end{aligned} \tag{1.22}$$

where we note that ρ_1, ρ_2 and σ_0 all depend on the frequency ω, as specified in (1.12) and (1.13). Then, we have the following result.

Proposition 1.3.4. *Let $\kappa \in \mathbb{C}$, given by (1.20), satisfying the dispersion relation (1.16) for a given frequency $\omega \in \mathbb{R}$. Then, its real and imaginary parts are given by*

$$\Re(\kappa) = \pm\frac{1}{2}\arccos\left(\frac{\mathscr{L}_1}{\cosh(2\Im(\kappa))}\right), \tag{1.23}$$

and

$$\Im(k) = \frac{1}{2}\operatorname{arcsinh}\left(\pm\sqrt{\frac{1}{2}\Big[\mathscr{L}_1^2 + \mathscr{L}_2^2 - 1 + \sqrt{(1-\mathscr{L}_1^2-\mathscr{L}_2^2)^2 + 4\mathscr{L}_2^2}\Big]}\right), \tag{1.24}$$

where $\mathscr{L}_1$ and $\mathscr{L}_2$ are given by (1.21) and (1.22), respectively. We, also, note that the choice of $+$ or $-$ should be the same in (1.23) and (1.24).

Proof. From (1.20), the dispersion relation (1.16) becomes

$$\cos(2\kappa_1 + i2\kappa_2) = \cos(\sigma_0)\cos(\sigma_0\rho_1 + i\sigma_0\rho_2) - \frac{1+(\rho_1+i\rho_2)^2}{2(\rho_1+i\rho_2)}\sin(\sigma_0)\sin(\sigma_0\rho_1 + i\sigma_0\rho_2),$$

which is,

$$\begin{aligned}&\cos(2\kappa_1)\cosh(2\kappa_2) - i\sin(2\kappa_1)\sinh(2\kappa_2) = \\ &\qquad = \cos(\sigma_0)\Big[\cos(\sigma_0\rho_1)\cosh(\sigma_0\rho_2) - i\sin(\sigma_0\rho_1)\sinh(\sigma_0\rho_2)\Big] -\end{aligned}$$

$$- \frac{1+\rho_1^2+2i\rho_1\rho_2-\rho_2^2}{2(\rho_1^2+\rho_2^2)}(\rho_1 - i\rho_2)\sin(\sigma_0)\Big[\sin(\sigma_0\rho_1)\cosh(\sigma_0\rho_2)+ \\ + i\cos(\sigma_0\rho_1)\sinh(\sigma_0\rho_2)\Big].$$

Taking real and imaginary parts, we obtain, for the real part,

$$\begin{aligned}\cos(2\kappa_1)\cosh(2\kappa_2) =& \cos(\sigma_0)\cos(\sigma_0\rho_1)\cosh(\sigma_0\rho_2)- \\ &- \frac{\sin(\sigma_0)}{2(\rho_1^2+\rho_2^2)}\Big[\rho_1(1+\rho_1^2+\rho_2^2)\sin(\sigma_0\rho_1)\cosh(\sigma_0\rho_2)- \\ &- \rho_2(\rho_2^2-1+\rho_1^2)\cos(\sigma_0\rho_1)\sinh(\sigma_0\rho_2)\Big],\end{aligned} \tag{1.25}$$

and, for the imaginary part,

$$\begin{aligned}\sin(2\kappa_1)\sinh(2\kappa_2) =& \cos(\sigma_0)\sin(\sigma_0\rho_1)\sinh(\sigma_0\rho_2)+ \\ &+ \frac{\sin(\sigma_0)}{2(\rho_1^2+\rho_2^2)}\Big[\rho_2(\rho_2^2-1+\rho_1^2)\sin(\sigma_0\rho_1)\cosh(\sigma_0\rho_2)+ \\ &+ \rho_1(1+\rho_1^2+\rho_2^2)\cos(\sigma_0\rho_1)\sinh(\sigma_0\rho_2)\Big].\end{aligned} \tag{1.26}$$

So, from (1.21) and (1.22), we obtain the system

$$\begin{cases}\cos(2\kappa_1)\cosh(2\kappa_2) = \mathscr{L}_1, \\ \sin(2\kappa_1)\sinh(2\kappa_2) = \mathscr{L}_2.\end{cases} \tag{1.27}$$

From the first equation, we immediately see that

$$\kappa_1 = \pm\frac{1}{2}\arccos\left(\frac{\mathscr{L}_1}{\cosh(2\kappa_2)}\right),$$

then, substituting into the second equation gives

$$\sin\left[\arccos\left(\frac{\mathscr{L}_1}{\cosh(2\kappa_2)}\right)\right]\sinh(2\kappa_2) = \pm\mathscr{L}_2.$$

We know that for $x \in [-1,1]$, we have the identity $\sin[\arccos(x)] = \sqrt{1-x^2}$. Hence, from the above, we get

$$\sqrt{1-\frac{\mathscr{L}_1^2}{\cosh^2(2\kappa_2)}}\sinh(2\kappa_2) = \pm\mathscr{L}_2. \tag{1.28}$$

Similarly, using the fact that $\cosh^2(x) - \sinh^2(x) = 1$ for $x \in \mathbb{R}$, we find that

$$\sqrt{1-\frac{\mathscr{L}_1^2}{1+\sinh^2(2\kappa_2)}}\sinh(2\kappa_2) = \pm\mathscr{L}_2. \tag{1.29}$$

Hence, we have

$$\sinh^4(2\kappa_2) + (1-\mathscr{L}_1^2-\mathscr{L}_2^2)\sinh^2(2\kappa_2) - \mathscr{L}_2^2 = 0.$$

Using the quadratic formula, this gives

$$\sinh^2(2\kappa_2) = \frac{1}{2}\Big[\mathscr{L}_1^2 + \mathscr{L}_2^2 - 1 + \sqrt{(1-\mathscr{L}_1^2-\mathscr{L}_2^2)^2 + 4\mathscr{L}_2^2}\Big],$$

and so, we get

$$\kappa_2 = \frac{1}{2}\operatorname{arcsinh}\left(\pm\sqrt{\frac{1}{2}\Big[\mathscr{L}_1^2 + \mathscr{L}_2^2 - 1 + \sqrt{(1-\mathscr{L}_1^2-\mathscr{L}_2^2)^2 + 4\mathscr{L}_2^2}\Big]}\right).$$

This gives the desired result. □

Remark 1.3.5. *Another way of viewing that the choice of + or − in* (1.23) *is the same as the one in* (1.24) *is from the fact that we have shown that if* $\kappa \in \mathbb{C}$ *satisfies* (1.16)*, then* $-\kappa$ *does as well, but* $\overline{\kappa}$ *does not.*

1.3.2.2. Imaginary part decay

From (1.24), we obtain a result on the decay of the imaginary part of the quasiperiodicity κ as $\omega \to \infty$. We will first state some preliminary results, before proving the main theorem.

Lemma 1.3.6. *Let the frequency-dependent contrast* $\rho \in \mathbb{C}$ *be given by* (1.13)*. Then, it holds*

$$\lim_{\omega\to\infty} |\rho| = 1, \tag{1.30}$$

$$\lim_{\omega\to\infty} |\Re(\rho)| = 1 \quad \textit{and} \quad \lim_{\omega\to\infty} |\Im(\rho)| = 0. \tag{1.31}$$

Proof. From (1.12), we have

$$\rho = \sqrt{1 + \frac{\alpha}{\varepsilon_0(1-\beta\omega^2 - i\gamma\omega)}},$$

which gives directly $\lim_{\omega\to\infty} |\rho| = 1$. This can be rewritten as

$$\rho = \sqrt{1 + \frac{\alpha}{\varepsilon_0}\frac{1-\beta\omega^2}{(1-\beta\omega^2)^2+\gamma^2\omega^2} + i\frac{\alpha}{\varepsilon_0}\frac{\gamma\omega}{(1-\beta\omega^2)^2+\gamma^2\omega^2}}$$

To ease the notation, let us write

$$a(\omega) := 1 + \frac{\alpha}{\varepsilon_0}\frac{1-\beta\omega^2}{(1-\beta\omega^2)^2+\gamma^2\omega^2} \quad \text{and} \quad b(\omega) := \frac{\alpha}{\varepsilon_0}\frac{\gamma\omega}{(1-\beta\omega^2)^2+\gamma^2\omega^2}. \tag{1.32}$$

Then, we have

$$\rho = \pm \left(\sqrt{\frac{\sqrt{a(\omega)^2 + b(\omega)^2} + a(\omega)}{2}} + i \frac{b(\omega)}{|b(\omega)|} \sqrt{\frac{\sqrt{a(\omega)^2 + b(\omega)^2} - a(\omega)}{2}} \right). \quad (1.33)$$

We observe, from (1.32), that, as $\omega \to \infty$,

$$a(\omega) = 1 + O\left(\frac{1}{\omega^2}\right) \quad \text{and} \quad b(\omega) = O\left(\frac{1}{\omega^3}\right), \quad (1.34)$$

which gives

$$\lim_{\omega \to \infty} a(\omega) = 1 \quad \text{and} \quad \lim_{\omega \to \infty} b(\omega) = 0.$$

Also, since $\alpha, \gamma, \varepsilon_0 > 0$, it holds that

$$\lim_{\omega \to \infty} \frac{b(\omega)}{|b(\omega)|} = 1.$$

Hence, combining these results, we get

$$\lim_{\omega \to \infty} |\rho_1| = \lim_{\omega \to \infty} \left| \sqrt{\frac{\sqrt{a(\omega)^2 + b(\omega)^2} + a(\omega)}{2}} \right| = 1$$

and

$$\lim_{\omega \to \infty} |\rho_2| = \lim_{\omega \to \infty} \left| \frac{b(\omega)}{|b(\omega)|} \sqrt{\frac{\sqrt{a(\omega)^2 + b(\omega)^2} - a(\omega)}{2}} \right| = 0.$$

This concludes the proof. □

Lemma 1.3.7. *As $\omega \to \infty$, we have that*

$$|\mathscr{L}_1| \leq 1 \quad \textit{and} \quad \mathscr{L}_2 \to 0, \quad (1.35)$$

where $\mathscr{L}_1 = \mathscr{L}_1(\omega)$ and $\mathscr{L}_2 = \mathscr{L}_2(\omega)$ were defined in (1.21) *and* (1.22).

Proof. From Lemma 1.3.6, we have that, as $\omega \to \infty$,

$$|\rho_1| \to 1, \quad |\rho_2| \to 0$$

and from (1.12), we have that

$$\sigma_0 \to \infty.$$

So, it is essential to understand the behaviour of $\sigma_0\rho_2$ as $\omega \to \infty$. Using the same notations as in the proof of Lemma 1.3.6, we have, without loss of generality on the $\pm$ of (1.33),

$$\rho_2 = \frac{b(\omega)}{|b(\omega)|}\sqrt{\frac{\sqrt{a(\omega)^2+b(\omega)^2}-a(\omega)}{2}},$$

and hence, from (1.12), we have

$$\sigma_0\rho_2 = \sqrt{\mu_0\varepsilon_0}\frac{b(\omega)}{|b(\omega)|}\sqrt{\frac{\sqrt{\omega^4\Big(a(\omega)^2+b(\omega)^2\Big)}-\omega^2 a(\omega)}{2}}.$$

From (1.34), we see that, as $\omega \to \infty$,

$$\omega^4 a(\omega)^2 = \omega^4 + O(1), \quad \omega^2 a(\omega) = \omega^2 + O(1)$$

and

$$\omega^4 b(\omega)^2 = O\left(\frac{1}{\omega^2}\right).$$

Hence, as $\omega \to \infty$,

$$\sqrt{\frac{\sqrt{\omega^4\Big(a(\omega)^2+b(\omega)^2\Big)}-\omega^2 a(\omega)}{2}} \to 0,$$

which gives,

$$\lim_{\omega\to\infty} \sigma_0\rho_2 = 0,$$

and so

$$\lim_{\omega\to\infty} |\cosh(\sigma_0\rho_2)| = 1 \quad \text{and} \quad \lim_{\omega\to\infty} |\sinh(\sigma_0\rho_2)| = 0. \tag{1.36}$$

Thus, (1.21) gives

$$\begin{aligned}\lim_{\omega\to\infty} |\mathscr{L}_1| &= \lim_{\omega\to\infty} \Big|\cos(\sigma_0)\cos(\sigma_0\rho_1) - \sin(\sigma_0)\sin(\sigma_0\rho_1)\Big| \\ &= \lim_{\omega\to\infty} \Big|\cos\Big(\sigma_0(1+\rho_1)\Big)\Big| \leq 1,\end{aligned}$$

which is the desired bound for $\mathscr{L}_1$. Similarly, from the triangle inequality applied on (1.22), we have

$$\begin{aligned}|\mathscr{L}_2| \leq |\sinh(\sigma_0\rho_2)| + \frac{1}{2(\rho_1^2+\rho_2^2)}\Big[&|\rho_2(\rho_2^2-1+\rho_1^2)||\cosh(\sigma_0\rho_2)| + \\ &+ |\rho_1|(1+\rho_1^2+\rho_2^2)|\sinh(\sigma_0\rho_2)|\Big].\end{aligned} \tag{1.37}$$

Using Lemma 1.3.6 and (1.36), we obtain

$$\lim_{\omega\to\infty} \mathscr{L}_2 = 0.$$

This concludes the proof. □

Using these results, we will describe the behaviour of the imaginary part κ_2 of the quasiperiodicity $\kappa \in \mathbb{C}$ as the frequency tends to infinity, i.e., $\omega \to \infty$.

Proposition 1.3.8. *Let us consider a complex quasiperiodicity $\kappa \in \mathbb{C}$ satisfying the dispersion relation* (1.16) *with $\alpha, \beta, \gamma \in \mathbb{R}_{>0}$. Then, it holds that*

$$\lim_{\omega \to \infty} \Im(\kappa) = 0. \tag{1.38}$$

Proof. Indeed, since $\kappa \in \mathbb{C}$, let us define $\kappa_1 := \Re(\kappa)$ and $\kappa_2 := \Im(\kappa)$. Then, from (1.24), we have that κ_2 is given by

$$\kappa_2 = \frac{1}{2}\text{arcsinh}\left(\pm\sqrt{\frac{1}{2}\left[\mathscr{L}_1^2 + \mathscr{L}_2^2 - 1 + \sqrt{(1 - \mathscr{L}_1^2 - \mathscr{L}_2^2)^2 + 4\mathscr{L}_2^2}\right]}\right).$$

From Lemma 1.3.7, we have that, as $\omega \to \infty$, $\mathscr{L}_1$ remains bounded, whereas $\mathscr{L}_2 \to 0$. Thus, the following holds

$$\lim_{\omega \to \infty} \left[\mathscr{L}_1^2 + \mathscr{L}_2^2 - 1 + \sqrt{(1 - \mathscr{L}_1^2 - \mathscr{L}_2^2)^2 + 4\mathscr{L}_2^2}\right] = \left[\mathscr{L}_1^2 - 1 + |1 - \mathscr{L}_1^2|\right] = 0,$$

since we have that $|\mathscr{L}_1| \leq 1$ also from Lemma 1.3.7. Then, from the continuity of the arcsinh$(\cdot)$ function, the desired result follows. □

The decay predicted by Proposition 1.3.8 is shown in Figure 1.3. Due to the damping in the model, the imaginary part has discernible peaks at the first few gaps, but then decays steadily to zero at higher frequencies.

1.3.3. The effect of singularities and damping

As mentioned before, the dispersion relation of the halide perovskite particles leads to dispersion curves which are not trivial to understand in terms of the traditional viewpoint of band gaps. In order to understand the behaviour, we will examine each distinct feature of the halide perovskite permittivity, to understand the effect it has on the spectrum of the photonic crystal.

In particular, we will begin with the simplest case when the permittivity is real and constant with respect to the frequency ω. Then, we will introduce a dispersive behaviour to the permittivity by adding singularities at non-zero frequencies. We will initially suppose that these poles lie on the real axis and will study the behaviour close to these regions. Finally, we will study the effect of introducing a complex permittivity, corresponding to damping. Taken together, these results will allow us to explain the spectra of a halide perovskite photonic crystal.

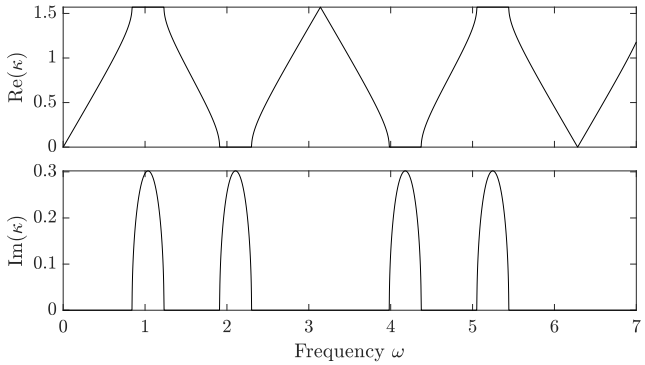

Figure 1.4.: The dispersion relation of a photonic crystal with frequency-independent material parameters. We model a material with permittivity given by (1.1) with $\alpha = 1$, $\beta = 0$ and $\gamma = 0$. The frequency ω is chosen to be real and the Bloch parameter κ allowed to take complex values. The permittivity is never singular in this case.

1.3.3.1. Constant permittivity

The first case we will consider is the one of a real-valued, non-dispersive permittivity, constant with respect to the frequency ω. In our setting this translates into having (1.1) with $\beta = \gamma = 0$ and $\alpha > 0$, i.e.,

$$\varepsilon(\omega) = \varepsilon_0 + \alpha \in \mathbb{R}_{>0}. \tag{1.39}$$

This setting has been studied quite extensively. We refer to [24], as a classical reference for studying the dispersive nature of waves in periodic systems. In Figure 1.4, we provide an example for the dispersion curves when the permittivity is constant and real. It is worth noting the following result.

Lemma 1.3.9. *Let $\varepsilon(\omega)$ be the real-valued, non-dispersive permittivity given by* (1.39)*. Then, if $\kappa \in \mathbb{C}$ is a quasiperiodicity satisfying* (1.16) *for a given frequency $\omega \in \mathbb{R}$, then so does $\overline{\kappa} \in \mathbb{C}$.*

Proof. Indeed, since $\varepsilon(\omega) \in \mathbb{R}_{>0}$, then $\rho \in \mathbb{R}_{>0}$. Let us take $\kappa \in \mathbb{C}$ satisfying (1.16). Then, we can write $\kappa = \kappa_1 + i\kappa_2$, with $\kappa_1, \kappa_2 \in \mathbb{R}$. Now, since $\rho > 0$, we can write

$$\cos(\sigma_0)\cos(\rho\sigma_0) - \frac{1+\rho^2}{2\rho}\sin(\sigma_0)\sin(\rho\sigma_0) =: A > 0.$$

Thus, (1.16) gives us

$$\cos(2\kappa_1 + 2i\kappa_2) = A,$$

which becomes the following system

$$\begin{cases} \cos(2\kappa_1)\cdot\cosh(2\kappa_2) = A, \\ \sin(2\kappa_1)\cdot\sinh(2\kappa_2) = 0. \end{cases}$$

This implies that

$$\kappa_2 = 0 \quad \text{or} \quad \kappa_1 = \frac{m}{2}\pi,\ m \in \mathbb{Z}.$$

If $\kappa_2 = 0$, then $\kappa = \kappa_1 \in \mathbb{R}$. Thus, $\kappa = \overline{\kappa}$, which gives the desired result. If $\kappa_1 = \frac{m}{2}\pi$, for $m \in \mathbb{Z}$, then κ satisfies (1.16) if and only if

$$\cosh(2\kappa_2) = \pm A. \tag{1.40}$$

Since $\cosh(\cdot)$ is an even function, we have that $-\kappa_2$ satisfies (1.40) for the same frequency ω. Hence, $\overline{\kappa} = \kappa_1 - i\kappa_2$ satisfies (1.16) and this concludes the proof. □

Crucially, the dispersion curves shown in Figure 1.4 consist of a countable sequence of disjoint bands in which κ is real valued. Between each band there is a band gap, defined in the sense of Definition 1.2.3, in which κ is purely imaginary, corresponding to the decay of the wave. The occurence of κ being either purely real or purely imaginary is the mechanism behind Lemma 1.3.9. As we will see below, when we add singularities or damping to the model, the band gap structure is less straightforward to interpret.

1.3.3.2. Singular permittivity with no damping

Let us now study the case where the permittivity has a dispersive (and singular) character with respect to the frequency ω, but there is no damping, i.e., we consider $\alpha, \beta > 0$ and $\gamma = 0$. This implies that

$$\varepsilon(\omega) = \varepsilon_0 + \frac{\alpha}{1 - \beta\omega^2}. \tag{1.41}$$

The interesting aspect in this setting is the existence of real poles for the permittivity. They are given by

$$\omega_{\pm}^{*} = \pm\frac{1}{\sqrt{\beta}}.$$

In Figure 1.5, we observe that near the pole of the permittivity there are infinitely many band gaps. This was similarly observed recently by [67]. Noting that a band gap occurs when the magnitude of the right-hand side of (1.16) is greater than one. We define the function

$$\begin{aligned} f(\omega) := &\cos\Big(\sigma_0(\omega)\Big)\cos\Big(\rho(\omega)\sigma_0(\omega)\Big) - \\ &- \frac{1+\rho(\omega)^2}{2\rho(\omega)}\sin\Big(\sigma_0(\omega)\Big)\sin\Big(\rho(\omega)\sigma_0(\omega)\Big), \end{aligned} \tag{1.42}$$

which is the right-hand side of (1.16). We will prove that this takes values greater than one on a countably infinite number of disjoint intervals within any neighbourhood of the singularity. To do so, we will introduce the following notation, which will be used in our analysis.

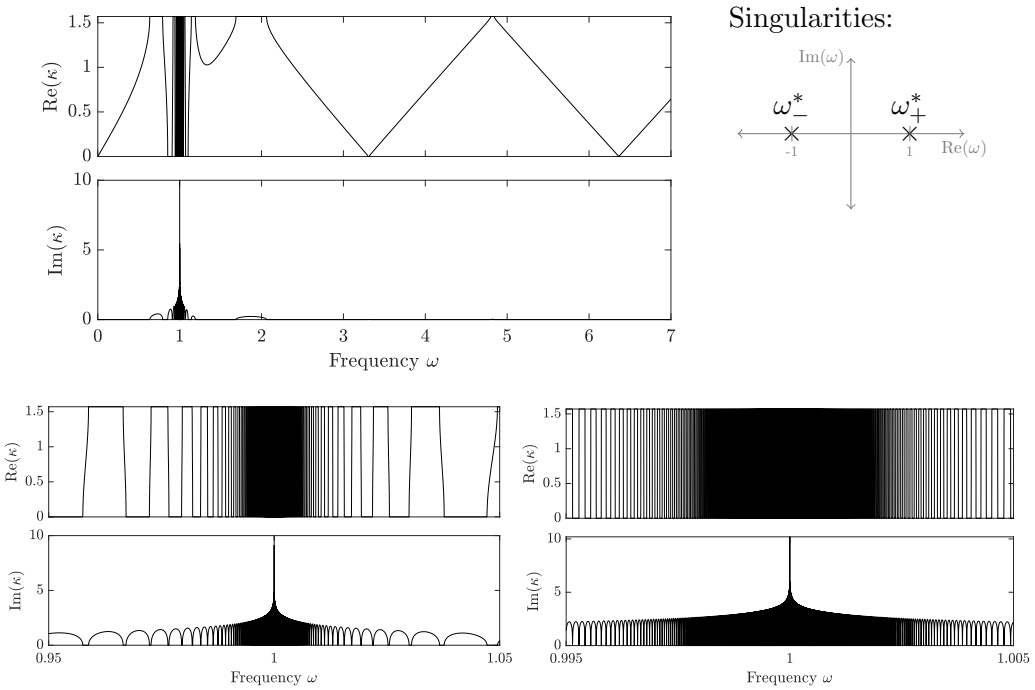

Figure 1.5.: The dispersion relation of a photonic crystal with frequency-independent material parameters. We model a material with permittivity given by (1.1) with $\alpha = 1$, $\beta = 1$ and $\gamma = 0$. The frequency ω is chosen to be real and the Bloch parameter κ allowed to take complex values. The permittivity is singular when $\omega = 1$. The lower two plots are display the same dispersion curves, zoomed into the region around the singularity.

Notation 1.3.10. *Let $x, y \in \mathbb{R}$. Then, we use $x \downarrow y$ when $x \to y$ and $x > y$. Similarly, we use $x \uparrow y$ when $x \to y$ and $x < y$.*

Then, close to a permittivity pole, the following holds.

Theorem 1.3.11. *Let ω^* denote a pole of the permittivity $\varepsilon(\omega)$ given by (1.41), i.e., $\omega^* \in \left\{\pm\frac{1}{\sqrt{\beta}}\right\}$. Then, for $\delta > 0$, the intervals $[\omega^* - \delta, \omega^*)$ and $(\omega^*, \omega^* + \delta]$ contain infinitely many disjoint sub-intervals, denoted by $\mathcal{I}_i$ and $\mathcal{J}_i$, $i = 1, 2, \ldots$, respectively, that are band gaps.*

Proof. We will first prove this result for the interval $[\omega^* - \delta, \omega)$, for $\delta > 0$. It suffices to show that there are infinitely many points $\omega_i^\dagger \in [\omega^* - \delta, \omega^*)$, $i = 1, 2, \ldots$, for $\delta > 0$ for which $f(\omega_i^\dagger) > 1$ or $f(\omega_i^\dagger) < -1$. Then, the continuity of f around these points gives us the existence of intervals of the form $\mathcal{I}_i := [\omega_i^\dagger - s, \omega_i^\dagger + s]$, for $i = 1, 2, \ldots$, for small $s > 0$, such that,

$$f(\omega) > 1 \quad \text{or} \quad f(\omega) < -1, \quad \forall\, \omega \in \mathcal{I}_i, \quad i = 1, 2, \ldots.$$

From (1.16) and (1.42), this gives

$$\cos(2\kappa) > 1 \quad \text{or} \quad \cos(2\kappa) < -1, \quad \forall\, \omega \in \mathcal{I}_i, \quad i = 1, 2, \ldots.$$

This is equivalent to the $\mathcal{I}_i$'s, $i = 1, 2, \ldots$ being band gaps, since κ becomes complex in these intervals, i.e. $|\Im(\kappa)| \neq 0$. Hence, since $|\Im(\kappa)|$ is continuous with respect to ω, we get that it has a local maximum in each of the $\mathcal{I}_i$'s, for $i = 1, 2, \ldots$.
We observe that $\lim_{\omega \uparrow \omega^*} \varepsilon(\omega) = +\infty$. Then, this implies that $\lim_{\omega \uparrow \omega^*} \rho(\omega) = +\infty$, and so, we get

$$\lim_{\omega \uparrow \omega^*} \frac{1 + \rho(\omega)^2}{2\rho(\omega)} = +\infty.$$

Also, as $\omega \uparrow \omega^*$, we have that σ_0 is constant and so, without loss of generality, we can assume that $\sin(\sigma_0) > 0$ (the same argument holds for taking $\sin(\sigma_0) < 0$). Hence, there exists $\delta_1 > 0$ such that for all $\omega \in [\omega^* - \delta_1, \omega^*)$, we have that

$$\frac{1 + \rho(\omega)^2}{2\rho(\omega)} > \frac{1}{\sin\Big(\sigma_0(\omega)\Big)} \geq 1. \tag{1.43}$$

Now, since $\lim_{\omega \uparrow \omega^*} \rho(\omega) = +\infty$, we have that

$$\lim_{\omega \uparrow \omega^*} \rho(\omega)\sigma_0(\omega) = +\infty. \tag{1.44}$$

This implies that, for all $K > 0$, there exists $\delta_2 > 0$ such that for all $\omega \in [\omega^* - \delta_2, \omega^*)$ it holds that $|\rho(\omega)\sigma_0(\omega)| > K$.
Now, let $\delta := \max\{\delta_1, \delta_2\}$ and let $I_\delta^{(-)} := [\omega^* - \delta, \omega^*)$. Then, (1.44) implies that

there exist two families of infinitely many points in $I_\delta^{(-)}$, denoted by $\{\omega_i^{(+)}\}_{i=1,\dots,\infty}$ and $\{\omega_i^{(-)}\}_{i=1,\dots,\infty}$, such that, for all $i = 1, \dots, \infty$, we have

$$\sin\left(\rho(\omega_i^{(+)})\omega_i^{(+)}\right) = 1 \quad \text{and} \quad \sin\left(\rho(\omega_i^{(-)})\omega_i^{(-)}\right) = -1. \tag{1.45}$$

We also note that this implies, for all $i = 1, \dots, \infty$, that

$$\cos\left(\rho(\omega_i^{(+)})\omega_i^{(+)}\right) = \cos\left(\rho(\omega_i^{(-)})\omega_i^{(-)}\right) = 0. \tag{1.46}$$

Thus, for all $i = 1, \dots, \infty$, we have

$$f\left(\omega_i^{(+)}\right) = -\frac{1+\rho(\omega_i^{(+)})^2}{2\rho(\omega_i^{(+)})}\sin\left(\sigma_0(\omega_i^{(+)})\right) < -1 \tag{1.47}$$

and

$$f\left(\omega_i^{(-)}\right) = \frac{1+\rho(\omega_i^{(-)})^2}{2\rho(\omega_i^{(-)})}\sin\left(\sigma_0(\omega_i^{(-)})\right) > 1. \tag{1.48}$$

In particular, without loss of generality, let us assume that $\omega_0^{(+)}$ is the smallest of the elements in both families $\{\omega_i^{(+)}\}_{i=1,\dots,\infty}$ and $\{\omega_i^{(-)}\}_{i=1,\dots,\infty}$. Then, the periodicity of $\sin(\cdot)$ shows that the elements of these families respect the following ordering:

$$\omega_0^{(+)} < \omega_0^{(-)} < \omega_1^{(+)} < \omega_1^{(-)} < \dots. \tag{1.49}$$

Now, the continuity of f around these points allows us to take $s > 0$ such that

$$f(\omega) < -1, \quad \forall\ \omega \in \left[\omega_i^{(+)} - s, \omega_i^{(+)} + s\right], \quad i = 1, 2, \dots,$$

$$f(\omega) > 1, \quad \forall\ \omega \in \left[\omega_i^{(-)} - s, \omega_i^{(-)} + s\right], \quad i = 1, 2, \dots,$$

and

$$\left[\omega_i^{(+)} - s, \omega_i^{(+)} + s\right] \bigcap \left[\omega_i^{(-)} - s, \omega_i^{(-)} + s\right] = \emptyset, \quad i = 1, 2, \dots\ .$$

Finally, the infinity of elements in the families $\{\omega_i^{(+)}\}_{i=1,\dots,\infty}$ and $\{\omega_i^{(-)}\}_{i=1,\dots,\infty}$ gives us the desired result.

We note that for the neighborhood of the form $\omega \in (\omega^*, \omega^* + \delta]$ for $\delta > 0$, the proof remains the same with the slight change of taking the limits as $\omega \downarrow \omega^*$. □

In addition to the occurrence of a countable number of band gaps close to the pole, in Figure (1.5), we observe that there is an interesting behaviour of the imaginary part $\Im(\kappa)$ of the quasiperiodicity κ as the frequency $\omega \in \mathbb{R}$ approaches a permittivity pole. In fact, we see that close to a pole, $|\Im(\kappa)|$ becomes arbitrarily big. This due to the resonance occurring here and is strongly related to the existence of infinitely many band gaps close to the pole. Actually, it is a corollary of Theorem 1.3.11.

Corollary 1.3.12. *Let $\omega \in \mathbb{R}$ and $\kappa \in \mathbb{C}$ be the associated quasiperiodicity satisfying the dispersion relation* (1.16) *and let $f(\omega)$ be the function defined in* (1.42). *Let $\omega^* \in \mathbb{R}$ denote a pole of the undamped permittivity $\varepsilon(\omega)$, given by* (1.41). *Then, for all $K > 0$, there exists $\delta > 0$, such that for all $p \in [-K, K]$, there exists $\omega_p \in [\omega^* - \delta, \omega^*)$ such that $\Im(\kappa(\omega_p)) = p$. That is, $|\Im(\kappa(\omega))|$ takes arbitrarily large values as $\omega \uparrow \omega^*$. The same result holds as $\omega \downarrow \omega^*$.*

Proof. From Theorem 1.3.11, we have that for all $K > 0$, there exists $\delta > 0$, such that, for all $\omega \in [\omega^* - \delta, \omega)$,

$$\frac{1 + \rho(\omega)^2}{2\rho(\omega)} > K.$$

We have that $\cos(\sigma_0(\omega))\cos(\rho(\omega)\sigma_0(\omega))$ remains bounded close to ω^* and because of the continuity of $\sin(\cdot)$, we can take $\sin(\sigma_0(\omega)) > 0$ in $[\omega^* - \delta, \omega)$. Then, it follows that, for all $K > 0$, in $[\omega^* - \delta, \omega)$,

$$\frac{1 + \rho(\omega)^2}{2\rho(\omega)} \sin\Big(\sigma_0(\omega)\Big) > K.$$

But, from Theorem (1.3.11), we have the existence of infinitely many points $\omega_0^{(+)} < \omega_0^{(-)} < \omega_1^{(+)} < \omega_1^{(-)} < \dots$ in $[\omega^* - \delta, \omega)$, for which, $\sin\Big(\rho(\omega)\sigma_0(\omega)\Big)$ oscillates between 1 and -1 in each of the intervals of the form $[\omega_0^{(+)}, \omega_0^{(-)}]$, $[\omega_0^{(-)}, \omega_1^{(+)}]$, $\dots$, denoted by $\mathcal{I}_i$, $i = 1, 2, \dots$. This implies that, for all $K > 0$, for all $p \in [-K, K]$, there exists $\omega_p \in \mathcal{I}_i$, for $i = 1, 2, \dots$, such that $f(\omega_p) = p$. Since this holds for all $K > 0$, it translates to f oscillating and taking all values between $+\infty$ and $-\infty$ in $[\omega^* - \delta, \omega^*)$ as we get closer to ω^*.
Now, from (1.16) and (1.42), we get that

$$\kappa = \frac{-i}{2} \ln\Big(f(\omega) \pm \sqrt{f(\omega)^2 - 1}\Big), \tag{1.50}$$

where $\ln(\cdot)$ denotes the complex logarithm. We see that

$$\Im(\kappa) = \frac{1}{2}\Re\Big(\ln\Big(f(\omega) \pm \sqrt{f(\omega)^2 - 1}\Big)\Big).$$

Although, since we are using the complex logarithm, we have that

$$\Re\Big(\ln\Big(f(\omega) \pm \sqrt{f(\omega)^2 - 1}\Big)\Big) = \ln\Big|f(\omega) \pm \sqrt{f(\omega)^2 - 1}\Big|.$$

Hence, since we have shown that in $[\omega^* - \delta, \omega^*)$, the function $f(\omega)$ oscillates between $+\infty$ and $-\infty$, we have that $\Big|f(\omega) \pm \sqrt{f(\omega)^2 - 1}\Big|$ has the same behaviour in $[\omega^* - \delta, \omega^*)$, but the oscillation takes place between 0 and $+\infty$. Finally, since $\ln(\cdot)$ is an increasing function, we obtain the desired result. Let us note that the proof is the same when we consider $\omega \downarrow \omega^*$, with the slight change that we consider neighborhoods of the form $(\omega^*, \omega^* + \delta]$.

□

1.3.3.3. Complex permittivity

We will now study the effect that introducing damping though allowing the permitivitty to be complex has on our one-dimensional system. Starting from the straightforward real-valued, non-dispersive model considered in Section 1.3.3.1, we subsequently add damping. For this, we take $\alpha \in \mathbb{C}$ and $\beta = \gamma = 0$, i.e.,

$$\varepsilon(\omega) = \varepsilon_0 + \alpha \in \mathbb{C}. \tag{1.51}$$

The dispersion curves for this setting are shown in Figure 1.6. They are plotted for α with successively larger imaginary parts, to show the effect of gradually increasing the damping. We see that the clear structure of successive bands and gaps is gradually blurred out, eventually to the point that the spectrum bears no clear relation to the original undamped spectrum.

In many ways, the spectrum we obtain in this setting appears to be similar to the actual halide perovskite particles, as plotted in Figure 1.3. Indeed, all of the results proved in subsection 1.3.2 hold, with the exception of the imaginary part decay. In fact, the converse is true, as made precise by the following result.

Lemma 1.3.13. *Let $\kappa \in \mathbb{C}$ and $\omega \in \mathbb{R}$ be a quasiperiodicity and a frequency, respectively, satisfying the dispersion relation* (1.16) *with complex-valued, non-dispersive permittivity given by* (1.51)*. Then,*

$$\lim_{\omega \to +\infty} |\Im(\kappa)| = +\infty. \tag{1.52}$$

Proof. Let us recall that κ_2, denoting the imaginary part of $\kappa \in \mathbb{C}$, is given by (1.24), where $\mathscr{L}_1$ and $\mathscr{L}_2$ are given by (1.21) and (1.22), respectively. We have that

$$\lim_{\omega \to \infty} \rho(\omega)\sigma_0(\omega) = +\infty, \tag{1.53}$$

since σ_0 is linear with respect to ω and ρ does not depend on ω in this setting. This implies

$$\lim_{\omega \to \infty} \sinh\Big(\rho(\omega)\sigma_0(\omega)\Big) = +\infty$$

and

$$\lim_{\omega \to \infty} \cosh\Big(\rho(\omega)\sigma_0(\omega)\Big) = +\infty.$$

We note that it is enough to show that

$$\lim_{\omega \to \infty} |\mathscr{L}_1| = \lim_{\omega \to \infty} |\mathscr{L}_2| = +\infty,$$

since applying this on (1.24) gives that $|\kappa_2| \to +\infty$ as $\omega \to +\infty$. Indeed, (1.21) gives that

$$\mathscr{L}_1 = C_1 \cosh(\sigma_0\rho_2) - C_2 \sinh(\sigma_0\rho_2),$$

(a) $\alpha = 1 + 0.001i$

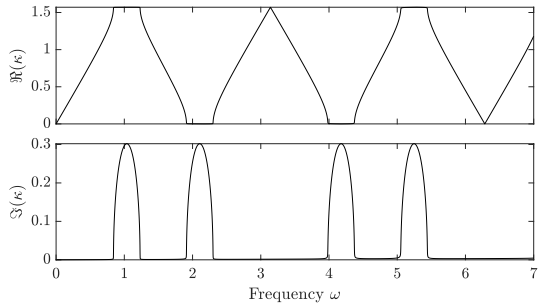

(b) $\alpha = 1 + 0.01i$

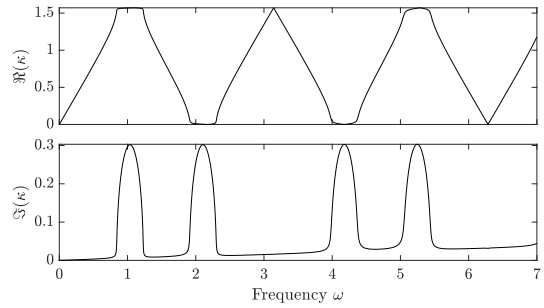

(c) $\alpha = 1 + 0.1i$

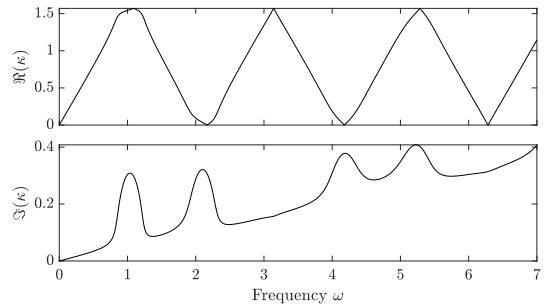

(d) $\alpha = 1 + i$

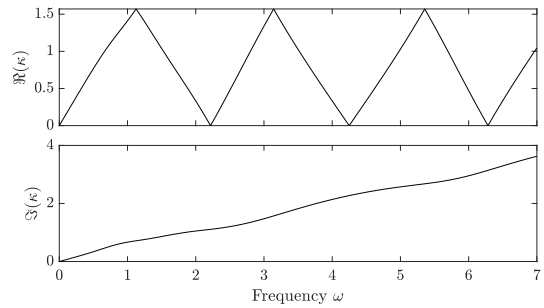

Figure 1.6.: The dispersion relation of a photonic crystal with frequency-independent complex-valued material parameters. We model a material with permittivity given by (1.1) with $\alpha \in \mathbb{C}$, $\beta = 0$ and $\gamma = 0$. The frequency ω is chosen to be real and the Bloch parameter κ allowed to take complex values. The permittivity is never singular in this case.

where

$$C_1 := \cos(\sigma_0)\cos(\sigma_0\rho_1) - \frac{\rho_1(1+\rho_1^2+\rho_2^2)}{2(\rho_1^2+\rho_2^2)}\sin(\sigma_0)\sin(\sigma_0\rho_1)$$

and

$$C_2 := \frac{\rho_2(\rho_1^2-1+\rho_2^2)}{2(\rho_1^2+\rho_2^2)}\sin(\sigma_0)\cos(\sigma_0\rho_1).$$

Using the exponential formulation of the hyperbolic trigonometric functions, we get

$$\mathscr{L}_1 = \frac{C_1-C_2}{2}e^{\sigma_0\rho_2} + \frac{C_1+C_2}{2}e^{-\sigma_0\rho_2}.$$

Now, we observe that, as $\omega \to +\infty$, C_1 and C_2 are both bounded and $C_1 - C_2 \neq 0$. Then, from (1.53), we get that

$$\lim_{\omega\to\infty} |\mathscr{L}_1| = +\infty.$$

Similarly, (1.22) gives that

$$\mathscr{L}_2 = \tilde{C}_1\sinh(\sigma_0\rho_2) - \tilde{C}_2\cosh(\sigma_0\rho_2),$$

where

$$\tilde{C}_1 := \cos(\sigma_0)\sin(\sigma_0\rho_1) + \frac{\rho_1(1+\rho_1^2+\rho_2^2)}{2(\rho_1^2+\rho_2^2)}\sin(\sigma_0)\cos(\sigma_0\rho_1)$$

and

$$\tilde{C}_2 := \frac{\rho_2(\rho_2^2-1+\rho_1^2)}{2(\rho_1^2+\rho_2^2)}\sin(\sigma_0)\sin(\sigma_0\rho_1).$$

Then, we can write

$$\mathscr{L}_2 = \frac{\tilde{C}_1+\tilde{C}_2}{2}e^{\sigma_0\rho_2} + \frac{\tilde{C}_2-\tilde{C}_1}{2}e^{-\sigma_0\rho_2}.$$

As before, we observe that, as $\omega \to +\infty$, $\tilde{C}_1$ and $\tilde{C}_2$ are both bounded and $\tilde{C}_1 - \tilde{C}_2 \neq 0$. Then, from (1.53), we get that

$$\lim_{\omega\to\infty} |\mathscr{L}_2| = +\infty.$$

This concludes the proof □

1.3.3.4. Discussion

The analysis in this section can be used to understand the dispersion diagram for the halide perovskite photonic crystal that was presented in Figure 1.3. There are two crucial observations. First, we saw in Section 1.3.3.2 that the introduction of singularities in the permittivity led to the creation of countably infinitely many band gaps in a neigbourhood of the pole, when the pole falls on the real axis. However, this exotic behaviour is not seen in Figure 1.3, due in part to the introduction of damping causing the poles to fall below the real axis. This effect can also be explained in terms of the results in Section 1.3.3.3, where we saw that the introduction of damping to a simple non-dispersive model smoothed out the band gaps. The behaviour shown in Figure 1.3 is a combination of these phenomena.

1.4. Multiple dimensions

Let us now treat the periodic structures in two- and three-dimensions. In this case, to be able to handle the problem concisely using asymptotic methods, we are interested in the case of small resonators. We will show how the results of the one-dimensional case can be generalised in multi-dimensional systems of finitely many resonators. This occurs since we expect that for sufficiently many resonators, this system converges to a periodic structure. We provide theoretical results for this setting.

1.4.1. Preliminaries

We will assume that there exists some fixed, smooth domain D, which is the union of the N disjoint subsets $D = D_1 \cup D_2 \cup \cdots \cup D_N$, such that Ω is given by

$$\Omega = \delta D + z, \tag{1.54}$$

for some position $z \in \mathbb{R}^d$, $d = 2, 3$, and characteristic size $0 < \delta \ll 1$. Then, making a change of variables, the quasiperiodic Helmholtz problem (1.8) becomes

$$\begin{cases} \Delta u^\kappa + \delta^2 \omega^2 \varepsilon(\omega) \mu_0 u^\kappa = 0 & \text{in } \mathcal{D}, \\ \Delta u^\kappa + \delta^2 k_0^2 u^\kappa = 0 & \text{in } \mathbb{R}^d \setminus \overline{D}, \\ u^\kappa|_+ - u^\kappa|_- = 0 & \text{on } \partial\mathcal{D}, \\ \frac{\partial u^\kappa}{\partial \nu}|_+ - \frac{\partial u^\kappa}{\partial \nu}|_- = 0 & \text{on } \partial\mathcal{D}, \\ u^\kappa(x_d, x_0) & \text{is } \kappa\text{-quasiperiodic in } x_d, \\ u^\kappa(x_d, x_0) & \text{satisfies the } \kappa\text{-quasiperiodic radiation condition as } |x_0| \to \infty. \end{cases} \tag{1.55}$$

We will also make an additional assumption on the dimensions of the nano-particles. This will allow us to prove an approximation for the values of the modes $u|_{D_i}$,

$i = 1, \dots, N$, on each particle. The assumption is one of *diluteness*, in the sense that the particles are small relative to the separation distances between them. To capture this, we introduce the parameter ρ_i to capture the size of the reference particles $D_1, \dots, D_N$. We define $\rho_i := \frac{1}{2}(\text{diam}(D_i))$, where $\text{diam}(D_i)$ is given by

$$\text{diam}(D_i) = \sup\{|x - y| : x, y \in D_i\}. \tag{1.56}$$

We will assume that each $\rho_i \to 0$ independently of δ. This regime means that the system is dilute in the sense that the particles are small relative to the distances between them.

We will first present certain general results for this system. Then we will give a more qualitative description of the two-dimensional setting.

1.4.2. Integral formulation

Let $G^k(x)$ be the outgoing Helmholtz Green's function in $\mathbb{R}^d$, defined as the unique solution to

$$(\Delta + k^2)G^k(x) = \delta_0(x) \quad \text{in } \mathbb{R}^d,$$

along with the outgoing radiation condition, where δ_0 is the Dirac delta. It is well known that G^k is given by

$$G^k(x) = \begin{cases} -\frac{i}{4}H_0^{(1)}(k|x|), & d = 2, \\ -\frac{e^{ik|x|}}{4\pi|x|}, & d = 3, \end{cases} \tag{1.57}$$

where $H_0^{(1)}$ is the Hankel function of first kind and order zero. We define the quasiperiodic Green's function $G^{\kappa,k}(x)$ as the Floquet transform of $G^k(x)$ in the first d_l coordinate dimensions, i.e.,

$$G^{\kappa,k}(x) = \begin{cases} -\frac{i}{4}\sum\limits_{m\in\Lambda} H_0^{(1)}(k|x-m|)e^{im\cdot\kappa}, & d = 2, \\ -\frac{1}{4\pi}\sum\limits_{m\in\Lambda} \frac{e^{ik|x-m|}}{|x-m|}e^{i\kappa\cdot m}, & d = 3. \end{cases} \tag{1.58}$$

Then, as it will be proved later in Chapter 4, we know that (1.8) has the following integral representation expression.

Theorem 1.4.1 (Lippmann-Schwinger integral representation formula)**.** *A function u^κ satisfies the differential system* (1.8) *if and only if it satisfies the following equation*

$$u^\kappa(x) - u^\kappa_{in}(x) = -\delta^2\omega^2\xi(\omega)\int_{\mathcal{D}} G^{\kappa,\delta k_0}(x-y)u(y)\mathrm{d}y, \quad x \in \mathbb{R}^d, \tag{1.59}$$

where the function $\xi : \mathbb{C} \to \mathbb{C}$ describes the permittivity contrast between $\mathcal{D}$ and the background and is given by

$$\xi(\omega) = \mu_0(\varepsilon(\omega) - \varepsilon_0).$$

1.4.3. Dispersion relation

We will now retrieve an expression which relates the subwavelength resonances of the system and the quasiperiodicities. The method used is similar to the one developed in Chapter 5 for systems of finitely many particles.

1.4.3.1. Matrix representation

Let us define the following κ-quasiperiodic integral operators

$$K_{D_i}^{\kappa,r} : u|_{D_i} \in L^2(D_i) \to -\int_{D_i} G^{\kappa,r}(x-y)u(y)\mathrm{d}y\Big|_{D_i} \in L^2(D_i) \tag{1.60}$$

and

$$R_{D_iD_j}^{\kappa,r} : u|_{D_i} \in L^2(D_i) \to -\int_{D_i} G^{\kappa,r}(x-y)u(y)\mathrm{d}y\Big|_{D_j} \in L^2(D_j). \tag{1.61}$$

Then, the scattering problem has the following matrix representation:

$$\begin{pmatrix} 1-\delta^2\omega^2\xi(\omega)K_{D_1}^{\kappa,\delta k_0} & -\delta^2\omega^2\xi(\omega)R_{D_2D_1}^{\kappa,\delta k_0} & \dots & -\delta^2\omega^2\xi(\omega)R_{D_ND_1}^{\kappa,\delta k_0} \\ -\delta^2\omega^2\xi(\omega)R_{D_1D_2}^{\kappa,\delta k_0} & 1-\delta^2\omega^2\xi(\omega)K_{D_2}^{\kappa,\delta k_0} & \dots & -\delta^2\omega^2\xi(\omega)R_{D_ND_2}^{\kappa,\delta k_0} \\ \vdots & \vdots & \ddots & \vdots \\ -\delta^2\omega^2\xi(\omega)R_{D_1D_N}^{\kappa,\delta k_0} & -\delta^2\omega^2\xi(\omega)R_{D_2D_N}^{\kappa,\delta k_0} & \dots & 1-\delta^2\omega^2\xi(\omega)K_{D_N}^{\kappa,\delta k_0} \end{pmatrix} \begin{pmatrix} u^\kappa|_{D_1} \\ u^\kappa|_{D_2} \\ \vdots \\ u^\kappa|_{D_N} \end{pmatrix} = \begin{pmatrix} u_{in}^\kappa|_{D_1} \\ u_{in}^\kappa|_{D_2} \\ \vdots \\ u_{in}^\kappa|_{D_N} \end{pmatrix}.$$

Since the scattered field is fully determined by the value within each resonator, we will introduce the notation

$$u_i^\kappa := u^\kappa|_{D_i}, \quad i = 1, \dots, N. \tag{1.62}$$

Then, the resonance problem is to find $\omega \in \mathbb{C}$, such that there exists $(u_1^\kappa, u_2^\kappa, \dots, u_N^\kappa) \in L^2(D_1) \times L^2(D_2) \times \cdots \times L^2(D_N)$, $u_i^\kappa \neq 0$, for $i = 1, \dots, N$, such that

$$\begin{pmatrix} 1-\delta^2\omega^2\xi(\omega)K_{D_1}^{\kappa,\delta k_0} & -\delta^2\omega^2\xi(\omega)R_{D_2D_1}^{\kappa,\delta k_0} & \dots & -\delta^2\omega^2\xi(\omega)R_{D_ND_1}^{\kappa,\delta k_0} \\ -\delta^2\omega^2\xi(\omega)R_{D_1D_2}^{\kappa,\delta k_0} & 1-\delta^2\omega^2\xi(\omega)K_{D_2}^{\kappa,\delta k_0} & \dots & -\delta^2\omega^2\xi(\omega)R_{D_ND_2}^{\kappa,\delta k_0} \\ \vdots & \vdots & \ddots & \vdots \\ -\delta^2\omega^2\xi(\omega)R_{D_1D_N}^{\kappa,\delta k_0} & -\delta^2\omega^2\xi(\omega)R_{D_2D_N}^{\kappa,\delta k_0} & \dots & 1-\delta^2\omega^2\xi(\omega)K_{D_N}^{\kappa,\delta k_0} \end{pmatrix} \begin{pmatrix} u_1^\kappa \\ u_2^\kappa \\ \vdots \\ u_N^\kappa \end{pmatrix} = \begin{pmatrix} 0 \\ 0 \\ \vdots \\ 0 \end{pmatrix}. \tag{1.63}$$

1.4.3.2. Resonances

Let us now retrieve the relation between the subwavelength resonant frequencies and the quasiperiodicities, obtained by studying the solutions to (1.63). We will first recall a definition and a lemma which will help in the analysis of the problem.

Definition 1.4.2. *Given $N \in \mathbb{N}$, we denote by $\lfloor N \rfloor : \mathbb{N} \to \{1, 2, \dots, N\}$ a modified version of the modulo function,* i.e.*, the remainder of euclidean division by N. In particular, for all $M \in \mathbb{N}$, there exists unique $\tau \in \mathbb{Z}_{\geq 0}$ and $r \in \mathbb{N}$ with $0 < r \leq N$, such that*

$$M = \tau \cdot N + r.$$

Then, we define $M\lfloor N \rfloor$ to be

$$M\lfloor N \rfloor := r.$$

We recall the diluteness assumption that we have made on our system, which is captured by considering small particle size ρ. We define $\rho := \frac{1}{2}\max_i(\mathrm{diam}(D_i))$ where $\mathrm{diam}(D_i)$ is given by

$$\mathrm{diam}(D_i) = \sup\{|x - y| : x, y \in D_i\}. \tag{1.64}$$

The next lemma is a variation of Lemma 5.2.7 in Chapter 5.

Lemma 1.4.3. *For all $i = 1, \dots, N$, we denote $u_i^\kappa = u^\kappa|_{D_i}$, where u^κ is a resonant mode, in the sense that it is a solution to* (1.59) *with no incoming wave. Then, for a characteristic size δ of the same order as ρ, we can write that*

$$u_i^\kappa = \langle u^\kappa, \phi_\kappa^{(i)} \rangle \phi_\kappa^{(i)} + O(\rho^2), \quad i = 1, \dots, N, \tag{1.65}$$

as $\rho \to 0$, where $\phi_\kappa^{(i)}$ denotes an eigenvector associated to the particle D_i of the potential $K_{D_i}^{\kappa,\delta k_0}$ and $\rho > 0$ denotes the particle size parameter of $D_1, \dots, D_N$. Here, δ and ρ are of the same order in the sense that $\delta = O(\rho)$ and $\rho = O(\delta)$. In this case, the error term holds uniformly for any small δ and ρ in a neighbourhood of 0.

Let us now state the main result of this section.

Theorem 1.4.4. *The resonance problem, as $\delta \to 0$ and $\rho \to 0$, with $\delta = O(\rho)$ and $\rho = O(\delta)$,* (1.63) *in dimensions $d = 2, 3$, becomes finding $\omega \in \mathbb{C}$ such that*

$$\det\Big(\mathcal{K}^\kappa(\omega)\Big) = 0,$$

where

$$\mathcal{K}^\kappa(\omega)_{ij} := \begin{cases} \langle R^{\kappa,\delta k_0}_{D_i D_{i+1\lfloor N \rfloor}} \phi_\kappa^{(i)}, \phi_\kappa^{(i+1\lfloor N \rfloor)} \rangle, & \text{if } i = j, \\ -\mathscr{A}_i^\kappa(\omega, \delta) \langle R^{\kappa,\delta k_0}_{D_j D_i} \phi_\kappa^{(j)}, \phi_\kappa^{(i)} \rangle \langle R^{\kappa,\delta k_0}_{D_i D_{i+1\lfloor N \rfloor}} \phi_\kappa^{(i)}, \phi_\kappa^{(i+1\lfloor N \rfloor)} \rangle, & \text{if } i \neq j, \end{cases} \tag{1.66}$$

Here, $k_0 = \omega\sqrt{\mu_0 \varepsilon_0}$ and

$$\mathscr{A}_i^\kappa(\omega, \delta) := \frac{\delta^2 \omega^2 \xi(\omega)}{1 - \delta^2 \omega^2 \xi(\omega) \lambda_\kappa^{(i)}}, \quad i = 1, ..., N, \tag{1.67}$$

with $\lambda_\kappa^{(i)}$ and $\phi_\kappa^{(i)}$ being an eigenvalue and the respective eigenvectors associated to the particle D_i of the potential $K_{D_i}^{\kappa,\delta k_0}$, for $i = 1, 2, \dots, N$.

Proof. We will provide an outline of the proof of this result, since it follows the exact same reasoning as, for example, the proof of Theorem 2.8 in [5]. Using the following pole pencil decomposition,

$$\left(1-\delta^2\omega^2\xi(\omega)K_{D_i}^{\kappa,\delta k_0}\right)^{-1}(\cdot)=\frac{\langle\cdot,\phi_\kappa^{(i)}\rangle\phi_\kappa^{(i)}}{1-\delta^2\omega^2\xi(\omega)\lambda_\kappa^{(i)}}+R_i[\omega](\cdot),\quad i=1,\dots,N,\quad (1.68)$$

we get that (1.63) is equivalent to the system of equations

$$u_i^\kappa-\frac{\delta^2\omega^2\xi(\omega)}{1-\delta^2\omega^2\xi(\omega)\lambda_\kappa^{(i)}}\sum_{j=1,j\neq 1}^{N}\langle R_{D_jD_i}^{\kappa,\delta k_0}u_j^\kappa,\phi_\kappa^{(i)}\rangle\phi_\kappa^{(i)}=0,\qquad \text{for each } i=1,\dots,N.$$

The above system is equivalent to

$$\langle R_{D_iD_{i+1\lfloor N\rfloor}}^{\kappa,\delta k_0}u_i^\kappa,\phi_\kappa^{(i+1\lfloor N\rfloor)}\rangle-$$
$$-\frac{\delta^2\omega^2\xi(\omega)}{1-\delta^2\omega^2\xi(\omega)\lambda_\kappa^{(i)}}\sum_{j=1,j\neq i}^{N}\langle R_{D_jD_i}^{\kappa,\delta k_0}u_j^\kappa,\phi_\kappa^{(i)}\rangle\langle R_{D_iD_{i+1\lfloor N\rfloor}}^{\kappa,\delta k_0}\phi_\kappa^{(i)},\phi_\kappa^{(i+1\lfloor N\rfloor)}\rangle=0.$$

From Lemma 1.4.3, we have

$$u_i^\kappa\simeq\langle u^\kappa,\phi_\kappa^{(i)}\rangle\phi_\kappa^{(i)},$$

which gives

$$\mathcal{K}^\kappa(\omega)\begin{pmatrix}\langle u^\kappa,\phi_\kappa^{(1)}\rangle\\ \langle u^\kappa,\phi_\kappa^{(2)}\rangle\\ \vdots\\ \langle u^\kappa,\phi_\kappa^{(N)}\rangle\end{pmatrix}=\begin{pmatrix}0\\0\\\vdots\\0\end{pmatrix},\quad (1.69)$$

where

$$\mathcal{K}^\kappa(\omega)_{ij}:=\begin{cases}\langle R_{D_iD_{i+1\lfloor N\rfloor}}^{\kappa,\delta k_0}\phi_\kappa^{(i)},\phi_\kappa^{(i+1\lfloor N\rfloor)}\rangle, & \text{if } i=j,\\ -\mathcal{A}_i^\kappa(\omega,\delta)\langle R_{D_jD_i}^{\kappa,\delta k_0}\phi_\kappa^{(j)},\phi_\kappa^{(i)}\rangle\langle R_{D_iD_{i+1\lfloor N\rfloor}}^{\kappa,\delta k_0}\phi_\kappa^{(i)},\phi_\kappa^{(i+1\lfloor N\rfloor)}\rangle, & \text{if } i\neq j.\end{cases}\quad (1.70)$$

Then, for the system to have a non-trivial solution, we require

$$\det\left(\mathcal{K}^\kappa(\omega)\right)=0,$$

which gives the desired result. □

1.4.4. The two-dimensional case

In the particular case of a two-dimensional system, it is possible to provide a more detailed and simplified version of the result in Theorem 1.4.4. In particular, we will

consider the setting where the periodic structure $\mathcal{D}$ is composed of $N \in \mathbb{N}$ resonators, denoted by $\mathcal{D}_i$, $i = 1, \dots, N$, which are repeated periodically in the lattice Λ. Let us recall that in dimension $d = 2$, the κ-quasiperiodic Green's function $G^{\kappa,r}(x)$ is given by

$$G^{\kappa,k}(x) = -\frac{i}{4} \sum_{m \in \Lambda} H_0^{(1)}\Big(k|x - m|\Big) e^{im\cdot\kappa}, \tag{1.71}$$

where $H_0^{(1)}$ denotes the Hankel function of the first kind of order zero and has the following asymptotic expansion as its argument goes to zero:

$$H_0^{(1)}(s) = \frac{2i}{\pi} \sum_{m=0}^{\infty} (-1)^m \frac{s^{2m}}{2^{2m}(m!)^2} \left(\log(\hat{\gamma} s) - \sum_{j=1}^{m} \frac{1}{j} \right). \tag{1.72}$$

1.4.4.1. Integral operators

We define the integral operators $K_{D_i}^{\kappa,(-1)} : L^2(D_i) \to L^2(D_i)$ and $K_{D_i}^{\kappa,(0)} : L^2(D_i) \to L^2(D_i)$ by

$$K_{D_i}^{\kappa,(-1)}[u](x) := -\frac{1}{2\pi} \log(\hat{\gamma}\delta k_0) \int_{D_i} \sum_{m \in \Lambda} e^{im\cdot\kappa} u(y) \mathrm{d}y \Big|_{D_i},$$

$$K_{D_i}^{\kappa,(0)}[u](x) := -\frac{1}{2\pi} \int_{D_i} \sum_{m \in \Lambda} \log\Big(|x - y - m|\Big) e^{im\cdot\kappa} u(y) \mathrm{d}y \Big|_{D_i},$$

and the integral operators $R_{D_iD_j}^{\kappa,(-1)} : L^2(D_i) \to L^2(D_j)$ and $R_{D_iD_j}^{\kappa,(0)} : L^2(D_i) \to L^2(D_j)$ by

$$R_{D_iD_j}^{\kappa,(-1)}[u](x) := -\frac{1}{2\pi} \log(\hat{\gamma}\delta k_0) \int_{D_i} \sum_{m \in \Lambda} e^{im\cdot\kappa} u(y) \mathrm{d}y \Big|_{D_j},$$

$$R_{D_iD_j}^{\kappa,(0)}[u](x) := -\frac{1}{2\pi} \int_{D_i} \sum_{m \in \Lambda} \log\Big(|x - y - m|\Big) e^{im\cdot\kappa} u(y) \mathrm{d}y \Big|_{D_j},$$

for $i = 1, \dots, N$. We will provide some results which will help us in the analysis of the problem.

Definition 1.4.5. *We define the integral operators $M_{D_i}^{\delta k_0}$ and $N_{D_iD_j}^{\delta k_0}$ for $i, j = 1, 2$ by*

$$M_{D_i}^{\delta k_0} := K_{D_i}^{\kappa,(-1)} + K_{D_i}^{\kappa,(0)} \quad \text{and} \quad N_{D_iD_j}^{\delta k_0} := R_{D_iD_j}^{\kappa,(-1)} + R_{D_iD_j}^{\kappa,(0)}. \tag{1.73}$$

From the asymptotic expansion of the Hankel function in (1.72), the following holds.

Proposition 1.4.6. *For the integral operators $K_{D_i}^{\kappa,\delta k_0}$ and $R_{D_iD_j}^{\kappa,\delta k_0}$, defined in* (1.60) *and* (1.61) *respectively, we can write*

$$K_{D_i}^{\kappa,\delta k_0} = M_{D_i}^{\kappa,\delta k_0} + O\Big(\delta^2 \log(\delta)\Big) \quad \text{and} \quad R_{D_iD_j}^{\kappa,\delta k_0} = N_{D_iD_j}^{\kappa,\delta k_0} + O\Big(\delta^2 \log(\delta)\Big), \tag{1.74}$$

as $\delta \to 0$ and with k_0 fixed.

1.4.4.2. Spectral results

We have the following spectral results for the operators $K_{D_i}^{\kappa,(-1)}$ and $K_{D_i}^{\kappa,\delta k_0}$, for $i = 1, \ldots, N$.

Lemma 1.4.7. *Let $\nu_{-1,i}^{(\kappa)}$ and $\Psi_{-1,i}^{(\kappa)}$ denote a non-zero eigenvalue and the associated eigenvector of the operator $K_{D_i}^{\kappa,(-1)}$, for $i = 1, \ldots, N$. Then,*

$$\nu_{-1,i}^{(\kappa)} = -\frac{|D_i|}{2\pi} \sum_{m \in \Lambda} e^{im\cdot\kappa} \quad \text{and} \quad \Psi_{-1,i}^{(\kappa)} = \hat{\mathbb{1}}_{D_i}, \tag{1.75}$$

for $i = 1, \ldots, N$, where $\hat{\mathbb{1}}_{D_i} := \frac{\mathbb{1}_{D_i}}{\sqrt{|D_i|}}$ and $|D_i|$ denotes the volume of D_i.

Proof. From the definition of $K_{D_i}^{\kappa,(-1)}$, for $i = 1, \ldots, N$, we observe that $K_{D_i}^{\kappa,(-1)}$ is independent of $x \in D_i$, and so, normalising on $L^2(D_i)$, we get

$$\Psi_{-1,i}^{(\kappa)} = \hat{\mathbb{1}}_{D_i}.$$

Then, the following must hold:

$$\begin{aligned} \nu_{-1,i}^{(\kappa)} \hat{\mathbb{1}}_{D_i} = K_{D_i}^{\kappa,(-1)}[\hat{\mathbb{1}}_{D_i}] \Rightarrow \nu_{-1,i}^{(\kappa)} \hat{\mathbb{1}}_{D_i} &= -\frac{|D_i|}{2\pi} \hat{\mathbb{1}}_{D_i} \sum_{m \in \Lambda} e^{im\cdot\kappa} \\ \Rightarrow \nu_{-1,i}^{(\kappa)} &= -\frac{|D_i|}{2\pi} \sum_{m \in \Lambda} e^{im\cdot\kappa}. \end{aligned}$$

This concludes the proof. □

Here, let us note that the eigenvector $\Psi_{-1,i}^{(\kappa)}$ of the operator $K_{D_i}^{\kappa,(-1)}$, for $i = 1, \ldots, N$, is unique since $K_{D_i}^{\kappa,(-1)}$ has range one.

Lemma 1.4.8. *Let $\nu_i^{(\kappa)}$ denote a non-zero eigenvalue of the operator $M_{D_i}^{\kappa,\delta k_0}$, for $i = 1, \ldots, N$, in dimension 2. Then, for small δ, it is approximately given by:*

$$\nu_i^{(\kappa)} = \log(\delta k_0 \hat{\gamma}) \nu_{-1,i}^{(\kappa)} + \langle K_{D_i}^{\kappa,(0)} \Psi_{-1,i}^{(\kappa)}, \Psi_{-1,i}^{(\kappa)} \rangle + O(\delta^2 \log(\delta)), \tag{1.76}$$

where $\nu_{-1,i}^{(\kappa)}$ and $\Psi_{-1,i}^{(\kappa)}$ denote the eigenvalue and the associated eigenvector of the potential $K_{D_i}^{\kappa,(-1)}$, for $i = 1, \ldots, N$, respectively.

Proof. This was proved in Lemma 4.2.10 of Chapter 4. □

Since we have considered identical resonators, the symmetry of the system leads to the following simple result.

Lemma 1.4.9. *Let $\nu_{-1,i}^{(\kappa)}$ denote the non-zero eigenvalue of the operator $K_{D_i}^{\kappa,(-1)}$, for $i = 1, \ldots, N$. Then, it holds that*

$$\nu_{-1,1}^{(\kappa)} = \nu_{-1,2}^{(\kappa)} = \cdots = \nu_{-1,N}^{(\kappa)} =: \nu_{-1}^{(\kappa)}.$$

1.4.4.3. Resonant frequencies

We will now state a more explicit version of Theorem 1.4.4. This is the main result of our analysis of the two-dimensional system, which fully characterises the resonant frequencies of the periodic system.

Proposition 1.4.10. *The resonance problem, as $\delta \to 0$ and $\rho \to 0$, with $\delta = O(\rho)$ and $\rho = O(\delta)$, (1.63) in dimensions $d = 2, 3$, becomes finding $\omega \in \mathbb{C}$ such that*

$$\det\left(\mathcal{K}^\kappa(\omega)\right) = 0,$$

where

$$\mathcal{K}^\kappa(\omega)_{ij} = \begin{cases} \langle N^{\kappa,\delta k_0}_{D_i D_{i+1\lfloor N\rfloor}} \hat{1}_{D_i}, \hat{1}_{D_{(i+1\lfloor N\rfloor)}} \rangle, & \text{if } i = j, \\ -\mathscr{A}_i^\kappa(\omega,\delta) \langle N^{\kappa,\delta k_0}_{D_j D_i} \hat{1}_{D_j}, \hat{1}_{D_i} \rangle \langle N^{\kappa,\delta k_0}_{D_i D_{i+1\lfloor N\rfloor}} \hat{1}_{D_i}, \hat{1}_{D_{(i+1\lfloor N\rfloor)}} \rangle, & \text{if } i \neq j. \end{cases} \tag{1.77}$$

Here, $k_0 = \omega\sqrt{\mu_0 \varepsilon_0}$ and

$$\mathscr{A}_i^\kappa(\omega,\delta) := \frac{\delta^2 \omega^2 \xi(\omega)}{1 - \delta^2 \omega^2 \xi(\omega) \nu^{(\kappa)}}, \quad i = 1, ..., N. \tag{1.78}$$

with $\nu^{(\kappa)}$ denoting a non-zero eigenvalue of the potential $M^{\kappa,\delta k_0}_{D_i}$, for $i = 1, 2, \ldots, N$.

Proof. This is a direct consequence of Theorem 1.4.4. We just have to apply (1.74) and (1.75) to (1.66) and get

$$\mathcal{K}^\kappa(\omega)_{ij} = \begin{cases} \langle N^{\kappa,\delta k_0}_{D_i D_{i+1\lfloor N\rfloor}} \hat{1}_{D_i}, \hat{1}_{D_{(i+1\lfloor N\rfloor)}} \rangle, & \text{if } i = j, \\ -\mathscr{A}_i^\kappa(\omega,\delta) \langle N^{\kappa,\delta k_0}_{D_j D_i} \hat{1}_{D_j}, \hat{1}_{D_i} \rangle \langle N^{\kappa,\delta k_0}_{D_i D_{i+1\lfloor N\rfloor}} \hat{1}_{D_i}, \hat{1}_{D_{(i+1\lfloor N\rfloor)}} \rangle, & \text{if } i \neq j, \end{cases}$$

which gives the desired result. □

1.5. Conclusion

We have used analytic methods to understand the dispersive nature of photonic crystals fabricated from metals with singular permittivities. In particular, we considered a Drude–Lorentz model inspired by halide perovskites that has poles in the lower complex plane. For a one-dimensional system, we characterised the effect that each feature of this model has on the dispersion relation. We showed that the introduction of singularities leads to the creation of countably many band gaps near the poles, whereas the introduction of damping smooths out the band gap structure. Finally, we showed how the integral methods developed in [3, 5] can be used to extend this theory to multi-dimensional systems.

2. Topological protection in the presence of dispersion

2.1. Introduction

One of the cornerstones of modern wave physics is the existence of strongly localised eigenmodes in perturbed periodic media. Strong localisation at specific frequencies is the starting point for the design of many wave guiding and control devices. The pre-eminent theory in the field of periodic waveguides is the notion of topological protection [43].

A corresponding mathematical theory for topologically protected modes has been developed. This theory first emerged in the setting of the Schrödinger equation [30, 31], but has since been extended to classical wave systems [50, 25]. Many of the seminal mathematical studies consider one-dimensional systems, since the fundamental mechanism requires an interface or edge to be introduced in just one axis of periodicity. However, multi-dimensional systems can be studied by using *e.g.* integral operators [10, 13] or a reduction to Dirac operators [32, 29, 15].

The existing mathematical theory mostly studies systems with frequency-independent material parameters. This is not only a natural toy model but gives a good description of several physical settings (*e.g.* microwaves and perfect conductors). However, many important materials are dispersive in desirable frequency ranges. This includes locally resonant systems (*e.g.* coupled Helmholtz resonators [75]) and most metals at optical frequencies. This work extends the mathematical theory of topologically protected modes to dispersive settings. The main theoretical challenge for doing so is that the spectrum of the differential operator can no longer be understood using standard linear eigenvalue theory. Instead, the spectrum is obtained through the solution of a non-linear eigenvalue problem. Further, many important dispersive materials have poles and singularities at certain frequencies [4, 67].

In this chapter, we will focus on materials whose permittivity is dispersive and real-valued (meaning there is no damping in the system). We exploit the work of [4] which characterised the Bloch spectrum as a function of the singularities of canonical dispersive permittivities. The main idea is to combine this theory with the work of [25] (and the previous works upon which it builds, *e.g.* [30, 50]), which uses the surface impedance to characterise the existence and topological protection of interface modes. This is a product of the work carried in [6].

2.2. Mathematical setting

Let us first present the mathematical setting in which we will work. We will consider materials composed of periodically repeating unit cells, within which the permittivity is allowed to vary as a function of both frequency and position. A crucial assumption will be that each unit cell is mirror symmetric. That is, the material's permittivity is described by a function $\varepsilon(x,\omega)$ which is periodic ($\varepsilon(x,\omega) = \varepsilon(x+1,\omega)$) and symmetric ($\varepsilon(x+h,\omega) = \varepsilon(x+1-h,\omega)$) in its first variable. Further, our analysis will require the assumption that $\varepsilon(x,\omega)$ is a piecewise differentiable, non-decreasing function of ω, in the sense that $\frac{\partial\varepsilon}{\partial\omega} \geq 0$ whenever the derivative exists.

We consider two dispersive materials A and B. Each one is of the form of a semi-infinite array. The arrays are glued together at $x_0 = 0$ and we assume that the material A expands towards $-\infty$ and the material B expands towards $+\infty$. In addition, we assume that each material is constructed by repeating periodically a unit cell. Each unit cell is the product of layering, i.e., it has particles of two different permittivities ε_1 and ε_2, satisfying the conditions above.

Let us denote by $D_i^{[1]}$, $i = 1, 2, \ldots, N+1$, and by $D_j^{[2]}$, $j = 1, 2, \ldots, N$, the particles of the unit cell with permittivity ε_1 and ε_2, respectively. Then, the permittivity of the system is defined as follows:

$$\varepsilon(x,\omega) = \begin{cases} \varepsilon_1(\omega), & x \in D^{[1]} := \bigcup_{i=1}^{N+1} D_i^{[1]}, \\ \varepsilon_2(\omega), & x \in D^{[2]} := \bigcup_{i=1}^{N} D_i^{[2]}. \end{cases} \tag{2.1}$$

We define the sequence $\{x_n\}_{n\in\mathbb{Z}}$ to be the set of endpoints of each one of the periodically repeated cells, i.e., $x_n = x_0 + n$ for $n \in \mathbb{Z}$. We take x_0 to be the glue point of the two materials and so for $n > 0$ we are in material B and for $n < 0$, we are in material A.

In Figure 2.1 we provide a schematic depiction of such an example of periodic cells for the materials A and B, respectively. Concerning the construction characteristics of the periodic cell, for materials A and B, we have three particles of permittivity ε_1, i.e., $D_1^{[1]}, D_2^{[1]}$ and $D_3^{[1]}$, and two particles of permittivity ε_2, i.e., $D_1^{[2]}$ and $D_2^{[2]}$. We note that our results can be generalised in settings where the number of particles in the periodic cells is greater. We also notice the geometry of each one of the periodic cells, i.e., the symmetric way in which the particles are placed in each periodic cell.

We are interested in finding eigenvalues

$$\mathcal{L}u = \omega^2 u \tag{2.2}$$

of the differential operator

$$\mathcal{L}u := -\frac{1}{\mu_0}\frac{\partial}{\partial x}\left(\frac{1}{\varepsilon(x,\omega)}\frac{\partial u}{\partial x}\right). \tag{2.3}$$

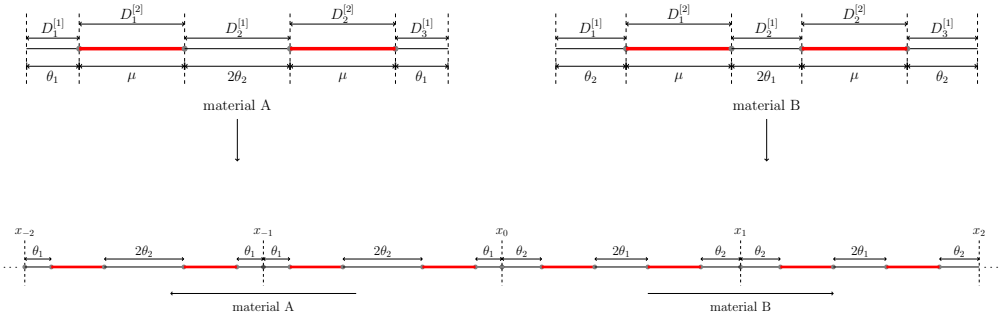

Figure 2.1.: An example of the setting studied. In the unit cell of each material we have 3 particles of permittivity ε_1 and 2 particles of permittivity ε_2. We notice the mirror symmetric way in which the particles are placed inside the periodic cells. Each material is constituted by a semi-infinite array created by periodically repeating the unit cell. Our structure is the result of gluing materials A and B at the point x_0.

In particular, the eigenmodes of interest are those which decay as $|x| \to \infty$, such that they are localised in a neighbourhood of the interface at $x_0 = 0$.

To find candidate eigenvalues ω^2 for which localised eigenmodes can occur, it is valuable to consider the Floquet-Bloch spectrum of the operators associated to materials A and B. This is the set of eigenmodes which satisfy the Floquet-Bloch quasi-periodicity conditions

$$u(x+1) = e^{i\kappa}u(x) \quad \text{and} \quad \frac{\partial u}{\partial x}(x+1) = e^{i\kappa}\frac{\partial u}{\partial x}(x), \tag{2.4}$$

for some $\kappa \in \mathcal{B} := [-\pi, \pi]$. Hence, these eigenmodes belong to the space of functions

$$H^2_\kappa := \Big\{ f \in H^2_{\text{loc}} : \ f(x+1) = e^{i\kappa} f(x), \ x \in \mathbb{R} \Big\}.$$

It follows that the localised eigenmodes that we are looking for, have to be in band gaps of the two materials. This happens because we are looking for solutions to (2.3), which decay as $|x| \to +\infty$. Thus, if the modes are in the bands, then from (2.4), we see that their magnitude is preserved. Let us also note here that we are interested in materials A and B which have overlapping band gaps, otherwise such modes cannot exist in this setting.

On its own, studying the spectrum of the operator $\mathcal{L}$ is a complicated task. This is due to the fact that there is a non-linear dependence of the operator on the eigenvalues ω^2 via $\varepsilon(x, \omega)$. In addition, the permittivity function ε may present certain aspect, e.g. poles, which make this analysis even harder. In Chapter 1, we have studied how these properties of the permittivity function affect the structure of the spectrum of the differential operator $\mathcal{L}$. In general, its spectrum will consist of countably many spectral bands. Unusual behaviour can occur near the poles of

the singularity, however, where there can be a countably infinite number of bands clustered within a finite region of the pole.

We will argue in the same way as in [25] and generalise these results to our dispersive setting. We will include proofs of most statements for completeness, although some are straighforward generalisations of [25]. Let us also note that in the case where the permittivity ε no longer depends on the frequency ω but only on x, we are in a similar setting as in [50].

2.3. Interface mode existence

The main theoretical challenge is to show that an interface mode exists for the structure composed of the two materials.

2.3.1. Impedance functions

Let us see a sufficient condition that needs to be satisfied for the interface mode to exist. We introduce the following notation.

Definition 2.3.1. *Let $f : \mathbb{R} \to \mathbb{C}$ be a continuous function and let $\alpha \in \mathbb{R}$. Then, we define*

$$f(\alpha^-) := \lim_{x \uparrow \alpha} f(x) \quad \text{and} \quad f(\alpha^+) := \lim_{x \downarrow \alpha} f(x).$$

The condition that needs to be satisfied for the interface mode to exist is continuity of both the solution and its derivative at the interface. Using the above notation, the continuity conditions that needs to be satisfied at the interface x_0 can be written as

$$u(x_0^-) = u(x_0^+) \quad \text{and} \quad \left(\frac{1}{\varepsilon_1(\omega)}\frac{\partial u}{\partial x}\right)(x_0^-) = \left(\frac{1}{\varepsilon_1(\omega)}\frac{\partial u}{\partial x}\right)(x_0^+). \tag{2.5}$$

We can now give the definition for the impedance functions.

Definition 2.3.2 (Surface impedances)**.** *We define the surface impedances of the problem* (2.2)*, as follows:*

$$Z^-(\omega) = -\frac{u(x_0^-)}{\frac{1}{\varepsilon_1(\omega)}\frac{\partial}{\partial x}u(x_0^-)} \quad \text{and} \quad Z^+(\omega) = \frac{u(x_0^+)}{\frac{1}{\varepsilon_1(\omega)}\frac{\partial}{\partial x}u(x_0^+)}, \quad \omega \in \mathbb{R}. \tag{2.6}$$

Then, the following result is a direct consequence of the continuity conditions (2.5).

Lemma 2.3.3. *Let $\mathfrak{A} \subset \mathbb{R}$. Then, a necessary and sufficient conditions for the existence of an interface localised mode u satisfying (2.2)-(2.4) for $x < x_0$ and $x > x_0$, for $\omega \in \mathfrak{A}$, is*

$$Z^+(\omega) + Z^-(\omega) = 0, \quad \omega \in \mathfrak{A}. \tag{2.7}$$

The question that arises naturally is whether a frequency $\omega \in \mathbb{R}$ exists such that this condition is satisfied and so, the global mode exists.

2.3.2. Dispersion relation

The quasiperiodic Helmholtz problem (2.2)-(2.4), for each material, is characterised by a dispersion relation. This is an expression which relates the quasiperiodicity κ with the frequency ω, such that it describes the spectral bands $\omega = \omega_n(\kappa)$. It is an equation of the form:

$$2\cos(\kappa) = f(\omega), \tag{2.8}$$

where $f : \mathbb{R} \to \mathbb{R}$ is a function that depends on the material parameters and the system's geometry. This function is variously known as the discriminant or Lyapunov function of the operator Λ [46]. Some examples are provided in *e.g.* [4, 56].

The analysis that follows stems from understanding the symmetries of the Bloch modes at the edged of the band gaps. Hence, it will be helpful to know that the maxima and minima of any band must occur at $\kappa = 0$ or $\kappa = \pm\pi$. This follows from the fact that the spectral bands are monotonic functions of κ within the reduced Brillouin zone $[0, \pi]$.

Lemma 2.3.4 (Frequency monotonicity)**.** *It holds that the frequency $\omega \in \mathbb{R}$ satisfying (2.8), as a function of the quasiperiodicity κ, is a monotonic function in the reduced Brillouin zone $[0, \pi]$.*

Proof. Indeed, we differentiate (2.8) with respect to the quasiperiodicity κ and we get

$$-2\sin(\kappa) = \frac{\partial f}{\partial \omega}\frac{\partial \omega}{\partial \kappa}.$$

We know that in $[0, \pi]$, it holds $-2\sin(\kappa) \leq 0$ with the zeros occurring in $\{0, \pi\}$. It is a direct consequence of this that $\frac{\partial \omega}{\partial \kappa}$ keeps a constant sign in $(0, \pi)$, otherwise there would exist $\kappa \in (0, \pi)$, such that $\sin(\kappa) = 0$, which is a contradiction. Also, if $\frac{\partial \omega}{\partial \kappa}(\kappa) = 0$, then $\kappa \in \{0, \pi\}$. Thus, $\omega(\kappa)$ is monotonic in the reduced Brillouin zone. This concludes the proof. □

Remark 2.3.5. *We note that the above property holds for any sufficiently smooth function $f : \mathbb{R} \to \mathbb{R}$.*

Thus, since ω is a monotonic function of κ in the reduced Brillouin zone, it follows that the edges of the spectrum are at 0 and π.

2.3.3. Mirror symmetry

Let us now focus on the geometry inside the periodic cells. The first thing we observe is the mirror symmetry which is established in the periodic cells of both materials. Indeed, we observe that for $x \in [0,1]$, we have

$$\varepsilon(x,\omega) = \varepsilon(1-x,\omega). \tag{2.9}$$

We introduce the parity operator $\mathcal{P}$, which acts on a function f as follows:

$$(\mathcal{P}f)(x) := f(1-x).$$

Using (2.3), the mirror symmetry implies

$$\mathcal{P}\mathcal{L}(-\kappa,\omega) = \mathcal{L}(\kappa,\omega)\mathcal{P}, \quad \forall \kappa \in \mathcal{B}. \tag{2.10}$$

As a direct consequence of (2.10), we have the following lemmas.

Lemma 2.3.6. *Let $\omega \in \mathbb{R}$. Then:*

- $\mathcal{L}(-\pi,\omega) = \mathcal{L}(\pi,\omega)$.
- *The differential operator $\mathcal{L}$ and the parity operator $\mathcal{P}$ commute at $\kappa \in \{0, \pm\pi\}$.*

Proof. We divide this proof in two parts, one for each result.

- We know that $\omega(-\kappa) = \omega(\kappa)$. Then, from (2.3), it follows directly that $\mathcal{L}(-\pi,\omega) = \mathcal{L}(\pi,\omega)$.
- From (2.10), we get

  $$\mathcal{P}\mathcal{L}(0,\omega) = \mathcal{L}(0,\omega)\mathcal{P}.$$

  We also get

  $$\mathcal{P}\mathcal{L}(-\pi,\omega) = \mathcal{L}(\pi,\omega)\mathcal{P}.$$

  We have shown that $\mathcal{L}(-\pi,\omega) = \mathcal{L}(\pi,\omega)$. This gives

  $$\mathcal{P}\mathcal{L}(\pi,\omega) = \mathcal{L}(\pi,\omega)\mathcal{P}$$

  and

  $$\mathcal{P}\mathcal{L}(-\pi,\omega) = \mathcal{L}(-\pi,\omega)\mathcal{P},$$

  which is the desired result.

This concludes the proof. □

In order to show the dependence of a solution u on the spatial variable x but also on both the quasiperiodicity κ and the frequency ω, we will use the notation $u^{[\kappa]}(x,\omega)$.

Lemma 2.3.7. *Let $\lambda_n(\kappa) := \omega_n^2(\kappa)$ be an eigenvalue of $\mathcal{L}(\kappa, \omega_n)$, with $u^{[\kappa]}(x, \omega_n)$ being the associated eigenvector. Then,*

- *$\mathcal{P}u^{[\kappa]}(x, \omega_n)$ is an eigenvector of $\mathcal{L}(-\kappa, \omega_n)$ with the same eigenvalue $\lambda_n(\kappa)$.*
- *$u^{[-\kappa]}(x, \omega_n)$ is also an eigenvector of $\mathcal{L}(-\kappa, \omega_n)$ with eigenvalue $\lambda_n(\kappa)$.*

Proof. We divide this proof in two parts, one for each result.

- We observe that (2.10) is symmetric in term of $\kappa \in \mathcal{B}$, in the following sense: for all $\kappa \in \mathcal{B}$, it holds that $-\kappa \in \mathcal{B}$, since we have taken $\mathcal{B} = [-\pi, \pi]$. Thus, replacing κ by $-\kappa$ in (2.10), we get

$$\mathcal{P}\mathcal{L}(\kappa, \omega) = \mathcal{L}(-\kappa, \omega)\mathcal{P}. \tag{2.11}$$

  We also know that

$$\mathcal{L}(\kappa, \omega_n)u^{[\kappa]}(x, \omega_n) = \lambda_n(\kappa)u^{[\kappa]}(x, \omega_n).$$

  Hence,

$$\begin{aligned}\mathcal{P}\mathcal{L}(\kappa, \omega_n)u^{[\kappa]}(x, \omega_n) &= \mathcal{P}\lambda_n(\kappa)u^{[\kappa]}(x, \omega_n) \\ &= \lambda_n(\kappa)\mathcal{P}u^{[\kappa]}(x, \omega_n).\end{aligned}$$

  So, from (2.11), we get

$$\mathcal{L}(-\kappa, \omega_n)\mathcal{P}u^{[\kappa]}(x, \omega_n) = \lambda_n(\kappa)\mathcal{P}u^{[\kappa]}(x, \omega_n),$$

  which gives the desired result.

- Let $\lambda_n(-\kappa)$ be an eigenvalue of $\mathcal{L}(-\kappa, \omega_n)$, with $u^{[-\kappa]}(x, \omega_n)$ being the associated eigenvector, for $\omega_n \in \mathbb{R}$ and $\kappa \in \mathcal{B}$. This implies that

$$\mathcal{L}(-\kappa, \omega_n)u^{[-\kappa]}(x, \omega_n) = \lambda_n(-\kappa)u_n^{[-\kappa]}(x, \omega_n).$$

  Although, we know that $\omega_n(-\kappa) = \omega_n(\kappa)$ and we have that $\lambda_n(\kappa) = \omega_n^2(\kappa)$. Hence, we get

$$\lambda_n(\kappa) = \lambda_n(-\kappa),$$

  which gives the desired result.

This concludes the proof. □

Lemma 2.3.8. *Let $\lambda_n(\kappa)$ be a non-degenerate eigenvalue of $\mathcal{L}(\kappa, \omega_n)$ with $u^{[\kappa]}(x, \omega_n)$ being the associated eigenvector, for κ at the band edges, i.e. $\kappa \in \{0, \pm\pi\}$. Then,*

$$u^{[\kappa]}(x, \omega_n) = \mathcal{P}u^{[\kappa]}(x, \omega_n) \quad \text{or} \quad u^{[\kappa]}(x, \omega_n) = -\mathcal{P}u^{[\kappa]}(x, \omega_n), \quad \text{for } \kappa \in \{0, \pm\pi\}.$$

Proof. Since we take $\lambda_n(\kappa)$ to be non-degenerate, there exists $\mu \in \mathbb{R}$ such that

$$u^{[-\kappa]}(x, \omega_n) = \mu \mathcal{P} u^{[\kappa]}(x, \omega_n). \tag{2.12}$$

Let us take κ to be at the band edges $\kappa \in \{0, \pm\pi\}$. We get for $\kappa = 0$

$$u^{[0]}(x, \omega_n) = \mu \mathcal{P} u^{[0]}(x, \omega_n).$$

We know that $\mathcal{P}\mathcal{P} = Id$. Thus, applying $\mathcal{P}$ on both sides, we get

$$\mathcal{P} u^{[0]}(x, \omega_n) = \mu u^{[0]}(x, \omega_n),$$

which gives

$$u^{[0]}(x, \omega_n) = \mu^2 u^{[0]}(x, \omega_n) \Rightarrow \mu^2 = 1.$$

Thus, either $\mu = 1$, in which case $\mathcal{P} u^{[0]}(x, \omega_n) = u^{[0]}(x, \omega_n)$, or $\mu = -1$, in which case $\mathcal{P} u^{[0]}(x, \omega_n) = -u^{[0]}(x, \omega_n)$.
Let us now take $\kappa = -\pi$. We have

$$u^{[\pi]}(x, \omega_n) = \mu \mathcal{P} u^{[-\pi]}(x, \omega_n).$$

Taking $\kappa = \pi$, we have

$$u^{[-\pi]}(x, \omega_n) = \mu \mathcal{P} u^{[\pi]}(x, \omega_n).$$

Combining these two expressions, we obtain

$$u^{[\pi]}(x, \omega_n) = \mu^2 \mathcal{P} u^{[\pi]}(x, \omega_n) \Rightarrow \mu^2 = 1$$

and

$$u^{[-\pi]}(x, \omega_n) = \mu^2 \mathcal{P} u^{[-\pi]}(x, \omega_n) \Rightarrow \mu^2 = 1.$$

Thus, either $\mu = 1$, in which case $\mathcal{P} u^{[\pi]}(x, \omega_n) = u^{[\pi]}(x, \omega_n)$ and $\mathcal{P} u^{[-\pi]}(x, \omega_n) = u^{[-\pi]}(x, \omega_n)$, or $\mu = -1$, in which case $\mathcal{P} u^{[\pi]}(x, \omega_n) = -u^{[\pi]}(x, \omega_n)$ and $\mathcal{P} u^{[-\pi]}(x, \omega_n) = -u^{[-\pi]}(x, \omega_n)$. This concludes the proof. □

We will call a function symmetric if $f = \mathcal{P} f$ and anti-symmetric if $f = -\mathcal{P} f$. Then, it is well known that due to the symmetry of the unit cell, combined with the periodicity or anti-periodicity that occurs when $\kappa \in \{0, \pi\}$, the modes at the edges of the bands must be either symmetric or anti-symmetric (see also [25]).

Lemma 2.3.9. *Let $\kappa \in \{0, \pi\}$ and let $\frac{\partial u}{\partial x}$ denote the spatial derivative of u. Then, either*

$$u \text{ is symmetric and } \frac{\partial u}{\partial x} \text{ is anti-symmetric,}$$

or

u is anti-symmetric and $\frac{\partial u}{\partial x}$ is symmetric.

Proof. Let us consider κ at the band edges 0 and π. Then, we know that either $u^{[\kappa]}(x,\omega_n) = \mathcal{P}u^{[\kappa]}(x,\omega_n)$ or $u^{[\kappa]}(x,\omega_n) = -\mathcal{P}u^{[\kappa]}(x,\omega_n)$. In the first case, we see that u_n is symmetric. In addition,

$$\begin{aligned} &u^{[\kappa]}(x,\omega_n) = \mathcal{P}u^{[\kappa]}(x,\omega_n) = u^{[\kappa]}(1-x,\omega_n) \Rightarrow \\ &\frac{\partial u^{[\kappa]}}{\partial x}(x,\omega_n) = -\frac{\partial u^{[\kappa]}}{\partial x}(1-x,\omega_n) = -\mathcal{P}\frac{\partial u^{[\kappa]}}{\partial x}(x,\omega_n), \end{aligned}$$

which shows that $\frac{\partial u}{\partial x}$ is anti-symmetric. Similarly, in the second case, we have that $\frac{\partial u}{\partial x}$ is anti-symmetric. Then,

$$u^{[\kappa]}(x,\omega_n) = -u^{[\kappa]}(1-x,\omega_n) \Rightarrow \frac{\partial u^{[\kappa]}}{\partial x}(x,\omega_n) = \frac{\partial u^{[\kappa]}}{\partial x}(x,\omega_n) = \mathcal{P}\frac{\partial u^{[\kappa]}}{\partial x}(x,\omega_n),$$

which shows that $\frac{\partial u}{\partial x}$ is symmetric. □

From now on, in order to ease the notation, we will suppress the dependence on the frequency ω_n, and have it indirectly at the subscripts, i.e., $u^{[\kappa]}(x,\omega_n) \equiv u_n^{[\kappa]}(x)$. A consequence of the symmetries characterised in Lemma 2.3.9 is that the modes at the edges of the spectral bands may have critical points at $x = 0$, which can be characterised based on the modes' symmetries. These symmetry arguments are similar to those in [25]. A specific proof for our setting is given in Appendix A.1.2.

Lemma 2.3.10. *Let $\kappa \in \{0,\pi\}$. Then, either*

$$u_n^{[\pi]}(0) = 0 \quad \textit{and} \quad \frac{\partial u_n^{[0]}}{\partial x}(0) = 0,$$

or

$$u_n^{[0]}(0) = 0 \quad \textit{and} \quad \frac{\partial u_n^{[\pi]}}{\partial x}(0) = 0.$$

2.3.4. Bulk index

Let us now define the notion of the bulk index. This is a topological property of the material which depends on the symmetry of the mode at the edges of a band.

Definition 2.3.11 (Bulk index)**.** *Let $\mathfrak{S} := [a,b]$ denote a band gap. Then, we define the bulk topological index $\mathcal{J}_{\mathfrak{S}}$ of the band gap $\mathfrak{S}$ as follows:*

$$\mathcal{J}_{\mathfrak{S}} := \begin{cases} +1, & \textit{if } u \textit{ is symmetric at } a, \\ -1, & \textit{if } u \textit{ is anti-symmetric at } a. \end{cases} \tag{2.13}$$

2.3.5. Frequency existence

Using the symmetry properties that we have proved, we will show that there exists $\omega \in \mathbb{R}$, such that (2.7) is satisfied.

2.3.5.1. Impedance evaluation

Let us now see what the impedance functions look like at the edges of a band gap. These edges occur for $\kappa \in \{0, \pi\}$. The dependence of the impedance functions on κ is a result of the dependence of the mode u on κ. We introduce the following notation:

$$Z_\kappa^\pm := Z^\pm \text{ at } \kappa,$$

for $\kappa \in \mathfrak{B}$. One of the main insights from the work of [25] is the dependence of the surface impedance on the symmetries of the eigenmodes (and, by definition, on the bulk index). This can be replicated in our setting with the following lemma.

Lemma 2.3.12. *It holds that either*

$$Z_0^\pm = \pm\infty \text{ and } Z_\pi^\pm = 0,$$

or

$$Z_0^\pm = 0 \text{ and } Z_\pi^\pm = \pm\infty.$$

Proof. As mentioned above, from the uniqueness of solution to (2.2), we know that, for $\kappa \in \{0, \pi\}$, we cannot have $u_n^{[\kappa]}(0) = \frac{\partial u_n^{[\kappa]}}{\partial x}(0) = 0$. Also, from Lemma 2.3.10, we have two cases for the values of u_n and $\frac{\partial u_n}{\partial x}$ at the band edges. We shall treat them separately.

In the first case, we know that

$$u_n^{[\pi]}(0) = 0 \quad \text{and} \quad \frac{\partial u_n^{[0]}}{\partial x}(0) = 0.$$

This implies that

$$\frac{\partial u_n^{[\pi]}}{\partial x}(0) \neq 0 \quad \text{and} \quad u_n^{[0]}(0) \neq 0.$$

Hence, combining these results at $\kappa = 0$, we get

$$\lim_{x \uparrow 0} Z_0^-(\omega) = \lim_{x \uparrow 0} -\frac{u^{[0]}(x, \omega)}{\frac{1}{\varepsilon_1(\omega)} \frac{\partial u^{[0]}}{\partial x}(x, \omega)} = \pm\infty$$

and

$$\lim_{x\downarrow 0} Z_0^+(\omega) = \lim_{x\downarrow 0} -\frac{u^{[0]}(x,\omega)}{\frac{1}{\varepsilon_1(\omega)}\frac{\partial u^{[0]}}{\partial x}(x,\omega)} = \pm\infty.$$

At $\kappa = \pi$, we see that

$$\lim_{x\uparrow 0} Z_\pi^-(\omega) = \lim_{x\uparrow 0} -\frac{u^{[\pi]}(x,\omega)}{\frac{1}{\varepsilon_1(\omega)}\frac{\partial u^{[\pi]}}{\partial x}(x,\omega)} = 0$$

and

$$\lim_{x\uparrow 0} Z_\pi^+(\omega) = \lim_{x\uparrow 0} -\frac{u^{[\pi]}(x,\omega)}{\frac{1}{\varepsilon_1(\omega)}\frac{\partial u^{[\pi]}}{\partial x}(x,\omega)} = 0.$$

For the second case, we know that

$$u_n^{[0]}(0) = 0 \quad \text{and} \quad \frac{\partial u_n^{[\pi]}}{\partial x}(0) = 0,$$

which implies that

$$\frac{\partial u_n^{[0]}}{\partial x}(0) \neq 0 \quad \text{and} \quad u_n^{[\pi]}(0) \neq 0.$$

Using the same reasoning as in the previous case, we get at $\kappa = 0$,

$$\lim_{x\uparrow 0} Z_0^-(\omega) = \lim_{x\uparrow 0} -\frac{u^{[0]}(x,\omega)}{\frac{1}{\varepsilon_1(\omega)}\frac{\partial u^{[0]}}{\partial x}(x,\omega)} = 0$$

and

$$\lim_{x\downarrow 0} Z_0^+(\omega) = \lim_{x\downarrow 0} -\frac{u^{[0]}(x,\omega)}{\frac{1}{\varepsilon_1(\omega)}\frac{\partial u^{[0]}}{\partial x}(x,\omega)} = 0.$$

Similarly, at $\kappa = \pi$, we get

$$\lim_{x\uparrow 0} Z_\pi^-(\omega) = \lim_{x\uparrow 0} -\frac{u^{[\pi]}(x,\omega)}{\frac{1}{\varepsilon_1(\omega)}\frac{\partial u^{[\pi]}}{\partial x}(x,\omega)} = \pm\infty$$

and

$$\lim_{x\uparrow 0} Z_\pi^+(\omega) = \lim_{x\uparrow 0} -\frac{u^{[\pi]}(x,\omega)}{\frac{1}{\varepsilon_1(\omega)}\frac{\partial u^{[\pi]}}{\partial x}(x,\omega)} = \pm\infty.$$

This concludes the proof. □

2.3.5.2. Impedance property

In order to ease the notation, let us define:

$$E(x,\omega) := \frac{1}{\varepsilon(x,\omega)} \quad \text{and} \quad \phi := \frac{\partial u}{\partial \omega}. \tag{2.14}$$

The following result is due to the work of [25], which says that the surface impedance functions are strictly decreasing functions of ω, within each band gap. For dispersive systems, this rests on the aforementioned assumption that ε is a non-decreasing function of ω. A proof of this result, specific to our setting, is given in Appendix A.1.1.

Theorem 2.3.13. *Let us assume that $\omega \in \mathfrak{A}$, where $\mathfrak{A} \subset \mathbb{R}$ is a band gap. Then, the surface impedance decreases with respect to the frequency, i.e.,*

$$\frac{\mathrm{d}Z^+}{\mathrm{d}\omega} < 0, \quad \frac{\mathrm{d}Z^-}{\mathrm{d}\omega} < 0, \qquad \textit{for } \omega \in \mathfrak{A}.$$

2.3.5.3. Interface mode existence

Let $\mathcal{L}_A$ and $\mathcal{L}_B$ denote the differential operator $\mathcal{L}$ for the material A and the material B, respectively. We define $\mathfrak{A}_A$ and $\mathfrak{A}_B$ to be two band gaps of $\mathcal{L}_A$ and $\mathcal{L}_B$, respectively. Let them be given by

$$\mathfrak{A}_A := [\omega_A^+, \omega_A^-] \quad \text{and} \quad \mathfrak{A}_B := [\omega_B^+, \omega_B^-].$$

Let us denote by $\mathfrak{A}$ the intersection of $\mathfrak{A}_A$ and $\mathfrak{A}_B$. We assume that it is non-empty, i.e.,

$$\mathfrak{A}_n = \mathfrak{A}_A \cap \mathfrak{A}_B \neq \emptyset.$$

This fact is directly related to the structure of the system, i.e., considering materials A and B whose repeatedly periodic unit cell has the same amount of particles. We denote it by

$$\mathfrak{A} := [\omega^+, \omega^-].$$

Finally, let us denote by $\mathcal{J}_A$ and $\mathcal{J}_B$ the bulk topological indices associated to the material A and the material B, respectively, in $\mathfrak{A}$.

Theorem 2.3.14. *If*

$$\mathcal{J}_A + \mathcal{J}_B \neq 0,$$

then no interface mode exists. If

$$\mathcal{J}_A + \mathcal{J}_B = 0,$$

then there exists a unique frequency $\omega_m \in \mathfrak{A}$, for which an interface mode exists.

Proof. We will divide the proof in two steps, one for each case.

Let us consider:

$$\mathcal{J}_A + \mathcal{J}_B \neq 0.$$

We will treat the case $\kappa = 0$. The same argument holds for $\kappa = \pi$. From (2.13), this implies that either u_A^+, u_B^+ are both symmetric or both anti-symmetric. Let us treat the case of both being symmetric. The anti-symmetric case follows the same reasoning. From Theorem 2.3.13, we have that Z^- is decreasing in $\mathfrak{A}$. Then, from Lemma 2.3.12, we have

$$Z_0^-(\omega_A^+) = +\infty \searrow Z_0^-(\omega_A^-) = 0 \ \text{ in } \mathfrak{A}_A.$$

Similarly, we get

$$Z_0^+(\omega_B^+) = +\infty \searrow Z_0^+(\omega_B^-) = 0 \ \text{ in } \mathfrak{A}_B.$$

We see directly that Lemma 2.3.3 does not hold, and hence, no interface mode exists.

Let us consider:

$$\mathcal{J}_A + \mathcal{J}_B = 0.$$

We will treat the case $\kappa = 0$. The same argument holds for $\kappa = \pi$. From (2.13), this implies that either u_A^+ is symmetric and u_B^+ is anti-symmetric, or u_A^+ is anti-symmetric and u_B^+ is symmetric. Let us focus on the first possibility. For the second one, the same argument will hold. So, we take

$$u_A^+ \text{ symmetric and } u_B^+ \text{ anti-symmetric at } \kappa = 0.$$

Then, from Lemma 2.3.12 and Theorem 2.3.13, we see that

$$Z_0^-(\omega_A^+) = +\infty \searrow Z_0^-(\omega_A^-) = 0 \ \text{ in } \mathfrak{A}_A.$$

Using the fact that u_B^+ is anti-symmetric, we get, from Lemma 2.3.12 and Theorem 2.3.13, that

$$Z_0^+(\omega_B^+) = 0 \searrow Z_0^+(\omega_B^-) = -\infty \ \text{ in } \mathfrak{A}_B.$$

Let us now study how $Z_0 := Z_0^- + Z_0^+$ behaves in $\mathfrak{A}$. Since $\mathfrak{A} \neq \emptyset$, we observe that

$$\min \mathfrak{A} \in \left\{\omega_A^+, \omega_B^+\right\}.$$

If $\min \mathfrak{A} = \omega_A^+$, then we see that

$$Z_0\left(\omega_A^+\right) = +\infty,$$

since $Z_0^-\left(\omega_A^+\right) = +\infty$ and $Z_0^+\left(\omega_A^+\right) \in \mathbb{R}_{<0}$. Also, if $\min \mathfrak{A} = \omega_B^+$, then we see that

$$Z_0\Big(\omega_B^+\Big) > 0,$$

since $Z_0^-\left(\omega_B^+\right) \in \mathbb{R}_{>0}$ and $Z_0^+\left(\omega_B^+\right) = 0$. Thus, in any case, we get that

$$Z_0\Big(\min \mathfrak{A}\Big) > 0.$$

Similarly, we have that

$$\max \mathfrak{A} \in \Big\{\omega_A^-, \omega_B^-\Big\}.$$

Then, if $\max \mathfrak{A} = \omega_A^-$, we see that

$$Z_0\Big(\omega_A^-\Big) < 0,$$

since $Z_0^-\left(\omega_A^-\right) = 0$ and $Z_0^+\left(\omega_A^-\right) \in \mathbb{R}_{<0}$. Also, if $\max \mathfrak{A} = \omega_B^-$, we have that

$$Z_0\Big(\omega_A^-\Big) = -\infty,$$

since $Z_0^-\left(\omega_A^-\right) \in \mathbb{R}_{>0}$ and $Z_0^+\left(\omega_A^-\right) = -\infty$. Hence, in any case, we observe that

$$Z_0\Big(\max \mathfrak{A}\Big) < 0.$$

To sum up these results, we have that

$$Z_0\Big(\min \mathfrak{A}\Big) > 0 \quad \text{and} \quad Z_0\Big(\max \mathfrak{A}\Big) < 0.$$

Then, from Theorem 2.3.13, we deduce that

$$\frac{\mathrm{d}Z_0}{\mathrm{d}\omega} < 0 \ \text{ in } \mathfrak{A}. \tag{2.15}$$

So, since Z_0 is continuous and strictly decreasing in $\mathfrak{A}$, there exists a unique point $\omega_m \in \mathfrak{A}$ at which $Z_0(\omega_m) = 0$. Therefore, a unique interface mode exists. This concludes the proof. □

Remark 2.3.15. *Here, let us recall that we have considered piecewise constant permittivities with respect to x but still dispersive with respect to ω. Although, as mentioned in Section 2.2, the analysis still applies on permittivity functions which respect the mirror symmetry in each periodic cell and the results remain the same.*

2.4. Zak phase

Let us now study the Zak phase, an invariant associated to one-dimensional crystals. This describes the topological properties of our system.

As mentioned at the beginning, we work in the space L^2_κ. We equip L^2_κ, with the following inner product:

$$\langle f, g\rangle_{\cdot} = \int_0^1 \mu_0 f(x)\overline{g}(x)\mathrm{d}x, \quad f, g \in L^2_\kappa. \tag{2.16}$$

Definition 2.4.1 (Berry connection). *We define the Berry connection $A_n(\kappa)$ of the n-th band to be*

$$A_n(\kappa) := -i\left\langle \frac{\partial u_n^{[\kappa]}}{\partial \kappa}, u_n^{[\kappa]} \right\rangle. \tag{2.17}$$

Definition 2.4.2 (Zak phase). *We define the Zak phase Θ_n of the n-th gap to be the integral of the Berry connection $A_n(\kappa)$ across the first Brillouin zone, i.e.,*

$$\Theta_n = \int_{-\pi}^{\pi} A_n(\kappa)\mathrm{d}\kappa. \tag{2.18}$$

To see that the Zak phase is well defined, we want to check that it is invariant $\mathrm{mod}(2\pi)$ with respect to phase changes of the eigenmode $u_n^{[\kappa]}$. This is because a normalised eigenmode (with $\|u_n^{[\kappa]}\| = 1$) can always be re-defined by changing the phase by an integer multiple of κ,

$$\tilde{u}_n^{[\kappa]} = e^{i\zeta\kappa}u_n^{[\kappa]},\ \zeta \in \mathbb{N}.$$

Under this transformation, we can calculate that

$$\begin{aligned}
\tilde{A}_n(\kappa) &= -i\left\langle \frac{\partial \tilde{u}_n^{[\kappa]}}{\partial x}, \tilde{u}_n^{[\kappa]} \right\rangle = -i\left\langle \frac{\partial}{\partial x}\left(e^{i\zeta\kappa}u_n^{[\kappa]}\right), e^{i\zeta\kappa}u_n^{[\kappa]} \right\rangle \\
&= -i\int_0^1 \mu_0 \left(e^{i\zeta\kappa}\frac{\partial u_n^{[\kappa]}}{\partial x}(x) + i\zeta e^{i\zeta\kappa}u_n^{[\kappa]}(x)\right)\overline{e^{i\zeta\kappa}u_n^{[\kappa]}(x)}\mathrm{d}x \\
&= A_n(\kappa) + \int_0^1 \mu_0 \zeta u_n^{[\kappa]}(x)\overline{u_n^{[\kappa]}(x)}\mathrm{d}x \\
&= A_n(\kappa) + \zeta.
\end{aligned}$$

Thus,

$$\int_{-\pi}^{\pi} \tilde{A}_n(\kappa)\mathrm{d}\kappa = \int_{-\pi}^{\pi} A_n(\kappa)\mathrm{d}\kappa + 2\zeta\pi,$$

which gives

$$\tilde{\Theta}_n(\kappa) = \Theta_n(\kappa) + 2\zeta\pi, \tag{2.19}$$

so $\tilde{\Theta}_n$ and Θ_n are equal $\mathrm{mod}(2\pi)$.

Theorem 2.4.3. *Let us assume that we have mirror symmetry and that the n-th eigenvalue of the operator $\mathcal{L}$ is non-degenerate. Then, it holds that $\Theta_n \mathrm{mod}(2\pi) \in \{0, \pi\}$.*

Proof. We recall that, for the assumptions for the theorem, $u_n^{[-\kappa]}$ and $\mathcal{P}u_n^{[\kappa]}$ are proportional to one another, i.e., there exists $\mu \in \mathbb{R}$, depending on κ, such that

$$u_n^{[-\kappa]} = \mu(\kappa)\mathcal{P}u_n^{[\kappa]}.$$

In addition, we have taken the modes to satisfy $\|u_n\| = 1$. Hence, we get $\|\mu(\kappa)\| = 1$ and so, we can write

$$u_n^{[-\kappa]} = e^{i\delta(\kappa)}\mathcal{P}u_n^{[\kappa]},$$

where $\delta(\kappa)$ is a locally smooth function of κ. Then, we see that

$$\frac{\partial}{\partial\kappa}u_n^{[-\kappa]} = \frac{\partial}{\partial\kappa}\left(e^{i\delta(\kappa)}\mathcal{P}u_n^{[\kappa]}\right) \Rightarrow \frac{\partial}{\partial\kappa}u_n^{[-\kappa]} = ie^{i\delta(\kappa)}\frac{\partial\delta}{\partial\kappa}\mathcal{P}u_n^{[\kappa]} + \frac{\partial\mathcal{P}u_n^{[\kappa]}}{\partial\kappa}e^{i\delta(\kappa)}.$$

Taking the inner product with $u_n^{[-\kappa]}$ on both sides, we see that

$$\begin{aligned}
\int_0^1 \mu_0 e^{i\delta(\kappa)}\frac{\partial\mathcal{P}u_n^{[\kappa]}}{\partial\kappa}(x)\overline{u_n^{[-\kappa]}}(x)\mathrm{d}x &= \int_0^1 \mu_0 e^{i\delta(\kappa)}\frac{\partial\mathcal{P}u_n^{[\kappa]}}{\partial\kappa}(x)\overline{e^{i\delta(\kappa)}\mathcal{P}u_n^{[\kappa]}}(x)\mathrm{d}x \\
&= \int_0^1 \mu_0\frac{\partial u_n^{[\kappa]}}{\partial\kappa}(1-x)\overline{u_n^{[\kappa]}}(1-x)\mathrm{d}x \\
&= -\int_1^0 \mu_0\frac{\partial u_n^{[\kappa]}}{\partial\kappa}(x)\overline{u_n^{[\kappa]}}(x)\mathrm{d}x \\
&= -iA_n(\kappa)
\end{aligned}$$

and

$$\begin{aligned}
\int_0^1 \mu_0 e^{i\delta(\kappa)}\frac{\partial\delta}{\partial\kappa}\mathcal{P}u_n^{[\kappa]}(x)\overline{u_n^{[-\kappa]}}(x)\mathrm{d}x &= \frac{\partial\delta}{\partial\kappa}\int_0^1 \mu_0 u_n^{[-\kappa]}(x)\overline{u_n^{[-\kappa]}}(x)\mathrm{d}x \\
&= i\frac{\partial\delta}{\partial\kappa}.
\end{aligned}$$

Thus, we get

$$iA_n(-\kappa) = -iA_n(\kappa) + i\frac{\partial\delta}{\partial\kappa}.$$

Multiplying by i and integrating over $[0, \pi]$, we get

$$-\int_0^\pi A_n(-\kappa)\mathrm{d}\kappa = \int_0^\pi A_n(\kappa)\mathrm{d}\kappa - \delta(\pi) + \delta(0),$$

which is

$$-\int_{-\pi}^0 A_n(\kappa)\mathrm{d}\kappa = \int_0^\pi A_n(\kappa)\mathrm{d}\kappa - \delta(\pi) + \delta(0).$$

Thus, we get

$$\Theta_n = \delta(\pi) - \delta(0).$$

From Lemma 2.3.8, we have that $\mu(\kappa) \in \{\pm, 1\}$, for $\kappa = 0, \pi$. This implies that $\delta(\kappa)\text{mod}(2\pi) \in \{0, \pi\}$, for $\kappa = 0, \pi$. If $\delta(\pi)\text{mod}(2\pi) = \delta(0)\text{mod}(2\pi)$, then $\Theta_n = 0$. If $\delta(\pi)\text{mod}(2\pi) \neq \delta(0)\text{mod}(2\pi)$, then the phase difference is always π. Thus, we get

$$\Theta_n \text{mod}(2\pi) \in \{0, \pi\}.$$

This concludes the proof. □

2.5. Asymptotic behaviour

We wish to study the asymptotic behaviour of the modes as $x \to \pm\infty$. For this, we will make use of the transfer matrix associated to this problem.

In the sections to follow, we will consider permittivity functions $\varepsilon(x, \omega)$ which are piecewise constant with respect to x in each particle. This method still applies for permittivities which are mirror symmetric with respect to x, but by suppressing this dependence, we obtain explicit expressions for the transfer matrices, and so, we have a more qualitative result.

2.5.1. Transfer matrix method

The transfer matrix method is a way of describing the mode u and its spatial derivative u' at each point on the structure with respect to the initial data vector $\left(u(0), \frac{\partial u}{\partial x}(0)\right)^\top$.

We define the segment matrices $\mathscr{T}(x, \omega)$ by

$$\mathscr{T}(l_x, \omega) := \begin{pmatrix} \cos(\sqrt{\mu_0\varepsilon(x,\omega)}\omega l_x) & \frac{\sin(\sqrt{\mu_0\varepsilon(x,\omega)}\omega l_x)}{\sqrt{\mu_0\varepsilon(x,\omega)}\omega} \\ -\sqrt{\mu_0\varepsilon(x,\omega)}\omega \sin(\sqrt{\mu_0\varepsilon(x,\omega)}\omega l_x) & \cos(\sqrt{\mu_0\varepsilon(x,\omega)}\omega l_x) \end{pmatrix}, \quad (2.20)$$

where l_x denotes the length of the part of the segment on which x lies.

Let us consider an interval I which is constituted by N segments of length l_i each, $i = 1, \ldots, N$. Then, we define the transfer matrix $T_I(\omega)$ over the interval I to be

$$T_I(\omega) := \prod_{i=1}^{N} \mathscr{T}(l_i, \omega). \quad (2.21)$$

If we define the vector $\tilde{u}(x) := \left(u(x), \frac{\partial u}{\partial x}(x)\right)^\top$, then the transfer matrix method describes the mode u at each point x based on the initial data at a point x_0, i.e.,

$$\tilde{u}(x) = T_{[x_0,x]}(\omega)\tilde{u}(x_0). \quad (2.22)$$

It is clear that the segment matrices $\mathscr{T}$ satisfy $\det(\mathscr{T}(x,\omega)) = 1$ for any x and ω. Hence, also, the transfer matrix T satisfies $\det(T(x,\omega)) \equiv 1$.

The mirror symmetry induced to the system gives

$$\varepsilon(x_n + h, \omega) = \varepsilon(x_{n+1} - h, \omega), \quad h \in [0,1), \ n \in \mathbb{N} \setminus \{0\}.$$

Let $T_p^{[j]}$ denote the transfer matrix over one periodic cell of the material j, with $j \in \{A, B\}$. Then, it holds, as in [26, 60], that

$$\begin{pmatrix} u(x_{n+1}) \\ \frac{\partial u}{\partial x}(x_{n+1}) \end{pmatrix} = \mathbb{1}_{\{n\geq 0\}} T_p^{[B]} \begin{pmatrix} u(x_n) \\ \frac{\partial u}{\partial x}(x_n) \end{pmatrix} + \mathbb{1}_{\{n<0\}} T_p^{[A]} \begin{pmatrix} u(x_n) \\ \frac{\partial u}{\partial x}(x_n) \end{pmatrix}, \tag{2.23}$$

for $n \in \mathbb{Z}$. Also, the symmetry of the system gives

$$\begin{pmatrix} u(x_{n-1}) \\ \frac{\partial u}{\partial x}(x_{n-1}) \end{pmatrix} = \mathbb{1}_{\{n\geq 0\}} S T_p^{[B]} S \begin{pmatrix} u(x_n) \\ \frac{\partial u}{\partial x}(x_n) \end{pmatrix} + \mathbb{1}_{\{n<0\}} S T_p^{[A]} S \begin{pmatrix} u(x_n) \\ \frac{\partial u}{\partial x}(x_n) \end{pmatrix}, \tag{2.24}$$

for $n \in \mathbb{Z}$, where the matrix S is given by

$$S := \begin{pmatrix} 1 & 0 \\ 0 & -1 \end{pmatrix}.$$

Here, let us note that with a direct calculation, we can see that $S = S^{-1}$.
Applying the quasiperiodic boundary conditions, we get, for each material i,

$$\tilde{u}(x_{n+1}) = e^{i\kappa} \tilde{u}(x_n).$$

Combining this with (2.23), we get the following problem

$$\left(T_p^{[j]}(\omega) - e^{i\kappa} I\right) \tilde{u}(x_n) = 0. \tag{2.25}$$

2.5.1.1. Spectral properties

Let us now state certain spectral properties of the transfer matrices.

Lemma 2.5.1. *Let $\omega \in \mathbb{R} \setminus \{\omega_p^{(\pm)}\}$. Then, $T_p^{[j]}$ has real eigenvalues denoted by $\lambda_1^{[j]}$ and $\lambda_2^{[j]}$, satisfying $|\lambda_1^{[j]}| < 1$ and $|\lambda_2^{[j]}| > 1$, for $j \in \{A, B\}$.*

Proof. Let $i \in \{A, B\}$. Since $\det(T_p^{[j]}(\omega)) = 1$, we get either

$$\lambda_1^{[j]}, \lambda_2^{[j]} \in \mathbb{R}, \quad \text{with} \quad |\lambda_1^{[j]}| < 1 \quad \text{and} \quad |\lambda_2^{[j]}| > 1,$$

or

$$\lambda_1^{[j]}, \lambda_2^{[j]} \in \mathbb{C}, \quad \text{with} \quad |\lambda_1^{[j]}| = |\lambda_2^{[j]}| = 1 \quad \text{and} \quad \lambda_1^{[j]} = \overline{\lambda_2^{[j]}}.$$

If the second case holds, then there exists κ such that $\lambda_1^{[j]} = e^{i\kappa}$, which implies that $\det\left(T_p^{[j]}(\omega) - e^{i\kappa} I\right) = 0$ and hence gives a contradiction. Thus, the first case holds, and so, we obtain the desired result. □

We use this result to obtain information about the asymptotic behaviour of the modes $u(x_n)$ as $n \to \pm\infty$.

Theorem 2.5.2. *The eigenfrequency ω of a localised eigenmode of the Helmholtz problem* (2.2) *must satisfy*

$$\begin{pmatrix} -V_{21}^{[B]}(\omega) & V_{11}^{[B]}(\omega) \end{pmatrix} \begin{pmatrix} V_{11}^{[A]}(\omega) \\ -V_{21}^{[A]}(\omega) \end{pmatrix} = 0, \tag{2.26}$$

where $(V_{11}^{[A]}(\omega), V_{21}^{[A]}(\omega))^\top$ is the eigenvector of the transfer matrix $T_p^{[A]}$ associated to the eigenvalue $|\lambda_1^{[A]}| < 1$ and $(V_{11}^{[B]}(\omega), V_{21}^{[B]}(\omega))^\top$ is the eigenvector of the transfer matrix $T_p^{[B]}$ associated to the eigenvalue $|\lambda_1^{[B]}| < 1$.

Proof. For $n \in \mathbb{N}_{>0}$, we have

$$\begin{aligned} \begin{pmatrix} u(x_n) \\ \frac{\partial u}{\partial x}(x_n) \end{pmatrix} &= (T_p^{[B]})^n(\omega) \begin{pmatrix} u(x_0) \\ \frac{\partial u}{\partial x}(x_0) \end{pmatrix} \\ &= V^{[B]} \begin{pmatrix} (\lambda_1^{[B]})^n & 0 \\ 0 & (\lambda_2^{[B]})^n \end{pmatrix} (V^{[B]})^{-1} \begin{pmatrix} u(x_0) \\ \frac{\partial u}{\partial x}(x_0) \end{pmatrix}, \end{aligned} \tag{2.27}$$

and for $n \in \mathbb{N}_{<0}$, from the symmetry condition (2.24), we have

$$\begin{pmatrix} u(x_n) \\ \frac{\partial u}{\partial x}(x_n) \end{pmatrix} = S T_p^{[A]} S \begin{pmatrix} u(x_{n+1}) \\ \frac{\partial u}{\partial x}(x_{n+1}) \end{pmatrix} \tag{2.28}$$

$$= S (T_p^{[A]})^{|n|} S \begin{pmatrix} u(x_0) \\ \frac{\partial u}{\partial x}(x_0) \end{pmatrix} \tag{2.29}$$

$$= S V^{[A]} \begin{pmatrix} (\lambda_1^{[A]})^n & 0 \\ 0 & (\lambda_1^{[A]})^n \end{pmatrix} (V^{[A]})^{-1} S \begin{pmatrix} u(x_0) \\ \frac{\partial u}{\partial x}(x_0) \end{pmatrix}, \tag{2.30}$$

where $\lambda_1^{[A]}, \lambda_2^{[A]}$, resp. $\lambda_1^{[B]}, \lambda_2^{[B]}$, are the eigenvalues of $T_p^{[A]}$, resp. $T_p^{[B]}$, with $|\lambda_1^{[A]}| < 1$ and $|\lambda_2^{[A]}| > 1$, resp. $|\lambda_1^{[B]}| < 1$ and $|\lambda_2^{[B]}| > 1$, and $V^{[A]}$, resp. $V^{[B]}$, is the matrix of the associated eigenvectors. We are looking for localised eigenmodes satisfying

$$\lim_{n \to \pm\infty} u(x_n) = 0 \quad \text{and} \quad \lim_{n \to \pm\infty} \frac{\partial u}{\partial x}(x_n) = 0.$$

We know that

$$\lim_{n \to \pm\infty} (\lambda_1^{[A]})^{|n|} = \lim_{n \to \pm\infty} (\lambda_1^{[B]})^{|n|} = 0$$

and

$$\lim_{n \to \pm\infty} (\lambda_2^{[A]})^{|n|} = \lim_{n \to \pm\infty} (\lambda_2^{[B]})^{|n|} \neq 0.$$

Thus, we wish to find $\omega, u(x_0)$ and $\frac{\partial u}{\partial x}(x_0)$ such that

$$\begin{pmatrix} -V_{21}^{[B]} & V_{11}^{[B]} \end{pmatrix} \begin{pmatrix} u(x_0) \\ \frac{\partial u}{\partial x}(x_0) \end{pmatrix} = 0 \quad \text{and} \quad \begin{pmatrix} -V_{21}^{[A]} & V_{11}^{[A]} \end{pmatrix} S \begin{pmatrix} u(x_0) \\ \frac{\partial u}{\partial x}(x_0) \end{pmatrix} = 0, \quad (2.31)$$

since $(V^{[j]})^{-1} = \frac{1}{\det(V)} \begin{pmatrix} V_{22}^{[j]} & -V_{12}^{[j]} \\ -V_{21}^{[j]} & V_{11}^{[j]} \end{pmatrix}$, $j \in \{A, B\}$ and so we multiply the eigenvalue $(\lambda_2^{[j]})^{|n|}$, $j \in \{A, B\}$ by the second row vector. Now, we observe that the second equation in (2.31) shows that $(u(x_0), \frac{\partial u}{\partial x}(x_0))$ is proportional to $(V_{11}^{[B]}, -V_{21}^{[B]})$. Applying this to the first equation in (2.31), we get

$$\begin{pmatrix} -V_{21}^{[B]} & V_{11}^{[B]} \end{pmatrix} \begin{pmatrix} V_{11}^{[A]} \\ -V_{21}^{[A]} \end{pmatrix} = 0,$$

which gives the desired result. □

2.5.1.2. Eigenmode decay

From this, we obtain the result concerning the decay of the localised eigenmodes as $n \to \pm\infty$.

Corollary 2.5.3. *A localised eigenmode u of (2.2), posed on a medium constituted by two semi-infinite arrays of different halide perovskites, and its associated eigenfrequency ω must satisfy*

$$u(x_n) = O\Big(|\lambda_1^{[A]}(\omega)|^{|n|}\Big) \quad \textit{and} \quad \frac{\partial u}{\partial x}(x_n) = O\Big(|\lambda_1^{[A]}(\omega)|^{|n|}\Big) \quad \textit{as } n \to -\infty,$$

$$u(x_n) = O\Big(|\lambda_1^{[B]}(\omega)|^{|n|}\Big) \quad \textit{and} \quad \frac{\partial u}{\partial x}(x_n) = O\Big(|\lambda_1^{[B]}(\omega)|^{|n|}\Big) \quad \textit{as } n \to +\infty,$$

where $\lambda_1^{[A]}$ is the eigenvalue of $T_p^{[A]}$ satisfying $|\lambda_1^{[A]}(\omega)| < 1$ and $\lambda_1^{[B]}$ is the eigenvalue of $T_p^{[B]}$ satisfying $|\lambda_1^{[B]}(\omega)| < 1$.

Proof. This is a direct result from the previous theorem. Indeed, from Theorem 2.5.2, we have that $(u(x_0), \frac{\partial u}{\partial x}(x_0))^\top$ is proportional to $(V_{11}^{[B]}, -V_{21}^{[B]})^\top$. Thus, we get from (2.27), for $n \in \mathbb{Z}_{>0}$

$$\begin{pmatrix} u(x_n) \\ \frac{\partial u}{\partial x}(x_n) \end{pmatrix} = (\lambda_1^{[B]})^n(\omega) \begin{pmatrix} V_{11}^{[B]} \\ V_{21}^{[B]} \end{pmatrix}$$

and from (2.28), for $n \in \mathbb{Z}_{<0}$,

$$\begin{pmatrix} u(x_n) \\ \frac{\partial u}{\partial x}(x_n) \end{pmatrix} = (\lambda_1^{[A]})^{|n|} S \begin{pmatrix} V_{11}^{[A]} \\ V_{21}^{[A]} \end{pmatrix}.$$

This concludes the proof. □

2.6. Robustness with respect to imperfections

Now that we have established the existence of an interface mode in each band gap for dispersive materials, which decays at infinity, we wish to study the effect of system perturbations. This happens in two different ways:

- Perturbations on the material parameters which have no effect on the symmetry inside each periodic cell. For this, we will introduce perturbations to the permittivity functions of the materials.
- Perturbations on the symmetry inside each periodic cell. To study this effect we will modify the length of two particles in each periodic cell, so that the symmetry breaks.

2.6.1. Theoretical results

2.6.1.1. Permittivity perturbation

First, we will study changes in the materials while the symmetry is preserved. To show this effect, we introduce the perturbation function $f : \mathbb{R} \to \mathbb{R}$, given by

$$f(x,\omega) := \begin{cases} f_1(\omega), & x \in D^{[1]}, \\ f_2(\omega), & x \in D^{[2]}. \end{cases} \tag{2.32}$$

The perturbation function f is a piecewise smooth function of the frequency ω and satisfies $\frac{\partial f}{\partial \omega} < +\infty$. Then, we define $\widetilde{\varepsilon}$ to be the perturbed permittivity of the system, given by

$$\widetilde{\varepsilon}(x,\omega) := \varepsilon(x,\omega) + \delta f(\omega) = \begin{cases} \varepsilon_1(\omega) + \delta f_1(\omega), & x \in D^{[1]}, \\ \varepsilon_2(\omega) + \delta f_2(\omega), & x \in D^{[2]}, \end{cases}$$

where $\delta > 0$ is the perturbation parameter. Then, we obtain the following perturbed problem

$$\begin{cases} \widetilde{\mathcal{L}}(\kappa,\omega)u = \omega^2 u, \\ u(x+1) = e^{i\kappa}u(x), \end{cases} \tag{2.33}$$

where

$$\widetilde{\mathcal{L}}u := -\frac{1}{\mu_0}\frac{\partial}{\partial x}\left(\frac{1}{\widetilde{\varepsilon}(x,\omega)}\frac{\partial u}{\partial x}\right). \tag{2.34}$$

The following definition follows naturally from the perturbation of the system.

Definition 2.6.1 (Perturbed impedance function)**.** *We define the surface impedances associated to the perturbed Helmholtz problem* (2.33) *by*

$$\widetilde{Z}^-(\omega) = -\frac{u(x_0^-)}{\frac{1}{\widetilde{\varepsilon}_1(\omega)}\frac{\partial}{\partial x}u(x_0^-)} \quad \text{and} \quad \widetilde{Z}^+(\omega) = \frac{u(x_0^+)}{\frac{1}{\widetilde{\varepsilon}_1(\omega)}\frac{\partial}{\partial x}u(x_0^+)}, \quad \omega \in \mathbb{R}. \tag{2.35}$$

We wish to show that, as $\delta \to 0$, an interface mode still exists. For the existence, Lemma 2.3.3 holds for the perturbed impedance functions. In addition, we observe that the symmetry of the system has been preserved by the perturbation of the permittivity. Hence, it is sufficient to show that the perturbed impedance functions remain decreasing. Then, because of the symmetry of the system, the rest of the arguments will hold and so, the result will follow.

Theorem 2.6.2. *Let us assume that $\omega \in \mathfrak{A}$, where $\mathfrak{A} \subset \mathbb{R}$ is a band gap. Then, the perturbed surface impedances, as $\delta \to 0$, are decreasing functions of the frequency ω, i.e.,*

$$\frac{\mathrm{d}\widetilde{Z}^{+}}{\mathrm{d}\omega} < 0, \quad \frac{\mathrm{d}\widetilde{Z}^{-}}{\mathrm{d}\omega} < 0, \qquad \text{for } \omega \in \mathfrak{A}.$$

Thus, we have shown that arbitrarily small perturbations on the permittivity of the system do not affect the existence of an interface mode. In addition, using the transfer matrix method (explained in Section 2.5.1), we can get an explicit expression of the solution to (2.33) with respect to the initial data $(u(0), \frac{\partial u}{\partial x}(0))$. Because of the continuous dependence of the solution on δ, it is direct that, as $\delta \to 0$, this solution converges to the one of (2.2). This translates to the following lemma.

Lemma 2.6.3. *Let u denote the asymptotically decaying interface mode of* (2.2) *in the band gap $\mathfrak{A}$ and let u_δ denote an asymptotically decaying interface mode associated to the permittivity perturbed problem* (2.33) *in the band gap $\mathfrak{A}_\delta$. Then, if $\mathfrak{A} \cap \mathfrak{A}_\delta \neq \emptyset$, it holds that*

$$\lim_{\delta \to 0} u_\delta = u.$$

2.6.1.2. Symmetry perturbation

Let us now introduce a structural perturbation to the system. This will result in breaking the symmetry inside each periodic cell. This phenomenon is easy to produce.

We have considered two semi-infinite materials A and B, each one constituted by a unit cell repeated periodically and glued together at $x_0 = 0$. We have assumed that each periodic cell is made of two different kinds of particles, one with permittivity $\varepsilon_1(\omega)$ and one with permittivity $\varepsilon_2(\omega)$, denoted by $D_i^{[1]}$ and $D_j^{[2]}$, with $i = 1, \ldots, N+1$ and $j = 1, \ldots, N$, respectively. The particles are ordered in the following way inside each periodic cell:

$$D_1^{[1]} \; - \; D_1^{[2]} \; - \; D_2^{[1]} \; - \; D_2^{[2]} \; - \; \ldots \; - \; D_N^{[2]} \; - \; D_{N+1}^{[1]}.$$

We call the position perturbation parameter $\sigma > 0$ and we apply the following procedure. In the material A, we increase the size of the particle $D_{N+1}^{[1]}$ by σ and we

decrease the size of the particle $D^{[1]}_{\frac{\lfloor N+2\rfloor}{2}}$ by σ. Then, in a similar way, in the material B we decrease the size of particle $D^{[1]}_1$ by σ and we increase the size of $D^{[1]}_{\frac{\lfloor N+2\rfloor}{2}}$ by σ. Hence, we manage to break the mirror symmetry governing each material. We will view this more analytically later in Figure 2.4, where we have considered a specific example for the model.

Let us note here that the position perturbation σ cannot take arbitrarily big values, as the size of the periodic cell has to remain unaffected. In fact, for this to happen, we require that

$$\sigma \leq \min_{A,B} \left\{ |D^{[1]}_1|, \left| D^{[1]}_{\frac{\lfloor N+2\rfloor}{2}} \right| \right\}, \tag{2.36}$$

where $\min_{A,B}$ denotes the minimum over materials A and B, and $|\cdot|$ denotes the size of each particle. Since we work in the one-dimensional setting, $|\cdot|$ denoted the length.

Once again, as in Section 2.6.1.1, using the transfer matrix method, we can see the continuous dependence that the decay mode has on the length of each particle. Thus, as a direct result, the following lemma holds.

Lemma 2.6.4. *Let u denote the asymptotically decaying interface mode of (2.2) in the band gap $\mathfrak{A}$ and let u_σ denote an asymptotically decaying interface mode associated to the position perturbation procedure described above in the band gap $\mathfrak{A}_\sigma$. Then, if $\mathfrak{A} \cap \mathfrak{A}_\sigma \neq \emptyset$, it holds that*

$$\lim_{\sigma \to 0} u_\sigma = u.$$

2.6.2. Numerical results

Let us now provide an example, in order to solidify the previous analysis. We consider dispersive particles with permittivity given by

$$\varepsilon(x,\omega) = \begin{cases} \varepsilon_1(\omega), & x \in D^{[1]}, \\ \varepsilon_2(\omega), & x \in D^{[2]}, \end{cases} \quad \text{where} \quad \varepsilon_i(\omega) := \varepsilon_0 + \frac{\alpha_i}{1-\beta_i\omega^2}, \quad \text{for} \ \ i = 1,2, \tag{2.37}$$

with $\varepsilon_0, \alpha_i, \beta_i \geq 0$, for $i = 1,2$. This permittivity function model is inspired from the examples treated in Chapter 1 and represents the undamped case of a Drude material or a halide perovskite. In order to obtain analytic results we consider the model for the periodic cells of materials A and B described in Figure 2.1. We note that, in this case, each periodic cell is constituted by five particles, three with permittivity $\varepsilon_1(\omega)$ and two with permittivity $\varepsilon_2(\omega)$. The particles have the following ordering:

$$D^{[1]}_1 \ - \ D^{[2]}_1 \ - \ D^{[1]}_2 \ - \ D^{[2]}_2 \ - \ D^{[1]}_3.$$

Let us denote by $\omega_{i,p}^{(\pm)}$ the poles of the permittivity (2.1), i.e.,

$$\omega_{i,p}^{(\pm)} = \pm\frac{\sqrt{\beta_i}}{\beta_i}. \tag{2.38}$$

We see that

$$\frac{\partial\varepsilon}{\partial\omega}(x,\omega) = \begin{cases} \frac{\partial\varepsilon_1}{\partial\omega}(\omega), & x \in D^{[1]}, \\ \frac{\partial\varepsilon_2}{\partial\omega}(\omega), & x \in D^{[2]}. \end{cases}$$

Thus, it holds

$$\begin{aligned} \frac{\partial\varepsilon_1}{\partial\omega}(\omega) &= \frac{\partial}{\partial\omega}\left(\varepsilon_0 + \frac{\alpha_1}{1-\beta_1\omega^2}\right) \\ &= \frac{2\alpha_1\beta_1\omega}{(1-\beta_1\omega^2)^2} \geq 0 \end{aligned}$$

and similarly

$$\frac{\partial\varepsilon_2}{\partial\omega}(\omega) \geq 0,$$

which gives

$$\frac{\partial\varepsilon}{\partial\omega}(x,\omega) \geq 0, \quad x \in \mathbb{R}.$$

Hence, Theorem 2.3.14 holds. This implies that if we consider a one-dimensional photonic crystal of the form of Figure 2.1 with permittivity given by (2.37), then, in each band gap, a topologically protected interface mode exists.

2.6.2.1. Permittivity perturbation

As mentioned previously, we will first study perturbations on the material parameters while keeping the symmetry inside each periodic cell intact. This occurs by introducing a perturbation to the permittivity of the particles and it gives rise to the perturbed system described by (2.33).

We can see that if the perturbation function f is constant, then the permittivity is not strongly affected. Hence we will consider perturbation functions which are dispersive with respect to the frequency ω. In order to simplify the analysis we will take $f_1(\omega) = f_2(\omega)$, for all $\omega \in \mathbb{R}$.

We will study the perturbation effect for two separate cases of perturbation functions:

1. Perturbation functions which satisfy the assumptions of the original permittivity. In particular, we will consider the following:

$$f(\omega) = -\frac{1}{\omega^2}. \tag{2.39}$$

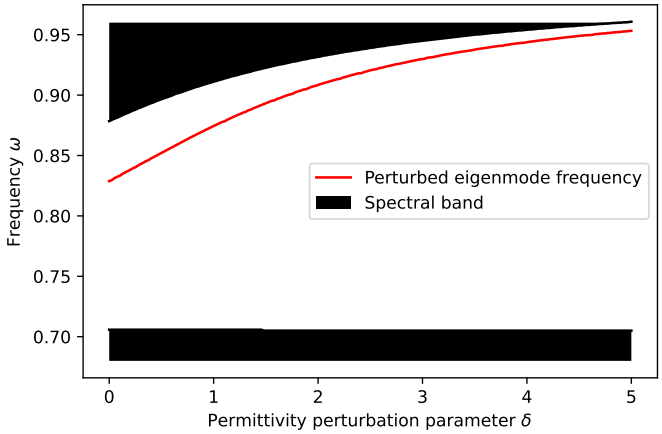

Figure 2.2.: Plot of the frequencies of the interface mode and the edges of the band gap as perturbations with magnitude δ that preserve the monotonicity condition are added. In particular, δ times the strictly increasing function (2.39) is added to the permittivity (2.37). This function is in full accordance with the initial assumptions on the material permittivities. We see that as $\delta \to 0$, the perturbed interface mode frequency converges to the unperturbed one, as stated in Lemma 2.6.3. As δ increases, the size of the band gap increases and the interface mode frequency increases but still remains inside the band gap.

2. Perturbation functions which does not satisfy the assumptions of the original permittivity. In particular, we will consider the following:

$$f(\omega) = \frac{1}{\omega^2}. \tag{2.40}$$

For both cases, we see directly the smoothness of the perturbation function. We will also work inside the first band gap of the problem (2.33). This region is away from zero, so we ensure that $\frac{\partial f}{\partial \omega} < +\infty$.

For the first case, we observe that as the perturbation parameter δ increases, the size of the band gap increases. Because of the monotonicity of the perturbation function ϕ, Theorem 2.3.14 holds and so a unique interface mode exists. This fact is shown in Figure 2.2, where we plot for each value of δ the value of the frequency ω of the interface mode. We observe that as δ increases, the interface mode frequency increases as well, which is natural, since the size of the band gap increases. We also note that, as $\delta \to 0$, the interface mode frequency converges to the one of the unperturbed interface mode, as shown in Lemma 2.6.3.

Let us now move to the second case. It holds that as δ increases, the size of the band gap decreases. This happens because the perturbation function f, which is

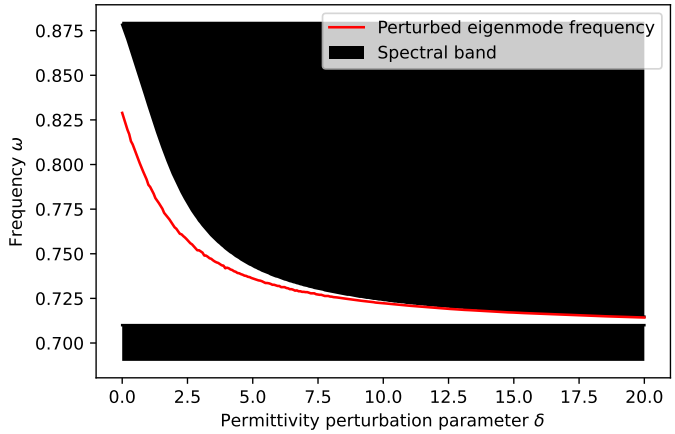

Figure 2.3.: Plot of the frequencies of the interface mode and the edges of the band gap as perturbations with magnitude δ that do not preserve the monotonicity condition are added. In particular, δ times the strictly decreasing function (2.40) is added to the permittivity (2.37). As a result, when δ is sufficiently large, the permittivity function does not respect the monotonicity assumption. Of course, we see that as $\delta \to 0$, the perturbed interface mode frequency converges to the unperturbed one, as stated in Lemma 2.6.3. As δ increases, the width of the band gap decreases. As a result, the perturbed interface mode frequency gets pushed outside of the band gap. Hence, a localised interface mode no longer exists for frequency ω in this band gap. The shaded areas are the spectral bands and the red line represents the frequency of the perturbed interface mode as the perturbation parameter δ increases. We observe that the band gap becomes small for large values of δ and that the perturbed interface mode frequency is pushed very close to the edge of the gap.

decreasing, becomes the dominating factor of the perturbed permittivity $\widetilde{\varepsilon}$. In Figure 2.3, we observe that as δ increases, the interface mode frequency ω decreases. In particular, for large values of δ, the band gap becomes very small. On the other hand, as $\delta \to 0$, the original permittivity is still the dominating factor of the perturbed permittivity and so, from Theorem 2.3.14, the interface mode still exists and converges to the unperturbed one.

This closing of the band gap poses problems for the physical implementation of these systems. In particular, since the edge mode approaches the edge of the band gap, its eigenfrequency will be close to that of a propagating Bloch mode. As a result, in any physical device, it is likely than any attempt to use this localised mode for wave guiding will fail as the nearby propagating mode will also be excited.

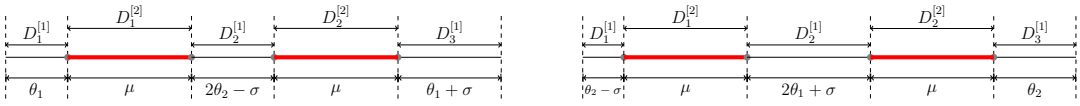

Perturbed material A

Perturbed material B

Figure 2.4.: Position perturbation on the periodic cells of each material. We have considered as values $\theta_1 = 0.1$, $\theta_2 = 0.15$ and $\mu = 0.25$. We notice that the largest possible value for σ is 0.15. We see that by modifying the sizes of the particles, the mirror symmetry inside the unit cell no longer holds.

2.6.2.2. Symmetry perturbation

Let us now treat the case where the symmetry of the periodic cells breaks. We will apply the procedure described in Section 2.6.1.2 on the model described in Figure 2.1. In particular, for material A, we reduce the size of the particle $D_2^{[1]}$ by σ and we increase the size of particle $D_3^{[1]}$ by σ. Similarly, for material B, we decrease the size of $D_1^{[1]}$ by σ and we increase the size of $D_2^{[1]}$ by the same amount. We depict this position perturbation graphically for the periodic cell of material A and B in Figure 2.4.

As it is already mentioned, the position perturbation parameter σ cannot take arbitrarily large values, since the length of the periodic cell has to remain the same. Thus, from the bound (2.36), we see that

$$0 \leq \sigma \leq \theta_2.$$

Studying the existence of an interface mode under the position perturbation regime is not in accordance with the argument we have presented in Theorem 2.3.14. In fact, our argument is based on the mirror symmetry governing the periodic cells and proposes a sufficient but not necessary condition for an interface mode to exist in a band gap. This symmetry breaks once the position perturbation takes place. What we can say with certainty is that, if the interface mode exists, then, as the position perturbation parameter $\sigma \to 0$, it converges to the unperturbed interface mode (Lemma 2.6.4). This result is illustrated in Figure 2.5, where we have plotted the interface mode frequency ω as a function of the position perturbation parameter σ inside a band gap.

2.7. Conclusion

Studying a one-dimensional system for dispersive materials, we used the mirror symmetry and the underlying periodic structure of our setting to show that localised interface modes exist. We explained the behaviour of the Zak phase, a topological

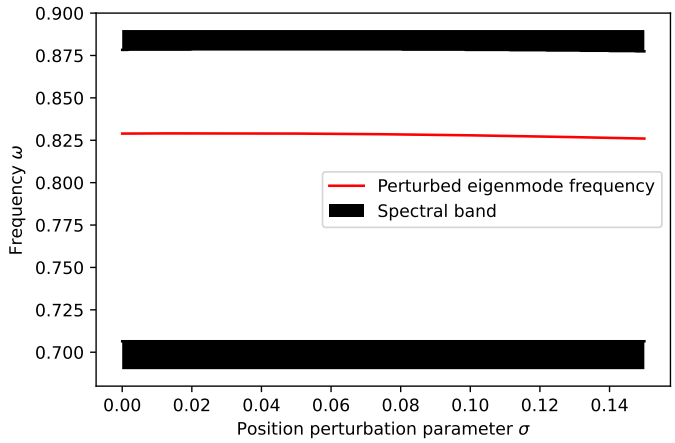

Figure 2.5.: Plot of the interface mode frequency ω as the position perturbation parameter σ increases. We notice that as $\sigma \to 0$, the perturbed interface mode frequency converges to the one of the unperturbed system. Also, we see that as σ increases, the break of the symmetry inside the unit cell is more drastic and so, the perturbed interface mode frequency diverges from the unperturbed one. Although, this divergence is quite small and the perturbed interface mode frequency remains inside the band gap. We note that the shaded areas denote the spectral bands.

invariant of the system, and we have provided the condition that the interface mode frequency needs to satisfy for these modes to decay at infinity. Finally, we introduced imperfections to the system in the form of perturbations on the material permittivity and the symmetry of the periodic cells and we showed how the decaying modes and their associated frequencies are affected.

3. Topological protection in the presence of damping

3.1. Introduction

As we have mentioned in the previous chapter, strongly localised waves in periodic media is a subject of intense research in both physics and mathematics. It comes as a natural consequence, that the study of topological protection is extended to materials with damping. This feature is present in materials such us metals and photonic crystals. It appears in the permittivity characterising these structures in the form of non-zero imaginary part. Physically, this implies that while the wave travels through the material, there is a change of energy.

In this chapter, we will focus on damped materials, i.e., materials with complex-valued permittivity functions. We have as our basis the work carried in Chapter 1 and in [25]. The theory developed in the previous works concern materials with no damping and takes into account only real frequencies. Using interface impedance function, it characterises the existence of interface modes. Building on that, we expand on complex frequencies and permittivities and establish similar results.

3.2. Mathematical setting

In this section, we will present the mathematical setting of a damped material with an interface. We provide the structural characteristics such a system along with the quasiperiodic differential problem which will help us show the wave localisation.

3.2.1. Damped systems

We consider two materials A and B. Each one is of the form of a semi-infinite array. The arrays are glued together at the origin and we assume that the material A expands towards $-\infty$ and the material B expands towards $+\infty$. In addition, we assume that each material is constructed by repeating periodically a unit cell. Each unit cell is the product of layering, i.e. it has particles different permittivities. We denote the permittivity function of material A by ε_A and of material B by ε_B.

Our assumptions on the permittivity functions are the following:

- complex-valued, i.e., $\varepsilon_j : \mathbb{R} \to \mathbb{C}$,
- periodic, i.e., $\varepsilon_j(x) = \varepsilon_j(x+1)$ and
- mirror-symmetric, i.e., $\varepsilon_j(x+h) = \varepsilon_j(x+1-h)$, for $h \in (0,1)$,

where $j = A, B$.

We define the sequence $\{x_n\}_{n\in\mathbb{Z}}$ to be the set of endpoints of each one of the periodically repeated cells, i.e., $x_n = x_0 + n$ for $n \in \mathbb{Z}$. We take x_0 to be the glue point of the two materials, i.e., the interface, and so, for $n < 0$, we are in material A and for $n > 0$, we are in material B.

3.2.2. Differential problem

The differential problem we are studying is the following:

$$\mathcal{L}u = \omega^2 u \tag{3.1}$$

with

$$\mathcal{L}u := -\frac{1}{\mu_0}\frac{\mathrm{d}}{\mathrm{d}x}\left(\frac{1}{\varepsilon(x)}\frac{\mathrm{d}u}{\mathrm{d}x}\right), \tag{3.2}$$

where $\mu_0 \in \mathbb{R}_{>0}$ is the magnetic permeability, which is constant, and $\omega \in \mathbb{C}$ is the frequency.

As in the previous chapter, our goal is to find eigenvalues of (3.2) for which the associated eigenmodes are localised in a neighborhood of the interface x_0 and decay as $|x| \to \infty$.

To find candidate eigenvalues ω^2 for which localised eigenmodes can occur, it is valuable to consider the Floquet-Bloch spectrum of the operators associated to materials A and B. This is the set of eigenmodes which satisfy the Floquet-Bloch quasi-periodicity conditions

$$u(x+1) = e^{i\kappa}u(x) \quad \text{and} \quad \frac{\partial u}{\partial x}(x+1) = e^{i\kappa}\frac{\partial u}{\partial x}(x), \tag{3.3}$$

for some $\kappa \in \mathcal{B} := [-\pi, \pi]$. Hence, these eigenmodes belong to the space of functions

$$H^2_\kappa := \left\{ f \in H^2_{\mathrm{loc}} : \ f(x+1) = e^{i\kappa} f(x), \ x \in \mathbb{R} \right\}.$$

With this formulation of the problem, we observe that for an eigenmode to be localised at the interface x_0, the associated eigenvalue has to lie in the spectral gaps of the problem (3.1)-(3.3). This holds since, for an eigenvalue in a spectral band, (3.3) gives that the magnitude of the associated eigenmode is preserved, which is a contradiction.

Let us also note here that we are interested in materials A and B with overlapping band gaps, otherwise such modes cannot exist in this setting.

Finally, we equip the space H^2_κ with the standard inner product $\langle \cdot, \cdot \rangle$, given by

$$\langle u, v \rangle = \int_{\mathbb{R}} u(x)\overline{v}(x)\mathrm{d}x, \quad \forall u, v \in H^2_\kappa. \tag{3.4}$$

3.3. Preliminaries

Let us start by recalling some notions which will be used for the analysis of the problem.

3.3.1. Impedance functions

We start by defining the notion of the impedance function.

Definition 3.3.1 (Interface impedance)**.** *We define the interface impedance of the problem* (3.1) *by*

$$Z(\omega) := Z_A(\omega) + Z_B(\omega), \quad \omega \in \mathbb{C}, \tag{3.5}$$

where Z_A and Z_B denote the surface impedances of materials A and B, respectively, given by

$$Z_A(\omega) = -\frac{u(x_0^-)}{\frac{1}{\varepsilon_1(\omega)}\frac{\partial}{\partial x}u(x_0^-)} \quad \text{and} \quad Z_B(\omega) = \frac{u(x_0^+)}{\frac{1}{\varepsilon_1(\omega)}\frac{\partial}{\partial x}u(x_0^+)}, \quad \omega \in \mathbb{C}. \tag{3.6}$$

Lemma 3.3.2. *Let $\mathfrak{A} \subset \mathbb{C}$. Then, a necessary and sufficient conditions for the existence of an interface localised mode in $\mathfrak{A}$ is*

$$Z_A(\omega) + Z_B(\omega) = 0, \quad \omega \in \mathfrak{A}. \tag{3.7}$$

3.3.2. Bulk index

Let us now define the bulk index. This topological property shows us the behaviour of u at the edges of a band gap.

Definition 3.3.3 (Bulk index)**.** *Let $\mathfrak{S}$ denote a band gap and a, b denote its edges. Then we define the associated bulk topological index $\mathcal{J}_\mathfrak{S}$ by*

$$\mathcal{J}_\mathfrak{S} := \begin{cases} +1, & \text{if } u \text{ is symmetric at } a, \\ -1, & \text{if } u \text{ is anti-symmetric at } a. \end{cases} \tag{3.8}$$

3.4. Undamped systems

Let us start by considering the case of undamped case, i.e. we are in the following regime

$$\Im(\varepsilon_A) = \Im(\varepsilon_B) = 0.$$

We denote by $Z^{(U)}$ the interface impedance function for the undamped systems, and by $Z_j^{(U)}$ the impedance function of material j, with $j = A, B$.

First, we will look at the case of $\omega \in \mathbb{R}$ and then we will study the case of $\omega \in \mathbb{C}$.

3.4.1. Real frequencies

This setting has been studied extensively in Chapter 2 and in [25]. Let $\mathcal{L}_A$ and $\mathcal{L}_B$ denote the differential operator $\mathcal{L}$ for the material A and the material B, respectively. We define $\tilde{\mathfrak{A}}_A^U$ and $\tilde{\mathfrak{A}}_B^U$ to be two band gaps of $\mathcal{L}_A$ and $\mathcal{L}_B$, respectively, for frequencies $\omega \in \mathbb{R}$, such that

$$\tilde{\mathfrak{A}}^U := \tilde{\mathfrak{A}}_A^U \cap \tilde{\mathfrak{A}}_B^U \neq \emptyset.$$

Let $\mathcal{J}_A$ and $\mathcal{J}_B$ be the bulk topological indices associated to the material A and the material B, respectively, in $\tilde{\mathfrak{A}}^U$.

In Chapter 2, existence and uniqueness of localised interface modes in a band-gap is proved.

Theorem 3.4.1. *If*

$$\mathcal{J}_A + \mathcal{J}_B \neq 0,$$

then no interface mode exists. If

$$\mathcal{J}_A + \mathcal{J}_B = 0,$$

then there exists a unique frequency $\omega_r \in \tilde{\mathfrak{A}}^U$, for which an interface mode exists.

3.4.2. Complex frequencies

Let us now consider complex frequencies ω while still having real valued permittivity functions. We denote by $\mathfrak{A}_A^U$ and $\mathfrak{A}_B^U$ two band gaps of $\mathcal{L}_A$ and $\mathcal{L}_B$, respectively, in this regime, such that

$$\mathfrak{A}^U := \mathfrak{A}_A^U \cap \mathfrak{A}_B^U \neq \emptyset.$$

Let us recall here that the difference between $\tilde{\mathfrak{A}}^U$ and $\mathfrak{A}^U$ is that for $\tilde{\mathfrak{A}}^U$ we have considered $\omega \in \mathbb{R}$ and for $\mathfrak{A}^U$ we have considered $\omega \in \mathbb{C}$.

Theorem 3.4.2. *If there exists $\omega^{\#} \in \tilde{\mathfrak{A}}^U$ such that $Z^{(U)}(\omega^{\#}) = 0$, then there exists at least one frequency $\omega \in \mathfrak{A}^U$ such that $Z^{(U)}(\omega) = 0$.*

Proof. Let us assume indeed that there exists $\omega^{\#} \in \tilde{\mathfrak{A}}^U$ such that

$$Z^{(U)}(\omega^{\#}) = 0.$$

We observe that $\tilde{\mathfrak{A}}^U \subset \mathfrak{A}^U$, since

$$\tilde{\mathfrak{A}}^U = \mathfrak{A}^U\Big|_{\mathbb{R}}.$$

This implies that

$$\omega^{\#} \in \mathfrak{A}^U.$$

This concludes the proof. □

Let us also prove the following lemma which will be of great importance later.

Lemma 3.4.3. *The interface impedance function $Z^{(U)}$ has no poles in $\mathfrak{A}^U \setminus \tilde{\mathfrak{A}}^U$.*

Proof. For Z to have a pole in $\mathfrak{A}^U \setminus \tilde{\mathfrak{A}}^U$, it means that there exists $\omega_p \in \mathfrak{A}^U \setminus \tilde{\mathfrak{A}}^U$ such that

$$Z_A^{(U)} = \infty \quad \text{or} \quad Z_B^{(U)} = \infty.$$

Let us assume that $Z_A^{(U)} = \infty$. This means that

$$\frac{\partial}{\partial x} u(x_0^-, \omega_p) = 0.$$

This implies that the boundary value problem

$$\begin{cases} \mathcal{L}u = \omega_p^2 u, \quad x \in [x_{-1}, x_0], \\ \dfrac{\partial}{\partial x} u(x_0^-) = 0, \end{cases} \tag{3.9}$$

admits a solution, where the differential operator $\mathcal{L}$ is given by (3.2). Although, we observe that with respect to the inner product (3.4), the differential operator $\mathcal{L}$ is self-adjoint (Appendix A.2.1). Hence, it admits only real eigenvalues which implies that $\omega_p^2 \in \mathbb{R}$. Since, in general, we consider frequencies with non-zero real parts, this implies that $\Im(\omega_p) = 0$. Thus, $\omega_p \in \tilde{\mathfrak{A}}^U$, which is a contradiction. The case $Z_B^{(U)} = \infty$ follows exactly the same reasoning. This concludes the proof. □

Combining this result with the dependence of u on the coefficients of (3.1), we obtain the following:

Lemma 3.4.4. *The interface impedance function $Z^{(U)}$ is holomorphic in $\mathfrak{A}^U$.*

3.5. Damped systems

Let us now still consider complex frequencies ω but move to complex valued permittivity functions ε_j, for $j = A, B$, with small imaginary part. More precisely, we introduce an arbitrary parameter $0 < \delta \ll 1$ and assume that

$$\lim_{\delta \to 0} \Im(\varepsilon_A)(\delta) = \lim_{\delta \to 0} \Im(\varepsilon_B)(\delta) = 0. \tag{3.10}$$

Essentially, by considering small imaginary parts for ε_A and ε_B, we view the case of complex permittivities as a perturbation of the case of real permittivities. Indeed, let us denote by $Z_j^{(D)}$, $j = A, B$, the impedance functions of materials A and B, respectively, and let $Z^{(D)}$ be the associated interface impedance. Then,

$$\lim_{\delta \to 0} Z_j^{(D)}(\omega) = Z_j^{(U)}(\omega), \tag{3.11}$$

for a fixed frequency $\omega \in \mathbb{C}$ and for $j = A, B$.

We denote by $\mathfrak{A}_A^D$ and $\mathfrak{A}_B^D$ two band gaps of $\mathcal{L}_A$ and $\mathcal{L}_B$, respectively, in this regime, such that

$$\mathfrak{A}^D := \mathfrak{A}_A^D \cap \mathfrak{A}_B^D \neq \emptyset.$$

Lemma 3.5.1. *The impedance functions $Z_A^{(D)}$ and $Z_B^{(D)}$ have no poles in the interior of $\mathfrak{A}^D$.*

Proof. We treat the case of $Z_A^{(D)}$. Then, using the same reasoning, the result for $Z_B^{(D)}$ will follow. We denote by $(\mathfrak{A}^D)^\circ$ the interior of $\mathfrak{A}^D$.

Let us assume that there exists $\omega_p \in (\mathfrak{A}^D)^\circ$ such that

$$Z_A^{(D)}(\omega_p) = \infty.$$

Then, for all $\varepsilon_p > 0$, there exists $r > 0$ such that, for all $\omega \in (\mathfrak{A}^D)^\circ$ satisfying $|\omega - \omega_p| < r$, it holds that

$$|Z_A^{(D)}(\omega)| > \varepsilon_p.$$

Then, applying the triangle inequality, we get

$$|Z_A^{(U)}(\omega)| + |Z_A^{(D)}(\omega) - Z_A^{(U)}(\omega)| > |Z_A^{(D)}(\omega)| > \varepsilon_p.$$

Now, letting our arbitrary parameter $\delta \to 0$, from (3.11), we have

$$\lim_{\delta \to 0} |Z_A^{(D)}(\omega) - Z_A^{(U)}(\omega)| = 0,$$

which gives

$$|Z_A^{(U)}(\omega)| > \varepsilon_p.$$

This translates to $Z_A^{(U)}$ having a pole at ω_p, which is a contradiction from Lemma 3.4.3. This concludes the proof. □

Combining this with the dependence of a solution u on the coefficients of (3.1), we have:

Lemma 3.5.2. *The impedance functions $Z_A^{(D)}$ and $Z_B^{(D)}$ are holomorphic in the interior of $\mathfrak{A}^D$.*

Applying Lemma 3.5.1 on (3.5), we get the following result.

Corollary 3.5.3. *The interface impedance $Z^{(D)}$ is holomorphic in the interior of $\mathfrak{A}^D$.*

This leads to the main result for damped systems.

Theorem 3.5.4. *Let us consider two band gaps $\mathfrak{A}^U$ and $\mathfrak{A}^D$ for $Z^{(U)}$ and $Z^{(D)}$, respectively, such that $\mathfrak{A}^U \cap \mathfrak{A}^D \neq \emptyset$. Let $Z^{(U)}$ have N roots in the interior of $\mathfrak{A}^U \cap \mathfrak{A}^D$. Then, for small δ, $Z^{(D)}$ has N roots in the interior of $\mathfrak{A}^U \cap \mathfrak{A}^D$, as well.*

Proof. Let $(\mathfrak{A}^U \cap \mathfrak{A}^D)^\circ$ denote the interior of $\mathfrak{A}^U \cap \mathfrak{A}^D$ and let $\{\omega_i\}_{i=1}^N$ be the set of roots of $Z^{(U)}$ in $(\mathfrak{A}^U \cap \mathfrak{A}^D)^\circ$. From Lemma (3.4.3) and Corollary (3.5.3), we get that, for each $i = 1, \ldots, N$, there exists $r_i > 0$, such that

$$Z^{(D)} \text{ and } Z^{(U)} \text{ are holomorphic in } N_i,$$

where

$$N_i := \left\{\omega \in \mathfrak{A}^U \cap \mathfrak{A}^D : \ |\omega - \omega_i| < r_i\right\} \subset (\mathfrak{A}^U \cap \mathfrak{A}^D)^\circ.$$

In addition, from (3.11), we know that

$$\lim_{\delta \to 0} |Z^{(D)}(\omega) - Z^{(U)}(\omega)| = 0, \quad \forall \omega \in \overline{\mathfrak{A}^U \cap \mathfrak{A}^D},$$

where $\overline{\mathfrak{A}^U \cap \mathfrak{A}^D}$ denotes the closure of $\mathfrak{A}^U \cap \mathfrak{A}^D$. It follows that, for small δ,

$$|Z^{(D)}(\omega)| > |Z^{(D)}(\omega) - Z^{(U)}(\omega)|, \quad \forall \omega \in \partial N_i,$$

since, for all $\kappa > 0$,

$$|Z^{(D)}(\omega) - Z^{(U)}(\omega)| < \kappa \quad \text{and} \quad |Z^{(D)}(\omega)| \neq 0, \quad \forall \omega \in \partial N_i, \quad i = 1, \ldots, N,$$

where ∂N_i denotes the boundary of N_i. Thus, we can apply Rouché's Theorem (Chapter 1, [16]) and obtain that $Z^{(D)}$ and $Z^{(U)}$ have the same number of roots in N_i, $i = 1, \ldots, N$.

Now, let us assume that there exists $\tilde{\omega} \in (\mathfrak{A}^U \cap \mathfrak{A}^D)^\circ \setminus \bigcup_{i=1}^N N_i$ such that $Z^{(U)}(\tilde{\omega}) \neq 0$ and $Z^{(D)}(\tilde{\omega}) = 0$. Thus, for all $\tilde{\varepsilon} > 0$, there exists $\tilde{r} > 0$, such that

$$|Z^{(D)}(\omega)| < \tilde{\varepsilon}, \quad \text{for all } \omega \text{ such that } |\omega - \tilde{\omega}| \leq \tilde{r}.$$

It holds that

$$\left||Z^{(D)}(\omega)+Z^{(U)}(\omega)|-|Z^{(U)}(\omega)|\right|<|Z^{(D)}(\omega)|<\tilde{\varepsilon}.$$

Letting $\delta\to 0$, this gives

$$|Z^{(U)}(\omega)|<\tilde{\varepsilon},\quad \text{for all } \omega \text{ such that } |\omega-\tilde{\omega}|\leq\tilde{r},$$

which translates to $\tilde{\omega}$ being a root for Z. This is a contradiction, since $\tilde{\omega}\in(\mathfrak{A}^U\cap\mathfrak{A}^D)^\circ\setminus\bigcup_{i=1}^N N_i$. This concludes the proof. □

3.6. Asymptotic behaviour

Our objective in this section is to obtain the asymptotic behaviour of the modes as $x\to+\infty$. For this, we will make use, as in Chapter 2, of the transfer matrix method associated to this problem.

3.6.1. Transfer matrix

Let us define

$$\tilde{u}(x):=\Big(u(x),u'(x)\Big)^\top. \tag{3.12}$$

The symmetry induced to the system is the following:

$$\varepsilon(x_n+h,\omega)=\varepsilon(x_{n+1}-h,\omega),\quad h\in[0,1),\ n\in\mathbb{N}\setminus\{0\}.$$

For $j=A,B$, we denote the transfer matrix associated to the periodic cell of material j by $T_p^{(j)}$, as described in Chapter 2.

The following result holds.

Lemma 3.6.1. *The transfer matrix $T_p^{(j)}$, for $j=A,B$, satisfies* $\det(T_p^{(j)})=1$.

We have that

$$\begin{pmatrix}u(x_{n+1})\\u'(x_{n+1})\end{pmatrix}=\mathbb{1}_{\{n\geq 0\}}T_p^{(B)}\begin{pmatrix}u(x_n)\\u'(x_n)\end{pmatrix}+\mathbb{1}_{\{n<0\}}T_p^{(A)}\begin{pmatrix}u(x_n)\\u'(x_n)\end{pmatrix}, \tag{3.13}$$

for $n\in\mathbb{Z}$.

From the symmetry of the model, we also get

$$\begin{pmatrix}u(x_{n-1})\\u'(x_{n-1})\end{pmatrix}=\mathbb{1}_{\{n\geq 0\}}ST_p^{(B)}S\begin{pmatrix}u(x_n)\\u'(x_n)\end{pmatrix}+\mathbb{1}_{\{n<0\}}ST_p^{(A)}S\begin{pmatrix}u(x_n)\\u'(x_n)\end{pmatrix}, \tag{3.14}$$

for $n \in \mathbb{Z}$, where

$$S = \begin{pmatrix} 1 & 0 \\ 0 & -1 \end{pmatrix}.$$

Here, let us note that with a direct calculation, we can see that $S = S^{-1}$.

Applying the quasiperiodic boundary conditions, we get

$$\tilde{u}(x_{n+1}) = e^{i\kappa}\tilde{u}(x_n).$$

Combining this with (3.13), we get the following problem:

$$\left(T_p^{(j)}(\omega) - e^{i\kappa}I\right)\tilde{u}(x_n) = 0, \quad n \in \mathbb{N}, \tag{3.15}$$

where $j = A$, if $n < 0$ and $j = B$, if $n > 0$. From (3.15), we obtain the dispersion relation for each material given by

$$\det\left(T_p^{(j)}(\omega) - e^{i\kappa}I\right) = 0, \quad j = A, B. \tag{3.16}$$

The dispersion relation relates the quasiperiodicity κ with the frequency ω of the system and gives the structure of the spectral bands and the spectral gaps of (3.1)-(3.3) for materials A and B.

From Chapter 2, we have the following spectral property for a transfer matrix $T_p^{(j)}$, $j = A, B$.

Lemma 3.6.2. *For $j = A, B$, the transfer matrix $T_p^{(j)}$ has real eigenvalues denoted by $\lambda_1^{(j)}$ and $\lambda_2^{(j)}$, satisfying $|\lambda_1^{(j)}| < 1$ and $|\lambda_2^{(j)}| > 1$.*

We use this result to obtain information about the asymptotic behaviour of the modes $u(x_n)$ as $n \to \pm\infty$.

3.6.2. Asymptotic behaviour of damped systems

In order to obtain the asymptotic behaviour of the eigenmodes as $n \to \pm\infty$, we follow the same reasoning as in Chapter 2. The result follows.

Theorem 3.6.3. *A localised eigenmode u of (3.1), posed on a medium constituted by two semi-infinite arrays of different materials with damping, and its associated eigenfrequency ω must satisfy*

$$u(x_n) = O\left(|\lambda_1^{(A)}(\omega)|^{|n|}\right) \quad \text{and} \quad u'(x_n) = O\left(|\lambda_1^{(A)}(\omega)|^{|n|}\right) \quad \text{as } n \to -\infty,$$

$$u(x_n) = O\left(|\lambda_1^{(B)}(\omega)|^{|n|}\right) \quad \text{and} \quad u'(x_n) = O\left(|\lambda_1^{(B)}(\omega)|^{|n|}\right) \quad \text{as } n \to +\infty,$$

where $\lambda_1^{(A)}$ is the eigenvalue of $T_p^{(A)}$ satisfying $|\lambda_1^{(A)}(\omega)| < 1$ and $\lambda_1^{(B)}$ is the eigenvalue of $T_p^{(B)}$ satisfying $|\lambda_1^{(B)}(\omega)| < 1$.

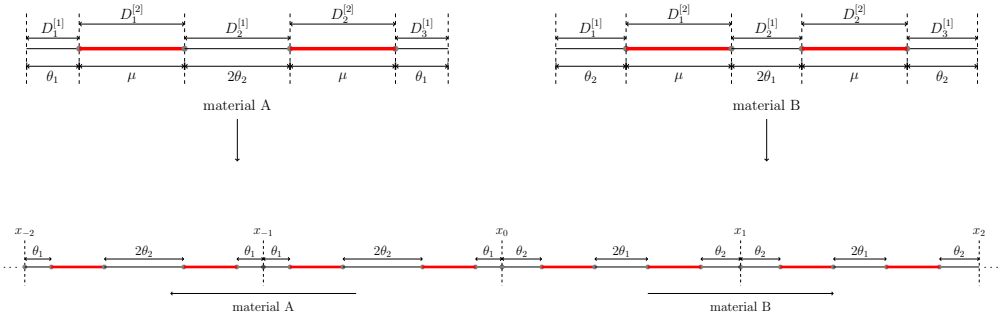

Figure 3.1.: An example of a damped system as studied in Section 3.7. In the unit cell of each material we have 3 particles of permittivity ε_1 and 2 particles of permittivity ε_2. We notice the mirror symmetric way in which the particles are placed inside the periodic cells. Each material is constituted by a semi-infinite array created by periodically repeating the unit cell. Our structure is the result of gluing materials A and B at the point x_0.

3.7. Numerical example

We now consider an example of a damped system and show our findings in the previous sections numerically.

3.7.1. Configuration

Let us consider two materials A and B, each one in the form of a semi-infinite array, glued at the interface x_0. Each material is constructed by a periodically repeated unit cell. Each unit cell is the product of layering; it contains five particles of two different permittivities ε_1 and ε_2. Each permittivity function satisfies the assumptions of Section 3.2.1. We denote by $D_i^{[1]}$, $i = 1, 2, 3$, and by $D_j^{[2]}$, $j = 1, 2$, the particles of the unit cell with permittivity ε_1 and ε_2, respectively. In particular, the particles obey the following ordering:

$$D_1^{[1]} \; - \; D_1^{[2]} \; - \; D_2^{[1]} \; - \; D_2^{[2]} \; - \; D_3^{[1]}.$$

A schematic depiction of this configuration is given in Figure 3.1.

In order to simplify our system, we will assume that the permittivities ε_1 and ε_2 are complex valued and constant on each particle. This translates to

$$\varepsilon(x,\omega) = \begin{cases} \varepsilon_1, & x \in D^{[1]} := \bigcup_{i=1}^{3} D_i^{[1]}, \\ \varepsilon_2, & x \in D^{[2]} := \bigcup_{i=1}^{2} D_i^{[2]}, \end{cases}$$

with $\varepsilon_1, \varepsilon_2 \in \mathbb{C}$. We consider an arbitrary parameter $\delta > 0$ and we assume that

$$\Im(\varepsilon_1) = c_1\delta \quad \text{and} \quad \Im(\varepsilon_2) = c_2\delta, \quad c_1, c_2 \in \mathbb{R}_{>0}.$$

This allows us to vary the damping of the system by taking different values of δ.

3.7.2. Band characterisation

The quasiperiodic Helmholtz problem (3.1)-(3.3), for each material, is characterised by a dispersion relation, as found in (3.16). This is an expression which relates the quasiperiodicity κ with the frequency ω, such that it describes the spectral bands $\omega = \omega_n(\kappa)$. It is an equation of the form:

$$2\cos(\kappa) = f(\omega), \tag{3.17}$$

where $f : \mathbb{R} \to \mathbb{R}$ is a function that depends on the material parameters and the system's geometry. This function is variously known as the discriminant or Lyapunov function of the operator Λ [46]. Some examples are provided in *e.g.* [4, 56].

From (3.17), we observe that, in order to be in a spectral band, the following two conditions need to be satisfied:

$$\Im(f(\omega)) = 0 \quad \text{and} \quad |f(\omega)| < 2. \tag{3.18}$$

We will use these conditions to identify the spectral bands and the band gaps of our quasiperiodic Helmholtz problem, i.e.,

- Band: both condition in (3.18) are satisfied.
- Band gap: at least one of the conditions in (3.18) in not satisfied.

3.7.3. Effect of damping on spectrum

A key feature of the proof given in Sections 3.4 and 3.5 is that, when we consider $\delta = 0$, i.e.,

$$\Im(\varepsilon_1) = \Im(\varepsilon_2) = 0,$$

we know that there exists a root ω_r of Z in the band gap, on the real axis.

In Figure 3.2, we observe how adding damping to the system affects the structure of the spectrum of (3.1). By fixing the material parameters and increasing the damping of the system, i.e., increasing δ, we observe a downwards shift of the spectral bands. In addition, we see how he location of the root of the interface impedance changes as the damping increases.

It is worth noting that Rouché's theorem holds for small δ. In fact, as δ increases the inequality condition of the theorem fails and hence we cannot use this tool. Although, from the numerics, we observe that even for larger values of the damping, a root for Z still exists in the according band gaps. In Figure 3.2, we have also tracked the behaviour of the root associated to the one of the undamped case in the complex plane. The key aspect of this is that it remains in a spectral band gap.

Along with this, in Figure 3.2, we provide also three example of fixed dampings which show how the spectral bands and the associated gaps look like. We see where the root of the interface impedance function Z is located in each spectral gap.

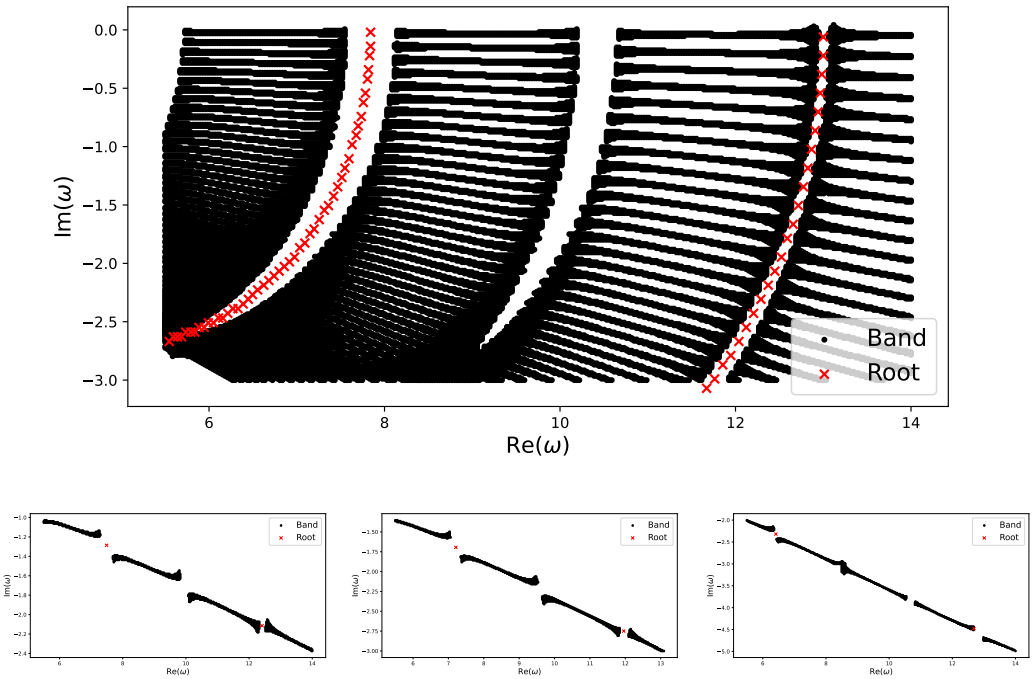

Figure 3.2.: Spectral bands of the damped system studied in Section 3.7. We observe how the increase in damping forces the bands to a downwards shift. Also, we notice how the position of a root of the interface impedance function $Z^{(D)}$ in a spectral gap changes as the damping changes. For three different and fixed values of damping, we provide the exact structure of the spectral bands.

3.7.4. Wave propagation

Apart from the material parameters, let us now also fix the damping. We take $\delta > 0$, so that $\Im(\varepsilon_1), \Im(\varepsilon_2) > 0$. For this specific damping, we consider a frequency in a spectral band gap of (3.1)-(3.3), for which the interface impedance function is zero, i.e., $Z^{(D)}(\omega) = 0$.

In Figure 3.3, we observe the decaying character of $|u|$ as $|x| \to \infty$. The red lines denote the positions of the endpoints x_i's. We see how u propagates at the interior of each unit cell, while its magnitude is localised around the interface x_0 and decays as we move further away from it. The blue curves denote the eigenvalue envelope given by Theorem 3.6.3. In particular, denoting the eigenvalue envelope by F, we have:

$$F(x_n) := \begin{cases} |\lambda_1^{(A)}(\omega)|^{|n|}, & n < 0, \\ |\lambda_1^{(B)}(\omega)|^{|n|}, & n > 0, \end{cases}$$

where $\lambda_1^{(A)}$ is the eigenvalue of $T_p^{(A)}$ satisfying $|\lambda_1^{(A)}(\omega)| < 1$ and $\lambda_1^{(B)}$ is the eigenvalue of $T_p^{(B)}$ satisfying $|\lambda_1^{(B)}(\omega)| < 1$. We observe how the eigenmode follows the decay rate of the eigenvalue envelope as $|x| \to \infty$. This is the expected behaviour indicated by Theorem 3.6.3.

3.8. Conclusion

Using the mirror symmetry and the underlying periodic structure of the mathematical setting considered, we have shown in Chapter 2 that localised interface modes exist for undamped materials with real frequencies. Having this as starting point, we prove the existence of localised modes for undamped materials with complex frequencies. Viewing the damped system as a perturbation regime of the undamped one by considering small dampings, with Rouché's theorem, we are also able to show the existence of localised modes for the damped case as well. Finally, we adapted the transfer matrix method to the case of damped systems and obtained the asymptotic behaviour of the localised modes, as $|x| \to \infty$, in terms of the eigenvalues of the transfer matrix of each material.

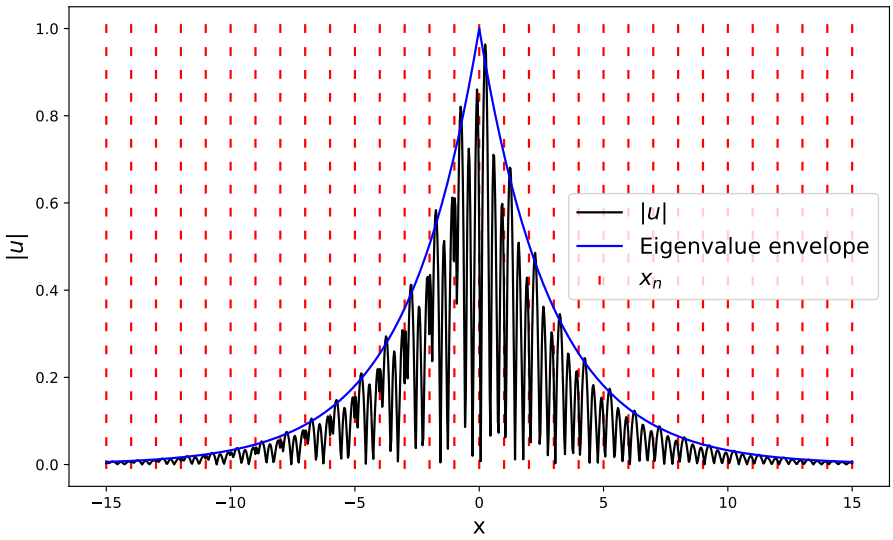

Figure 3.3.: For fixed damping, we see the behaviour of an interface localised mode as $|x| \to \infty$, for the damped system considered in Section 3.7. The eigenvalue envelope shows the decay rates in terms of the eigenvalues of the transfer matrices, as described in Theorem 3.6.3.

4. Subwavelength halide perovskite resonators

4.1. Introduction

Halide perovskites are materials which are increasingly being used in optical devices. Their underlying chemistry consists of octohedral-shaped crystalline lattices containing atoms of heavier halides, such as chlorine, bromine and iodine [2]. When used in microscopic devices, their high absorption coefficient helps absorb the complete visible spectrum. This, combined with the fact that they are cheap and easy to manufacture, means they are playing a prominent role in the production of electromagnetic devices [36, 38, 52, 64, 72].

The dielectric permittivity of a halide perovskite, denoted by ε, show the highly non-linear character of these materials. It depends on both the frequency ω of the system and the wavenumber k, while damping is also present. We will consider the following simplified form of ε:

$$\varepsilon(\omega, k) = \varepsilon_0 + \frac{\alpha}{\beta - \omega^2 + \eta k^2 - i\gamma\omega}, \tag{4.1}$$

where $\alpha, \beta, \gamma, \eta$ are the material parameters, taken to be positive constants.

Dielectric nano-particles, and other electromagnetic metamaterials, have been studied using various techniques. In the case of extreme material parameters, such as small particle size or large material contrast, asymptotic methods can be used [8, 9, 18, 34]. Likewise, homogenisation has been used to characterise materials with periodic micro-structures [22, 37]. Multiple scattering formulations are popular, particularly when a convenient choice of geometry (e.g. cylindrical or spherical resonators) facilitates explicit formulas [70]. We will use integral methods to study a general class of geometries and will extend the previous theory, e.g. [8], to the case of dispersive materials.

For simplicity, let us consider the Helmholtz equation as a model of the propagation of time-harmonic waves. We will use an approach based on representing the scattered solution using a Lippmann-Schwinger integral formulation and then using asymptotic methods to characterise the resonant frequencies in terms of the eigenvalues of the resulting integral operator (which turns out to be the Newtonian potential). This approach can handle a very general class of resonator shapes and can be adapted to study solutions to the Maxwell's equations [17]. A similar method

was used in [8] for a simpler, non-dispersive setting. We will show that the asymptotic theory developed in [8] and elsewhere can be developed to model real-world settings and can be used to influence high-impact design problems.

We will first introduce the problem setting and retrieve its integral formulation. Then, we will study the one particle case for three and two dimensions, using integral techniques to formulate the subwavelength resonant problem and asymptotic approximations to study the resonant frequencies. Using these methods, we describe the hybridisation of two halide perovskite resonators. Again, we treat the three- and two-dimensional cases separately. Passing from the integral to a matrix formulation of the problem, we obtain the hybridised subwavelength resonant frequencies. Finally, we examine the case of spherical resonators, making use of the fact that eigenvalues and eigenfunctions of the Newtonian potential can be computed explicitly in this case (see also [41]). We show that our findings are qualitatively consistent with the ones of [8]. Hence, we show that the asymptotic techniques used in [8] can be generalised to less straightforward and more impactful physical settings. This chapter is from the work carried in [3].

4.2. Single Resonators

In this section, we present the Helmholtz formulation of the mathematical problem considered for one halide perovskite subwavelength resonator. We present the integral methods used for both the two- and three-dimensional case and, using asymptotic analysis techniques, we provide formulas for the subwavelength resonances.

4.2.1. Problem Setting

Consider a single resonator occupying a bounded domain $\Omega \subset \mathbb{R}^d$, for $d \in \{2, 3\}$. We assume that the particle is non-magnetic, so that the magnetic permeability μ_0 is constant on all of $\mathbb{R}^d$. We will consider a time-harmonic wave with frequency $\omega \in \mathbb{C}$ (which we assume to have positive real part). The wavenumber in the background $\mathbb{R}^d \setminus \overline{\Omega}$ is given by $k_0 := \omega\varepsilon_0\mu_0$ and we will use k to denote the wavenumber within Ω. We, then, consider the following Helmholtz model for light propagation:

$$\begin{cases} \Delta u + \omega^2 \varepsilon(\omega, k)\mu_0 u = 0 & \text{in } \Omega, \\ \Delta u + k_0^2 u = 0 & \text{in } \mathbb{R}^d \setminus \overline{\Omega}, \\ u|_+ - u|_- = 0 & \text{on } \partial\Omega, \\ \frac{\partial u}{\partial \nu}|_+ - \frac{\partial u}{\partial \nu}|_- = 0 & \text{on } \partial\Omega, \\ u(x) - u_{in}(x) & \text{satisfies the outgoing radiation condition as } |x| \to \infty, \end{cases} \tag{4.2}$$

where u_{in} is the incident wave, assumed to satisfy

$$(\Delta + k_0^2)u_{in} = 0 \quad \text{in } \mathbb{R}^d,$$

and the appropriate outgoing radiation condition is the Sommerfeld radiation condition, which requires that

$$\lim_{|x|\to\infty} |x|^{\frac{d-1}{2}} \left(\frac{\partial}{\partial |x|} - ik_0 \right) (u(x) - u_{in}(x)) = 0. \tag{4.3}$$

In particular, we are interested in the case of small resonators. Thus, we will assume that there exists some fixed, smooth and bounded domain D, containing the origin, such that Ω is given by

$$\Omega = \delta D + z, \tag{4.4}$$

for some position $z \in \mathbb{R}^d$ and characteristic size $0 < \delta \ll 1$. Then, making a change of variables, the Helmholtz problem (4.2) becomes

$$\begin{cases} \Delta u + \delta^2 \omega^2 \varepsilon(\omega, k) \mu_0 u = 0 & \text{in } D, \\ \Delta u + \delta^2 k_0^2 u = 0 & \text{in } \mathbb{R}^d \setminus \overline{D}, \end{cases} \tag{4.5}$$

along with the same transmission conditions on ∂D and far-field behaviour. The behaviour of resonators which is of interest is when $\delta \ll k_0^{-1}$, meaning that the system can be described as being *subwavelength*. We will study this by performing asymptotics in the regime that the frequency ω is fixed while the size $\delta \to 0$.
We will characterise solutions to (4.2) in terms of the system's resonant frequencies. For a given wavenumber k, we define $\omega = \omega(k)$ to be a *resonant frequency* if it is such that there exists a non-trivial solution u to (4.2) in the case that $u_{in} = 0$.

4.2.2. Integral Formulation

Let $G(x, k)$ be the outgoing Helmholtz Green's function in $\mathbb{R}^d$, defined as the unique solution to

$$(\Delta + k^2) G(x, k) = \delta_0(x) \quad \text{in } \mathbb{R}^d,$$

along with the outgoing radiation condition (4.3). It is well known that G is given by

$$G(x, k) = \begin{cases} -\frac{i}{4} H_0^{(1)}(k|x|), & d = 2, \\ -\frac{e^{ik|x|}}{4\pi |x|}, & d = 3, \end{cases} \tag{4.6}$$

where $H_0^{(1)}$ is the Hankel function of first kind and order zero.

Theorem 4.2.1 (Lippmann-Schwinger Integral Representation Formula)**.** *The solution to the Helmholtz problem (4.2) is given by*

$$u(x) - u_{in}(x) = -\delta^2 \omega^2 \xi(\omega, k) \int_D G(x - y, \delta k_0) u(y) \mathrm{d}y, \quad x \in \mathbb{R}^d, \tag{4.7}$$

where the function $\xi : \mathbb{C} \to \mathbb{C}$ describes the permittivity contrast between D and the background and is given by

$$\xi(\omega, k) = \mu_0 (\varepsilon(\omega, k) - \varepsilon_0).$$

Proof. We see from (4.5) that $\Delta u + \delta^2\omega^2\varepsilon(\omega,k)\mu_0 u = 0$ in D, so it holds that

$$\Delta u + \delta^2 k_0^2 u = -\delta^2\omega^2\xi(\omega,k)u,$$

where $\xi(\omega,k) = \mu_0(\varepsilon(\omega,k) - \varepsilon_0)$. Therefore, the Helmholtz problem (4.5) becomes

$$(\Delta + \delta^2 k_0^2)(u(y) - u_{in}(y)) = -\delta^2\omega^2\xi(\omega,k)u(y)\chi_D(y), \quad y \in \mathbb{R}^d \setminus \partial D,$$

with χ_D being the indicator function of the set D. Then, we know that for $x \in \mathbb{R}^d$ and $y \in \mathbb{R}^d \setminus \partial D$, the following identity holds:

$$\begin{aligned}\nabla_y \cdot \Big[G(x-y,\delta k_0)\nabla_y\Big(u(y) - u_{in}(y)\Big) - \Big(u(y) - u_{in}(y)\Big)\nabla_y G(x-y,\delta k_0)\Big] \\ = -\delta^2\omega^2\xi(\omega,k)u(y)G(x-y,\delta k_0)\chi_D(y) - \Big(u(y) - u_{in}(y)\Big)\delta_0(x-y).\end{aligned}$$

Let S_R be a large sphere with radius R large enough so that $D \subset S_R$. Integrating the above identity over $y \in S_r \setminus \partial D$ and letting $R \to +\infty$, we can use the radiation condition (4.3) in the far field and the transmission conditions on ∂D to obtain the desired integral representation formula. □

We are interested in understanding how the formula from Theorem 4.2.1 behaves in the case that δ is small. In particular, we wish to understand the operator $K_D^{\delta k_0} : L^2(D) \to L^2(D)$ given by

$$K_D^{\delta k_0}[u](x) = -\int_\Omega G(x-y,\delta k_0)u(y)\mathrm{d}y, \qquad x \in D. \tag{4.8}$$

The Helmholtz Green's function has helpful asymptotic expansions which facilitate this. However, the behaviour is quite different in two and three dimensions, so we must now consider these two settings separately. We will first work on the three-dimensional case, and then treat the two-dimensional setting as the asymptotic expansions are more complicated.

4.2.3. Reformulation as a Subwavelength Resonance Problem

In order to reveal the behaviour of the system of nano-particles, we will characterise the properties of the operator $K_D^{\delta k_0}$. We observe that the Lippmann-Schwinger formulation (4.7) of the problem is equivalent to

$$(u - u_{in})(x) = \delta^2\omega^2\xi(\omega,k)K_D^{\delta k_0}[u](x).$$

This is equivalent to

$$(I - \delta^2\omega^2\xi(\omega,k)K_D^{\delta k_0})[u](x) = u_{in}(x),$$

which gives

$$u(x) = (I - \delta^2\omega^2\xi(\omega,k)K_D^{\delta k_0})^{-1}[u_{in}](x),$$

for all $x \in D$, where I denotes the identity operator. Then, the subwavelength resonance problem is to find $\omega \in \mathbb{C}$ close to 0, such that the operator $(I-\delta^2\omega^2\xi(\omega,k)K_D^{\delta k_0})^{-1}$ is singular, or equivalently, such that there exists $u \in L^2(D)$, $u \neq 0$ with

$$u(x) - \delta^2\omega^2\xi(\omega,k)\int_D G(x-y,\delta k_0)u(y)\mathrm{d}y = 0, \quad \text{for } x \in D. \tag{4.9}$$

4.2.4. Three Dimensions

We consider the three-dimensional case, $d = 3$. Let us define the Newtonian potential on D to be $K_D^{(0)} : L^2(D) \to L^2(D)$ such that

$$\begin{aligned} K_D^{(0)}[u](x) :&= -\int_D u(y)G(x-y,0)\mathrm{d}y \\ &= -\frac{1}{4\pi}\int_D \frac{1}{|x-y|}u(y)\mathrm{d}y. \end{aligned} \tag{4.10}$$

Similarly, we define the operators $K_D^{(n)} : L^2(D) \to L^2(D)$, for $n = 1, 2, \ldots$, as

$$K_D^{(n)}[u](x) = -\frac{i}{4\pi}\int_D \frac{(i|x-y|)^{n-1}}{n!}u(y)\mathrm{d}y. \tag{4.11}$$

Then, in order to capture the behaviour of $K_D^{\delta k_0}$ for small δ, we can use an asymptotic expansion in terms of small δ.

Lemma 4.2.2. *Suppose that $d = 3$. The operator $K_D^{\delta k_0}$ can be rewritten as*

$$K_D^{\delta k_0} = \sum_{n=0}^{\infty}(\delta k_0)^n K_D^{(n)},$$

where the series converges in the $L^2(D) \to L^2(D)$ operator norm if δk_0 is small enough.

Proof. This follows from an application of the Taylor expansion on the operator $K_D^{\delta k_0}$. Indeed, using Taylor expansion on the second variable of G, we can see that

$$G(x-y,\delta k_0) = \sum_{n=0}^{\infty}(\delta k_0)^n \frac{\partial^n G}{\partial k^n}(x-y,k)\Big|_{k=0}.$$

Since we are working in three dimensions,

$$G(x,k) = -\frac{e^{ik|x|}}{4\pi|x|}$$

and thus,

$$G(x-y,0) = -\frac{1}{4\pi|x-y|}$$

and

$$\frac{\partial^n G}{\partial k^n}(x-y,k) = -\frac{i}{4\pi}\frac{(i|x-y|)^{n-1}}{n!}, \quad \text{for } n>0.$$

Hence,

$$\begin{aligned} G(x-y,\delta k_0) &= \sum_{n=0}^{\infty}(\delta k_0)^n \frac{\partial^n G}{\partial k^n}(x-y,k)\Big|_{k=0} \\ &= \sum_{n=0}^{\infty}(\delta k_0)^n \left(-\frac{i}{4\pi}\right)\frac{(i|x-y|)^{n-1}}{n!} \end{aligned}$$

and then, multiplying by u and integrating over D, gives

$$K_D^{\delta k_0}[u](y) = \sum_{n=0}^{\infty}(\delta k_0)^n K_D^{(n)}[u](y),$$

which is the desired result. □

4.2.4.1. Eigenvalue Calculation

In order to study the operator $K_D^{\delta k_0}$, we need to find its eigenvalues. From Lemma 4.2.2, if k_0 is fixed then we can write our operator as

$$K_D^{\delta k_0} = K_D^{(0)} + \delta k_0 K_D^{(1)} + O(\delta^2) \quad \text{as } \delta \to 0. \tag{4.12}$$

Since we know that $K_D^{(0)}$ is self-adjoint, we know that it admits eigenvalues. Let us denote such an eigenvalue by λ_0, and by u_0 the associated eigenvector. Let us now consider the problem

$$K_D^{\delta k_0} u_\delta = \lambda_\delta u_\delta, \tag{4.13}$$

where λ_δ denotes an eigenvalue of the operator $K_D^{\delta k_0}$ and u_δ denotes the associated eigenvector. The compactness of the operator $K_D^{\delta k_0}$ gives us the existence of isolated eigenvectors. We wish to express λ_δ as a function of λ_0, for small values of δ, which is a classical idea in perturbation theory. This is possible, since $K_D^{(0)}$ is a compact operator and hence, all the eigenvalues are isolated, except from 0. Using this eigenvalue problem, we will find the resonant frequency ω_s and the associated wavenumber k_s of the halide perovskite nano-particle.

Proposition 4.2.3. *Let λ_δ denote a non-zero eigenvalue of the operator $K_D^{\delta k_0}$ in dimension three. Then, if δ is small, it is approximately given by*

$$\lambda_\delta \approx \lambda_0 + \delta k_0 \langle K_D^{(1)} u_0, u_0\rangle. \tag{4.14}$$

Proof. Using Theorem 2.3 of [42], eigenvalue perturbation formulas of this kind are straightforward to obtain, provided that the unperturbed eigenvalue is semi-simple. Since $K_D^{(0)}$ is compact, all its non-zero eigenvalues are simple and isolated. Consequently, we know that there exists an expansion of the form $\lambda_\delta = \lambda_0 + \delta A$, for some constant A which it remains to calculate. We start by truncating the $O(\delta^2)$ term in the expansion (4.12). Then, we have that

$$\begin{aligned} K_D^{\delta k_0} u_\delta = \lambda_\delta u_\delta \;&\Leftrightarrow\; \left(K_D^{(0)} + \delta k_0 K_D^{(1)}\right) u_\delta = \lambda_\delta u_\delta \\ &\Leftrightarrow\; \langle \left(K_D^{(0)} + \delta k_0 K_D^{(1)}\right) u_\delta, u_0 \rangle = \langle \lambda_\delta u_\delta, u_0 \rangle. \end{aligned}$$

Since $K_D^{(0)}$ is self-adjoint, we have that

$$\lambda_0 \langle u_\delta, u_0 \rangle + \delta k_0 \langle K_D^{(1)} u_\delta, u_0 \rangle = \lambda_\delta \langle u_\delta, u_0 \rangle.$$

Finally, since $u_\delta \approx u_0$ we find that

$$\begin{aligned} \lambda_\delta &= \lambda_0 + \delta k_0 \frac{\langle K_D^{(1)} u_\delta, u_0 \rangle}{\langle u_\delta, u_0 \rangle} \\ &\approx \lambda_0 + \delta k_0 \langle K_D^{(1)} u_0, u_0 \rangle, \end{aligned}$$

which is the desired result. □

The following corollary is a direct consequence of Proposition 4.14.

Corollary 4.2.4. *Let λ_δ denote an eigenvalue of the operator $K_D^{\delta k_0}$ in three dimensions. Then, if δ is small, it is approximately given by*

$$\lambda_\delta \approx \lambda_0 - \frac{i}{4\pi} \delta k_0 \mathbb{B}, \tag{4.15}$$

where $\mathbb{B} := (\int_D u_0(y) \mathrm{d}y)^2$ is a constant.

Proof. From (4.11), we get that

$$\begin{aligned} K_D^{(1)}[u](x) &= -\frac{i}{4\pi} \int_D \frac{(i|x-y|)^{1-1}}{1!} u(y) \mathrm{d}y \\ &= -\frac{i}{4\pi} \int_D u(y) \mathrm{d}y. \end{aligned}$$

Let us define the constant $\mathbb{B} := (\int_D u_0(y) \mathrm{d}y)^2$. Then, we observe that

$$\begin{aligned} \langle K_D^{(1)} u_0, u_0 \rangle &= \int_D \left(-\frac{i}{4\pi}\right) u_0(y) \int_D \overline{u_0}(x) \mathrm{d}x \mathrm{d}y \\ &= -\frac{i}{4\pi} \left(\int_D u_0(y) \mathrm{d}y \right)^2 \\ &= -\frac{i}{4\pi} \mathbb{B}. \end{aligned}$$

Substituting into (4.14) gives the desired result. □

4.2.4.2. Frequency and wavenumber

Let us now find the resonant frequency ω_δ and wavenumber k_δ associated to this eigenvalue, which will also constitute the basis of our analysis of the operator $K_D^{\delta k_0}$. From (4.9), we see that if $u = u_\varepsilon$, then $1 = \delta^2\omega^2\xi(\omega, k)\lambda_\delta$ so, using Corollary 4.15 we have that

$$\varepsilon(\omega, k) = \frac{1}{\mu_0\delta^2\omega^2\left(\lambda_0 - \frac{i}{4\pi}\delta k_0\mathbb{B}\right)} + \varepsilon_0. \tag{4.16}$$

In order to study halide perovskite particles, we want the permittivity $\varepsilon(\omega, k)$ to be given by (4.1), that is,

$$\varepsilon(\omega, k) = \varepsilon_0 + \frac{\alpha}{\beta - \omega^2 + \eta k^2 - i\gamma\omega}, \tag{4.17}$$

where $\alpha, \beta, \gamma, \eta$ are positive constants. Comparing the two expressions (4.16) and (4.17) we see that

$$\begin{cases} \alpha\mu_0\delta^2\omega^2\lambda_0 - \beta + \omega^2 - \eta k^2 = 0, \\ \gamma\omega - \mu_0\frac{1}{4\pi}\alpha\delta^3\omega^2 k_0\mathbb{B} = 0. \end{cases} \tag{4.18}$$

We study these two equations separately. First, we look at the second equation of (4.18). We have that

$$\omega\left(\gamma - \mu_0\frac{1}{4\pi}\alpha\delta^3\omega k_0\mathbb{B}\right) = 0,$$

meaning that

$$\omega = 0 \quad \text{or} \quad \omega = \frac{4\pi\gamma}{\alpha\mu_0\delta^3 k_0\mathbb{B}}.$$

For $\omega = \frac{4\pi\gamma}{\alpha\mu_0\delta^3 k_0\mathbb{B}}$, we obtain that

$$\eta k^2 = (1 + \alpha\mu_0\delta^2\lambda_0)\omega^2 - \beta,$$

which has solutions

$$k = \pm\sqrt{\frac{16\pi^2\gamma^2(1 + \alpha\mu_0\delta^2\lambda_0)}{\alpha^2\mu_0^2\delta^6 k_0^2\mathbb{B}^2\eta} - \frac{\beta}{\eta}}. \tag{4.19}$$

The case of $\omega = 0$ is not of physical interest here. Thus, denoting this specific frequency by ω_δ and the associated wavenumber by k_δ, we will work with

$$\omega_\delta = \frac{4\pi\gamma}{\alpha\mu_0\delta^3 k_0\mathbb{B}} \quad \text{and} \quad k_\delta = \sqrt{\frac{16\pi^2\gamma^2(1 + \alpha\mu_0\delta^2\lambda_0)}{\alpha^2\mu_0^2\delta^6 k_0^2\mathbb{B}^2\eta} - \frac{\beta}{\eta}}, \tag{4.20}$$

where we have chosen the wavenumber k_δ to be positive.

4.2.4.3. Asymptotic analysis

Let us now return to the problem of studying the singularities of the operator $(I - \delta^2\omega^2\xi(\omega,k)K_D^{\delta k_0})^{-1}$. We have the following equivalence:

$$(I - \delta^2\omega^2\xi(\omega,k)K_D^{\delta k_0})^{-1} = 0 \;\Leftrightarrow\; \left(I - \delta^2\omega^2\xi(\omega,k)\sum_{n=0}^{\infty}(\delta k_0)^n K_D^{(n)}\right)^{-1} = 0.$$

We define

$$A_n := \delta^2\omega^2\xi(\omega,k)K_D^{(n)} = -\delta^2\omega^2\xi(\omega,k)\frac{i}{4\pi}\int_D \frac{(i|x-y|)^{n-1}}{n!}u(y)\mathrm{d}y.$$

Then, it holds that

$$\begin{aligned}\left(I - \delta^2\omega^2\xi(\omega,k)\sum_{n=0}^{\infty}(\delta k_0)^n K_D^{(n)}\right)^{-1} &= \left(I - \sum_{n=0}^{\infty}(\delta k_0)^n A_n\right)^{-1}\\ &= \sum_{i=0}^{\infty}\left((I - A_0 - \delta k_0 A_1)^{-1}\sum_{n=2}^{\infty}(\delta k_0)^n A_n\right)^i (I - A_0 - \delta k_0 A_1)^{-1}\\ &= (I - A_0 - \delta k_0 A_1)^{-1} +\\ &\quad + (I - A_0 - \delta k_0 A_1)^{-1}(\delta k_0)^2 A_2 (I - A_0 - \delta k_0 A_1)^{-1} + O(\delta^4).\end{aligned}$$

Thus, the above equivalence yields

$$(I - \delta^2\omega^2\xi(\omega,k)K_D^{\delta k_0})^{-1} = 0 \;\Leftrightarrow\; \left(I - \delta^2\omega^2\xi(\omega,k)\sum_{n=0}^{\infty}(\delta k_0)^n K_D^{(n)}\right)^{-1} = 0 \;\Leftrightarrow$$
$$(I - A_0 - \delta k_0 A_1)^{-1} + (I - A_0 - \delta k_0 A_1)^{-1}(\delta k_0)^2 A_2 (I - A_0 - \delta k_0 A_1)^{-1} + O(\delta^4) = 0.$$

Using this expression, we obtain the following proposition.

Proposition 4.2.5. *Let $d = 3$ and let ω_δ be defined by (4.20). Then, as $\delta \to 0$, the $O(\delta^4)$ approximation of the subwavelength resonant frequencies ω_s and the associated wavenumbers k_s of the single halide perovskite resonator $\Omega = \delta D + z$ satisfy*

$$1 - \delta^2\omega_s^2\xi(\omega_s,k_s)\lambda_\delta = -\delta^4 k_0^2\omega_s^2\xi(\omega_s,k_s)\langle K_D^{(2)}[u_\delta], u_\delta\rangle. \tag{4.21}$$

Proof. For $\psi \in L^2(D)$, and dropping the $O(\delta^4)$ term, we have

$$\Big[(I - A_0 - \delta k_0 A_1)^{-1} + (I - A_0 - \delta k_0 A_1)^{-1}(\delta k_0)^2 A_2 (I - A_0 - \delta k_0 A_1)^{-1}\Big][\psi] = 0. \tag{4.22}$$

We apply a pole-pencil decomposition, as it is defined in [14], to the term $(I - A_0 - \delta k_0 A_1)^{-1}[\psi]$ and obtain

$$(I - A_0 - \delta k_0 A_1)^{-1}[\psi] = \frac{\langle u_\delta, \psi\rangle u_\delta}{1 - \delta^2\omega_s^2\xi(\omega_s,k_s)\lambda_\delta} + R(\delta)[\psi],$$

where the remainder term $R(\delta)[\psi]$ can be dropped. Hence, (4.22) is, at leading order, equivalent to

$$\frac{\langle u_\delta, \psi\rangle u_\delta}{1-\delta^2\omega^2\xi(\omega_s,k_s)\lambda_\delta} + \frac{\langle u_\delta, \psi\rangle u_\delta}{1-\delta^2\omega_s^2\xi(\omega_s,k_s)\lambda_\delta}(\delta k_0)^2 A_2 \frac{\langle u_\delta, \psi\rangle u_\delta}{1-\delta^2\omega_s^2\xi(\omega_s,k_s)\lambda_\delta} = 0,$$

which reduces to

$$\frac{u_\delta}{1-\delta^2\omega_s^2\xi(\omega_s,k_s)\lambda_\delta} + \frac{u_\delta\langle K_D^{(2)}[u_\delta], u_\delta\rangle}{(1-\delta^2\omega_s^2\xi(\omega_s,k_s)\lambda_\delta)^2}\delta^4 k_0^2\omega_s^2\xi(\omega_s,k_s) = 0,$$

which can be rearranged to give the desired result. □

Remark 4.2.6. *In the appendix, we will recover a formula for* $\langle K_D^{(2)}[u_\delta], u_\delta\rangle$.

Before we move on to the consequences of this proposition, we recall that

$$K_D^{(2)}[u](x) = -\frac{i}{4\pi}\int_D \frac{i|x-y|}{2}u(y)\mathrm{d}y = \frac{1}{8\pi}\int_D |x-y|u(y)\mathrm{d}y.$$

Thus, we can define the constant $\mathbb{F}$ to be such that

$$\langle K_D^{(2)}[u_\delta], u_\delta\rangle = \int K_D^{(2)}[u_\delta](x)\overline{u_\delta}(x)\mathrm{d}x = \frac{1}{8\pi}\int_D\int_D |x-y|u_\delta(y)\overline{u_\delta}(x)\mathrm{d}y\mathrm{d}x =: \frac{1}{8\pi}\mathbb{F}.$$

So, from (4.21), we see that

$$1-\delta^2\omega_s^2\xi(\omega_s,k_s)\lambda_\delta = -\frac{\delta^4 k_0^2\omega_s^2\xi(\omega_s,k_s)}{8\pi}\mathbb{F}. \tag{4.23}$$

Then, the following two corollaries are immediate consequences of the Proposition 4.2.5.

Corollary 4.2.7. *Let* $d = 3$. *Then, as* $\delta \to 0$, *the* $O(\delta^8)$ *approximation of the subwavelength resonant frequencies of the halide perovskite resonator* $\Omega = \delta D + z$ *are given by*

$$1 - \frac{\omega_s^2}{\omega_\delta^2}\lambda_\delta(\varepsilon(\omega_s,k_s)-\varepsilon_0)\frac{64\pi^2\gamma^2}{\alpha^2\mu_0\delta^4 k_0^2\mathbb{B}^2} = -\frac{\delta^4\omega_s^2 k_0^2\xi(\omega_s,k_s)}{8\pi}\mathbb{F}. \tag{4.24}$$

Proof. By a direct calculation and using (4.20), we have

$$\begin{aligned}
1-\delta^2\omega_s^2\xi(\omega_s,k_s)\lambda_\delta &= 1-\delta^2\omega_s^2\mu_0(\varepsilon(\omega_s,k_s)-\varepsilon_0)\lambda_\delta \\
&\overset{(4.20)}{=} 1-\delta^2\frac{\omega_s^2}{\omega_\delta^2}\mu_0(\varepsilon(\omega_s,k_s)-\varepsilon_0)\lambda_\delta\frac{64\pi^2\gamma^2}{\alpha^2\mu_0^2\delta^4 k_0^2\mathbb{B}^2} \\
&= 1-\frac{\omega_s^2}{\omega_\delta^2}\lambda_\delta(\varepsilon(\omega_s,k_s)-\varepsilon_0)\frac{64\pi^2\gamma^2}{\alpha^2\mu_0\delta^4 k_0^2\mathbb{B}^2}.
\end{aligned}$$

Then, using (4.23), the result follows. □

Corollary 4.2.8. *Let $d = 3$. Then, as $\delta \to 0$, the $O(\delta^4)$ approximation of the subwavelength resonant frequencies of the halide perovskite resonator $\Omega = \delta D + z$ can be computed as*

$$1 - \delta^2 \omega_s^2 \xi(\omega_s, k_s)\lambda_\delta = -\frac{\omega_s^2}{\omega_\delta^2}(\varepsilon(\omega_s, k_s) - \varepsilon_0)\frac{8\pi\gamma^2\mathbb{F}}{\alpha^2\mu_0\delta^2\mathbb{B}^2}. \tag{4.25}$$

Proof. Again, we can calculate this directly:

$$\begin{aligned}\frac{\delta^4 k_0^2 \omega_s^2 \xi(\omega_s, k_s)}{8\pi}\mathbb{F} &= \frac{1}{8\pi}\delta^4\frac{\omega_s^2}{\omega_\delta^2}k_0^2\mu_0(\varepsilon(\omega_s, k_s) - \varepsilon_0)\omega_\delta^2 \\ &\overset{(4.20)}{=} \frac{1}{8\pi}\frac{\omega_s^2}{\omega_\delta^2}\delta^4 k_0^2\mu_0(\varepsilon(\omega_s, k_s) - \varepsilon_0)\frac{64\pi^2\gamma^2}{\alpha^2\mu_0^2\delta^4 k_0^2\mathbb{B}^2} \\ &= \frac{\omega_s^2}{\omega_\delta^2}(\varepsilon(\omega_s, k_s) - \varepsilon_0)\frac{8\pi\gamma^2}{\alpha^2\mu_0\delta^2\mathbb{B}^2}.\end{aligned}$$

Then, using (4.23), the result follows. □

We finish our analysis of the three-dimensional case with the following proposition.

Proposition 4.2.9. *Let $d = 3$. For ω close to the resonant frequency ω_s, the field scattered by the halide perovskite nano-particle $\Omega = \delta D + z$ can be approximated by*

$$u(x) - u_{in}(x) \approx \frac{1 + \delta^2\omega^2 G(x - z, \delta k_0)\xi(\omega, k)}{\delta^2\omega^2\left(\lambda_\delta - \lambda_0 + \frac{i}{4\pi}\delta k_0\mathbb{B}\right)\xi(\omega, k)}\langle u_{in}, u_\delta\rangle\int_D u_\delta, \quad x \in D,$$

for $|x - z| \gg \frac{2\pi}{\omega\sqrt{\varepsilon(\omega,k)\mu_0}}$.

Proof. Our goal is to find $u \in L^2(D)$, $u \neq 0$ such that (4.9) is satisfied. Using the pole-pencil decomposition, for $x \in D$, we can rewrite

$$\begin{aligned}u(x) - u_{in}(x) \approx &- \delta^2\omega^2\xi(\omega, k)G(x - z, \delta k_0)\frac{\langle u_{in}, u_\delta\rangle\int_D u_\delta}{1 - \delta^2\omega^2\xi(\omega, k)\lambda_\delta} + \\ &+ \delta^4 k_0^2\omega^2\xi(\omega, k)\frac{\langle K_D^{(2)}[u_\delta], u_\delta\rangle\langle u_{in}, u_\delta\rangle\int_D u_\delta}{(1 - \delta^2\omega^2\xi(\omega, k)\lambda_\delta)^2}.\end{aligned}$$

Using (4.21) and plugging it in the above expression, we obtain

$$\begin{aligned}u(x) - u_{in}(x) \approx\ & -\delta^2\omega^2\xi(\omega, k)G(x - z, \delta k_0)\frac{\langle u_{in}, u_\delta\rangle\int_D u_\delta}{-\delta^4 k_0^2\omega^2\xi(\omega, k)\langle K_D^{(2)}[u_\delta], \upsilon_\delta\rangle} \\ &+ \delta^4 k_0^2\omega^2\xi(\omega, k)\frac{\langle K_D^{(2)}[u_\delta], u_\delta\rangle\langle u_{in}, u_\delta\rangle\int_D u_\delta}{\delta^8 k_0^4\omega^4\xi(\omega, k)^2\langle K_D^{(2)}[u_\delta], \upsilon_\delta\rangle^2} \\ =\ & \frac{G(x - z, \delta k_0)\langle u_{in}, u_\delta\rangle\int_D u_\delta}{\delta^2 k_0^2\langle K_D^{(2)}[u_\delta], u_\delta\rangle} + \frac{\langle u_{in}, u_\delta\rangle\int_D u_\delta}{\delta^4 k_0^2\omega^2\xi(\omega, k)\langle K_D^{(2)}[u_\delta], u_\delta\rangle}.\end{aligned}$$

Thus, defining the constant $\mathbb{F} := 8\pi\langle K_D^{(2)}[u_\delta], u_\delta\rangle$, we obtain

$$u(x) - u_{in}(x) \approx \frac{8\pi\Big(1 + \delta^2\omega^2 G(x-z, \delta k_0)\xi(\omega,k)\Big)}{\delta^4 k_0^2 \omega^2 \xi(\omega,k)\mathbb{F}} \langle u_{in}, u_\delta\rangle \int_D u_\delta. \tag{4.26}$$

From Appendix A.3.1.1, we have that

$$\mathbb{F} = \frac{8\pi}{\delta^2 k_0^2}\left(\lambda_\delta - \lambda_0 + \frac{i}{4\pi}\delta k_0 \mathbb{B}\right).$$

Plugging it into (4.26), we obtain

$$\begin{aligned} u(x) - u_{in}(x) &\approx \\ &\approx \frac{8\pi\Big(1 + \delta^2\omega^2 G(x-z, \delta k_0)\xi(\omega,k)\Big)}{\delta^4 k_0^2 \omega^2 \xi(\omega,k)\mathbb{F}} \frac{\delta^2 k_0^2}{8\pi} \frac{1}{\lambda_\delta - \lambda_0 + \frac{i}{4\pi}\delta k_0 \mathbb{B}} \langle u_{in}, u_\delta\rangle \int_D u_\delta, \end{aligned}$$

from which the result follows. □

4.2.5. Two dimensions

We now turn our attention to the two-dimensional setting. We define the Newtonian potential on D, $K_D^{(0)} : L^2(D) \to L^2(D)$, by

$$K_D^{(0)}[u](x) := -\int_D u(y) G(x-y, 0)\mathrm{d}y = -\frac{1}{2\pi}\int_D \log|x-y| u(y)\mathrm{d}y.$$

We also define the operators $K_D^{(-1)} : L^2(D) \to L^2(D)$ and $K_D^{(n)} : L^2(D) \to L^2(D)$ by

$$K_D^{(-1)}[u](x) := -\frac{1}{2\pi}\int_D u(y)\mathrm{d}y$$

and

$$K_D^{(n)}[u](x) := \int_D \frac{\partial^n}{\partial k^n} G(x-y,k)\Big|_{k=0} u(y)\mathrm{d}y.$$

Then, from the asymptotic expansion of the Hankel function, we have the following result.

Lemma 4.2.10. *Suppose that $d = 2$. Then, for fixed $k_0 \in \mathbb{C}$, the operator $K_D^{\delta k_0}$ satisfies*

$$K_D^{\delta k_0} = \log(\delta k_0 \hat{\gamma}) K_D^{(-1)} + K_D^{(0)} + (\delta k_0)^2 \log(\hat{\gamma}\delta k_0) K_D^{(1)} + O(\delta^4 \log\delta), \tag{4.27}$$

as $\delta \to 0$, with convergence in the $L^2(D) \to L^2(D)$ operator norm and the constant $\hat{\gamma}$ being given by $\hat{\gamma} := \frac{1}{2}k_0 \exp(\gamma - \frac{i\pi}{2})$, where γ is the Euler constant.

4.2.5.1. Eigenvalue calculation

We use the same notation for u_δ as in Section 4.2.4.1. Let us consider the eigenvalue problem

$$K_D^{\delta k_0} u_\delta = \lambda_\delta u_\delta, \tag{4.28}$$

where λ_δ denotes a non-zero eigenvalue of the operator $K_D^{\delta k_0}$, and u_δ denotes an associated eigenvector. As in the case of dimension $d = 3$, we now wish to express λ_δ in terms of, for small values of δ. This is possible since $K_D^{(-1)}$ is a compact operator.

Proposition 4.2.11. *Let λ_δ denote a non-zero eigenvalue of the operator $K_D^{\delta k_0}$ in dimension 2. Then, for small δ, it is approximately given by*

$$\lambda_\delta \approx \log(\delta k_0 \hat{\gamma})\lambda_{-1} + \langle K_D^{(0)} u_{-1}, u_{-1}\rangle + (\delta k_0)^2 \log(\delta k_0 \hat{\gamma})\langle K_D^{(1)} u_{-1}, u_{-1}\rangle, \tag{4.29}$$

where λ_{-1} and u_{-1} are an eigenvalue and the associated eigenvector of the potential $K_D^{(-1)}$.

Proof. Since $K_D^{(-1)}$ is a compact operator, it has simple eigenvalues so we can use Theorem 2.3 of [42]. We start by dropping the $O(\delta^4 \log(\delta))$ term on the expansion (4.27). Then, we have that

$$\begin{aligned} K_D^{\delta k_0} u_\delta = \lambda_\delta u_\delta \;&\Leftrightarrow\; (\log(\delta k_0 \hat{\gamma}) K_D^{(-1)} + K_D^{(0)} + (\delta k_0)^2 \log(\delta k_0 \hat{\gamma}) K_D^{(1)}) u_\delta = \lambda_\delta u_\delta \\ &\Leftrightarrow\; \log(\delta k_0 \hat{\gamma})\lambda_{-1}\langle u_\delta, u_0\rangle + \langle K_D^{(0)} u_\delta, u_{-1}\rangle + \\ &\quad + (\delta k_0)^2 \log(\delta k_0 \hat{\gamma})\langle K_D^{(1)} u_\delta, u_{-1}\rangle = \lambda_\delta \langle u_\delta, u_{-1}\rangle. \end{aligned}$$

Therefore, assuming that $u_\delta \approx u_{-1}$, we can see that

$$\lambda_\delta \approx \log(\delta k_0 \hat{\gamma})\lambda_{-1} + \langle K_D^{(0)} u_{-1}, u_{-1}\rangle + (\delta k_0)^2 \log(\delta k_0 \hat{\gamma})\langle K_D^{(1)} u_{-1}, u_{-1}\rangle,$$

which is the desired result. □

The following corollary is a direct consequence of the above proposition.

Corollary 4.2.12. *Let λ_δ denote an eigenvalue of the operator $K_D^{\delta k_0}$ in dimension 2. Then, for small δ, it is approximately given by*

$$\lambda_\delta \approx \log(\delta k_0 \hat{\gamma})\lambda_{-1} - \frac{\mathbb{P}}{2\pi} - \frac{i(\delta k_0)^2 \log(\delta k_0 \hat{\gamma})\mathbb{G}}{4\pi}, \tag{4.30}$$

where $\mathbb{P}$ and $\mathbb{G}$ are constants that depend on u_{-1}.

Proof. We observe that

$$\begin{aligned}\langle K_D^{(0)} u_{-1}, u_{-1}\rangle &= \int_D \left(-\frac{1}{2\pi}\int_D \log|x-y| u_{-1}(y)\mathrm{d}y\right)\overline{u_{-1}}(x)\mathrm{d}x \\ &= -\frac{1}{2\pi}\int_D\int_D \log|x-y| u_{-1}(y)\overline{u_{-1}}(x)\mathrm{d}y\mathrm{d}x \\ &=: -\frac{1}{2\pi}\mathbb{P}.\end{aligned}$$

Then, for $u \in L^2(D)$,

$$\begin{aligned}K_D^{(1)}[u](x) &= \int_D \frac{\partial}{\partial k} G(x-y,k)\Big|_{k=0} u(y)\mathrm{d}y \\ &= \int_D \frac{\partial}{\partial k}\left(-\frac{i}{4}H_0^{(1)}(k|x-y|)\right)\Big|_{k=0} u(y)\mathrm{d}y \\ &= -\frac{i}{4\pi}\int_D \frac{u(y)}{|x-y|}\mathrm{d}y,\end{aligned}$$

and so, we have

$$\begin{aligned}\langle K_D^{(1)} u_{-1}, u_{-1}\rangle &= \int_D \left(-\frac{i}{4\pi}\int_D \frac{u_{-1}(y)}{|x-y|}\mathrm{d}y\right)\overline{u_{-1}}(x)\mathrm{d}x \\ &= -\frac{i}{4\pi}\int_D\int_D \frac{u_{-1}(y)\overline{u_{-1}}(x)}{|x-y|}\mathrm{d}y\mathrm{d}x \\ &=: -\frac{i}{4\pi}\mathbb{G}.\end{aligned}$$

Hence, from (4.29), we obtain the desired result. □

4.2.5.2. Frequency and wavenumber

Let us now find the frequency ω_δ and the wavenumber k_δ associated to this eigenvalue, which will also constitute the basis of our analysis of the operator $K_D^{\delta k_0}$. We see that (4.9) gives us that

$$1 = \delta^2\omega^2\xi(\omega,k)\lambda_\delta \;\Leftrightarrow\; 1 = \delta^2\omega^2\mu_0(\varepsilon(\omega,k)-\varepsilon_0)\lambda_\delta.$$

Using the expression (4.29) for λ_δ, we see that

$$\varepsilon(\omega,k) = \frac{1}{\mu_0\delta^2\omega^2\left(\log(\delta k_0\hat{\gamma})\lambda_{-1} - \frac{\mathbb{P}}{2\pi} - \frac{i(\delta k_0)^2\log(\delta k_0\hat{\gamma})\mathbb{G}}{4\pi}\right)} + \varepsilon_0.$$

Arguing in the same way as in Section 4.2.4.2 and comparing the two permittivity expressions, we obtain the following system:

$$\begin{cases} 4\pi\alpha\delta^2\omega^2\mu_0\log(\delta k_0\hat{\gamma})\lambda_{-1} - 2\mathbb{P}\alpha\delta^2\omega^2\mu_0 - 4\pi\beta + 4\pi\omega^2 - 4\pi\eta k^2 = 0, \\ -\alpha\delta^4\omega^2\mu_0 k_0^2\log(\delta k_0\hat{\gamma})\mathbb{G} + 4\pi\gamma\omega = 0. \end{cases} \tag{4.31}$$

From the second equation in (4.31), we see that

$$\omega(-\alpha\delta^4\omega\mu_0 k_0^2\log(\delta k_0\hat{\gamma})\mathbb{G}+4\pi\gamma)=0,$$

which shows us that

$$\omega=0 \quad \text{or} \quad \omega=\frac{4\pi\gamma}{\alpha\delta^4\mu_0 k_0^2\log(\delta k_0\hat{\gamma})\mathbb{G}}.$$

For $\omega=\frac{4\pi\gamma}{\alpha\delta^4\mu_0 k_0^2\log(\delta k_0\hat{\gamma})\mathbb{G}}$, we obtain the equation

$$\begin{aligned}&4\pi\alpha\delta^2\mu_0\lambda_{-1}\log(\delta k_0\hat{\gamma})\frac{16\pi^2\gamma^2}{\alpha^2\delta^8\mu_0^2k_0^4\log(\delta k_0\hat{\gamma})^2\mathbb{G}^2}-\\&-2\mathbb{P}\alpha\delta^2\mu_0\frac{16\pi^2\gamma^2}{\alpha^2\delta^8\mu_0^2k_0^4\log(\delta k_0\hat{\gamma})^2\mathbb{G}^2}-4\pi\beta+\\&+4\pi\frac{16\pi^2\gamma^2}{\alpha^2\delta^8\mu_0^2k_0^4\log(\delta k_0\hat{\gamma})^2\mathbb{G}^2}-4\pi\eta k^2=0,\end{aligned}$$

which has the solutions

$$k=\pm\sqrt{-\frac{\beta}{\eta}+\Big(2\pi\alpha\delta^2\mu_0\lambda_{-1}\log(\delta k_0\hat{\gamma})-\alpha\delta^2\mu_0\mathbb{P}+2\pi\Big)\frac{8\pi\gamma^2}{\eta\alpha^2\delta^8\mu_0^2k_0^4\log(\delta k_0\hat{\gamma})^2\mathbb{G}^2}}.$$

Yet again, we discard the case of $\omega=0$, as there is no physical interest. Denoting the frequency by ω_δ and the wavenumber by λ_δ, we will work with

$$\begin{aligned}\omega_\delta&=\frac{4\pi\gamma}{\alpha\delta^4\mu_0 k_0^2\log(\delta k_0\hat{\gamma})\mathbb{G}},\\k_\delta&=\sqrt{-\frac{\beta}{\eta}+\Big(2\pi\alpha\delta^2\mu_0\lambda_{-1}\log(\delta k_0\hat{\gamma})-\alpha\delta^2\mu_0\mathbb{P}+2\pi\Big)\frac{8\pi\gamma^2}{\eta\alpha^2\delta^8\mu_0^2k_0^4\log(\delta k_0\hat{\gamma})^2\mathbb{G}^2}},\end{aligned}\tag{4.32}$$

where we have chosen the wavenumber to be positive.

4.2.5.3. Asymptotic analysis

Let us consider ω near ω_δ, and define the coefficients

$$c_n=\begin{cases}\log(\delta k_0\hat{\gamma}), & n=-1,\\1, & n=0,\\(\delta k_0)^{2n}\log(\delta k_0\hat{\gamma}), & n\geq 1.\end{cases}$$

Then, we can write

$$K_D^{\delta k_0}=\sum_{n=-1}^{+\infty}c_nK_D^{(n)}.$$

We are interested in studying the singularities of the operator $(I-\delta^2\omega^2\xi(\omega,k)K_D^{\delta k_0})^{-1}$. Setting $B_n := \delta^2\omega^2\xi(\omega,k)K_D^{(n)}$, we find that $(I-\delta^2\omega^2\xi(\omega,k)K_D^{\delta k_0})^{-1}=0$ can be written as

$$\left(I-\sum_{n=-1}^{+\infty}c_nB_n\right)^{-1}=0,$$

which can be expanded to give

$$\left(I-\log(\delta k_0\hat{\gamma})B_{-1}-B_0-(\delta k_0)^2\log(\delta k_0\hat{\gamma})B_1-\sum_{n\geq 2}^{+\infty}c_nB_n\right)^{-1}=0,$$

which yields

$$\mathfrak{L}+\mathfrak{L}(\delta k_0)^4\log(\delta k_0\hat{\gamma})B_2\mathfrak{L}+O(\delta^6)=0,$$

where we have defined,

$$\mathfrak{L}:=\Big(I-\log(\delta k_0\hat{\gamma})B_{-1}-B_0-(\delta k_0)^2\log(\delta k_0\hat{\gamma})B_1\Big)^{-1}. \tag{4.33}$$

Using this expression, we have the following proposition.

Proposition 4.2.13. *Let $d=2$ and let ω_δ be defined by (4.32). Then, as $\delta\to 0$, the $O(\delta^4)$ approximations of the subwavelength resonant frequencies ω_s and the associated wavenumbers k_s of the single halide perovskite resonator $\Omega=\delta D+z$ satisfy*

$$1-\delta^2\omega_s^2\xi(\omega_s,k_s)\lambda_\delta=-\delta^6k_0^4\log(\delta k_0\hat{\gamma})\omega_s^2\xi(\omega_s,k_s)\langle K_D^{(2)}[u_\delta],u_\delta\rangle. \tag{4.34}$$

Proof. Applying a pole-pencil decomposition, we obtain

$$\Big(I-\log(\delta k_0\hat{\gamma})B_{-1}-B_0-(\delta k_0)^2\log(\delta k_0\hat{\gamma})B_1\Big)^{-1}[\cdot]=\frac{\langle\cdot,u_\delta\rangle u_\delta}{1-\delta^2\omega_s^2\xi(\omega_s,k_s)\lambda_\delta}+R(\omega_s)[\cdot],$$

where the remainder $R(\omega_s)$ is analytic in a neighborhood of ω_δ and can be dropped. Thus, dropping the $O(\delta^6)$ term, we find for $\psi\in L^2(D)$ that

$$\Big[\mathfrak{L}+\mathfrak{L}(\delta k_0)^4\log(\delta k_0\hat{\gamma})B_2\mathfrak{L}\Big](\psi)=0.$$

Applying a pole-pencil decomposition on (4.33), we get

$$\frac{\langle\psi,u_\delta\rangle u_\delta}{1-\delta^2\omega_s^2\xi(\omega_s,k_s)\lambda_\delta}+\frac{\langle\psi,u_\delta\rangle u_\delta}{1-\delta^2\omega_s^2\xi(\omega_s,k_s)\lambda_\delta}(\delta k_0)^4\log(\delta k_0\hat{\gamma})B_2\frac{\langle\psi,u_\delta\rangle u_\delta}{1-\delta^2\omega_s^2\xi(\omega_s,k_s)\lambda_\delta}=0.$$

This implies that

$$1-\delta^2\omega_s^2\xi(\omega_s,k_s)\lambda_\delta=-\delta^6k_0^4\log(\delta k_0\hat{\gamma})\omega_s^2\xi(\omega_s,k_s)\langle K_D^{(2)}[u_\delta],u_\delta\rangle,$$

which is the desired result. □

In order to obtain the associated consequences of this proposition, we observe that, since $d = 2$, we have that

$$\begin{aligned} K_D^{(2)}[u_\delta](x) &= \int_D \frac{\partial^2}{\partial k^2} G(x-y,k)\Big|_{k=0} u_\delta(y)\mathrm{d}y \\ &= \int_D \frac{\partial^2}{\partial k^2}\left(-\frac{i}{4}H_0^{(1)}(k|x|)\right)\Big|_{k=0} \\ &= -\frac{i}{4}\int_D -\frac{1}{\pi|x-y|^2}u_\delta(y)\mathrm{d}y \\ &= \frac{i}{4\pi}\int_D \frac{u_\delta(y)}{|x-y|^2}\mathrm{d}y. \end{aligned}$$

Hence,

$$\langle K_D^{(2)}[u_\delta], u_\delta\rangle = \int_D \left(\frac{i}{4\pi}\int_D \frac{u_\delta(y)}{|x-y|^2}\mathrm{d}y\right)\overline{u_\delta}(x)\mathrm{d}x \tag{4.35}$$

$$= \frac{i}{4\pi}\int_D\int_D \frac{u_\delta(y)\overline{u_\delta}(x)}{|x-y|^2}\mathrm{d}y\mathrm{d}x \tag{4.36}$$

$$=: \frac{i}{4\pi}\mathbb{S}. \tag{4.37}$$

So, we get that (4.34) is equivalent to

$$1-\delta^2\omega_s^2\xi(\omega_s,k_s)\lambda_\delta = \frac{-i\delta^6k_0^4\log(\delta k_0\hat{\gamma})\omega_s^2\xi(\omega_s,k_s)\mathbb{S}}{4\pi}. \tag{4.38}$$

Remark 4.2.14. *In Appendix A.3.1.2 of this paper, we recover a formula for* $\mathbb{S}$.

Then, the next two corollaries follow as immediate results.

Corollary 4.2.15. *Let* $d = 2$. *Then, as* $\delta \to 0$, *the* $O(\delta^{10}\log(\delta)^3)$ *approximation of the subwavelength resonant frequencies of the halide perovskite resonator* $\Omega = \delta D + z$ *can be computed as*

$$1-\frac{\omega_s^2}{\omega_\delta^2}\cdot\frac{16\pi^2\gamma^2\lambda_\delta\Big(\varepsilon(\omega_s,k_s)-\varepsilon_0\Big)}{\alpha^2\delta^6\mu_0k_0^4\log(\delta k_0\hat{\gamma})^2\mathbb{G}^2} = -\frac{i\delta^6k_0^4\log(\delta k_0\hat{\gamma})\omega_s^2\xi(\omega_s,k_s)\mathbb{S}}{4\pi}. \tag{4.39}$$

Proof. By a direct computation, we observe that

$$\begin{aligned} 1-\delta^2\omega_s^2\xi(\omega_s,k_s)\lambda_\delta &= 1-\delta^2\omega_s^2\mu_0\Big(\varepsilon(\omega_s,k_s)-\varepsilon_0\Big)\lambda_\delta\frac{\omega_\delta^2}{\omega_\delta^2} \\ &\overset{(4.32)}{=} 1-\delta^2\frac{\omega_s^2}{\omega_\delta^2}\mu_0\Big(\varepsilon(\omega_s,k_s)-\varepsilon_0\Big)\lambda_\delta\frac{16\pi^2\gamma^2}{\alpha^2\delta^8\mu_0^2k_0^4\log(\delta k_0\hat{\gamma})^2\mathbb{G}^2} \\ &= 1-\frac{\omega_s^2}{\omega_\delta^2}\cdot\frac{16\pi^2\gamma^2\lambda_\delta\Big(\varepsilon(\omega_s,k_s)-\varepsilon_0\Big)}{\alpha^2\delta^6\mu_0k_0^4\log(\delta k_0\hat{\gamma})^2\mathbb{G}^2}, \end{aligned}$$

and thus, (4.38) gives the desired result. □

Corollary 4.2.16. *Let $d = 2$. Then, as $\delta \to 0$, the $O(\delta^4 \log(\delta))$ approximation of the subwavelength resonant frequencies of the halide perovskite resonator $\Omega = \delta D + z$ can be computed as*

$$1 - \delta^2 \omega_s^2 \xi(\omega_s, k_s)\lambda_\delta = -\frac{\omega_s^2}{\omega_\varepsilon^2} \cdot \frac{4\pi i \mathbb{S}\gamma^2 \Big(\varepsilon(\omega_s, k_s) - \varepsilon_0\Big)}{\alpha^2 \delta^2 \log(\delta k_0 \hat{\gamma}) \mu_0 \mathbb{G}^2}. \tag{4.40}$$

Proof. Again, to show this, we need to make a straightforward calculation:

$$\begin{aligned}
\frac{i\delta^6 k_0^4 \log(\delta k_0 \hat{\gamma}) \omega_s^2 \xi(\omega_s, k_s)\mathbb{S}}{4\pi} &= \frac{i}{4\pi}\ \delta^6\ k_0^4\ \log(\delta k_0 \hat{\gamma})\ \frac{\omega_s^2}{\omega_\delta^2}\ \mathbb{S}\ \mu_0\ \Big(\varepsilon(\omega_s, k_s) - \varepsilon_0\Big)\ \omega_\delta^2 \\
&\overset{(4.32)}{=} \frac{i}{4\pi}\ \delta^6\ k_0^4\ \log(\delta k_0 \hat{\gamma})\ \frac{\omega_s^2}{\omega_\delta^2}\ \mathbb{S}\ \mu_0\ \Big(\varepsilon(\omega_s, k_s) - \varepsilon_0\Big)\ \frac{16\pi^2\gamma^2}{\alpha^2 \delta^8 \mu_0^2 k_0^4 \log(\delta k_0 \hat{\gamma})^2 \mathbb{G}^2} \\
&= \frac{\omega_s^2}{\omega_\varepsilon^2} \cdot \frac{4\pi i \mathbb{S}\gamma^2 \Big(\varepsilon(\omega_s, k_s) - \varepsilon_0\Big)}{\alpha^2 \delta^2 \log(\delta k_0 \hat{\gamma}) \mu_0 \mathbb{G}^2}.
\end{aligned}$$

Hence, (4.38) gives the desired result. □

We continue our analysis in the same way as in the previous case.

Proposition 4.2.17. *Let $d = 2$. For ω real close to the resonant frequency ω_s, the following approximation for the field scattered by the halide perovskite nano-particle $\Omega = \delta D + z$ holds:*

$$u(x) - u_{in}(x) \approx \frac{4\pi \Big(1 + \delta^2 \omega^2 \xi(\omega, k) G(x - z, \delta k_0)\Big)}{i\delta^6 k_0^4 \omega^2 \log(\delta k_0 \hat{\gamma}) \omega^2 \xi(\omega, k)\mathbb{S}} \langle u_{in}, u_\delta \rangle \int_D u_\delta, \quad x \in D, \tag{4.41}$$

for $|x - z| \gg \frac{2\pi}{\omega\sqrt{\varepsilon(\omega,k)\mu_0}}$.

Proof. As we mentioned at the beginning or our analysis, our goal is to find $u \in L^2(D)$, $u \neq 0$, such that (4.9) is satisfied. Using the pole-pencil decomposition on this Lippmann-Schwinger formulation of the problem, we can rewrite, for $x \in D$, as in Corollary 2.3 in [8],

$$\begin{aligned}
u(x) - u_{in}(x) \ \approx & - \delta^2 \omega^2 \xi(\omega, k) G(x - z, \delta k_0) \frac{\langle u_{in}, u_\delta \rangle \int_D u_\delta}{1 - \delta^2 \omega^2 \xi(\omega, k)\lambda_\delta} + \\
& + \delta^6 k_0^4 \log(\delta k_0 \hat{\gamma}) \omega^2 \xi(\omega, k) \frac{\langle K_D^{(2)}[u_\delta], u_\delta \rangle \langle u_{in}, u_\delta \rangle \int_D u_\delta}{\Big(1 - \delta^2 \omega^2 \xi(\omega, k)\lambda_\delta\Big)^2},
\end{aligned}$$

which, using (4.38), becomes:

$$u(x) - u_{in}(x) \ \approx \ \frac{G(x - z, \delta k_0)\langle u_{in}, u_\delta \rangle \int_D u_\delta}{\delta^4 k_0^4 \log(\delta k_0 \hat{\gamma}) \langle K_D^{(2)}[u_\delta], u_\delta \rangle} + \frac{\langle u_{in}, u_\delta \rangle \int_D u_\delta}{\delta^6 k_0^4 \omega^2 \log(\delta k_0 \hat{\gamma}) \omega^2 \xi(\omega, k) \langle K_D^{(2)}[u_\delta], u_\delta \rangle}.$$

From (4.35), this gives

$$u(x) - u_{in}(x) \;\approx\; \frac{4\pi\Big(1+\delta^2\omega^2\xi(\omega,k)G(x-z,\delta k_0)\Big)}{i\delta^6 k_0^4\omega^2\log(\delta k_0\hat{\gamma})\omega^2\xi(\omega,k)\mathbb{S}}\langle u_{in},u_\delta\rangle\int_D u_\delta,$$

which is the desired result. □

We finish our analysis with the following result.

Proposition 4.2.18. *Let $d=2$ and δ be small enough. Then, the $o(\delta^4)$ approximation of the subwavelength resonant frequencies ω_s of the halide perovskite nano-particle $\Omega=\delta D+z$ satisfies*

$$\begin{aligned}1-\delta^2\omega_s^2\xi(\omega_s,k_s)\Bigg(&-\frac{|D|}{2\pi}\log(\delta k_0\hat{\gamma})+\langle K_D^{(0)}[\hat{\mathbb{I}}_D],\hat{\mathbb{I}}_D\rangle+\\&+\delta^2k_0^2\log(\delta)\langle K_D^{(1)}[\hat{\mathbb{I}}_D],\hat{\mathbb{I}}_D\rangle\Bigg)=O\big(\delta^4\big),\end{aligned}\tag{4.42}$$

where $|D|$ is the volume of D and $\hat{\mathbb{I}}_D=\mathbb{I}_D/\sqrt{|D|}$.

Proof. We want to find $\omega_s\in\mathbb{C}$ such that

$$\Big(I-\delta^2\omega_s^2\xi(\omega_s,k_s)K_D^{\delta k_0}\Big)[u](x)=0,$$

which, for small δ, can be written as

$$\begin{aligned}\Bigg(I-\delta^2\omega_s^2\xi(\omega_s,k_s)\Big(\log(\delta k_0\hat{\gamma})K_D^{(-1)}+K_D^{(0)}+&(\delta k_0)^2\log(\delta k_0\hat{\gamma})K_D^{(1)}\Big)\Bigg)[u](x)=\\&=O\Big(\delta^6\log(\delta)\Big).\end{aligned}$$

Let us denote

$$M_D^{\delta k_0}:=\log(\delta k_0\hat{\gamma})K_D^{(-1)}+K_D^{(0)}+(\delta k_0)^2\log(\delta k_0\hat{\gamma})K_D^{(1)}.$$

We take $\nu(\delta)\in\sigma(M_D^{\delta k_0})$ and consider the eigenvalue problem for $M_D^{\delta k_0}$:

$$M_D^{\delta k_0}[\Psi]=\nu(\delta)\Psi.\tag{4.43}$$

We employ the ansatz

$$\begin{aligned}\Psi(\delta)&=\Psi_0+O\left(\frac{1}{\log(\delta)}\right),\\ \nu(\delta)&=\log(\delta)\nu_0+\nu_1+\delta^2\log(\delta)\nu_2+O\Big(\delta^2\Big).\end{aligned}$$

From (4.43) and the fact that $\delta^2\log(\delta k_0\hat{\gamma}) = \delta^2\log(\delta) + O(\delta^2)$ we have that

$$\Big(\log(\delta)K_D^{(-1)} + \log(k_0\hat{\gamma})K_D^{(-1)} + K_D^{(0)} + (\delta k_0)^2\log(\delta)K_D^{(1)}\Big)[\Psi_0] = \\ = \Big(\log(\delta)\nu_0 + \nu_1 + \delta^2\log(\delta)\nu_2\Big)[\Psi_0] + O\Big(\delta^2\Big).$$

Equating the $O(\log\delta)$ terms gives

$$\begin{aligned} K_D^{(-1)}[\Psi_0] = \nu_0\Psi_0 &\Rightarrow \nu_0\hat{\mathbb{I}}_D = K_D^{(-1)}[\hat{\mathbb{I}}_D] \\ &\Rightarrow \nu_0\hat{\mathbb{I}}_D = -\frac{|D|}{2\pi}\hat{\mathbb{I}}_D \\ &\Rightarrow \nu_0 = -\frac{|D|}{2\pi}. \end{aligned}$$

Then, equating the $O(1)$ terms gives

$$\log(k_0\hat{\gamma})K_D^{(-1)}[\hat{\mathbb{I}}_D] + K_D^{(0)}[\hat{\mathbb{I}}_D] = \nu_1\hat{\mathbb{I}}_D \Rightarrow \nu_1\hat{\mathbb{I}}_D = -\frac{|D|}{2\pi}\log(k_0\hat{\gamma})\hat{\mathbb{I}}_D + K_D^{(0)}[\hat{\mathbb{I}}_D] \\ \Rightarrow \nu_1 = -\frac{|D|}{2\pi}\log(k_0\hat{\gamma}) + \langle K_D^{(0)}[\hat{\mathbb{I}}_D], \hat{\mathbb{I}}_D\rangle.$$

Using the same reasoning for the $O\Big(\delta^2\log(\delta)\Big)$ terms, we get

$$\nu_2\hat{\mathbb{I}}_D = k_0^2K_D^{(1)}[\hat{\mathbb{I}}_D] \Rightarrow \nu_2 = k_0^2\langle K_D^{(1)}[\hat{\mathbb{I}}_D], \hat{\mathbb{I}}_D\rangle.$$

Thus,

$$\begin{aligned} \nu(\delta) &= \log(\delta)\nu_0 + \nu_1 + \delta^2\log(\delta)\nu_2 + O\Big(\delta^2\Big) \\ &= -\frac{|D|}{2\pi}\log(\delta) - \frac{|D|}{2\pi}\log(k_0\hat{\gamma}) + \langle K_D^{(0)}[\hat{\mathbb{I}}_D], \hat{\mathbb{I}}_D\rangle + \delta^2k_0^2\log(\delta)\langle K_D^{(1)}[\hat{\mathbb{I}}_D], \hat{\mathbb{I}}_D\rangle + \\ &\quad + O\Big(\delta^2\Big) \\ &= -\frac{|D|}{2\pi}\log(\delta k_0\hat{\gamma}) + \langle K_D^{(0)}[\hat{\mathbb{I}}_D], \hat{\mathbb{I}}_D\rangle + \delta^2k_0^2\log(\delta)\langle K_D^{(1)}[\hat{\mathbb{I}}_D], \hat{\mathbb{I}}_D\rangle + O\Big(\delta^2\Big). \end{aligned}$$

Using these expressions, $1 - \delta^2\omega_s^2\xi(\omega_s, k_s)M_D^{\delta k_0} = O(\delta^6\log(\delta))$ can be rewritten as

$$1 - \delta^2\omega_s^2\xi(\omega_s, k_s)\Bigg(-\frac{|D|}{2\pi}\log(\delta k_0\hat{\gamma}) + \langle K_D^{(0)}[\hat{\mathbb{I}}_D], \hat{\mathbb{I}}_D\rangle + \delta^2k_0^2\log(\delta)\langle K_D^{(1)}[\hat{\mathbb{I}}_D], \hat{\mathbb{I}}_D\rangle \\ + O\Big(\delta^2\Big)\Bigg) = O\Big(\delta^6\log(\delta)\Big),$$

from which the result follows. □

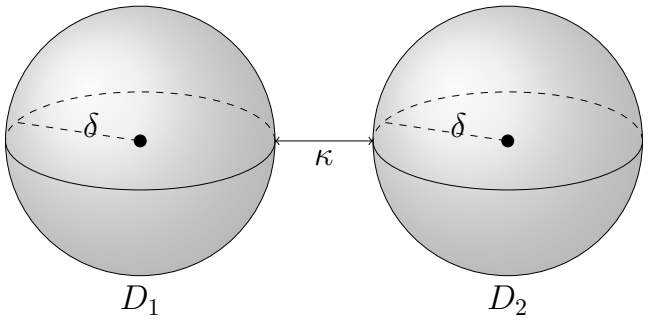

Figure 4.1.: Two identical spherical halide perovskite resontators D_1 and D_2 of radius δ, made from the same material, placed at a distance κ from each other.

4.3. Hybridisation of two resonators

In this section, we study the resonance problem for a system of two halide perovskite subwavelength resonators. Using the integral formulation of the problem, we obtain a matrix representation form which we use to obtain the expressions describing the subwavelength resonance in both the the two- and the three-dimensional setting.

4.3.1. Three Dimensions

Let us consider two identical halide perovskite resontators D_1 and D_2 (e.g. the speres in Figure 4.1), made from the same material. From now on, we will denote the permittivity by $\xi(\omega, k)$, where ω is the frequency and k the associated wavenumber. In order to generalise our results, we will define it by

$$\xi(\omega, k) := \frac{\mu_0 \alpha}{\beta - \omega^2 + \eta k^2 - i\gamma\omega}, \tag{4.44}$$

where the positive constants α, β, γ and η characterise the material.

Then, since there is an interaction between the two resonators, the field $u - u_{in}$ scattered by the two particles will be given by the following representation formula:

$$(u - u_{in})(x) = -\delta^2\omega^2\xi(\omega, k)\left[\int_{D_1} G(x - y, \delta k_0)u(y)\mathrm{d}y + \int_{D_2} G(x - y, \delta k_0)u(y)\mathrm{d}y\right], \tag{4.45}$$

for $x \in \mathbb{R}^d$.

Definition 4.3.1. *We define the integral operators $K_{D_i}^{\delta k_0}$ and $R_{D_iD_j}^{\delta k_0}$, for $i, j = 1, 2$, by*

$$K_{D_i}^{\delta k_0} : u\big|_{D_i} \in L^2(D_i) \longmapsto -\int_{D_i} G(x - y, \delta k_0)u(y)\mathrm{d}y\Big|_{D_i} \in L^2(D_i)$$

and

$$R^{\delta k_0}_{D_iD_j} : u\big|_{D_i} \in L^2(D_i) \longmapsto -\int_{D_i} G(x-y,\delta k_0)u(y)\mathrm{d}y\Big|_{D_j} \in L^2(D_j).$$

Then, the following lemma is a direct consequence of these definitions.

Lemma 4.3.2. *The scattering problem (4.45) can be restated, using the Definition 4.3.1, as*

$$\begin{pmatrix} 1-\delta^2\omega^2\xi(\omega,k)K^{\delta k_0}_{D_1} & -\delta^2\omega^2\xi(\omega,k)R^{\delta k_0}_{D_2D_1} \\ -\delta^2\omega^2\xi(\omega,k)R^{\delta k_0}_{D_1D_2} & 1-\delta^2\omega^2\xi(\omega,k)K^{\delta k_0}_{D_2} \end{pmatrix} \begin{pmatrix} u|_{D_1} \\ u|_{D_2} \end{pmatrix} = \begin{pmatrix} u_{in}|_{D_1} \\ u_{in}|_{D_2} \end{pmatrix}. \tag{4.46}$$

Thus, the scattering resonance problem is to find ω such that the operator in (4.46) is singular, or equivalently, such that there exists $(u_1,u_2) \in L^2(D_1)\times L^2(D_2)$, $(u_1,u_2)\neq 0$, such that

$$\begin{pmatrix} 1-\delta^2\omega^2\xi(\omega,k)K^{\delta k_0}_{D_1} & -\delta^2\omega^2\xi(\omega,k)R^{\delta k_0}_{D_2D_1} \\ -\delta^2\omega^2\xi(\omega,k)R^{\delta k_0}_{D_1D_2} & 1-\delta^2\omega^2\xi(\omega,k)K^{\delta k_0}_{D_2} \end{pmatrix} \begin{pmatrix} u_1 \\ u_2 \end{pmatrix} = \begin{pmatrix} 0 \\ 0 \end{pmatrix}. \tag{4.47}$$

Theorem 4.3.3. *Let $d=3$. Then, the hybridised subwavelength resonant frequencies ω satisfy*

$$\Big(1-\delta^2\omega^2\xi(\omega,k)\lambda_\delta\Big)^2 - \delta^4\omega^4\xi(\omega,k)^2\langle R^{\delta k_0}_{D_1D_2}\phi^{(\delta)}_1,\phi^{(\delta)}_2\rangle\langle R^{\delta k_0}_{D_2D_1}\phi^{(\delta)}_2,\phi^{(\delta)}_1\rangle = 0, \tag{4.48}$$

where $\phi^{(\delta)}_i$, for $i=1,2$, is the eigenfunction associated to the eigenvalue λ_δ of the potential $K^{\delta k_0}_{D_i}$.

Proof. We observe that (4.47) is equivalent to

$$\begin{pmatrix} 1-\delta^2\omega^2\xi(\omega,k)K^{\delta k_0}_{D_1} & 0 \\ 0 & 1-\delta^2\omega^2\xi(\omega,k)K^{\delta k_0}_{D_2} \end{pmatrix} \begin{pmatrix} u_1 \\ u_2 \end{pmatrix} - \delta^2\omega^2\xi(\omega,k) \begin{pmatrix} 0 & R^{\delta k_0}_{D_2D_1} \\ R^{\delta k_0}_{D_1D_2} & 0 \end{pmatrix} \begin{pmatrix} u_1 \\ u_2 \end{pmatrix} = 0,$$

which gives

$$\begin{pmatrix} u_1 \\ u_2 \end{pmatrix} - \delta^2\omega^2\xi(\omega,k) \begin{pmatrix} \Big(1-\delta^2\omega^2\xi(\omega,k)K^{\delta k_0}_{D_1}\Big)^{-1} & 0 \\ 0 & \Big(1-\delta^2\omega^2\xi(\omega,k)K^{\delta k_0}_{D_2}\Big)^{-1} \end{pmatrix} \begin{pmatrix} R^{\delta k_0}_{D_2D_1}u_2 \\ R^{\delta k_0}_{D_1D_2}u_1 \end{pmatrix} = 0. \tag{4.49}$$

Let us now apply a pole-pencil decomposition on the operators $\Big(1-\delta^2\omega^2\xi(\omega,k)K^{\delta k_0}_{D_i}\Big)^{-1}$, for $i=1,2$. We see that

$$\Big(1-\delta^2\omega^2\xi(\omega,k)K^{\delta k_0}_{D_1}\Big)^{-1}(\cdot) = \frac{\langle\cdot,\phi^{(\delta)}_1\rangle\phi^{(\delta)}_1}{1-\delta^2\omega^2\xi(\omega,k)\lambda_\delta} + R_1[\omega](\cdot)$$

and

$$\left(1-\delta^2\omega^2\xi(\omega,k)K_{D_2}^{\delta k_0}\right)^{-1}(\cdot)=\frac{\langle\cdot,\phi_2^{(\delta)}\rangle\phi_2^{(\delta)}}{1-\delta^2\omega^2\xi(\omega,k)\lambda_\delta}+R_2[\omega](\cdot),$$

where the remainder terms $R_1[\omega](\cdot)$ and $R_2[\omega](\cdot)$ are holomorphic for ω in a neighborhood of ω_δ, so can be neglected. Then, (4.49), is equivalent to

$$\begin{pmatrix}u_1\\u_2\end{pmatrix}-\delta^2\omega^2\xi(\omega,k)\begin{pmatrix}\frac{\langle\cdot,\phi_1^{(\delta)}\rangle\phi_1^{(\delta)}}{1-\delta^2\omega^2\xi(\omega,k)\lambda_\delta} & 0\\ 0 & \frac{\langle\cdot,\phi_2^{(\delta)}\rangle\phi_2^{(\delta)}}{1-\delta^2\omega^2\xi(\omega,k)\lambda_\delta}\end{pmatrix}\begin{pmatrix}R_{D_2D_1}^{\delta k_0}u_2\\ R_{D_1D_2}^{\delta k_0}u_1\end{pmatrix}=0.$$

This gives us the system

$$\begin{cases}u_1-\frac{\delta^2\omega^2\xi(\omega,k)}{1-\delta^2\omega^2\xi(\omega,k)\lambda_\delta}\langle R_{D_2D_1}^{\delta k_0}u_2,\phi_1^{(\delta)}\rangle\phi_1^{(\delta)}=0,\\ u_2-\frac{\delta^2\omega^2\xi(\omega,k)}{1-\delta^2\omega^2\xi(\omega,k)\lambda_\delta}\langle R_{D_1D_2}^{\delta k_0}u_1,\phi_2^{(\delta)}\rangle\phi_2^{(\delta)}=0.\end{cases}$$

Applying the operator $R_{D_1D_2}^{\delta k_0}$ (resp. $R_{D_2D_1}^{\delta k_0}$) to the first (resp. second) equation, and then applying $\langle\cdot,\phi_2^{(\varepsilon)}\rangle$ (resp. $\langle\cdot,\phi_1^{(\varepsilon)}\rangle$), we find that

$$\begin{cases}\langle R_{D_1D_2}^{\delta k_0}u_1,\phi_2^{(\delta)}\rangle-\frac{\delta^2\omega^2\xi(\omega,k)}{1-\delta^2\omega^2\xi(\omega,k)\lambda_\delta}\langle R_{D_1D_2}^{\delta k_0}\phi_1^{(\delta)},\phi_2^{(\delta)}\rangle\langle R_{D_2D_1}^{\delta k_0}u_2,\phi_1^{(\delta)}\rangle=0,\\ \langle R_{D_2D_1}^{\delta k_0}u_2,\phi_1^{(\delta)}\rangle-\frac{\delta^2\omega^2\xi(\omega,k)}{1-\delta^2\omega^2\xi(\omega,k)\lambda_\delta}\langle R_{D_2D_1}^{\delta k_0}\phi_2^{(\delta)},\phi_1^{(\delta)}\rangle\langle R_{D_1D_2}^{\delta k_0}u_1,\phi_2^{(\delta)}\rangle=0.\end{cases}$$

This system has a solution only if its determinant is zero. That is, if

$$1-\frac{\delta^4\omega^4\xi(\omega,k)^2}{\left(1-\delta^2\omega^2\xi(\omega,k)\lambda_\delta\right)^2}\langle R_{D_1D_2}^{\delta k_0}\phi_1^{(\delta)},\phi_2^{(\delta)}\rangle\langle R_{D_2D_1}^{\delta k_0}\phi_2^{(\delta)},\phi_1^{(\delta)}\rangle=0,$$

which gives the desired result. □

The following corollary is a direct result of Theorem 4.3.3.

Corollary 4.3.4. *Let $d=3$. Then, the hybridised subwavelength resonant frequencies are given by*

$$\omega=\frac{i\gamma\pm\sqrt{-\gamma^2-4\Gamma(\beta+\eta k^2)}}{2\Gamma},\qquad(4.50)$$

$$\textit{where}\qquad\Gamma=-1-\delta^2\alpha\lambda_\delta\pm\alpha\delta^2\sqrt{\langle R_{D_1D_2}^{\delta k_0}\phi_1^{(\delta)},\phi_2^{(\delta)}\rangle\langle R_{D_2D_1}^{\delta k_0}\phi_2^{(\delta)},\phi_1^{(\delta)}\rangle}.$$

where ϕ_i^δ, for $i=1,2$, is the eigenfunction associated to the eigenvalue λ_δ of the potential $K_{D_i}^{\delta k_0}$ and the $\pm$ in the two expressions do not have to agree.

Proof. We introduce the notation $\mathbb{K}:=\langle R_{D_1D_2}^{\delta k_0}\phi_1^{(\delta)},\phi_2^{(\delta)}\rangle$ and $\mathbb{M}:=\langle R_{D_2D_1}^{\delta k_0}\phi_2^{(\delta)},\phi_1^{(\delta)}\rangle$. Then, (4.48) becomes

$$\left(1-\delta^2\omega^2\xi(\omega,k)\lambda_\delta\right)^2-\delta^4\omega^4\xi(\omega,k)^2\mathbb{K}\mathbb{M}=0$$

$$\begin{aligned}
&\Leftrightarrow 1 - \delta^2\omega^2\xi(\omega,k)\lambda_\delta \pm \delta^2\omega^2\xi(\omega,k)\sqrt{\mathbb{K}\mathbb{M}} = 0 \\
&\Leftrightarrow \left(-1 - \delta^2\alpha\lambda_\delta \pm \alpha\delta^2\sqrt{\mathbb{K}\mathbb{M}}\right)\omega^2 - i\gamma\omega + \beta + \eta k^2 = 0,
\end{aligned}$$

and the roots to this second degree polynomial are given by

$$\omega = \frac{i\gamma \pm \sqrt{-\gamma^2 - 4\Gamma(\beta + \eta k^2)}}{2\Gamma},$$

where

$$\Gamma = -1 - \delta^2\alpha\lambda_\delta \pm \alpha\delta^2\sqrt{\mathbb{K}\mathbb{M}},$$

with the two $\pm$ not necessarily agreeing. Finally, substituting the expressions for $\mathbb{K}$ and $\mathbb{M}$, we obtain the result. □

4.3.2. Two Dimensions

Let us move on to the case of dimension $d = 2$. For simplicity, we again consider two identical halide perovskite resontators D_1 and D_2, made from the same material with permittivity given by the formula (4.44). We define the operators $K_{D_i}^{\delta k_0}$ and $R_{D_iD_j}^{\delta k_0}$, for $i, j = 1, 2$, as in Definition 4.3.1 and we continue by defining the following integral operators.

Definition 4.3.5. *We define the integral operators $M_{D_i}^{\delta k_0}$ and $N_{D_iD_j}^{\delta k_0}$ for $i, j = 1, 2$ as*

$$M_{D_i}^{\delta k_0} := \hat{K}_{D_i}^{\delta k_0} + K_{D_i}^{(0)} + (\delta k_0)^2 \log(\delta k_0 \hat{\gamma}) K_{D_i}^{(1)},$$

and

$$N_{D_iD_j}^{\delta k_0} := \hat{K}_{D_iD_j}^{\delta k_0} + R_{D_iD_j}^{(0)} + (\delta k_0)^2 \log(\delta k_0 \hat{\gamma}) R_{D_iD_j}^{(1)},$$

where

$$\begin{aligned}
K_{D_i}^{(0)} : u\Big|_{D_i} \in L^2(D_i) &\longmapsto \int_{D_i} G(x-y,0)u(y)\mathrm{d}y\Big|_{D_i} \in L^2(D_i), \\
\hat{K}_{D_i}^{\delta k_0} : u\Big|_{D_i} \in L^2(D_i) &\longmapsto \log(\hat{\gamma}\delta k_0)\hat{K}_{D_i}[u]\Big|_{D_i} \in L^2(D_i), \\
\hat{K}_{D_i} : u\Big|_{D_i} \in L^2(D_i) &\longmapsto -\frac{1}{2\pi}\int_{D_i} u(y)\mathrm{d}y\Big|_{D_i} \in L^2(D_i), \\
K_{D_i}^{(1)} : u\Big|_{D_i} \in L^2(D_i) &\longmapsto \int_{D_i} \frac{\partial}{\partial k} G(x-y,k)\Big|_{k=0} u(y)\mathrm{d}y\Big|_{D_i} \in L^2(D_i),
\end{aligned}$$

and

$$R_{D_iD_j}^{(0)} : u\Big|_{D_i} \in L^2(D_i) \longmapsto \int_{D_i} G(x-y,0)u(y)\mathrm{d}y\Big|_{D_j} \in L^2(D_j),$$

$$\hat{K}^{\delta k_0}_{D_iD_j} : u\Big|_{D_i} \in L^2(D_i) \longmapsto \log(\hat{\gamma}\delta k_0)\hat{K}_{D_iD_j}[u]\Big|_{D_j} \in L^2(D_j),$$
$$\hat{K}_{D_iD_j} : u\Big|_{D_i} \in L^2(D_i) \longmapsto -\frac{1}{2\pi}\int_{D_i} u(y)\mathrm{d}y\Big|_{D_j} \in L^2(D_j),$$
$$R^{(1)}_{D_iD_j} : u\Big|_{D_i} \in L^2(D_i) \longmapsto \int_{D_i} \frac{\partial}{\partial k}G(x-y,k)\Big|_{k=0} u(y)\mathrm{d}y\Big|_{D_j} \in L^2(D_j).$$

We observe the following result.

Proposition 4.3.6. *For the integral operators $K^{\delta k_0}_{D_i}$ and $R^{\delta k_0}_{D_iD_j}$, we can write*

$$K^{\delta k_0}_{D_i} = M^{\delta k_0}_{D_i} + O\Big(\delta^4\log(\delta)\Big), \quad \text{and} \quad R^{\delta k_0}_{D_iD_j} = N^{\delta k_0}_{D_iD_j} + O\Big(\delta^4\log(\delta)\Big), \tag{4.51}$$

as $\delta \to 0$ and with k_0 fixed.

Proof. The proof is a direct result of the expansion of the Green's function in dimension $d = 2$. Indeed, for $u|_{D_i} \in L^2(D_i)$, we observe that

$$\begin{aligned}
K^{\delta k_0}_{D_i}[u](x) &= -\int_{D_i} G(x-y,\delta k_0)u(y)\mathrm{d}y\Big|_{D_i} \\
&= -\int_{D_i} \Big(\log(\hat{\gamma}\delta k_0)\frac{1}{2\pi} + G(x-y,0) + (\delta k_0)^2\log(\delta k_0\hat{\gamma})\frac{\partial}{\partial k}G(x-y,k)\Big|_{k=0} \\
&\qquad + O\Big(\delta^4\log(\delta)\Big)\Big)u(y)\mathrm{d}y\Big|_{D_i} \\
&= \Big(\hat{K}^{\delta k_0}_{D_i} + K^{(0)}_{D_i} + (\delta k_0)^2\log(\delta k_0\hat{\gamma})K^{(1)}_{D_i}\Big)[u](x) + O\Big(\delta^4\log(\delta)\Big) \\
&= M^{\delta k_0}_{D_i}[u](x) + O\Big(\delta^4\log(\delta)\Big).
\end{aligned}$$

Similarly, for $u|_{D_i} \in L^2(D_i)$,

$$\begin{aligned}
R^{\delta k_0}_{D_iD_j}[u](x) &= -\int_{D_i} G(x-y,\delta k_0)u(y)\mathrm{d}y\Big|_{D_j} \in L^2(D_j) \\
&= -\int_{D_i} \Big(\log(\hat{\gamma}\delta k_0)\frac{1}{2\pi} + G(x-y,0) + (\delta k_0)^2\log(\delta k_0\hat{\gamma})\frac{\partial}{\partial k}G(x-y,k)\Big|_{k=0} \\
&\quad + O\Big(\delta^4\log(\delta)\Big)\Big)u(y)\mathrm{d}y\Big|_{D_j} \\
&= \Big(\hat{K}^{\delta k_0}_{D_iD_j} + R^{(0)}_{D_iD_j} + (\delta k_0)^2\log(\delta k_0\hat{\gamma})R^{(1)}_{D_iD_j}\Big)[u](x) + O\Big(\delta^4\log(\delta)\Big) \\
&= N^{\delta k_0}_{D_iD_j}[u](x) + O(\delta^4\log(\delta)).
\end{aligned}$$

□

Therefore, our problem is to determine the frequencies ω and the associated wavenumber k, for which the following holds:

$$\begin{pmatrix} I - \delta^2\omega^2\xi(\omega,k)K^{\delta k_0}_{D_1} & -\delta^2\omega^2\xi(\omega,k)R^{\delta k_0}_{D_2D_1} \\ -\delta^2\omega^2\xi(\omega,k)R^{\delta k_0}_{D_1D_2} & I - \delta^2\omega^2\xi(\omega,k)K^{\delta k_0}_{D_2} \end{pmatrix}\begin{pmatrix} u_1 \\ u_2 \end{pmatrix} = \begin{pmatrix} 0 \\ 0 \end{pmatrix} \tag{4.52}$$

for nontrivial $u := (u_1, u_2)$, such that $u|_{D_i} \in L^2(D_i)$, for $i = 1, 2$.

Proposition 4.3.7. *Let $d = 2$. Then, the hybridised subwavelength resonant frequencies ω satisfy*

$$\begin{aligned} 1 - \delta^2\omega^2\xi(\omega,k)\Bigg(&- \frac{|D_1|}{2\pi}\log(\hat{\gamma}\delta k_0)(1 \pm 1) + \langle K_{D_1}^{(0)}[\hat{\mathbb{I}}_{D_1}], \hat{\mathbb{I}}_{D_1}\rangle \\ &+ (\delta k_0)^2 \log(\delta k_0\hat{\gamma})\langle K_{D_1}^{(1)}[\hat{\mathbb{I}}_{D_1}], \hat{\mathbb{I}}_{D_1}\rangle \pm \langle R_{D_2D_1}^{(0)}[\hat{\mathbb{I}}_{D_2}], \hat{\mathbb{I}}_{D_1}\rangle \\ &\pm (\delta k_0)^2 \log(\delta k_0\hat{\gamma})\langle R_{D_2D_1}^{(1)}[\hat{\mathbb{I}}_{D_2}], \hat{\mathbb{I}}_{D_1}\rangle \Bigg) = 0, \end{aligned} \tag{4.53}$$

where the $\pm$ symbols coincide.

Proof. The first thing that we do is to observe that, by applying the expansion (4.51) to (4.52), we reach the problem

$$\begin{pmatrix} I - \delta^2\omega^2\xi(\omega,k)M_{D_1}^{\delta k_0} & -\delta^2\omega^2\xi(\omega,k)N_{D_2D_1}^{\delta k_0} \\ -\delta^2\omega^2\xi(\omega,k)N_{D_1D_2}^{\delta k_0} & I - \delta^2\omega^2\xi(\omega,k)M_{D_2}^{\delta k_0} \end{pmatrix} \begin{pmatrix} u_1 \\ u_2 \end{pmatrix} = \begin{pmatrix} O\Big(\delta^4\log(\delta)\Big) \\ O\Big(\delta^4\log(\delta)\Big) \end{pmatrix}.$$

We note that $|D_1| = |D_2|$. Then, using the symmetries of the dimer, let us denote

$$\begin{aligned} \hat{\nu}(\delta) :&= -\frac{|D_1|}{2\pi}\log(\delta k_0\hat{\gamma}) + \langle K_{D_1}^{(0)}[\hat{\mathbb{I}}_{D_1}], \hat{\mathbb{I}}_{D_1}\rangle + (\delta k_0)^2\log(\delta k_0\hat{\gamma})\langle K_{D_1}^{(1)}[\hat{\mathbb{I}}_{D_1}], \hat{\mathbb{I}}_{D_1}\rangle \\ &= -\frac{|D_2|}{2\pi}\log(\delta k_0\hat{\gamma}) + \langle K_{D_2}^{(0)}[\hat{\mathbb{I}}_{D_2}], \hat{\mathbb{I}}_{D_2}\rangle + (\delta k_0)^2\log(\delta k_0\hat{\gamma})\langle K_{D_2}^{(1)}[\hat{\mathbb{I}}_{D_2}], \hat{\mathbb{I}}_{D_2}\rangle, \end{aligned}$$

and

$$\hat{\eta} := \langle N_{D_1D_2}^{\delta k_0}[\hat{\mathbb{I}}_{D_1}], \hat{\mathbb{I}}_{D_2}\rangle = \langle N_{D_2D_1}^{\delta k_0}[\hat{\mathbb{I}}_{D_2}], \hat{\mathbb{I}}_{D_1}\rangle.$$

In addition, we have that

$$\hat{K}_{D_iD_j}^{\delta k_0}[\hat{\mathbb{I}}_{D_i}] = \hat{K}_{D_j}^{\delta k_0}[\hat{\mathbb{I}}_{D_j}].$$

Now, we define the quantity $\nu(\delta)$ to be the eigenvalues of the operator $M_{D_i}^{\delta k_0}$, that is,

$$\nu(\delta) = \langle M_{D_1}^{\delta k_0}[\Psi_{D_1}], \Psi_{D_1}\rangle = \langle M_{D_2}^{\delta k_0}[\Psi_{D_2}], \Psi_{D_2}\rangle,$$

for the eigenfunctions $\Psi_{D_i}(\delta) \in L^2(D_i)$, $\Psi_{D_i}(\delta) = \hat{\mathbb{I}}_{D_i} + O\left(\frac{1}{\log(d)}\right)$. Thus, we have that (4.52) is equivalent to

$$\begin{pmatrix} u_1 \\ u_2 \end{pmatrix} - \delta^2\omega^2\xi(\omega,k) \begin{pmatrix} \Big(I - \delta^2\omega^2\xi(\omega,k)M_{D_1}^{\delta k_0}\Big)^{-1} & 0 \\ 0 & \Big(I - \delta^2\omega^2\xi(\omega,k)M_{D_2}^{\delta k_0}\Big)^{-1} \end{pmatrix} \begin{pmatrix} N_{D_2D_1}^{\delta k_0}u_2 \\ N_{D_1D_2}^{\delta k_0}u_1 \end{pmatrix} = 0. \tag{4.54}$$

Applying a pole-pencil decomposition, we observe that

$$\left(I - \delta^2\omega^2\xi(\omega,k)M_{D_i}^{\delta k_0}\right)^{-1}[\cdot] = \frac{\langle\cdot,\hat{\mathbb{I}}_{D_i}\rangle\hat{\mathbb{I}}_{D_i}}{1-\delta^2\omega^2\xi(\omega,k)\nu(\delta)} + R[\omega](\cdot),$$

where the remainder terms $R[\omega](\cdot)$ can be neglected. Hence, (4.54) is equivalent to

$$\begin{cases} u_1 - \delta^2\omega^2\xi(\omega,k)\frac{\langle N_{D_2D_1}^{\delta k_0}u_2,\hat{\mathbb{I}}_{D_1}\rangle\hat{\mathbb{I}}_{D_1}}{1-\delta^2\omega^2\xi(\omega,k)\nu(\delta)} = 0, \\ u_2 - \delta^2\omega^2\xi(\omega,k)\frac{\langle N_{D_1D_2}^{\delta k_0}u_1,\hat{\mathbb{I}}_{D_2}\rangle\hat{\mathbb{I}}_{D_2}}{1-\delta^2\omega^2\xi(\omega,k)\nu(\delta)} = 0, \end{cases}$$

which is equivalent to

$$\begin{cases} \langle N_{D_1D_2}^{\delta k_0}u_1,\hat{\mathbb{I}}_{D_2}\rangle - \frac{\delta^2\omega^2\xi(\omega,k)}{1-\delta^2\omega^2\xi(\omega,k)\nu(\delta)}\langle N_{D_1D_2}^{\delta k_0}\hat{\mathbb{I}}_{D_1},\hat{\mathbb{I}}_{D_2}\rangle\langle N_{D_2D_1}^{\delta k_0}u_2,\hat{\mathbb{I}}_{D_1}\rangle = 0, \\ \langle N_{D_2D_1}^{\delta k_0}u_2,\hat{\mathbb{I}}_{D_1}\rangle - \frac{\delta^2\omega^2\xi(\omega,k)}{1-\delta^2\omega^2\xi(\omega,k)\nu(\delta)}\langle N_{D_2D_1}^{\delta k_0}\hat{\mathbb{I}}_{D_2},\hat{\mathbb{I}}_{D_1}\rangle\langle N_{D_1D_2}^{\delta k_0}u_1,\hat{\mathbb{I}}_{D_2}\rangle = 0. \end{cases}$$

For this to have a solution, we need the determinant of the matrix induced by this system to be zero. This gives

$$1 - \frac{\delta^4\omega^4\xi(\omega,k)^2}{(1-\delta^2\omega^2\xi(\omega,k)\nu(\delta))^2}\langle N_{D_1D_2}^{\delta k_0}\hat{\mathbb{I}}_{D_1},\hat{\mathbb{I}}_{D_2}\rangle\langle N_{D_2D_1}^{\delta k_0}\hat{\mathbb{I}}_{D_2},\hat{\mathbb{I}}_{D_1}\rangle = 0.$$

Given the symmetry of our setting, we have that

$$\langle N_{D_1D_2}^{\delta k_0}\hat{\mathbb{I}}_{D_1},\hat{\mathbb{I}}_{D_2}\rangle = \langle N_{D_2D_1}^{\delta k_0}\hat{\mathbb{I}}_{D_2},\hat{\mathbb{I}}_{D_1}\rangle,$$

and hence, we get

$$1 - \delta^2\omega^2\xi(\omega,k)\nu(\delta) \pm \delta^2\omega^2\xi(\omega,k)\langle N_{D_1D_2}^{\delta k_0}\hat{\mathbb{I}}_{D_1},\hat{\mathbb{I}}_{D_2}\rangle = 0.$$

This is equivalent to

$$\begin{aligned} 1 - \delta^2\omega^2\xi(\omega,k)\Bigg(&- \frac{|D_1|}{2\pi}\log(\delta k_0\hat{\gamma})(1\pm 1) + \langle K_{D_1}^{(0)}[\hat{\mathbb{I}}_{D_1}],\hat{\mathbb{I}}_{D_1}\rangle \\ &+ (\delta k_0)^2\log(\delta k_0\hat{\gamma})\langle K_{D_1}^{(1)}[\hat{\mathbb{I}}_{D_1}],\hat{\mathbb{I}}_{D_1}\rangle \pm \langle R_{D_2D_1}^{(0)}[\hat{\mathbb{I}}_{D_2}],\hat{\mathbb{I}}_{D_1}\rangle \\ &\pm (\delta k_0)^2\log(\delta k_0\hat{\gamma})\langle R_{D_2D_1}^{(1)}[\hat{\mathbb{I}}_{D_2}],\hat{\mathbb{I}}_{D_1}\rangle\Bigg) = 0, \end{aligned}$$

which is the desired result. □

4.4. Example: circular resonators

In this section, we illustrate our results for the case of two-dimensional circular halide perovskite resonators. We can find the resonant frequencies of a single particle ω_s by solving (4.38). Similarly, the hybridised resonant frequencies of a pair of circular

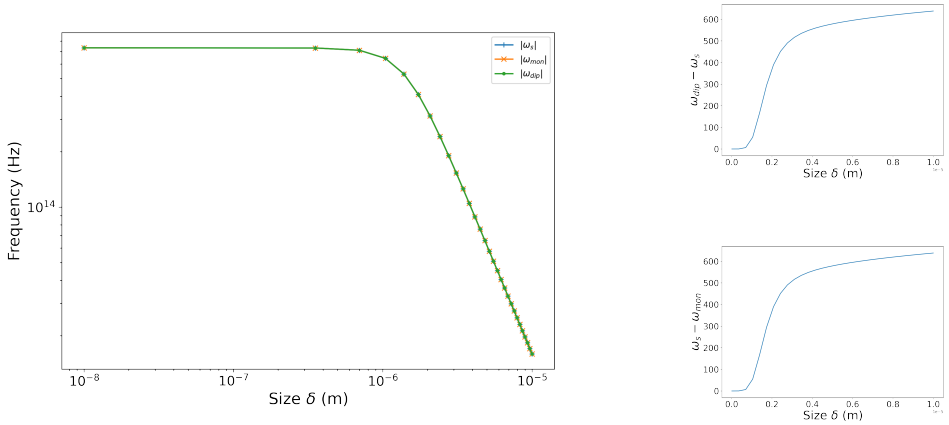

Figure 4.2.: Behaviour of the subwavelength resonances for small circular nano-particles of radius δ. The resonant frequency ω_s of a single circular methylammonium lead chloride nano-particle is shown. For two circular nano-particles, made from the same material, we see how the hybridisation causes the frequencies ω_{dip} (dipole) and ω_{mon} (monopole) to shift either side of ω_s.

resonators can be found by solving (4.53). The two solutions of (4.53) are denoted by ω_{mon} and ω_{dip}, to describe their monopolar and dipolar characteristics. As is expected from other hybridised systems, it holds that $\omega_{\text{mon}} < \omega_{\text{dip}}$. We plot these three frequencies as a function of the particle size δ in Figure 4.2(a). Parameter values are chosen to corresponding to methylammonium lead chloride ($MAPbCl_3$), which is a popular halide perovskite [52]. We notice that the resonant frequencies for these resonators lies in the range of visible frequencies, when the particles are hundreds of nanometres in size. This puts the system in the appropriate subwavelength regime that was required for our asymptotic method.

One thing we observe from Figure 4.2 is that in the $\delta \to 0$ limit, the frequencies coincide. This is because the nano-particles behave as isolated, identical resonators when δ is very small. Then, as δ increases the single-particle resonance ω_s always stays between the monopole and dipole frequencies of the hybridised case. In Figure 4.2(a) it appears that the three resonances coincide, however in Figures 4.2(b) and 4.2(c) we plot $\omega_s - \omega_{\text{mon}}$ and $\omega_{\text{dip}} - \omega_s$ to show that the three values differ by several hundred Hertz and satisfy $\omega_{\text{mon}} < \omega_s < \omega_{\text{dip}}$. The phenomenon of the dipole frequency ω_d being shifted above ω_s and the monopole frequency ω_m being shifted below ω_s is a typical behaviour of hybridised resonator systems, see e.g. [9].

4.5. Conclusion

We have established a new mathematical approach for modelling halide perovskite resonators. This is a significant development of the existing theory of subwave-

length resonators [8, 9], as it generalises the techniques to dispersive settings where the permittivity of the material depends non-linearly on both the frequency and the wavenumber. Given the growing use of halide perovskites in engineering applications, this theory will have a significant impact on the design of advanced devices [38, 47]. The integral methods used here are able to describe a very broad class of resonator shapes, so are an ideal approach for studying complex geometries, such as the biomimetic eye developed by [36].

5. Highly dispersive subwavelength resonator systems

5.1. Introduction

When multiple resonators are allowed to influence one another coupling interactions take place, which can often be complex and difficult to model. Understanding how these interactions depend on the shapes, sizes and positions of resonators has allowed scientists and engineers to design devices with exotic and remarkable properties. Some notable examples include effectively negative material parameters [58, 71], cloaking devices [54, 27] and bio-inspired structural colouration [66, 77]. The word *metamaterial* is a broad term that is often used as a catchall term to encompass materials whose emergent properties arise due to geometry and structure (as opposed to purely from chemistry) [40].

For designing complex devices, it is valuable to be able to model systems of coupled resonators without the need for expensive numerical simulations (*e.g.* with commercial finite element packages). For this reason, there has been significant mathematical interest in developing concise models for coupled resonator systems. A prominent field in this direction is multiple scattering theory [69]. These techniques are particularly effective for modelling either small (point) scatterers or systems whose geometry admits explicit representations (*e.g.* cylinders or spheres) [70, 35]. For homogeneous circles and spheres, the prominent approach in this direction is *Mie theory*, named after Gustav Mie who famously developed so-called multipole solutions for electromagnetic scattering by a sphere [53]. These expressions have been used many times in the literature for designing complex devices and metamaterials [76]. To describe resonators with general and possibly complex shapes, integral methods can be used [14]. On top of this, asymptotic techniques have helped provide concise characterisations of complex problems. Homogenisation can be used characterise the effective properties of materials with periodic [22, 37], quasi-periodic [23] or random [33] micro-structures. Local properties can also be deduced through asymptotic approaches. For example, asymptotic expansions can be computed when resonators are very small or have highly contrasting material parameters [8, 9].

Extending existing asymptotic and integral methods to models of dispersive resonators, with physically realistic material parameters, has proved to be a challenging problem. Some recent progress has been made for the well-known Drude model [20] and for halide perovskites as demonstrated in Chapter 4. In these cases, resonant frequencies of the coupled resonator system cannot be found by solving a simple

eigenvalue problem, as the associated eigenvalue problem inherits the non-linearity of the permittivity relation.

In this chapter, we will use integral methods to study a broad class of geometries of halide perovskite resonators. This extends the theory developed in Chapter 4 for one and two resonators to the case of three or more halide perovskite nano-particles. In Section 5.2, we will present the integral formulation of the resonance problem that we are studying. We will use asymptotic techniques to show how this system can be approximated in the case that the resonators are small. In Section 5.3, we will show how these results can be used to find the resonant frequencies of a coupled system of circular halide perovskite resonators and present numerical visualisations. Our results will be for a two-dimensional differential system, however we will show (in the appendix) how these results can easily be modified to three dimensions.

In the final part of this chapter, in Section 5.4, we will use our asymptotic results to treat an inverse design problem. In particular, given three wavelengths of visible light, we will show that a system of three identical circular halide perovskite resonators can be chosen to resonate at those wavelengths and present an efficient strategy for deriving the appropriate geometry. This problem is inspired by the sensitivity of retinal receptor cells to three colours of light (red, blue and green). This shows that, with the help of our mathematical insight, it is possible to add customisable colour perception to bioinspired artificial eyes [36, 48]. This is from the work carried in [5].

5.2. Asymptotic analysis

5.2.1. Problem setting

Let us consider $N \in \mathbb{N}$ halide perovskite resonators $D_1, D_2, \ldots, D_N$ occupying a bounded domain $\Omega \subset \mathbb{R}^d$, for $d \in \{2, 3\}$. We assume that the resonators have permittivity given by

$$\varepsilon(\omega, k) = \varepsilon_0 + \frac{\alpha}{\beta - \omega^2 + \eta k^2 - i\gamma\omega}, \tag{5.1}$$

where $\alpha, \beta, \gamma, \eta$ are positive constants. This is motivated by the formula for the permittivity of halide perovskites reported in [52]. The non-linear dependence on both the frequency ω and the wavenumber k are responsible for the complex, dispersive behaviour of the material. We assume that the particles are non-magnetic, so that the magnetic permeability μ_0 is constant on all of $\mathbb{R}^d$.

We consider the Helmholtz equation as a model for the propagation of time-harmonic waves with frequency ω. This is a reasonable model for the scattering of transverse magnetic polarised light (see *e.g.* [55, Remark 2.1] for a discussion). The wavenumber in the background $\mathbb{R}^d \setminus \overline{\Omega}$ is given by $k_0 := \omega\varepsilon_0\mu_0$ and we will use k to denote the wavenumber within Ω. Let us note here that, from now on, we will suppress

the dependence of k_0 on ω for brevity. We, then, consider the following Helmholtz model for light propagation:

$$\begin{cases} \Delta u + \omega^2 \varepsilon(\omega, k)\mu_0 u = 0 & \text{in } \Omega, \\ \Delta u + k_0^2 u = 0 & \text{in } \mathbb{R}^d \setminus \overline{\Omega}, \\ u|_+ - u|_- = 0 & \text{on } \partial\Omega, \\ \frac{\partial u}{\partial \nu}|_+ - \frac{\partial u}{\partial \nu}|_- = 0 & \text{on } \partial\Omega, \\ u(x) - u_{in}(x) & \text{satisfies the outgoing radiation condition as } |x| \to \infty, \end{cases} \tag{5.2}$$

where u_{in} is the incident wave, assumed to satisfy

$$(\Delta + k_0^2)u_{in} = 0 \quad \text{in } \mathbb{R}^d,$$

and the appropriate outgoing radiation condition is the Sommerfeld radiation condition, which requires that

$$\lim_{|x|\to\infty} |x|^{\frac{d-1}{2}} \left(\frac{\partial}{\partial |x|} - ik_0 \right) \Big(u(x) - u_{in}(x) \Big) = 0. \tag{5.3}$$

In particular, we are interested in the case of small resonators. Thus, we will assume that there exists some fixed domain D, which the the union of N disjoint subsets $D = D_1 \cup D_2 \cup \cdots \cup D_N$, such that Ω is given by

$$\Omega = \delta D + z, \tag{5.4}$$

for some position $z \in \mathbb{R}^d$ and characteristic size $0 < \delta \ll 1$. Then, making a change of variables, the Helmholtz problem (5.2) becomes

$$\begin{cases} \Delta u + \delta^2 \omega^2 \varepsilon(\omega, k)\mu_0 u = 0 & \text{in } D, \\ \Delta u + \delta^2 k_0^2 u = 0 & \text{in } \mathbb{R}^d \setminus \overline{D}, \end{cases} \tag{5.5}$$

along with the same transmission conditions on ∂D and far-field behaviour. We are interested in the *subwavelength* behaviour of the system, which occurs when $\delta \ll k_0^{-1}$. We will study this by performing asymptotics in the regime that the frequency ω is fixed while the size $\delta \to 0$. We will characterise solutions to (5.2) in terms of the system's resonant frequencies. For a given wavenumber k, we define $\omega = \omega(k)$ to be a *resonant frequency* if it is such that there exists a non-trivial solution u to (4.2) in the case that $u_{in} = 0$.

We will also make an additional assumption on the dimensions of the nano-particles. This will allow us to prove an approximation for the values of the modes $u|_{D_i}$, $i = 1, \ldots, N$, on each particle. The assumption is one of *diluteness*, in the sense that the particles are small relative to the separation distances between them. To capture this, we introduce the parameter ρ_i to capture the size of the reference particles $D_1, \ldots, D_N$. We define $\rho_i := \frac{1}{2}(\text{diam}(D_i))$ where $\text{diam}(D_i)$ is given by

$$\text{diam}(D_i) = \sup\{|x - y| : x, y \in D_i\}. \tag{5.6}$$

We will assume that each $\rho_i \to 0$ independently of δ. This regime means that the system is dilute in the sense that the particles are small relative to the distances between them. These scales described by δ and ρ_i are depicted in Figure 5.1.

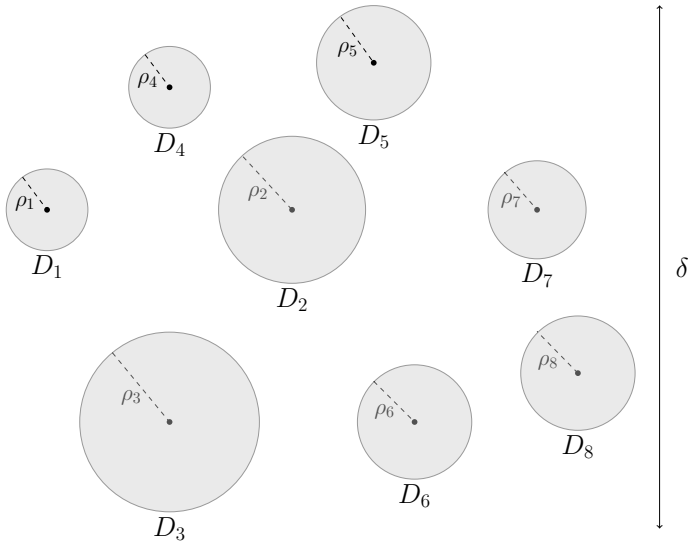

Figure 5.1.: A system of eight circular resonators. Here, we see how δ parametrizes the size of our system. Also, for the diluteness assumption, for a circular particle D_i, $i = 1, \ldots, 8$, we have that the parameter ρ_i is the radius of D_i.

5.2.2. Integral formulation

Let $G(x, k)$ be the outgoing Helmholtz Green's function in $\mathbb{R}^d$, defined as the unique solution to $(\Delta + k^2)G(x, k) = \delta_0(x)$ in $\mathbb{R}^d$, along with the outgoing radiation condition (5.3). It is well known that G is given by

$$G(x,k) = \begin{cases} -\frac{i}{4}H_0^{(1)}(k|x|), & d = 2, \\ -\frac{e^{ik|x|}}{4\pi|x|}, & d = 3, \end{cases} \tag{5.7}$$

where $H_0^{(1)}$ is the Hankel function of first kind and order zero. Then, as in Chapter 4, we have the following result, which gives an integral representation of the scattering problem.

Theorem 5.2.1 (Lippmann-Schwinger integral representation formula)**.** *A function u satisfies the differential system* (5.2) *if and only if it satisfies the following equation*

$$u(x) - u_{in}(x) = -\delta^2\omega^2\xi(\omega, k)\int_D G(x - y, k_0\delta)u(y)\mathrm{d}y, \quad x \in \mathbb{R}^d, \tag{5.8}$$

where the function $\xi : \mathbb{C} \to \mathbb{C}$ describes the permittivity contrast between D and the background and is given by

$$\xi(\omega, k) = \mu_0(\varepsilon(\omega, k) - \varepsilon_0).$$

Thus, a resonant mode of the system (5.2) is a non-trivial solution u to the integral equation (5.8) that exists when $u_{in}(x) = 0$. Since the domains $D_1, \dots, D_N$ are disjoint, the field $u - u_{in}$ scattered by the N particles can be written as

$$(u - u_{in})(x) = -\delta^2 \omega^2 \xi(\omega, k) \sum_{i=1}^{N} \int_{D_i} G(x - y, k_0 \delta) u(y), \quad \text{for } x \in \mathbb{R}^d. \tag{5.9}$$

We are interested in understanding how the formula (5.8) behaves in the case that δ is small. For this, the asymptotic expansions of the Green's function will be of great help. Although, we have to distinguish the cases of two and three dimensions, since these expansions differ in each case. We will work on the two-dimensional setting as the asymptotic expansions are more complicated. The same method can be used in three-dimensions, although the analysis is slightly easier. We present some of the key details in Appendix A.4.1.

5.2.3. Two-dimensional analysis

Let us assume that we work in dimension $d = 2$ and let us consider N halide perovskite resonators $D_1, D_2, \dots, D_N$, made from the same material. We define the operators $K_{D_i}^{k_0\delta}$ and $R_{D_i D_j}^{k_0\delta}$, for $i, j = 1, 2, \dots, N$, $i \neq j$, as follows.

Definition 5.2.2. *We define the integral operators $K_{D_i}^{k_0\delta}$ and $R_{D_i D_j}^{k_0\delta}$, for $i, j = 1, 2, ..., N$, by*

$$K_{D_i}^{k_0\delta} : u\big|_{D_i} \in L^2(D_i) \longmapsto -\int_{D_i} G(x - y, k_0\delta) u(y) \mathrm{d}y \Big|_{D_i} \in L^2(D_i)$$

and

$$R_{D_i D_j}^{k_0\delta} : u\big|_{D_i} \in L^2(D_i) \longmapsto -\int_{D_i} G(x - y, k_0\delta) u(y) \mathrm{d}y \Big|_{D_j} \in L^2(D_j).$$

We continue by recalling from Chapter 4 some results concerning the asymptotic behaviour of these integral operators.

Definition 5.2.3. *We define the integral operators $M_{D_i}^{k_0\delta}$ and $N_{D_i D_j}^{k_0\delta}$, for $i, j = 1, 2, \dots, N$, $i \neq j$, as*

$$M_{D_i}^{k_0\delta} := \hat{K}_{D_i}^{k_0\delta} + K_{D_i}^{(0)} + (k_0\delta)^2 \log(k_0\delta\hat{\gamma}) K_{D_i}^{(1)},$$

and

$$N_{D_i D_j}^{k_0\delta} := \hat{K}_{D_i D_j}^{k_0\delta} + R_{D_i D_j}^{(0)} + (k_0\delta)^2 \log(k_0\delta\hat{\gamma}) R_{D_i D_j}^{(1)},$$

where

$$K_{D_i}^{(0)} : u\Big|_{D_i} \in L^2(D_i) \longmapsto \int_{D_i} G(x-y,0)u(y)\mathrm{d}y\Big|_{D_i} \in L^2(D_i),$$
$$\hat{K}_{D_i}^{k_0\delta} : u\Big|_{D_i} \in L^2(D_i) \longmapsto -\frac{1}{2\pi}\log(\hat{\gamma}k_0\delta)\int_{D_i} u(y)\mathrm{d}y\Big|_{D_i} \in L^2(D_i),$$
$$K_{D_i}^{(1)} : u\Big|_{D_i} \in L^2(D_i) \longmapsto \int_{D_i} \frac{\partial}{\partial k}G(x-y,k)\Big|_{k=0} u(y)\mathrm{d}y\Big|_{D_i} \in L^2(D_i),$$

and

$$R_{D_iD_j}^{(0)} : u\Big|_{D_i} \in L^2(D_i) \longmapsto \int_{D_i} G(x-y,0)u(y)\mathrm{d}y\Big|_{D_j} \in L^2(D_j),$$
$$\hat{K}_{D_iD_j}^{k_0\delta} : u\Big|_{D_i} \in L^2(D_i) \longmapsto -\frac{1}{2\pi}\log(\hat{\gamma}k_0\delta)\int_{D_i} u(y)\mathrm{d}y\Big|_{D_j} \in L^2(D_j),$$
$$R_{D_iD_j}^{(1)} : u\Big|_{D_i} \in L^2(D_i) \longmapsto \int_{D_i} \frac{\partial}{\partial k}G(x-y,k)\Big|_{k=0} u(y)\mathrm{d}y\Big|_{D_j} \in L^2(D_j).$$

Proposition 5.2.4. *For the integral operators $K_{D_i}^{k_0\delta}$ and $R_{D_iD_j}^{k_0\delta}$, we can write*

$$K_{D_i}^{k_0\delta} = M_{D_i}^{k_0\delta} + O\Big(\delta^4\log(\delta)\Big), \quad \text{and} \quad R_{D_iD_j}^{k_0\delta} = N_{D_iD_j}^{k_0\delta} + O\Big(\delta^4\log(\delta)\Big), \tag{5.10}$$

as $\delta \to 0$ and with k_0 fixed.

Since the scattered field is fully determined by the value within each resonator, we will introduce the notation

$$u_i := u|_{D_i}, \quad i = 1, \dots, N. \tag{5.11}$$

Then, the resonance problem is to find $\omega \in \mathbb{C}$, such that there exists $(u_1, u_2, \dots, u_N) \in L^2(D_1) \times L^2(D_2) \times \cdots \times L^2(D_N)$, $u_i \neq 0$, for $i = 1, \dots, N$, such that

$$\begin{pmatrix} 1-\delta^2\omega^2\xi(\omega,k)M_{D_1}^{k_0\delta} & -\delta^2\omega^2\xi(\omega,k)N_{D_2D_1}^{k_0\delta} & \dots & -\delta^2\omega^2\xi(\omega,k)N_{D_ND_1}^{k_0\delta} \\ -\delta^2\omega^2\xi(\omega,k)N_{D_1D_2}^{k_0\delta} & 1-\delta^2\omega^2\xi(\omega,k)M_{D_2}^{k_0\delta} & \dots & -\delta^2\omega^2\xi(\omega,k)N_{D_ND_2}^{k_0\delta} \\ \vdots & \vdots & \ddots & \vdots \\ -\delta^2\omega^2\xi(\omega,k)N_{D_1D_N}^{k_0\delta} & -\delta^2\omega^2\xi(\omega,k)N_{D_2D_N}^{k_0\delta} & \dots & 1-\delta^2\omega^2\xi(\omega,k)M_{D_N}^{k_0\delta} \end{pmatrix} \begin{pmatrix} u_1 \\ u_2 \\ \vdots \\ u_N \end{pmatrix} = \begin{pmatrix} 0 \\ 0 \\ \vdots \\ 0 \end{pmatrix}. \tag{5.12}$$

To ease the notation in what follows, let us define a modified version of the modulo function. This is modified to always return strictly positive values (this is important it will be used for matrix indices later). In particular, it is chosen so that $N\lfloor N \rfloor = N$ for any $N \in \mathbb{N}$.

Definition 5.2.5. *Given $N \in \mathbb{N}$, we denote by $\lfloor N \rfloor : \mathbb{N} \to \{1, 2, \dots, N\}$ a modified version of the modulo function,* i.e.*, the remainder of euclidean division by N. In*

particular, for all $M \in \mathbb{N}$, there exists unique $\tau \in \mathbb{Z}_{\geq 0}$ and $r \in \mathbb{N}$ with $0 < r \leq N$, such that

$$M = \tau \cdot N + r.$$

Then, we define $M\lfloor N \rfloor$ to be

$$M\lfloor N \rfloor := r.$$

Here, let us state the following lemma, which will be used to prove the main results of this subsection.

Lemma 5.2.6. *For $i = 1, \ldots, N$, let $\phi_i^{(\delta)}$ denote the eigenvector associated to the particle D_i of the potential $M_{D_i}^{k_0\delta}$. Then, we have that*

$$\phi_i^{(\delta)} = \hat{1}_{D_i} + O\left(\frac{1}{\log \delta}\right), \quad i = 1, \ldots, N,$$

where $\hat{1}_{D_i} = \frac{1_{D_i}}{\sqrt{|D_i|}}$ and $|D_i|$ is used to denote the volume of D_i.

Proof. We refer to Appendix A of [8] for the complete proof of this statement. The main idea is to notice that the first order of the expansion of the operator $M_{D_i}^{k_0\delta}$ is independent of $x \in D$. Hence, the eigenvectors $\phi_i^{(\delta)}$, $i = 1, 2, ..., N$, should be constant functions, meaning they can be approximated as $\phi_i^{(\delta)} = \hat{1}_{D_i} + O(\frac{1}{\log(\delta)})$, where $\hat{1}_{D_i} = \frac{1_{D_i}}{\sqrt{|D_i|}}$. □

We recall the diluteness assumption that we have made on our system, which is captured by considering small particle size ρ. We define $\rho := \frac{1}{2}\max_i(\mathrm{diam}(D_i))$ where $\mathrm{diam}(D_i)$ is given by

$$\mathrm{diam}(D_i) = \sup\{|x - y| : x, y \in D_i\}. \tag{5.13}$$

Then, in the case that ρ is small, we have the following lemma, which will be used later.

Lemma 5.2.7. *For all $i = 1, \ldots, N$, we denote $u_i = u|_{D_i}$, where u is a resonant mode, in the sense that it is a solution to (5.8) with no incoming wave. Then, for characteristic size δ of the same order as ρ, we can write that*

$$u_i = \langle u, \phi_i^{(\delta)} \rangle \phi_i^{(\delta)} + O(\rho^2), \quad i = 1, \ldots, N, \tag{5.14}$$

as $\rho \to 0$, where $\phi_i^{(\delta)}$ denotes the eigenvector associated to the particle D_i of the potential $M_{D_i}^{k_0\delta}$ and $\rho > 0$ denotes the particle size parameter of $D_1, \ldots, D_N$. Here, δ and ρ are of the same order in the sense that $\delta = O(\rho)$ and $\rho = O(\delta)$. In this case, the error term holds uniformly for any small δ and ρ in a neighbourhood of 0.

Proof. We refer to Appendix A.4.2. □

We can now state the main result in the two-dimensional case.

Theorem 5.2.8. *The scattering resonance problem in two dimensions becomes, at leading order as $\delta \to 0$ and $\rho \to 0$, with $\delta = O(\rho)$ and $\rho = O(\delta)$, finding $\omega \in \mathbb{C}$ such that*

$$\det(\mathcal{L}) = 0,$$

where the matrix $\mathcal{L}$ is given by

$$\mathcal{L}_{ij} = \begin{cases} \langle N^{k_0\delta}_{D_i D_{i+1\lfloor N\rfloor}} \phi^{(\delta)}_i, \phi^{(\delta)}_{i+1\lfloor N\rfloor} \rangle, & \text{if } i = j, \\ -\mathcal{B}_i(\omega,\delta) \langle N^{k_0\delta}_{D_j D_i} \phi^{(\delta)}_j, \phi^{(\delta)}_i \rangle \langle N^{k_0\delta}_{D_i D_{i+1\lfloor N\rfloor}} \phi^{(\delta)}_i, \phi^{(\delta)}_{i+1\lfloor N\rfloor} \rangle, & \text{if } i \neq j. \end{cases} \tag{5.15}$$

Here, $k_0 = \mu_0 \varepsilon_0 \omega$ and

$$\mathcal{B}_i(\omega,\delta) := \frac{\delta^2 \omega^2 \xi(\omega,k)}{1 - \delta^2 \omega^2 \xi(\omega,k) \nu^{(i)}_\delta}, \quad i = 1, 2, ..., N, \tag{5.16}$$

with $\nu^{(i)}_\delta$ and $\phi^{(\delta)}_i$ being the eigenvalues and the respective eigenvectors associated to the particle D_i of the potential $M^{k_0\delta}_{D_i}$, for $i = 1, 2, \ldots, N$.

Proof. We observe that the integral formulation (5.12) is equivalent to

$$\begin{pmatrix} u_1 \\ u_2 \\ \vdots \\ u_N \end{pmatrix} - \delta^2 \omega^2 \xi(\omega,k) \mathbb{M} \begin{pmatrix} \sum_{j=1, j\neq 1}^{N} N^{k_0\delta}_{D_j D_1} u_j \\ \sum_{j=1, j\neq 2}^{N} N^{k_0\delta}_{D_j D_2} u_j \\ \vdots \\ \sum_{j=1, j\neq N}^{N} N^{k_0\delta}_{D_j D_N} u_j \end{pmatrix} = \begin{pmatrix} 0 \\ 0 \\ \vdots \\ 0 \end{pmatrix}, \tag{5.17}$$

where $\mathbb{M}$ is the diagonal matrix given by

$$\mathbb{M}_{ij} = \begin{cases} \left(1 - \delta^2 \omega^2 \xi(\omega,k) M^{k_0\delta}_{D_i}\right)^{-1}, & \text{if } i = j, \\ 0, & \text{if } i \neq j, \end{cases}$$

for $i, j = 1, \ldots, N$. From the pole-pencil decomposition, for $i = 1, 2, \ldots, N$, we have

$$\left(1 - \delta^2 \omega^2 \xi(\omega,k) M^{k_0\delta}_{D_i}\right)^{-1} (\cdot) = \frac{\langle \cdot, \phi^{(\delta)}_i \rangle \phi^{(\delta)}_i}{1 - \delta^2 \omega^2 \xi(\omega,k) \nu^{(i)}_\delta} + R_i[\omega](\cdot).$$

We recall that, as in Chapter 4, the remainder term $R_i[\omega](\cdot)$ can be neglected. Thus, (5.17) gives

$$\begin{pmatrix} u_1 \\ u_2 \\ \vdots \\ u_N \end{pmatrix} - \delta^2\omega^2\xi(\omega,k)\tilde{\mathbb{M}} \begin{pmatrix} \sum_{j=1,j\neq 1}^{N} N^{k_0\delta}_{D_jD_1}u_j \\ \sum_{j=1,j\neq 2}^{N} N^{k_0\delta}_{D_jD_2}u_j \\ \vdots \\ \sum_{j=1,j\neq N}^{N} N^{k_0\delta}_{D_jD_N}u_j \end{pmatrix} = \begin{pmatrix} 0 \\ 0 \\ \vdots \\ 0 \end{pmatrix},$$

where $\tilde{\mathbb{M}}$ is the diagonal matrix given by

$$\tilde{\mathbb{M}}_{ij} = \begin{cases} \frac{\langle\cdot,\phi_i^{(\delta)}\rangle\phi_i^{(\delta)}}{1-\delta^2\omega^2\xi(\omega,k)\nu_\delta^{(i)}}, & \text{if } i=j, \\ 0, & \text{if } i\neq j. \end{cases}$$

This is equivalent to the following system

$$u_i - \frac{\delta^2\omega^2\xi(\omega,k)}{1-\delta^2\omega^2\xi(\omega,k)\nu_\delta^{(i)}} \sum_{j=1,j\neq i}^{N} \langle N^{k_0\delta}_{D_jD_i}u_j, \phi_i^{(\delta)}\rangle\phi_i^{(\delta)} = 0, \quad \text{for each } i=1,\dots,N. \tag{5.18}$$

Then, applying the operator $N^{k_0\delta}_{D_iD_{i+1\lfloor N\rfloor}}$ to (5.18) for each i and taking the product with $\phi^{(\delta)}_{i+1\lfloor N\rfloor}$, gives

$$\begin{aligned} &\langle N^{k_0\delta}_{D_iD_{i+1\lfloor N\rfloor}}u_i, \phi^{(\delta)}_{i+1\lfloor N\rfloor}\rangle - \\ &\qquad - \mathcal{B}_i(\omega,\delta) \sum_{j=1,j\neq i}^{N} \langle N^{k_0\delta}_{D_jD_i}u_j, \phi_i^{(\delta)}\rangle \langle N^{k_0\delta}_{D_iD_{i+1\lfloor N\rfloor}}\phi_i^{(\delta)}, \phi^{(\delta)}_{i+1\lfloor N\rfloor}\rangle = 0, \end{aligned} \tag{5.19}$$

for each $i=1,\dots,N$. We observe that for $j=1,\dots,N$, from Lemma 5.2.7, the following approximation formula holds:

$$u_j \simeq \langle u, \phi_j^{(\delta)}\rangle\phi_j^{(\delta)}.$$

Applying this to (5.19), we get

$$\begin{aligned} &\langle N^{k_0\delta}_{D_iD_{i+1\lfloor N\rfloor}}\phi_i^{(\delta)}, \phi^{(\delta)}_{i+1\lfloor N\rfloor}\rangle\langle u, \phi_i^{(\delta)}\rangle - \\ &\qquad - \mathcal{B}_i(\omega,\delta) \sum_{j=1,j\neq i}^{N} \langle N^{k_0\delta}_{D_jD_i}\phi_j^{(\delta)}, \phi_i^{(\delta)}\rangle \langle N^{k_0\delta}_{D_iD_{i+1\lfloor N\rfloor}}\phi_i^{(\delta)}, \phi^{(\delta)}_{i+1\lfloor N\rfloor}\rangle\langle u, \phi_j^{(\delta)}\rangle = 0, \end{aligned} \tag{5.20}$$

for each $i = 1, \ldots, N$. This system has the matrix representation

$$\mathcal{L}\begin{pmatrix} \langle u, \phi_1^{(\delta)} \rangle \\ \langle u, \phi_2^{(\delta)} \rangle \\ \vdots \\ \langle u, \phi_N^{(\delta)} \rangle \end{pmatrix} = \begin{pmatrix} 0 \\ 0 \\ \vdots \\ 0 \end{pmatrix}, \tag{5.21}$$

where $\mathcal{L}$ is given by (5.15), which is the desired result. □

Corollary 5.2.9. *It holds that for* $1 \leq i, j \leq N$,

$$\mathcal{L}_{ij} = \begin{cases} \langle N^{k_0\delta}_{D_i D_{i+1\lfloor N \rfloor}} \hat{1}_{D_i}, \hat{1}_{D_{i+1\lfloor N \rfloor}} \rangle, & \text{if } j = i, \\ -\mathcal{B}_i(\omega, \delta) \langle N^{k_0\delta}_{D_i D_{i+1\lfloor N \rfloor}} \hat{1}_{D_i}, \hat{1}_{D_{i+1\lfloor N \rfloor}} \rangle^2, & \text{if } j = i + 1\lfloor N \rfloor, \\ -\mathcal{B}_i(\omega, \delta) \langle N^{k_0\delta}_{D_i D_j} \hat{1}_{D_i}, \hat{1}_{D_j} \rangle \langle N^{k_0\delta}_{D_i D_{i+1\lfloor N \rfloor}} \hat{1}_{D_i}, \hat{1}_{D_{i+1\lfloor N \rfloor}} \rangle, & \text{otherwise.} \end{cases} \tag{5.22}$$

Proof. We have from Lemma 5.2.6 that the eigenvectors $\phi_i^{(\delta)}$, $i = 1, 2, ..., N$, are by $\phi_i^{(\delta)} = \hat{1}_{D_i} + O(\frac{1}{\log(\delta)})$, where $\hat{1}_{D_i} = \frac{1_{D_i}}{\sqrt{|D_i|}}$. Then, we can directly see the symmetry argument

$$\langle N^{k_0\delta}_{D_i D_j} \hat{1}_{D_i}, \hat{1}_{D_j} \rangle = \langle N^{k_0\delta}_{D_j D_i} \hat{1}_{D_j}, \hat{1}_{D_i} \rangle.$$

This implies that

$$\mathcal{L}_{i,i+1\lfloor N \rfloor} = -\mathcal{B}_i(\omega, \delta) \langle N^{k_0\delta}_{D_i D_j} \hat{1}_{D_i}, \hat{1}_{D_{i+1\lfloor N \rfloor}} \rangle^2,$$

which gives the desired result. □

5.3. Computation of the coupled resonant frequencies

In Theorem 5.2.8, we have derived an asymptotic formula for the resonant frequencies. This amounts to finding the ω such that $\det(\mathcal{L}(\omega)) = 0$. In this section, we will show how to use this asymptotic formula to calculate the resonant frequencies for physical examples. This calculation is not straightforward, since the integral operators have highly non-linear dependence on ω. However, an explicit formula can be derived under an additional assumption. Furthermore, Muller's method can be used to find the the frequencies for which the coefficient matrix is singular, given appropriate initial guesses.

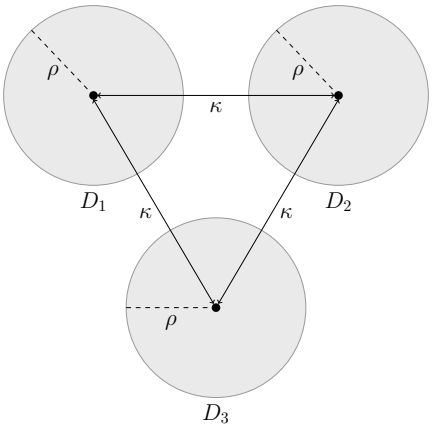

Figure 5.2.: A system of three identical circular resonators can be modelled concisely using our asymptotic method. We study halide perovskite resontators D_1, D_2 and D_3 of radius ρ, made from the same material, with centers placed at a distance κ from each other.

5.3.1. Example: Three circular resonators

Let us consider the case of having three identical circular halide perovskite resonators D_1, D_2 and D_3. We will assume that the particles are placed at the same distance κ from each other. This geometry is sketched in Figure 5.2 and will serve as a suitable example to demonstrate our method. In order to ease the notation, let us write

$$N_{12}(\omega,\delta) := \langle N^{k_0\delta}_{D_1D_2}\hat{1}_{D_1}, \hat{1}_{D_2}\rangle, \qquad N_{23}(\omega,\delta) := \langle N^{k_0\delta}_{D_2D_3}\hat{1}_{D_2}, \hat{1}_{D_3}\rangle$$

and

$$N_{31}(\omega,\delta) := \langle N^{k_0\delta}_{D_3D_1}\hat{1}_{D_3}, \hat{1}_{D_1}\rangle.$$

In order to accelerate the numerical computations and facilitate explicit analytic results, we will make an additional assumption. This assumption is that $N_{ij}(\omega,\delta)$ has no a priori dependence on the frequency ω. This is justified in the specific case of halide perovskite nano-particles since ε_0 is of the same magnitude as the characteristic size δ. This assumption does not discard the dispersive nature of our system with respect to the frequency $\omega \in \mathbb{C}$, since this dependence is due to the terms $\mathcal{B}_i(\omega,\delta)$, $i = 1,\dots,N$, where the non-linear dispersive permittivity relation appears. Further, since we are working with the frequencies of the visible light, it holds that ω is of the same magnitude as δ^{-2}. Thus, it is reasonable to assume that δk_0 is constant with respect to ω. Since the dependence of N_{ij} on ω always takes this form, we can assume it to be approximately independent of ω. We will make this assumption for the results presented in this subsection, and it will be of great importance in studying the inverse design problem in the following section. We write $N_{12}(\omega,\delta) = N_{12}(\delta), N_{23}(\omega,\delta) = N_{23}(\delta)$ and $N_{31}(\omega,\delta) = N_{31}(\delta)$. Also, since

the resonators are identical, it means that they are made from the same material and have the same symmetry. As a result, it holds that $\mathcal{B}_1(\omega,\delta) = \mathcal{B}_2(\omega,\delta) = \mathcal{B}_3(\omega,\delta) =: \mathcal{B}(\omega,\delta)$. Thus, the matrix $\mathcal{L}$ can be rewritten as

$$\mathcal{L} = \begin{pmatrix} N_{12}(\delta) & -\mathcal{B}(\omega,\delta)N_{12}(\delta)^2 & -\mathcal{B}(\omega,\delta)N_{12}(\delta)N_{31}(\delta) \\ -\mathcal{B}(\omega,\delta)N_{12}(\delta)N_{23}(\delta) & N_{23}(\delta) & -\mathcal{B}(\omega,\delta)N_{23}(\delta)^2 \\ -\mathcal{B}(\omega,\delta)N_{31}(\delta)^2 & -\mathcal{B}(\omega,\delta)N_{23}(\delta)N_{31}(\delta) & N_{31}(\delta) \end{pmatrix}. \tag{5.23}$$

Then, seeking ω such that $\det(\mathcal{L}) = 0$, gives that

$$2N_{12}(\delta)N_{23}(\delta)N_{31}(\delta)\mathcal{B}(\omega,\delta)^3 + \Big(N_{12}(\delta)^2 + N_{23}(\delta)^2 + N_{31}(\delta)^2\Big)\mathcal{B}(\omega,\delta)^2 - 1 = 0. \tag{5.24}$$

We solve (5.24) for $\mathcal{B}(\omega,\delta)$ and denote the three solutions by $\mathbb{B}_i$, for $i = 1,2,3$. Then, solving for $\omega \in \mathbb{C}$ in (5.16), we have

$$\Big[\mu_0\alpha\delta^2 + \mathbb{B}_i + \mathbb{B}_i\mu_0\alpha\delta^2\nu(\delta)\Big]\omega^2 + i\mathbb{B}_i\gamma\omega - \mathbb{B}_i\beta - \mathbb{B}_i\eta k^2 = 0,$$

from which we obtain

$$\omega_i = \frac{-i\mathbb{B}_i\gamma \pm \sqrt{-\mathbb{B}_i^2\gamma^2 + 4\Big(\mathbb{B}_i\beta + \mathbb{B}_i\eta k^2\Big)\Big(\mu_0\alpha\delta^2 + \mathbb{B}_i + \mathbb{B}_i\mu_0\alpha\delta^2\nu(\delta)\Big)}}{2\Big(\mu_0\alpha\delta^2 + \mathbb{B}_i + \mathbb{B}_i\mu_0\alpha\delta^2\nu(\delta)\Big)}, \quad i = 1,2,3. \tag{5.25}$$

It is helpful to illustrate these results by comparing the case of three resonators to one- and two-particle systems. We plot all these frequencies as a function of the particle size in Figure 5.3. The resonant frequency for one particle is denoted by $\omega_s^{(1)}$ and the subwavelength frequencies for the case of two particles will be denoted by $\omega_{\text{mon}}^{(2)}$ and $\omega_{\text{dip}}^{(2)}$. These systems were explored in detail in Chapter 4, where it was shown that that $\omega_{\text{mon}}^{(2)} < \omega_s^{(1)} < \omega_{\text{dip}}^{(2)}$ as a result of the hybridisation. For the case of three particles, we denote the frequencies by $\omega_1^{(3)}, \omega_2^{(3)}$ and $\omega_3^{(3)}$, and we observe that there is also an ordering between them $\omega_1^{(3)} < \omega_2^{(3)} < \omega_3^{(3)}$. Parameter values are chosen to corresponding to methylammonium lead chloride ($MAPbCl_3$), which is a popular halide perovskite [52]. We notice that the resonant frequencies for these resonators lies in the range of visible frequencies, when the particles are hundreds of nanometres in size. This puts the system in the appropriate subwavelength regime that was required for our asymptotic method. As $\delta \to 0$, the frequencies of the different cases converge to $\omega_s^{(1)}$. This is because the nano-particles behave as isolated, identical resonators when δ is very small. Then, as δ increases, we observe that there is a separation between the frequencies of the two particle and three particle case $\omega_1^{(3)} < \omega_{\text{mon}}^{(2)} < \omega_2^{(3)} < \omega_{\text{dip}}^{(2)} < \omega_3^{(3)}$. In Figures 5.3(b) and 5.3(c), we can see more clearly this separation. This is the effect of the hybridisation on the system of resonators.

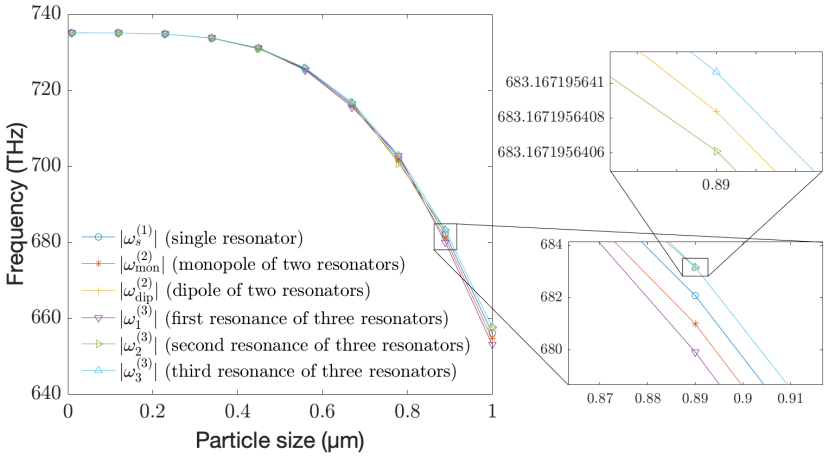

Figure 5.3.: Behaviour of the subwavelength resonances for small circular nanoparticles of radius δ. For three circular methylammonium lead chloride nano-particles, we see how the hybridisation causes the frequencies $\omega_1^{(3)}, w_2^{(3)}$ and $\omega_3^{(3)}$ to shift, relative to the uncoupled resonant frequency of a single particle. We compare them with the hybridised frequencies $\omega_{\text{mon}}^{(2)}, \omega_{\text{dip}}^{(2)}$ of the two circular particle case and the resonant frequency $\omega_s^{(1)}$ of the single particle. All the resonators are identical, in the sense that they are the same size and made from the same material (methylammonium lead chloride).

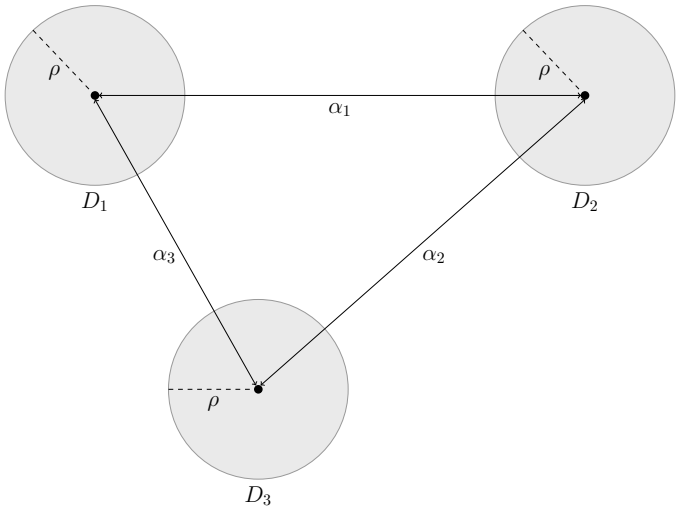

Figure 5.4.: Our asymptotic results can be used to design a system of three identical resonators with specific resonant frequencies. We study a system of three identical circular halide perovskite resonators D_1, D_2 and D_3, each with radius ρ, with centers placed at distances $\operatorname{dist}(D_1, D_2) = \alpha_1, \operatorname{dist}(D_2, D_3) = \alpha_2$ and $\operatorname{dist}(D_1, D_3) = \alpha_3$.

5.4. Inverse design

In this section, we will use our asymptotic results to tackle an inverse design problem. Let us assume that we are given three identical two-dimensional circular halide perovskite resonators D_1, D_2 and D_3 of radius $\rho \in \mathbb{R}_{>0}$ and three frequencies $\omega_1, \omega_2, \omega_3 \in \mathbb{C}$. Again, we will assume that we are working with nano-particles and that the frequencies given are of the visible light, and so of order δ^{-2}. We want to find the appropriate geometry such that the system of three particles resonates at ω_1, ω_2 and ω_3. This toy problem is inspired by human vision, which is sensitive to three different colours, and the desire to design systems capable of giving colour perception to bioinspired artificial eyes made from halide perovskites [36, 48].

Let us denote the separation distances as

$$\alpha_1 = \operatorname{dist}(D_1, D_2), \quad \alpha_2 = \operatorname{dist}(D_2, D_3), \quad \alpha_3 = \operatorname{dist}(D_1, D_3).$$

The configuration is sketched in Figure 5.4. Then, our problem is finding $\alpha_1, \alpha_2, \alpha_3 \in \mathbb{R}$, such that

$$\det(\mathcal{L})(\omega_1, \delta) = \det(\mathcal{L})(\omega_2, \delta) = \det(\mathcal{L})(\omega_3, \delta) = 0,$$

where $\mathcal{L}$ is the coefficient matrix given by (5.22). This translates into finding

$(\alpha_1, \alpha_2, \alpha_3) \in \mathbb{R}^3$, such that

$$\begin{cases} 2\mathcal{B}(\omega_1,\delta)^3 N_{12}(\delta)N_{23}(\delta)N_{13}(\delta) + \mathcal{B}(\omega_1,\delta)^2\Big(N_{12}(\delta)^2 + N_{23}(\delta)^2 + N_{13}(\delta)^2\Big) - 1 = 0, \\ 2\mathcal{B}(\omega_2,\delta)^3 N_{12}(\delta)N_{23}(\delta)N_{13}(\delta) + \mathcal{B}(\omega_2,\delta)^2\Big(N_{12}(\delta)^2 + N_{23}(\delta)^2 + N_{13}(\delta)^2\Big) - 1 = 0, \\ 2\mathcal{B}(\omega_3,\delta)^3 N_{12}(\delta)N_{23}(\delta)N_{13}(\delta) + \mathcal{B}(\omega_3,\delta)^2\Big(N_{12}(\delta)^2 + N_{23}(\delta)^2 + N_{13}(\delta)^2\Big) - 1 = 0. \end{cases} \tag{5.26}$$

Here, let us note that we have suppressed the dependence of the terms N_{ij}, $i,j = 1,2,3$, $i \neq j$ on the frequencies $\omega_i \in \mathbb{C}$, for $i = 1,2,3$, since, as mentioned in the previous subsection, it makes physical sense for our model, and the dispersive character is still preserved.

Our design strategy will have two steps. First, we will find the appropriate characteristic size in order for (5.26) to admit a solution. Then, we derive the condition on the separation distances that is required to give the desired resonant frequencies.

5.4.1. Linearity of off-diagonal entries

In order to handle (5.26), it will be helpful to establish how the coefficients N_{ij} depend on the distances between the particles, in the case that δ is small. Let us first show the following lemma which we will use later and is a consequence of working with small, circular particles.

Lemma 5.4.1. *Let $d \in \mathbb{R}$ be fixed and $A \in \mathbb{C}$ be given by $A = R\cos(t) + iR\sin(t)$, where $R, t \in \mathbb{R}$. Then, as $R \to 0$, we have that*

$$|A + d| = |A| + d + O(R).$$

Proof. We observe that

$$\begin{aligned} |A + d|^2 &= |R\cos(t) + iR\sin(t) + d|^2 \\ &= R^2\cos^2(t) + 2dR\cos(t) + d^2 + R^2 sin^2(t) \end{aligned}$$

and

$$\Big(|A| + d\Big)^2 = R^2\cos^2(t) + R^2\sin^2(t) + 2d|R\cos(t) + iR\sin(t)| + d^2.$$

Hence, as $R \to 0$,

$$|A + d|^2 = \Big(|A| + d\Big)^2 + O(R),$$

which gives the desired result. □

We will now state a fundamental result which contributes a lot to the analysis of the system.

Theorem 5.4.2. *There exists* $\mathbb{S} = \mathbb{S}(\delta), \mathbb{Q} = \mathbb{Q}(\delta) \in \mathbb{C}$, *such that as* $\delta \to 0$

$$N_{ij}(\delta) = \mathbb{S} + \mathbb{Q}\mathrm{dist}(D_i, D_j) + O(\delta^4), \quad i, j = 1, \ldots, N,$$

where $\mathrm{dist}(D_i, D_j)$ *denotes the distance between the unscaled particles* D_i *and* D_j, *which does not depend on* δ.

Proof. Let us recall that

$$\begin{aligned} N_{ij}(\delta) &= \langle N^{k_0\delta}_{D_iD_j}\hat{1}_{D_i}, \hat{1}_{D_j}\rangle \\ &= \langle \hat{K}^{k_0\delta}_{D_iD_j}\hat{1}_{D_i}, \hat{1}_{D_j}\rangle + \langle R^{(0)}_{D_iD_j}\hat{1}_{D_i}, \hat{1}_{D_j}\rangle + (k_0\delta)^2\log(k_0\delta\hat{\gamma})\langle R^{(1)}_{D_iD_j}\hat{1}_{D_i}, \hat{1}_{D_j}\rangle. \end{aligned}$$

We will look at this expression term by term. We observe that

$$\langle \hat{K}^{k_0\delta}_{D_iD_j}\hat{1}_{D_i}, \hat{1}_{D_j}\rangle = -\frac{1}{2\pi}\log(k_0\delta\hat{\gamma})\int_{D_j}\int_{D_i}\hat{1}_{D_i}(y)\mathrm{d}y\hat{1}_{D_j}(x)\mathrm{d}x.$$

Since there is no distance element appearing in the integrand, there is not dependence on the distance between the particles D_i and D_i. Thus, this is a constant with respect to the resonator distance,

$$K_{ij} := \langle \hat{K}^{k_0\delta}_{D_iD_j}\hat{1}_{D_i}, \hat{1}_{D_j}\rangle \tag{5.27}$$

Next, we have

$$\begin{aligned} &\langle R^{(0)}_{D_iD_j}\hat{1}_{D_i}, \hat{1}_{D_j}\rangle = -\frac{1}{2\pi}\int_{D_j}\int_{D_i}\log|x-y|\hat{1}_{D_i}(y)\mathrm{d}y\hat{1}_{D_j}(x)\mathrm{d}x \\ &= -\frac{1}{2\pi\sqrt{|D_i||D_j|}}\int_0^{2\pi}\int_0^{\rho}\int_0^{2\pi}\int_0^{\rho}\log\Big|r_xe^{it_x} - r_ye^{it_y} + \mathrm{dist}(D_i, D_j)\Big|r_yr_x\mathrm{d}r_y\mathrm{d}t_y\mathrm{d}r_x\mathrm{d}t_x, \end{aligned}$$

where we have changed to polar coordinates and used the fact that the particles are circular and identical. From this, we also get $|D_1| = |D_2| = |D_3| = \pi\rho^2$. In addition, using the Taylor expansion of the logarithm function and Lemma 5.4.1, we have

$$\log\Big|r_xe^{it_x} - r_ye^{it_y} + \mathrm{dist}(D_i, D_j)\Big| \simeq \Big|r_xe^{it_x} - r_ye^{it_y}\Big| + \mathrm{dist}(D_i, D_j) - 1 + O(\rho^2).$$

If we define

$$R^{(0)} := -\frac{1}{2\pi^2\rho^2}\int_0^{2\pi}\int_0^{\rho}\int_0^{2\pi}\int_0^{\rho}\Big(\Big|r_xe^{it_x} - r_ye^{it_y}\Big| - 1\Big)r_yr_x\mathrm{d}r_y\mathrm{d}t_y\mathrm{d}r_x\mathrm{d}t_x,$$

then we have that

$$\langle R^{(0)}_{D_iD_j}\hat{1}_{D_i}, \hat{1}_{D_j}\rangle = R^{(0)} - \frac{\rho^2}{2}\mathrm{dist}(D_i, D_j) + O(\rho^4). \tag{5.28}$$

The last term can be rewritten as

$$\langle R^{(1)}_{D_iD_j}\hat{1}_{D_i}, \hat{1}_{D_j}\rangle = -\frac{i}{4\pi}\int_{D_j}\int_{D_i}\frac{1}{|x-y|}\hat{1}_{D_i}(y)\mathrm{d}y\hat{1}_{D_j}(x)\mathrm{d}x$$

$$= \frac{-i}{4\pi^2\rho^2}\int_0^{2\pi}\int_0^{\rho}\int_0^{2\pi}\int_0^{\rho}\frac{r_y r_x}{\left|r_x e^{it_x} - r_y e^{it_y} + \mathrm{dist}(D_i, D_j)\right|}\mathrm{d}r_y\mathrm{d}t_y\mathrm{d}r_x\mathrm{d}t_x.$$

Again, using the Taylor expansion and Lemma 5.4.1, we have

$$\frac{1}{\left|r_x e^{it_x} - r_y e^{it_y} + \mathrm{dist}(D_i, D_j)\right|} \simeq 2 + \mathrm{dist}(D_i, D_j) - \left|r_x e^{it_x} - r_y e^{it_y}\right| + O(\rho^2)$$

Hence, defining

$$R^{(1)} := \frac{-i}{4\pi^2\rho^2}\int_0^{2\pi}\int_0^{\rho}\int_0^{2\pi}\int_0^{\rho}\left(2 - \left|r_x e^{it_x} - r_y e^{it_y}\right|\right) r_y r_x \mathrm{d}r_y\mathrm{d}t_y\mathrm{d}r_x\mathrm{d}t_x,$$

gives

$$\langle R^{(1)}_{D_i D_j}\hat{1}_{D_i}, \hat{1}_{D_j}\rangle = R^{(1)} - \frac{i\rho^2}{4}\mathrm{dist}(D_i, D_j) + O(\rho^4). \tag{5.29}$$

Gathering the results (5.27), (5.28) and (5.29), we obtain

$$\begin{aligned} N_{ij}(\delta) =& K_{ij} + R^{(0)} + (k_0\delta)^2\log(k_0\delta\hat{\gamma})R^{(1)} + & (5.30)\\ &+ \left[-\frac{\rho^2}{2} - \frac{i\rho^2}{4}(k_0\delta)^2\log(k_0\delta\hat{\gamma})\right]\mathrm{dist}(D_i, D_j) + O(\delta^4), & (5.31)\end{aligned}$$

and thus, by defining

$$\mathbb{S}_{ij} := K_{ij} + R^{(0)} + (k_0\delta)^2\log(k_0\delta\hat{\gamma})R^{(1)}$$

and

$$\mathbb{Q} := -\frac{\rho^2}{2} - \frac{i\rho^2}{4}(k_0\delta)^2\log(k_0\delta\hat{\gamma}),$$

we get

$$N_{ij}(\delta) = \mathbb{S}_{ij} + \mathbb{Q}\mathrm{dist}(D_i, D_j) + O(\delta^4).$$

Since the particles are identical, we have directly that $\mathbb{S}_{12} = \mathbb{S}_{23} = \mathbb{S}_{13} =: \mathbb{S}$, from which the result follows. □

Remark 5.4.3. *We note that this theorem can also be generalised to the cases where the resonators are not circular. The adaptation required would be a change in the definitions of* $\mathbb{S}$ *and* $\mathbb{Q}$*.*

The above theorem allows us to write

$$\begin{gathered} N_{12} = \mathbb{S} + \mathbb{Q}\alpha_1 + O(\delta^4), \quad N_{23} = \mathbb{S} + \mathbb{Q}\alpha_2 + O(\delta^4) \\ \text{and} \quad N_{13} = \mathbb{S} + \mathbb{Q}\alpha_3 + O(\delta^4). \end{gathered} \tag{5.32}$$

5.4.2. Condition on characteristic size

The first thing that we wish to understand is when the system (5.26) has a solution. Let us write

$$X = N_{12}N_{23}N_{13} \qquad \text{and} \qquad Y = N_{12}^2 + N_{23}^2 + N_{13}^2.$$

Then, (5.26) becomes

$$\begin{cases} 2\mathcal{B}(\omega_1,\delta)^3 X + \mathcal{B}(\omega_1,\delta)^2 Y - 1 = 0, \\ 2\mathcal{B}(\omega_2,\delta)^3 X + \mathcal{B}(\omega_2,\delta)^2 Y - 1 = 0, \\ 2\mathcal{B}(\omega_3,\delta)^3 X + \mathcal{B}(\omega_3,\delta)^2 Y - 1 = 0. \end{cases} \tag{5.33}$$

Using the Gauss elimination process, we get that the following equation needs to be satisfied

$$\begin{aligned} \mathcal{B}(\omega_3,\delta)^2 \Big[\mathcal{B}(\omega_1,\delta)^3 - \mathcal{B}(\omega_2,\delta)^3\Big] \Big[\mathcal{B}(\omega_3,\delta) - \mathcal{B}(\omega_1,\delta)\Big] = \\ = \mathcal{B}(\omega_2,\delta)^2 \Big[\mathcal{B}(\omega_1,\delta)^3 - \mathcal{B}(\omega_3,\delta)^3\Big] \Big[\mathcal{B}(\omega_2,\delta) - \mathcal{B}(\omega_1,\delta)\Big]. \end{aligned}$$

Expanding this, we obtain that the characteristic size δ needs to satisfy

$$\begin{aligned} \delta^2\nu(\delta) = & \frac{-1}{3\omega_1^2\xi(\omega_1,k)\omega_2^2\xi(\omega_2,k)\omega_3^2\xi(\omega_3,k)} \cdot \Big[\omega_1^4\xi(\omega_1,k)^2\omega_3^6\xi(\omega_3,k)^3 - \\ & - \omega_1^6\xi(\omega_1,k)^3\omega_3^4\xi(\omega_3,k)^2 + \omega_2^6\xi(\omega_2,k)^3\omega_3^4\xi(\omega_3,k)^2 - \\ & - \omega_1^4\xi(\omega_1,k)^2\omega_2^6\xi(\omega_2,k)^3 + \omega_1^6\xi(\omega_1,k)^3\omega_2^4\xi(\omega_2,k)^2 - \\ & - \omega_2^4\xi(\omega_2,k)^2\omega_3^6\xi(\omega_3,k)^3\Big] \cdot \Big[\omega_1^2\xi(\omega_1,k)\omega_2^4\xi(\omega_2,k)^2 + \\ & + \omega_2^2\xi(\omega_2,k)\omega_3^4\xi(\omega_3,k)^2 + \omega_1^4\xi(\omega_1,k)^2\omega_3^2\xi(\omega_3,k) - \\ & - \omega_1^2\xi(\omega_1,k)\omega_3^4\xi(\omega_3,k)^2 - \omega_2^4\xi(\omega_2,k)^2\omega_3^2\xi(\omega_3,k) - \\ & - \omega_1^4\xi(\omega_1,k)^2\omega_2^2\xi(\omega_2,k)\Big]^{-1}, \end{aligned} \tag{5.34}$$

for (5.33) to have a solution.

5.4.3. Condition on separation distances

We assume that the condition (5.34) is satisfied. Then, we can reduce our study of the system (5.33) to finding a solution to

$$\begin{cases} 2\mathcal{B}(\omega_1,\delta)^3 X + \mathcal{B}(\omega_1,\delta)^2 Y - 1 = 0, \\ 2\mathcal{B}(\omega_2,\delta)^3 X + \mathcal{B}(\omega_2,\delta)^2 Y - 1 = 0. \end{cases} \tag{5.35}$$

This gives

$$X = \frac{\mathcal{B}(\omega_2,\delta)^2\Big[\mathcal{B}(\omega_2,\delta)-\mathcal{B}(\omega_1,\delta)\Big]-\Big[\mathcal{B}(\omega_2,\delta)^3-\mathcal{B}(\omega_1,\delta)^3\Big]}{2\mathcal{B}(\omega_1,\delta)\mathcal{B}(\omega_2,\delta)^2\Big[\mathcal{B}(\omega_2,\delta)\mathcal{B}(\omega_1,\delta)^2-\mathcal{B}(\omega_1,\delta)^3\Big]} \tag{5.36}$$

and

$$Y = \frac{\mathcal{B}(\omega_2,\delta)^3-\mathcal{B}(\omega_1,\delta)^3}{\mathcal{B}(\omega_1,\delta)^2\mathcal{B}(\omega_2,\delta)^2\Big[\mathcal{B}(\omega_2,\delta)-\mathcal{B}(\omega_1,\delta)\Big]}. \tag{5.37}$$

Fixing these values for X and Y and varying $\alpha_3 \in \mathbb{R}$, we get from (5.26),

$$\alpha_2(\alpha_3) = \frac{1}{\mathbb{Q}}\left(-\mathbb{S} \pm \sqrt{\frac{-C \pm \sqrt{C^2-4X^2(\mathbb{S}+\mathbb{Q}\alpha_3)^2}}{2(\mathbb{S}+\mathbb{Q}\alpha_3)^2}}\right), \tag{5.38}$$

where $C = (\mathbb{S}+\mathbb{Q}\alpha_3)^2[(\mathbb{S}+\mathbb{Q}\alpha_3)^2 - Y]$ and

$$\alpha_1(\alpha_3) = \frac{1}{\mathbb{Q}}\left(\frac{X}{\Big(\mathbb{S}+\mathbb{Q}\alpha_2(\alpha_3)\Big)\Big(\mathbb{S}+\mathbb{Q}\alpha_3\Big)} - \mathbb{S}\right). \tag{5.39}$$

Let us also note here, that in order for the distances found to make geometric sense, we require

$$\Big|\alpha_3 - \alpha_2(\alpha_3)\Big| \le \alpha_1(\alpha_3) \le \Big|\alpha_3 + \alpha_2(\alpha_3)\Big|, \tag{5.40}$$

which gives an additional condition on $\alpha_3 \in \mathbb{R}$. Therefore, we conclude that the distances α_1, α_2 and α_3 must lie in the one-dimensional space given by

$$\left\{\begin{pmatrix}\alpha_1(\alpha_3)\\ \alpha_2(\alpha_3)\\ \alpha_3\end{pmatrix} : \alpha_3 \in \mathbb{R} \text{ such that (5.40) holds and } \delta \in \mathbb{R} \text{ is given by (5.34)}\right\}. \tag{5.41}$$

5.5. Conclusion

We have developed an approach for modelling a coupled system of many subwavelength halide perovskite resonators. Their highly dispersive material parameters makes this a challenging problem, but, given their rapidly growing usage in electromagnetic devices, efficient mathematical methods like ours are becoming increasingly valuable. Our method is sufficiently concise that we have been able to use it for an inverse design problem, which would have required significant computational effort to solve using numerical simulation methods. These results can accelerate the design of advanced photonic devices [38, 47], including those with complicated structures and geometries, such as the biomimetic eye developed by [36].

A. Appendices

A.1. Appendix to Chapter 2

A.1.1. Proofs of impedance monotonicity

A.1.1.1. Proof of Theorem 2.3.13

Proof of Theorem 2.3.13. We assume that we are working in a band gap $\mathfrak{A}$. We apply $\frac{\partial}{\partial\omega}$ on both sides of (2.2) and we get, using (2.14), that

$$\frac{\partial}{\partial\omega}\left[\frac{\partial}{\partial x}\left(E(x,\omega)\frac{\partial u}{\partial x}\right)\right] = \frac{\partial}{\partial\omega}\Big(-\mu_0\omega^2 u\Big),$$

which is, from (2.14),

$$\frac{\partial}{\partial x}\left[\frac{\partial}{\partial\omega}\left(E(x,\omega)\frac{\partial u}{\partial x}\right)\right] = -2\mu_0\omega u - \mu_0\omega^2\phi$$

and so

$$\frac{\partial}{\partial x}\left[\frac{\partial E}{\partial\omega}(x,\omega)\frac{\partial u}{\partial x} + E(x,\omega)\frac{\partial\phi}{\partial x}\right] = -2\mu_0\omega u - \mu_0\omega^2\phi. \tag{A.1}$$

Also, we have

$$\frac{\mathrm{d}Z^+}{\mathrm{d}\omega} = \frac{\partial}{\partial\omega}\left(\frac{u}{Eu}\right) = \frac{1}{\left(E\frac{\partial u}{\partial x}\right)^2}\left[E\frac{\partial u}{\partial x}\phi - u\left(\frac{\partial E}{\partial\omega}\frac{\partial u}{\partial x} + E\frac{\partial\phi}{\partial x}\right)\right].$$

Let us define the Wronskian $\mathcal{W}$ by

$$\mathcal{W} := E\frac{\partial u}{\partial x}\phi - u\left(\frac{\partial E}{\partial\omega}\frac{\partial u}{\partial x} + E\frac{\partial\phi}{\partial x}\right). \tag{A.2}$$

Then, we get

$$\frac{\mathrm{d}Z_R}{\mathrm{d}\omega} = \frac{\mathcal{W}}{\left(E\frac{\partial u}{\partial x}\right)^2}.$$

We observe that

$$\frac{\partial\mathcal{W}}{\partial x} = \frac{\partial}{\partial x}\left[E\frac{\partial u}{\partial x}\phi - u\left(\frac{\partial E}{\partial\omega}\frac{\partial u}{\partial x} + E\frac{\partial\phi}{\partial x}\right)\right]$$

$$
\begin{aligned}
&= \frac{\partial E}{\partial x}\frac{\partial u}{\partial x}\phi + E\left(\frac{\partial u^2}{\partial x^2}\phi + \frac{\partial u}{\partial x}\frac{\partial \phi}{\partial x}\right) - \frac{\partial u}{\partial x}\left(\frac{\partial E}{\partial \omega}\frac{\partial u}{\partial x} + E\frac{\partial \phi}{\partial x}\right) - \\
&\quad - u\frac{\partial}{\partial x}\left(\frac{\partial E}{\partial \omega}\frac{\partial u}{\partial x} + E\frac{\partial \phi}{\partial x}\right) \\
&= \frac{\partial E}{\partial x}\frac{\partial u}{\partial x}\phi + E\frac{\partial u^2}{\partial x^2}\phi + E\frac{\partial u}{\partial x}\frac{\partial \phi}{\partial x} - \left(\frac{\partial u}{\partial x}\right)^2\frac{\partial E}{\partial \omega} - E\frac{\partial u}{\partial x}\frac{\partial \phi}{\partial x} - \\
&\quad - u\frac{\partial}{\partial x}\left(\frac{\partial E}{\partial \omega}\frac{\partial u}{\partial x} + E\frac{\partial \phi}{\partial x}\right) \\
&= \frac{\partial E}{\partial x}\frac{\partial u}{\partial x}\phi + E\frac{\partial u^2}{\partial x^2}\phi - \left(\frac{\partial u}{\partial x}\right)^2\frac{\partial E}{\partial \omega} - u\frac{\partial}{\partial x}\left(\frac{\partial E}{\partial \omega}\frac{\partial u}{\partial x} + E\frac{\partial \phi}{\partial x}\right) \\
&= \phi\frac{\partial}{\partial x}\left(E\frac{\partial u}{\partial x}\right) - u\frac{\partial}{\partial x}\left(\frac{\partial E}{\partial \omega}\frac{\partial u}{\partial x} + E\frac{\partial \phi}{\partial x}\right) - \left(\frac{\partial u}{\partial x}\right)^2\frac{\partial E}{\partial \omega}.
\end{aligned}
$$

Applying (2.2) and (A.1), we get

$$
\begin{aligned}
\frac{\partial \mathcal{W}}{\partial x} &= -\phi\mu_0\omega^2 u - u(-2\omega\mu_0 u - \mu_0\omega^2\phi) - \left(\frac{\partial u}{\partial x}\right)^2\frac{\partial E}{\partial \omega} \\
&= 2\mu_0\omega u^2 - \left(\frac{\partial u}{\partial x}\right)^2\frac{\partial E}{\partial \omega},
\end{aligned}
$$

which gives

$$
\frac{\partial \mathcal{W}}{\partial x} = 2\mu_0\omega u^2 - \left(\frac{\partial u}{\partial x}\right)^2\frac{\partial E}{\partial \omega}. \tag{A.3}
$$

Integrating with respect to x over the material B, i.e. on $[0, +\infty]$, we have

$$
\lim_{x\to+\infty} \mathcal{W}(x,w) - \mathcal{W}(0,w) = 2\mu_0\omega\int_0^{+\infty} u^2 \mathrm{d}x - \int_0^{+\infty}\left(\frac{\partial u}{\partial x}\right)^2\frac{\partial E}{\partial \omega}\mathrm{d}x.
$$

We know that when the frequency is inside a band gap, the field vanishes as $x \to +\infty$. This implies that

$$
\lim_{x\to+\infty} \mathcal{W}(x,w) = 0,
$$

and so

$$
\mathcal{W}(0,w) = \int_0^{+\infty}\left(\frac{\partial u}{\partial x}\right)^2\frac{\partial E}{\partial \omega}\mathrm{d}x - 2\mu_0\omega\int_0^{+\infty} u^2\mathrm{d}x.
$$

We know that $\frac{\partial \varepsilon}{\partial \omega} \geq 0$. This gives

$$
\frac{\partial E}{\partial \omega} = \frac{\partial}{\partial \omega}\left(\frac{1}{\varepsilon}\right) = \frac{-1}{\varepsilon^2}\frac{\partial \varepsilon}{\partial \omega} \leq 0.
$$

Hence,

$$
\int_0^{+\infty}\left(\frac{\partial u}{\partial x}\right)^2\frac{\partial E}{\partial \omega}\mathrm{d}x \leq 0.
$$

Therefore, we get

$$\frac{\mathrm{d}Z^+}{\mathrm{d}\omega} = \frac{1}{\left(E\frac{\partial u}{\partial x}\right)^2}\left(-2\mu_0\omega\int_0^{+\infty} u^2\mathrm{d}x + \int_0^{+\infty}\left(\frac{\partial u}{\partial x}\right)^2\frac{\partial E}{\partial \omega}\mathrm{d}x\right) < 0.$$

We apply the same argument for Z^- and we obtain similarly that

$$\frac{\mathrm{d}Z^-}{\mathrm{d}\omega} < 0.$$

This concludes the proof.

□

A.1.1.2. Proof of Theorem 2.6.2

Proof of Theorem 2.6.2. The proof follows the same reasoning as the one of Lemma 2.3.3. We first define $\widetilde{E}$ by

$$\widetilde{E}(x,\omega) := \frac{1}{\widetilde{\varepsilon}(x,\omega)}.$$

Applying $\frac{\partial}{\partial\omega}$ on both sides of (2.33), we get

$$\frac{\partial}{\partial x}\left[\frac{\partial\widetilde{E}}{\partial\omega}(x,\omega)\frac{\partial u}{\partial x} + \widetilde{E}(x,\omega)\frac{\partial\phi}{\partial x}\right] = -2\mu_0\omega u - \mu_0\omega^2\phi, \tag{A.4}$$

where $\phi := \frac{\partial u}{\partial\omega}$. Also, we have

$$\frac{\mathrm{d}\widetilde{Z}^+}{\mathrm{d}\omega} = \frac{1}{\left(\widetilde{E}\frac{\partial u}{\partial x}\right)^2}\left[\widetilde{E}\frac{\partial u}{\partial x}\phi - u\left(\frac{\partial\widetilde{E}}{\partial\omega}\frac{\partial u}{\partial x} + \widetilde{E}\frac{\partial\phi}{\partial x}\right)\right].$$

We define the perturbed Wronskian $\widetilde{\mathcal{W}}$ by

$$\widetilde{\mathcal{W}} := \widetilde{E}\frac{\partial u}{\partial x}\phi - u\left(\frac{\partial\widetilde{E}}{\partial\omega}\frac{\partial u}{\partial x} + \widetilde{E}\frac{\partial\phi}{\partial x}\right), \tag{A.5}$$

which gives

$$\frac{\mathrm{d}\widetilde{Z}^+}{\mathrm{d}\omega} = \frac{\widetilde{\mathcal{W}}}{\left(\widetilde{E}\frac{\partial u}{\partial x}\right)^2}.$$

It follows that

$$\frac{\partial\widetilde{\mathcal{W}}}{\partial x} = \phi\frac{\partial}{\partial x}\left(\widetilde{E}\frac{\partial u}{\partial x}\right) - u\frac{\partial}{\partial x}\left(\frac{\partial\widetilde{E}}{\partial\omega}\frac{\partial u}{\partial x} + \widetilde{E}\frac{\partial\phi}{\partial x}\right) - \left(\frac{\partial u}{\partial x}\right)^2\frac{\partial\widetilde{E}}{\partial\omega},$$

and so, from (2.33) and (A.4), we get

$$\frac{\partial \widetilde{\mathcal{W}}}{\partial x} = 2\mu_0 \omega u^2 - \left(\frac{\partial u}{\partial x}\right)^2 \frac{\partial \widetilde{E}}{\partial \omega}.$$

Integrating with respect to x over the perturbed material B, i.e. on $[0, +\infty]$, we have

$$\lim_{x\to+\infty} \widetilde{\mathcal{W}}(x,w) - \widetilde{\mathcal{W}}(0,w) = 2\mu_0\omega \int_0^{+\infty} u^2 \mathrm{d}x - \int_0^{+\infty} \left(\frac{\partial u}{\partial x}\right)^2 \frac{\partial \widetilde{E}}{\partial \omega} \mathrm{d}x.$$

We know that when in a band gap, the field vanishes as $x \to +\infty$. This implies that

$$\lim_{x\to+\infty} \widetilde{\mathcal{W}}(x,w) = 0,$$

and so

$$\widetilde{\mathcal{W}}(0,w) = \int_0^{+\infty} \left(\frac{\partial u}{\partial x}\right)^2 \frac{\partial \widetilde{E}}{\partial \omega} \mathrm{d}x - 2\mu_0\omega \int_0^{+\infty} u^2 \mathrm{d}x.$$

We observe that

$$\begin{aligned}
\frac{\partial \widetilde{E}}{\partial \omega} &= \frac{\partial}{\partial \omega}\left(\frac{1}{\widetilde{\varepsilon}(x,\omega)}\right) \\
&= \frac{\partial}{\partial \omega}\left(\frac{1}{\varepsilon(x,\omega) + \delta f(\omega)}\right) \\
&= \frac{-1}{\Big(\varepsilon(x,\omega) + \delta f(\omega)\Big)^2}\left(\frac{\partial \varepsilon}{\partial \omega} + \delta \frac{\partial f}{\partial \omega}\right).
\end{aligned}$$

Thus, since $\frac{\partial f}{\partial \omega} < +\infty$, we get

$$\lim_{\delta\to 0} \frac{\partial \widetilde{E}}{\partial \omega} = \frac{-1}{\varepsilon(x,\omega)^2} \frac{\partial \varepsilon}{\partial \omega} \leq 0,$$

since we have that $\frac{\partial \varepsilon}{\partial \omega} \geq 0$. Hence,

$$\lim_{\delta\to 0} \int_0^{+\infty} \left(\frac{\partial u}{\partial x}\right)^2 \frac{\partial \widetilde{E}}{\partial \omega} \mathrm{d}x \leq 0.$$

Therefore, at $x = 0$, we get

$$\lim_{\delta\to 0} \frac{\mathrm{d}\widetilde{Z}^+}{\mathrm{d}\omega} = \lim_{\delta\to 0} \frac{1}{\left(\widetilde{E}\frac{\partial u}{\partial x}\right)^2} \left(-2\mu_0\omega \int_0^{+\infty} u^2 \mathrm{d}x + \int_0^{+\infty} \left(\frac{\partial u}{\partial x}\right)^2 \frac{\partial \widetilde{E}}{\partial \omega} \mathrm{d}x\right) < 0.$$

The same argument holds for $\widetilde{Z}^-$ and so, we obtain that

$$\frac{\mathrm{d}\widetilde{Z}^-}{\mathrm{d}\omega} < 0.$$

This concludes the proof. □

A.1.2. Characterisation of eigenmode symmetries

Proof of Lemma 2.3.10. The first thing that we notice is that we cannot have $u_n^{[0]}(0) = \frac{\partial u_n^{[0]}}{\partial x}(0) = 0$ or $u_n^{[\pi]}(0) = \frac{\partial u_n^{[\pi]}}{\partial x}(0) = 0$, since by the uniqueness of solution to the problem (2.2), it would mean $u_n \equiv 0$. Then, from the Lemma 2.3.9, we have two different cases. We will treat each one separately:

We have u_n being symmetric and $\frac{\partial u_n}{\partial x}$ being anti-symmetric. At $\kappa = \pi$, from the symmetry of u_n, we have that

$$u_n^{[\pi]}(0) = \mathcal{P} u_n^{[\pi]}(0) = u_n^{[\pi]}(1)$$

and from (2.4), it holds that

$$u_n^{[\pi]}(0) = e^{i\pi} u_n^{[\pi]}(1) = -u_n^{[\pi]}(1).$$

Combining the two, we get

$$u_n^{[\pi]}(0) = 0.$$

Then, at $\kappa = 0$, since $\frac{\partial u_n}{\partial x}$ is anti-symmetric, we have that

$$\frac{\partial u_n^{[0]}}{\partial x}(0) = -\mathcal{P}\frac{\partial u_n^{[0]}}{\partial x}(0) = -\frac{\partial u_n^{[0]}}{\partial x}(1).$$

But, from (2.4), we have

$$\frac{\partial u_n^{[0]}}{\partial x}(0) = e^0 \frac{\partial u_n^{[0]}}{\partial x}(1) = \frac{\partial u_n^{[0]}}{\partial x}(1).$$

Combining the two, we get

$$\frac{\partial u_n^{[0]}}{\partial x}(0) = 0.$$

This gives the desired result.

The second case is u_n being anti-symmetric and $\frac{\partial u_n}{\partial x}$ being symmetric. At $\kappa = 0$, the anti-symmetry of u_n gives

$$u_n^{[0]}(0) = -\mathcal{P} u_n^{[0]}(0) = -u_n^{[0]}(1)$$

and the quasiperiodic boundary condition (2.4) gives

$$u_n^{[0]}(0) = e^0 u_n^{[0]}(1) = u_n^{[0]}(1).$$

Combining the two, we get

$$u_n^{[0]}(0) = 0.$$

Then, at $\kappa = \pi$, since $\frac{\partial u_n}{\partial x}$ is symmetric, we have that

$$\frac{\partial u_n^{[\pi]}}{\partial x}(0) = \mathcal{P}\frac{\partial u_n^{[\pi]}}{\partial x}(0) = \frac{\partial u_n^{[\pi]}}{\partial x}(1).$$

But, from (2.4), we have

$$\frac{\partial u_n^{[\pi]}}{\partial x}(0) = e^{i\pi}\frac{\partial u_n^{[\pi]}}{\partial x}(1) = -\frac{\partial u_n^{[\pi]}}{\partial x}(1).$$

Combining the two, we get

$$\frac{\partial u_n^{[\pi]}}{\partial x}(0) = 0.$$

This gives the desired result. This concludes the proof. □

A.2. Appendix to Chapter 3

A.2.1. Self-adjointness in Lemma 3.4.3

We consider the boundary value problem (3.9). In order to show that the operator $\mathcal{L}$ is self-adjoint, let us consider two solutions, u and v, of (3.9). We will show that

$$\langle \mathcal{L}u, v\rangle = \langle u, \mathcal{L}v\rangle,$$

where the inner product $\langle\cdot,\cdot\rangle$ is defined in (3.4).

It holds

$$\begin{aligned}
\langle \mathcal{L}u, v\rangle &= \int_{x_{-1}}^{x_0} \frac{1}{\mu_0}\frac{\partial}{\partial x}\left(\frac{1}{\varepsilon(x)}\frac{\partial}{\partial x}u(x)\right)\overline{v}(x)\mathrm{d}x \\
&= \left[\frac{1}{\mu_0}\frac{1}{\varepsilon(x)}\frac{\partial}{\partial x}u(x)\overline{v}(x)\right]_{x_{-1}}^{x_0} - \int_{x_{-1}}^{x_0}\frac{1}{\mu_0}\frac{\partial}{\partial x}u(x)\frac{1}{\varepsilon(x)}\frac{\partial}{\partial x}\overline{v}(x)\mathrm{d}x \\
&= -\frac{1}{\mu_0}\frac{1}{\varepsilon(x_{-1})}\frac{\partial}{\partial x}u(x_{-1})\overline{v}(x_{-1}) - \int_{x_{-1}}^{x_0}\frac{1}{\mu_0}\frac{\partial}{\partial x}u(x)\frac{1}{\varepsilon(x)}\frac{\partial}{\partial x}\overline{v}(x)\mathrm{d}x,
\end{aligned}$$

since $\frac{\partial}{\partial x}u(x_0^-) = 0$. Then,

$$\begin{aligned}
\langle \mathcal{L}u, v\rangle &= -\frac{1}{\mu_0}\frac{1}{\varepsilon(x_{-1})}\frac{\partial}{\partial x}u(x_{-1})\overline{v}(x_{-1}) - \left[\frac{1}{\mu_0}u(x)\frac{1}{\varepsilon(x)}\frac{\partial}{\partial x}\overline{v}(x)\right]_{x_{-1}}^{x_0} + \\
&\quad + \int_{x_{-1}}^{x_0} u(x)\frac{1}{\mu_0}\frac{\partial}{\partial x}\left(\frac{1}{\varepsilon(x)}\frac{\partial}{\partial x}\overline{v}(x)\right)\mathrm{d}x \\
&= \int_{x_{-1}}^{x_0} u(x)\frac{1}{\mu_0}\frac{\partial}{\partial x}\left(\frac{1}{\varepsilon(x)}\frac{\partial}{\partial x}\overline{v}(x)\right)\mathrm{d}x \\
&= \langle u, \mathcal{L}v\rangle,
\end{aligned}$$

since if v is a solution of (3.9), by taking complex conjugate in (3.1), so is $\overline{v}$. This concludes the proof.

A.3. Appendix to Chapter 4

A.3.1. Calculation of asymptotic constants

A.3.1.1. Calculation of Three-dimensional Constants

We derive a formula for $\mathbb{F}$, which was a crucial quantity in Section 4.2.4.3, in the case of a single three-dimensional halide perovskite resonator. We have that

$$\langle K_D^{(2)}[u_\delta], u_\delta \rangle = \frac{1}{8\pi}\mathbb{F}.$$

From (4.23), we observe that

$$\delta^2\omega^2\xi(\omega,k) = \frac{8\pi}{8\pi\lambda_\delta - \delta^2 k_0^2\mathbb{F}}.$$

Also, we know that $\xi(\omega,k) = \mu_0(\varepsilon(\omega,k) - \varepsilon_0)$, and we have shown that

$$\varepsilon(\omega,k) = \varepsilon_0 + \frac{1}{\mu_0\delta^2\omega^2\left(\lambda_0 - \frac{i}{4\pi}\delta k_0\mathbb{B}\right)}.$$

Substituting this into the above equation, we get

$$\mathbb{F} = \frac{8\pi}{\delta^2 k_0^2}\Big(\lambda_\delta - \lambda_0 + \frac{i}{4\pi}\delta k_0\mathbb{B}\Big).$$

Therefore, we obtain that

$$\langle K_D^{(2)}[u_\delta], u_\delta \rangle = \frac{1}{\delta^2 k_0^2}\Big(\lambda_\delta - \lambda_0 + \frac{i}{4\pi}\delta k_0\mathbb{B}\Big).$$

A.3.1.2. Calculation of Two-dimensional Constants

We derive a formula for $\mathbb{S}$, which was a crucial quantity in Section 4.2.5.3, in the case of a single two-dimensional halide perovskite resonator. We have that

$$\langle K_D^{(2)}[u_\delta], u_\delta \rangle = \frac{i}{4\pi}\mathbb{S}.$$

From (4.38), we can obtain an expression for $\mathbb{S}$. Indeed, (4.38) is equivalent to

$$4\pi = \delta^2\omega^2\xi(\omega,k)\Big(4\pi\lambda_\delta - i\delta^4 k_0^4\log(\delta k_0\hat{\gamma})\mathbb{S}\Big).$$

We know that $\xi(\omega,k) = \mu_0\Big(\varepsilon(\omega,k) - \varepsilon_0\Big)$ and we have shown that

$$\varepsilon(\omega,k) = \frac{1}{\mu_0\delta^2\omega^2\left(\log(\delta k_0\hat{\gamma})\lambda_{-1} - \frac{\mathbb{P}}{2\pi} - \frac{i(\delta k_0)^2\log(\delta k_0\hat{\gamma})\mathbb{G}}{4\pi}\right)} + \varepsilon_0.$$

Substituting this into the above equality, we get

$$\mathbb{S} = \frac{-i}{\delta^4 k_0^4 \log(\delta k_0 \hat{\gamma})}\Big(4\pi(\lambda_\delta - \log(\delta k_0\hat{\gamma})\lambda_{-1}) + 2\mathbb{P} + i(\delta k_0)^2 \log(\delta k_0\hat{\gamma})\mathbb{G}\Big).$$

Therefore, we obtain that

$$\langle K_D^{(2)}[u_\delta], u_\delta\rangle = \frac{1}{4\pi\delta^4 k_0^4 \log(\delta k_0\hat{\gamma})}\Big(4\pi(\lambda_\delta - \log(\delta k_0\hat{\gamma})\lambda_{-1}) + 2\mathbb{P} + i(\delta k_0)^2 \log(\delta k_0\hat{\gamma})\mathbb{G}\Big).$$

A.4. Appendix to Chapter 5

A.4.1. Three-dimensional analysis for N resonators

Here, we present the fundamentals of the analysis of the problem in the three-dimensional setting. We consider $N \in \mathbb{N}$ halide perovskite resontators $D_1, D_2, \ldots, D_N$, made from the same material. We consider the integral operators $K_{D_i}^{k_0\delta}$ and $R_{D_iD_j}^{k_0\delta}$, for $i, j = 1, 2, ..., N$ defined as in Definition 5.2.2. Then, the following lemma is a direct consequence of these definitions.

Lemma A.4.1. *The scattering problem (5.9) can be restated, using the Definition 5.2.2, as*

$$\begin{pmatrix} 1-\delta^2\omega^2\xi(\omega,k)K_{D_1}^{k_0\delta} & -\delta^2\omega^2\xi(\omega,k)R_{D_2D_1}^{k_0\delta} & \ldots & -\delta^2\omega^2\xi(\omega,k)R_{D_ND_1}^{k_0\delta} \\ -\delta^2\omega^2\xi(\omega,k)R_{D_1D_2}^{k_0\delta} & 1-\delta^2\omega^2\xi(\omega,k)K_{D_2}^{k_0\delta} & \ldots & -\delta^2\omega^2\xi(\omega,k)R_{D_ND_2}^{k_0\delta} \\ \vdots & \vdots & \ddots & \vdots \\ -\delta^2\omega^2\xi(\omega,k)R_{D_1D_N}^{k_0\delta} & -\delta^2\omega^2\xi(\omega,k)R_{D_2D_N}^{k_0\delta} & \ldots & 1-\delta^2\omega^2\xi(\omega,k)K_{D_N}^{k_0\delta} \end{pmatrix} \begin{pmatrix} u|_{D_1} \\ u|_{D_2} \\ \vdots \\ u|_{D_N} \end{pmatrix} = \begin{pmatrix} u_{in}|_{D_1} \\ u_{in}|_{D_2} \\ \vdots \\ u_{in}|_{D_N} \end{pmatrix}. \tag{A.6}$$

Thus, the scattering resonance problem is to find ω such that the operator in (A.6) is singular, or equivalently, such that there exists $(u_1, u_2, ..., u_N) \in L^2(D_1) \times L^2(D_2) \times ... \times L^2(D_N)$, $(u_1, u_2, ..., u_N) \neq \mathbf{0}$, such that

$$\begin{pmatrix} 1-\delta^2\omega^2\xi(\omega,k)K_{D_1}^{k_0\delta} & -\delta^2\omega^2\xi(\omega,k)R_{D_2D_1}^{k_0\delta} & \ldots & -\delta^2\omega^2\xi(\omega,k)R_{D_ND_1}^{k_0\delta} \\ -\delta^2\omega^2\xi(\omega,k)R_{D_1D_2}^{k_0\delta} & 1-\delta^2\omega^2\xi(\omega,k)K_{D_2}^{k_0\delta} & \ldots & -\delta^2\omega^2\xi(\omega,k)R_{D_ND_2}^{k_0\delta} \\ \vdots & \vdots & \ddots & \vdots \\ -\delta^2\omega^2\xi(\omega,k)R_{D_1D_N}^{k_0\delta} & -\delta^2\omega^2\xi(\omega,k)R_{D_2D_N}^{k_0\delta} & \ldots & 1-\delta^2\omega^2\xi(\omega,k)K_{D_N}^{k_0\delta} \end{pmatrix} \begin{pmatrix} u_1 \\ u_2 \\ \vdots \\ u_N \end{pmatrix} = \begin{pmatrix} 0 \\ 0 \\ \vdots \\ 0 \end{pmatrix}. \tag{A.7}$$

This gives the main result of the three-dimensional case.

Theorem A.4.2. *The scattering resonance problem in three dimensions becomes finding $\omega \in \mathbb{C}$, such that*

$$\det(\mathcal{K}) = 0,$$

where the matrix $\mathcal{K}$ is given by

$$\mathcal{K}_{ij} = \begin{cases} \langle R^{k_0\delta}_{D_iD_{i+1\lfloor N\rfloor}} \phi_i^{(\delta)}, \phi_{i+1\lfloor N\rfloor}^{(\delta)} \rangle, & \text{if } i = j, \\ -\mathcal{A}_i(\omega,\delta)\langle R^{k_0\delta}_{D_jD_i}\phi_j^{(\delta)}, \phi_i^{(\delta)}\rangle\langle R^{k_0\delta}_{D_iD_{i+1\lfloor N\rfloor}}\phi_i^{(\delta)}, \phi_{i+1\lfloor N\rfloor}^{(\delta)}\rangle, & \text{if } i \neq j, \end{cases} \tag{A.8}$$

where $k_0 = \mu_0\varepsilon_0\omega$ and

$$\mathcal{A}_i(\omega,\delta) := \frac{\delta^2\omega^2\xi(\omega,k)}{1-\delta^2\omega^2\xi(\omega,k)\lambda_\delta^{(i)}}, \quad i = 1, ..., N, \tag{A.9}$$

where $\lambda_\delta^{(i)}$ and $\phi_i^{(\delta)}$ are the eigenvalues and the respective eigenvectors associated to the particle D_i of the potential $K_{D_i}^{k_0\delta}$, for $i = 1, 2, \ldots, N$.

Proof. We observe that (A.7) is equivalent to

$$\begin{pmatrix} 1-\delta^2\omega^2\xi(\omega,k)K_{D_1}^{k_0\delta} & 0 & \dots & 0 \\ 0 & 1-\delta^2\omega^2\xi(\omega,k)K_{D_2}^{k_0\delta} & \dots & 0 \\ \vdots & \vdots & \ddots & \vdots \\ 0 & 0 & \dots & 1-\delta^2\omega^2\xi(\omega,k)K_{D_N}^{k_0\delta} \end{pmatrix} \begin{pmatrix} u_1 \\ u_2 \\ \vdots \\ u_N \end{pmatrix}$$
$$- \delta^2\omega^2\xi(\omega,k) \begin{pmatrix} 0 & R^{k_0\delta}_{D_2D_1} & \dots & R^{k_0\delta}_{D_ND_1} \\ R^{k_0\delta}_{D_1D_2} & 0 & \dots & R^{k_0\delta}_{D_ND_2} \\ \vdots & \vdots & \ddots & \vdots \\ R^{k_0\delta}_{D_1D_N} & R^{k_0\delta}_{D_2D_N} & \dots & 0 \end{pmatrix} \begin{pmatrix} u_1 \\ u_2 \\ \vdots \\ u_N \end{pmatrix} = \begin{pmatrix} 0 \\ 0 \\ \vdots \\ 0 \end{pmatrix},$$

which gives

$$\begin{pmatrix} u_1 \\ u_2 \\ \vdots \\ u_N \end{pmatrix} - \delta^2\omega^2\xi(\omega,k)\mathbb{N} \begin{pmatrix} \sum_{j=1,j\neq1}^{N} R^{k_0\delta}_{D_jD_1}u_j \\ \sum_{j=1,j\neq2}^{N} R^{k_0\delta}_{D_jD_2}u_j \\ \vdots \\ \sum_{j=1,j\neq N}^{N} R^{k_0\delta}_{D_jD_N}u_j \end{pmatrix} = \begin{pmatrix} 0 \\ 0 \\ \vdots \\ 0 \end{pmatrix}, \tag{A.10}$$

where $\mathbb{N}$ is the diagonal matrix given by

$$\mathbb{N}_{ij} = \begin{cases} \left(1-\delta^2\omega^2\xi(\omega,k)K_{D_i}^{k_0\delta}\right)^{-1}, & \text{if } i = j, \\ 0, & \text{if } i \neq j. \end{cases}$$

Let us now apply a pole-pencil decomposition on the operators $\left(1-\delta^2\omega^2\xi(\omega,k)K_{D_i}^{k_0\delta}\right)^{-1}$, for $i = 1, 2, \ldots, N$. We see that

$$\left(1-\delta^2\omega^2\xi(\omega,k)K_{D_i}^{k_0\delta}\right)^{-1}(\cdot) = \frac{\langle\cdot, \phi_i^{(\delta)}\rangle\phi_i^{(\delta)}}{1-\delta^2\omega^2\xi(\omega,k)\lambda_\delta^{(i)}} + R_i[\omega](\cdot),$$

where $\lambda_\delta^{(i)}$ and $\phi_i^{(\delta)}$ are the eigenvalues and the respective eigenvectors of the potential $K_{D_i}^{k_0\delta}$ associated to the particle D_i, for $i = 1, 2, \ldots, N$. We also recall that the remainder terms $R_i[\omega](\cdot)$ can be neglected, as in Chapter 4. Then, (A.10) becomes

$$\begin{pmatrix} u_1 \\ u_2 \\ \vdots \\ u_N \end{pmatrix} - \delta^2\omega^2\xi(\omega,k)\tilde{\mathbb{N}} \begin{pmatrix} \sum_{j=1,j\neq 1}^{N} R_{D_jD_1}^{k_0\delta} u_j \\ \sum_{j=1,j\neq 2}^{N} R_{D_jD_2}^{k_0\delta} u_j \\ \vdots \\ \sum_{j=1,j\neq N}^{N} R_{D_jD_N}^{k_0\delta} u_j \end{pmatrix} = \begin{pmatrix} 0 \\ 0 \\ \vdots \\ 0 \end{pmatrix},$$

where the matrix $\tilde{\mathbb{N}}$ is given by

$$\tilde{\mathbb{N}}_{ij} = \begin{cases} \frac{\langle \cdot, \phi_i^{(\delta)} \rangle \phi_i^{(\delta)}}{1-\delta^2\omega^2\xi(\omega,k)\lambda_\delta^{(i)}}, & \text{if } i = j, \\ 0, & \text{if } i \neq j. \end{cases}$$

This is equivalent to the system of equations

$$u_i - \frac{\delta^2\omega^2\xi(\omega,k)}{1-\delta^2\omega^2\xi(\omega,k)\lambda_\delta^{(i)}} \sum_{j=1,j\neq 1}^{N} \langle R_{D_jD_i}^{k_0\delta} u_j, \phi_i^{(\delta)} \rangle \phi_i^{(\delta)} = 0, \quad \text{for each } i = 1, \ldots, N.$$

We apply on the i-th line the operator $R_{D_iD_{i+1\lfloor N \rfloor}}^{k_0\delta}$ and then take the product with $\phi_{i+1\lfloor N \rfloor}^{(\delta)}$. Then, we find that

$$\begin{aligned} &\langle R_{D_iD_{i+1\lfloor N \rfloor}}^{k_0\delta} u_i, \phi_{i+1\lfloor N \rfloor}^{(\delta)} \rangle - \\ &\quad - \frac{\delta^2\omega^2\xi(\omega,k)}{1-\delta^2\omega^2\xi(\omega,k)\lambda_\delta^{(i)}} \sum_{j=1,j\neq i}^{N} \langle R_{D_jD_i}^{k_0\delta} u_j, \phi_i^{(\delta)} \rangle \langle R_{D_iD_{i+1\lfloor N \rfloor}}^{k_0\delta} \phi_i^{(\delta)}, \phi_{i+1\lfloor N \rfloor}^{(\delta)} \rangle = 0, \end{aligned} \tag{A.11}$$

for each $i = 1, \ldots, N$. Then, using the definition (A.9), the system (A.11) becomes

$$\begin{aligned} &\langle R_{D_iD_{i+1\lfloor N \rfloor}}^{k_0\delta} u_i, \phi_{i+1\lfloor N \rfloor}^{(\delta)} \rangle - \\ &\quad - \mathcal{A}_i(\omega,\delta) \sum_{j=1,j\neq i}^{N} \langle R_{D_jD_i}^{k_0\delta} u_j, \phi_i^{(\delta)} \rangle \langle R_{D_iD_{i+1\lfloor N \rfloor}}^{k_0\delta} \phi_i^{(\delta)}, \phi_{i+1\lfloor N \rfloor}^{(\delta)} \rangle = 0, \end{aligned} \tag{A.12}$$

for each $i = 1, \ldots, N$. Applying (5.14) to (A.12), we reach the linear system of equations

$$\mathcal{K} \begin{pmatrix} \langle u, \phi_1^{(\delta)} \rangle \\ \langle u, \phi_2^{(\delta)} \rangle \\ \vdots \\ \langle u, \phi_N^{(\delta)} \rangle \end{pmatrix} = \begin{pmatrix} 0 \\ 0 \\ \vdots \\ 0 \end{pmatrix}, \tag{A.13}$$

where $\mathcal{K}$ is the matrix given by (A.8). □

A.4.2. Proof of Lemma 5.2.7

Proof. We will show that the approximation formula (5.14) holds for sufficiently small $\rho \to 0$, when δ is also small. It is important to check the uniformity of these results with respect to δ. In particular, we will take $\rho > 0$ such that $\rho \to 0$ at the same rate as $\delta \to 0$. That is, $\rho = O(\delta)$ and $\delta = O(\rho)$. This gives the uniformity of the error term with respect to a small characteristic size δ.

Our argument is based on Theorem 2.10 of [21]. In particular, once we have shown that the assumptions of this Theorem hold, Lemma 5.2.7 will follow directly. We will present this proof in the two-dimensional setting, but it could easily be modified to three dimensions. Also, for simplicity, we will consider identical resonators, but the proof will be the same for particles of different sizes.

Recall that in Corollary 5.2.9 we showed that $\phi_i^{(\delta)} = \hat{1}_{D_i}$, for $i = 1, 2, .., N$. As a result, the desired approximation $u_i \simeq \langle u, \phi_i^{(\delta)} \rangle \phi_i^{(\delta)} + O(\rho^2)$ from (5.14) is equivalent to $u_i \simeq \langle u, \hat{1}_{D_i} \rangle \hat{1}_{D_i} + O(\rho^2)$. In order to be able to work with fixed spaces of functions, let us fix a large compact domain $K \subset \mathbb{R}^2$, which contains all the resonators D, i.e., $D \subset K$. Then, for $g \in L^2(K)$, we define the operator p_δ as follows

$$p_\rho : g \longmapsto \langle g, \hat{1}_{D_i} \rangle \hat{1}_{D_i} \in L^2(K). \tag{A.14}$$

To be able to use Theorem 2.10 of [21], the conditions that need to be satisfied are the following:

1. It holds that

$$\lim_{\rho \to 0} \|p_\rho u_i\|_{L^2(K)} = \|u_i\|_{L^2(K)}, \quad \forall i = 1, \ldots, N.$$

2. For every compact set $\mathcal{C} \subset \mathbb{C} \setminus \{0\}$, it holds

$$\sup_{\omega \in \mathcal{C}} \|\mathcal{L}\|_{\sup} < \infty,$$

   uniformly for all $\delta > 0$ and all $\rho > 0$, where the norm $\|\cdot\|_{\sup}$ is defined for a square matrix $P \in \mathbb{C}^{N \times N}$ as $\|P\|_{\sup} = \sup_{1 \le i,j \le N} |P_{ij}|$.

3. $\langle u, \hat{1}_{D_i} \rangle \hat{1}_{D_i}$ converges regularly to u_i, *i.e.*,
   - $\lim_{\rho \to 0} \|\mathcal{L} p_\rho u - \mathcal{F} u\|_{\sup} = 0$, where $\mathcal{F}u$ denotes our system without the use of the approximation formula (5.14).
   - For every subsequence ρ' of ρ, it holds that $\lim_{\rho' \to 0} \|u_i - p_{\rho'} u_i\|_{L^2(D)} = 0, \quad \forall i = 1, \ldots, N$.

Let us proceed to their proof.

A.4.2.1. First condition: Convergence in norm

It holds that

$$\begin{aligned}\|p_\rho u_i\|_{L^2(K)} &= \left(\int_K \left|\int_D u(y)\hat{1}_{D_i}(y)\mathrm{d}y\hat{1}_{D_i}(x)\right|^2 \mathrm{d}x\right)^{\frac{1}{2}} \\ &= \left(\frac{1}{|D_i|^2}\int_{D_i}\left|\int_{D_i} u(y)\mathrm{d}y\right|\mathrm{d}x\right)^{\frac{1}{2}} \\ &= \frac{1}{\sqrt{|D_i|}}\left|\int_{D_i} u(y)\mathrm{d}y\right|.\end{aligned}$$

Then, from the Cauchy-Schwartz inequality,

$$\|p_\rho u_i\|_{L^2(K)} \leq \frac{1}{\sqrt{|D_i|}}\left(\int_{D_i}|u(y)|^2\mathrm{d}y\int_{D_i}1\mathrm{d}y\right)^{\frac{1}{2}} = \|u_i\|_{L^2(K)}.$$

We can also see that, as $\rho \to 0$,

$$\|u_i\|_{L^2(K)} \to 0.$$

Hence, we have that

$$\lim_{\rho\to 0}\|p_\rho u_i\|_{L^2(K)} = \|u_i\|_{L^2(K)}. \tag{A.15}$$

A.4.2.2. Second condition: Matrix norm boundedness

We need to show that, for every compact $\mathcal{C} \subset \mathbb{C}\setminus\{0\}$,

$$\sup_{\omega\in\mathcal{C}}\|\mathcal{L}\|_{\sup} = \sup_{\omega\in\mathcal{C}}\left(\sup_{1\leq i,j\leq N}|\mathcal{L}_{ij}|\right) < \infty. \tag{A.16}$$

Indeed, let $\mathcal{C}$ denote a compact subset of $\mathbb{C}\setminus\{0\}$. Then, $\mathcal{C}$ is closed and bounded, which implies that there exist $s_1, s_2 \in \mathcal{C}$ such that $|s_1| \leq |\omega| \leq |s_2|$, for all $\omega \in \mathcal{C}$. This gives the following bounds:

$$\log|s_1| \leq \log|\omega| \leq \log|s_2| \quad \text{and} \quad |s_1|^2\log|s_1| \leq |\omega|^2\log|\omega| \leq |s_2|^2\log|s_2|, \tag{A.17}$$

and so, from Definition 5.2.3, we get

$$\sup_{\omega\in\mathcal{C}}\left|\langle N_{D_jD_i}^{k_0\delta}\hat{1}_{D_j},\hat{1}_{D_i}\rangle\right| < \infty, \tag{A.18}$$

for all $i, j = 1,\ldots,N$, with $i \neq j$. Then, from (5.16), we see that the dependence of $\mathcal{B}(\omega,\delta)$ on ρ is due to the term $\nu_\delta^{(i)}$. Since it holds that $\nu_\delta^{(i)} \to 0$ as $\rho \to 0$, we can see that $\mathcal{B}(\omega,\delta)$ converges to a limit independent of ρ. Also, we note that

$\nu_\delta^{(i)}$ is increasing with respect to ρ, meaning the maximum and minimum of $\mathcal{B}(\omega,\delta)$ for any ρ in a neighbourhood of zero are well defined and we can derive bounds that are independent of ρ. Hence, from (5.16) and (A.17), we get that there exist $\mathcal{F}_1, \mathcal{F}_2 \in [0,\infty)$ such that

$$\mathcal{F}_1 \leq |\mathcal{B}(\omega,\delta)| \leq \mathcal{F}_2 \tag{A.19}$$

for all $\omega \in \mathcal{C}$, which gives

$$\sup_{\omega\in\mathcal{C}} \Big|\mathcal{B}(\omega,\delta)\Big| < \infty. \tag{A.20}$$

Applying (A.18) and (A.20) to the definition of $\mathcal{L}$ in (5.22), we obtain the desired bound (A.16).

A.4.2.3. Third condition: Approximation convergence

For the next part, we have to show a convergence result as $\rho \to 0$ on the matrix formulations of the problem before and after using (5.14). We will provide this in the setting of three resonators, since the calculations are lengthy and similar for $N \in \mathbb{N}$ particles and so can be easily extrapolated. In this case, we have $\mathcal{L}p_\rho u = \Big((\mathcal{L}p_\rho u)_1, (\mathcal{L}p_\rho u)_2, (\mathcal{L}p_\rho u)_3\Big)^\top$, where

$$\begin{aligned}(\mathcal{L}p_\rho u)_i =& \langle N^{k_0\delta}_{D_iD_{i+1\lfloor 3\rfloor}}\hat{1}_{D_i}, \hat{1}_{D_{i+1\lfloor 3\rfloor}}\rangle\langle u, \hat{1}_{D_i}\rangle - \\ &- \mathcal{B}(\omega,\delta)\langle N^{k_0\delta}_{D_iD_{i+1\lfloor 3\rfloor}}\hat{1}_{D_i}, \hat{1}_{D_{i+1\lfloor 3\rfloor}}\rangle^2\langle u, \hat{1}_{D_{i+1\lfloor 3\rfloor}}\rangle \\ &- \mathcal{B}(\omega,\delta)\langle N^{k_0\delta}_{D_iD_{i+1\lfloor 3\rfloor}}\hat{1}_{D_i}, \hat{1}_{D_{i+1\lfloor 3\rfloor}}\rangle\langle N^{k_0\delta}_{D_{i+2\lfloor 3\rfloor}D_i}\hat{1}_{D_{i+2\lfloor 3\rfloor}}, \hat{1}_{D_i}\rangle\langle u, \hat{1}_{D_{i+2\lfloor 3\rfloor}}\rangle,\end{aligned}$$

for $i = 1,2,3$ and we define $\mathcal{F}u$ to be our system before the approximation, *i.e.*,

$$\mathcal{F}u = \begin{pmatrix} \langle N^{k_0\delta}_{D_1D_2}u_1, \hat{1}_{D_2}\rangle - \mathcal{B}(\omega,\delta)\Big[\langle N^{k_0\delta}_{D_2D_1}u_2, \hat{1}_{D_1}\rangle + \langle N^{k_0\delta}_{D_3D_1}u_3, \hat{1}_{D_1}\rangle\Big]\langle N^{k_0\delta}_{D_1D_2}\hat{1}_{D_1}, \hat{1}_{D_2}\rangle \\ \langle N^{k_0\delta}_{D_1D_2}u_1, \hat{1}_{D_2}\rangle - \mathcal{B}(\omega,\delta)\Big[\langle N^{k_0\delta}_{D_2D_1}u_2, \hat{1}_{D_1}\rangle + \langle N^{k_0\delta}_{D_3D_1}u_3, \hat{1}_{D_1}\rangle\Big]\langle N^{k_0\delta}_{D_1D_2}\hat{1}_{D_1}, \hat{1}_{D_2}\rangle \\ \langle N^{k_0\delta}_{D_3D_1}u_3, \hat{1}_{D_1}\rangle - \mathcal{B}(\omega,\delta)\Big[\langle N^{k_0\delta}_{D_1D_3}u_1, \hat{1}_{D_3}\rangle + \langle N^{k_0\delta}_{D_2D_3}u_2, \hat{1}_{D_3}\rangle\Big]\langle N^{k_0\delta}_{D_3D_1}\hat{1}_{D_3}, \hat{1}_{D_1}\rangle \end{pmatrix}.$$

We want to show that

$$\lim_{\rho\to 0} \|\mathcal{L}p_\rho u - \mathcal{F}u\|_{\sup} = 0. \tag{A.21}$$

Indeed, let us treat this difference at each entry separately. Since, the operators repeat themselves with different indices, and the particles are identical, whatever we show for the first entry holds for the rest. Hence, our study focuses on

$$\begin{aligned}\mathcal{W} := \lim_{\rho\to 0} \Big|&\langle N^{k_0\delta}_{D_1D_2}\hat{1}_{D_1}, \hat{1}_{D_2}\rangle\langle u, \hat{1}_{D_1}\rangle - \mathcal{B}(\omega,\delta)\langle N^{k_0\delta}_{D_1D_2}\hat{1}_{D_1}, \hat{1}_{D_2}\rangle^2\langle u, \hat{1}_{D_2}\rangle \\ &- \mathcal{B}(\omega,\delta)\langle N^{k_0\delta}_{D_1D_2}\hat{1}_{D_1}, \hat{1}_{D_2}\langle N^{k_0\delta}_{D_3D_1}\hat{1}_{D_3}, \hat{1}_{D_1}\rangle\langle u, \hat{1}_{D_3}\rangle - \Big(\langle N^{k_0\delta}_{D_1D_2}u_1, \hat{1}_{D_2}\rangle\end{aligned}$$

$$- \mathcal{B}(\omega,\delta)\Big[\langle N^{k_0\delta}_{D_2D_1}u_2,\hat{1}_{D_1}\rangle + \langle N^{k_0\delta}_{D_3D_1}u_3,\hat{1}_{D_1}\rangle\Big]\langle N^{k_0\delta}_{D_1D_2}\hat{1}_{D_1},\hat{1}_{D_2}\rangle\Big)\Big|.$$

We are going to split $\mathcal{W}$ into three differences

$$\mathcal{W}_1 := \langle N^{k_0\delta}_{D_1D_2}\hat{1}_{D_1},\hat{1}_{D_2}\rangle\langle u,\hat{1}_{D_1}\rangle - \langle N^{k_0\delta}_{D_1D_2}u_1,\hat{1}_{D_2}\rangle,$$

$$\mathcal{W}_2 := \mathcal{B}(\omega,\delta)\langle N^{k_0\delta}_{D_2D_1}u_2,\hat{1}_{D_1}\rangle\langle N^{k_0\delta}_{D_1D_2}\hat{1}_{D_1},\hat{1}_{D_2}\rangle - \mathcal{B}(\omega,\delta)\langle N^{k_0\delta}_{D_1D_2}\hat{1}_{D_1},\hat{1}_{D_2}\rangle^2\langle u,\hat{1}_{D_2}\rangle$$

and

$$\begin{aligned}\mathcal{W}_3 :=& \mathcal{B}(\omega,\delta)\langle N^{k_0\delta}_{D_3D_1}u_3,\hat{1}_{D_1}\rangle\langle N^{k_0\delta}_{D_1D_2}\hat{1}_{D_1},\hat{1}_{D_2}\rangle - \\ &- \mathcal{B}(\omega,\delta)\langle N^{k_0\delta}_{D_1D_2}\hat{1}_{D_1},\hat{1}_{D_2}\langle N^{k_0\delta}_{D_3D_1}\hat{1}_{D_3},\hat{1}_{D_1}\rangle\langle u,\hat{1}_{D_3}\rangle.\end{aligned}$$

We will study them separately to show the convergence result. Let us recall that for $u \in L^2(D)$

$$N^{k_0\delta}_{D_iD_j}u = \hat{K}^{k_0\delta}_{D_iD_j}u + R^{(0)}_{D_iD_j}u + (k_0\delta)^2\log(k_0\delta\hat{\gamma})R^{(1)}_{D_iD_j}u.$$

Then, we have

$$\begin{aligned}\mathcal{W}_1 &= \frac{1}{|D_1|\sqrt{|D_2|}}\langle N^{k_0\delta}_{D_1D_2}1_{D_1},1_{D_2}\rangle\langle u,1_{D_1}\rangle - \frac{1}{\sqrt{|D_2|}}\langle N^{k_0\delta}_{D_1D_2}u_1,1_{D_2}\rangle \\ &= \frac{1}{|D_1|\sqrt{|D_2|}}\langle \hat{K}^{k_0\delta}_{D_1D_2}1_{D_1},1_{D_2}\rangle\langle u,1_{D_1}\rangle - \frac{1}{\sqrt{|D_2|}}\langle \hat{K}^{k_0\delta}_{D_1D_2}u_1,1_{D_2}\rangle + \\ &\quad + \frac{1}{|D_1|\sqrt{|D_2|}}\langle R^{(0)}_{D_1D_2}1_{D_1},1_{D_2}\rangle\langle u,1_{D_1}\rangle - \frac{1}{\sqrt{|D_2|}}\langle R^{(0)}_{D_1D_2}u_1,1_{D_2}\rangle + \\ &\quad + (k_0\delta)^2\log(k_0\delta\hat{\gamma})\Bigg(\frac{1}{|D_1|\sqrt{|D_2|}}\langle R^{(1)}_{D_1D_2}1_{D_1},1_{D_2}\rangle\langle u,1_{D_1}\rangle - \\ &\quad - \frac{1}{\sqrt{|D_2|}}\langle R^{(1)}_{D_1D_2}u_1,1_{D_2}\rangle\Bigg).\end{aligned}$$

We observe that

$$\begin{aligned}&\frac{1}{|D_1|\sqrt{|D_2|}}\langle \hat{K}^{k_0\delta}_{D_1D_2}1_{D_1},1_{D_2}\rangle\langle u,1_{D_1}\rangle - \frac{1}{\sqrt{|D_2|}}\langle \hat{K}^{k_0\delta}_{D_1D_2}u_1,1_{D_2}\rangle = \\ &= -\frac{1}{|D_1|\sqrt{|D_2|}}\frac{1}{2\pi}\log(k_0\delta\hat{\gamma})\int_{D_2}\int_{D_1}\mathrm{d}y\mathrm{d}x\int_{D_1}u(x)\mathrm{d}x - \\ &\quad - \frac{1}{\sqrt{|D_2|}}\frac{1}{2\pi}\log(k_0\delta\hat{\gamma})\int_{D_2}\int_{D_1}u(y)\mathrm{d}y\mathrm{d}x \\ &= -\frac{1}{2\pi}\log(k_0\delta\hat{\gamma})\int_{D_1}u(x)\mathrm{d}x\left[\frac{1}{|D_1|\sqrt{|D_2|}}|D_1||D_2| - \frac{1}{\sqrt{|D_2|}}|D_2|\right] \\ &= 0.\end{aligned}$$

Also,

$$\frac{1}{|D_1|\sqrt{|D_2|}}\langle R^{(0)}_{D_1D_2}1_{D_1},1_{D_2}\rangle\langle u,1_{D_1}\rangle - \frac{1}{\sqrt{|D_2|}}\langle R^{(0)}_{D_1D_2}u_1,1_{D_2}\rangle =$$

$$
\begin{aligned}
&= \frac{1}{|D_1|\sqrt{|D_2|}} \int_{D_2}\int_{D_1} \log|x-y|\mathrm{d}y\mathrm{d}x \int_{D_1} u(x)\mathrm{d}x - \\
&\quad - \frac{1}{\sqrt{|D_2|}} \int_{D_2}\int_{D_1} \log|x-y|u(y)\mathrm{d}y\mathrm{d}x \\
&= \mathcal{W}_1^{(1)}.
\end{aligned}
$$

We know that for $y \in D_1$ and $x \in D_2$, it holds

$$\log|\alpha_1 - 2\rho| \leq \log|x-y| \leq \log|\alpha_1 + 2\rho|. \tag{A.22}$$

This gives

$$\sqrt{|D_2|}\log|\alpha_1 - 2\rho| \int_{D_1} u(x)\mathrm{d}x - \sqrt{|D_2|}\log|\alpha_1 + 2\rho| \int_{D_1} u(x)\mathrm{d}x \leq \mathcal{W}_1^{(1)} \tag{A.23}$$

and

$$\mathcal{W}_1^{(1)} \leq \sqrt{|D_2|}\log|\alpha_1 + 2\rho| \int_{D_1} u(x)\mathrm{d}x - \sqrt{|D_2|}\log|\alpha_1 - 2\rho| \int_{D_1} u(x)\mathrm{d}x. \tag{A.24}$$

It is direct that as $\rho \to 0$, the left-hand side of (A.23) and the right-hand side of (A.24), both converge to 0. Thus, as $\rho \to 0$,

$$\mathcal{W}_1^{(1)} \to 0.$$

Then,

$$
\begin{aligned}
&\frac{1}{|D_1|\sqrt{|D_2|}} \langle R^{(1)}_{D_1D_2} 1_{D_1}, 1_{D_2}\rangle \langle u, 1_{D_1}\rangle - \frac{1}{\sqrt{|D_2|}} \langle R^{(1)}_{D_1D_2} u_1, 1_{D_2}\rangle = \\
&= \frac{1}{|D_1|\sqrt{|D_2|}} \int_{D_2}\int_{D_1} \frac{1}{|x-y|}\mathrm{d}y\mathrm{d}x \int_{D_1} u(x)\mathrm{d}x - \frac{1}{\sqrt{|D_2|}} \int_{D_2}\int_{D_1} \frac{u(y)}{|x-y|}\mathrm{d}y\mathrm{d}x \\
&= \mathcal{W}_1^{(2)}.
\end{aligned}
$$

We know that for $y \in D_1$ and $x \in D_2$, it holds

$$\frac{1}{|\alpha_1 + 2\rho|} \leq \frac{1}{|x-y|} \leq \frac{1}{|\alpha_1 - 2\rho|}. \tag{A.25}$$

This gives

$$\frac{\sqrt{|D_2|}}{|\alpha_2 + 2\rho|} \int_{D_1} u(x)\mathrm{d}x - \frac{\sqrt{|D_2|}}{|\alpha_2 - 2\rho|} \int_{D_1} u(x)\mathrm{d}x \leq \mathcal{W}_1^{(2)} \tag{A.26}$$

and

$$\mathcal{W}_1^{(2)} \leq \frac{\sqrt{|D_2|}}{|\alpha_2 - 2\rho|} \int_{D_1} u(x)\mathrm{d}x - \frac{\sqrt{|D_2|}}{|\alpha_2 + 2\rho|} \int_{D_1} u(x)\mathrm{d}x. \tag{A.27}$$

Again, we see that as $\rho \to 0$, the left-hand side of (A.26) and the right-hand side of (A.27), both converge to 0. Thus, as $\rho \to 0$,

$$\mathcal{W}_1^{(2)} \to 0.$$

Thus, gathering these results, we get that

$$\mathcal{W}_1 = \mathcal{W}_1^{(1)} + (k_0\delta)^2 \log(k_0\delta\hat{\gamma})\mathcal{W}_1^{(2)},$$

which, at hand, shows that, as $\rho \to 0$,

$$\mathcal{W}_1 \to 0.$$

Let us now show the convergence of $\mathcal{W}_2$ as $\rho \to 0$. Then, we note that this also gives the convergence of $\mathcal{W}_3$, since the calculations are of the same order. Keeping in mind that $\lim_{\rho\to 0} \mathcal{B}(\omega, \delta)$ is finite, we will study

$$\tilde{\mathcal{W}}_2 := \frac{\mathcal{W}_2}{\mathcal{B}(\omega,\delta)} = \langle N^{k_0\delta}_{D_2D_1} u_2, \hat{1}_{D_1}\rangle \langle N^{k_0\delta}_{D_1D_2}\hat{1}_{D_1}, \hat{1}_{D_2}\rangle - \langle N^{k_0\delta}_{D_1D_2}\hat{1}_{D_1}, \hat{1}_{D_2}\rangle^2 \langle u, \hat{1}_{D_2}\rangle,$$

which is

$$\begin{aligned}
\tilde{\mathcal{W}}_2 = &\Big[\langle \hat{K}^{k_0\delta}_{D_2D_1} u_2, \hat{1}_{D_1}\rangle \langle \hat{K}^{k_0\delta}_{D_1D_2}\hat{1}_{D_1}, \hat{1}_{D_2}\rangle - \langle \hat{K}^{k_0\delta}_{D_1D_2}\hat{1}_{D_1}, \hat{1}_{D_2}\rangle^2 \langle u, \hat{1}_{D_2}\rangle\Big] + \\
&+ \Big[\langle R^{(0)}_{D_2D_1} u_2, \hat{1}_{D_1}\rangle \langle R^{(0)}_{D_1D_2}\hat{1}_{D_1}, \hat{1}_{D_2}\rangle - \langle R^{(0)}_{D_1D_2}\hat{1}_{D_1}, \hat{1}_{D_2}\rangle^2 \langle u, \hat{1}_{D_2}\rangle\Big] + \\
&+ \Big((k_0\delta)^2 \log(k_0\delta\hat{\gamma})\Big)^2 \Big[\langle R^{(1)}_{D_2D_1} u_2, \hat{1}_{D_1}\rangle \langle R^{(1)}_{D_1D_2}\hat{1}_{D_1}, \hat{1}_{D_2}\rangle - \\
&- \langle R^{(1)}_{D_1D_2}\hat{1}_{D_1}, \hat{1}_{D_2}\rangle^2 \langle u, \hat{1}_{D_2}\rangle\Big] + \Big[\langle \hat{K}^{k_0\delta}_{D_1D_2}\hat{1}_{D_1}, \hat{1}_{D_2}\rangle \langle R^{(0)}_{D_2D_1} u_2, \hat{1}_{D_1}\rangle + \\
&+ \langle \hat{K}^{k_0\delta}_{D_1D_2} u_2, \hat{1}_{D_1}\rangle \langle R^{(0)}_{D_2D_1}\hat{1}_{D_2}, \hat{1}_{D_1}\rangle - \\
&- 2\langle \hat{K}^{k_0\delta}_{D_1D_2}\hat{1}_{D_1}, \hat{1}_{D_2}\rangle \langle R^{(0)}_{D_1D_2}\hat{1}_{D_1}, \hat{1}_{D_2}\rangle \langle u, \hat{1}_{D_2}\rangle\Big] + \\
&+ (k_0\delta)^2 \log(k_0\delta\hat{\gamma})\Big[\langle \hat{K}^{k_0\delta}_{D_1D_2}\hat{1}_{D_1}, \hat{1}_{D_2}\rangle \langle R^{(1)}_{D_2D_1} u_2, \hat{1}_{D_1}\rangle + \\
&+ \langle \hat{K}^{k_0\delta}_{D_1D_2} u_2, \hat{1}_{D_2}\rangle \langle R^{(1)}_{D_2D_1}\hat{1}_{D_2}, \hat{1}_{D_1}\rangle - \\
&- 2\langle \hat{K}^{k_0\delta}_{D_1D_2}\hat{1}_{D_1}, \hat{1}_{D_2}\rangle \langle R^{(1)}_{D_1D_2}\hat{1}_{D_1}, \hat{1}_{D_2}\rangle \langle u, \hat{1}_{D_2}\rangle\Big] + \\
&+ (k_0\delta)^2 \log(k_0\delta\hat{\gamma})\Big[\langle R^{(0)}_{D_1D_2}\hat{1}_{D_1}, \hat{1}_{D_2}\rangle \langle R^{(1)}_{D_2D_1} u_2, \hat{1}_{D_1}\rangle + \\
&+ \langle R^{(0)}_{D_1D_2} u_2, \hat{1}_{D_2}\rangle \langle R^{(1)}_{D_2D_1}\hat{1}_{D_2}, \hat{1}_{D_1}\rangle - \\
&- 2\langle R^{(0)}_{D_1D_2}\hat{1}_{D_1}, \hat{1}_{D_2}\rangle \langle R^{(1)}_{D_1D_2}\hat{1}_{D_1}, \hat{1}_{D_2}\rangle \langle u, \hat{1}_{D_2}\rangle\Big] \\
=: &\tilde{\mathcal{W}}_2^{(1)} + \tilde{\mathcal{W}}_2^{(2)} + \Big((k_0\delta)^2 \log(k_0\delta\hat{\gamma})\Big)^2 \tilde{\mathcal{W}}_2^{(3)} + \tilde{\mathcal{W}}_2^{(4)} \\
&+ (k_0\delta)^2 \log(k_0\delta\hat{\gamma})\tilde{\mathcal{W}}_2^{(5)} + (k_0\delta)^2 \log(k_0\delta\hat{\gamma})\tilde{\mathcal{W}}_2^{(6)}.
\end{aligned}$$

We will consider each of the $\tilde{\mathcal{W}}_2^{(i)}, i = 1, \ldots, 6$ separately. We observe that

$$\tilde{\mathcal{W}}_2^{(1)} = \frac{1}{4\pi^2} \log(k_0\delta\hat{\gamma})^2 \Bigg[\frac{1}{|D_1|\sqrt{|D_2|}} \int_{D_1}\int_{D_2} u(y)\mathrm{d}y\mathrm{d}x \int_{D_1}\int_{D_2} \mathrm{d}y\mathrm{d}x -$$

$$- \frac{1}{|D_1||D_2|\sqrt{|D_2|}} \left(\int_{D_1} \int_{D_2} \mathrm{d}y\mathrm{d}x \right)^2 \int_{D_2} u(y)\mathrm{d}y \Bigg] = 0.$$

Then,

$$\tilde{\mathcal{W}}_2^{(2)} = \langle R^{(0)}_{D_1D_2} \hat{1}_{D_1}, \hat{1}_{D_2} \rangle \Big[\langle R^{(0)}_{D_2D_1} u_2, \hat{1}_{D_1} \rangle - \langle R^{(0)}_{D_1D_2} \hat{1}_{D_1}, \hat{1}_{D_2} \rangle \langle u, \hat{1}_{D_2} \rangle \Big].$$

We know that, as $\rho \to 0$,

$$\langle R^{(0)}_{D_1D_2} \hat{1}_{D_1}, \hat{1}_{D_2} \rangle \to 0$$

and, up to changing the indices, from (A.23) and (A.24), we have shown that as $\rho \to 0$

$$\langle R^{(0)}_{D_2D_1} u_2, \hat{1}_{D_1} \rangle - \langle R^{(0)}_{D_1D_2} \hat{1}_{D_1}, \hat{1}_{D_2} \rangle \langle u, \hat{1}_{D_2} \rangle \to 0.$$

Thus, as $\rho \to 0$, it holds that

$$\tilde{\mathcal{W}}_2^{(2)} \to 0.$$

Using the same reasoning, we have,

$$\tilde{\mathcal{W}}_2^{(3)} = \Big((k_0\delta) \log(k_0\delta\hat{\gamma}) \Big)^2 \langle R^{(1)}_{D_2D_1} \hat{1}_{D_2}, \hat{1}_{D_1} \rangle \Big[\langle R^{(1)}_{D_2D_1} u_2, \hat{1}_{D_1} \rangle - \langle R^{(1)}_{D_2D_1} \hat{1}_{D_2}, \hat{1}_{D_1} \rangle \Big]$$

where, as $\rho \to 0$,

$$\langle R^{(1)}_{D_1D_2} \hat{1}_{D_1}, \hat{1}_{D_2} \rangle \to 0$$

and, up to changing the indices, from (A.26) and (A.27), we have, as $\rho \to 0$

$$\langle R^{(1)}_{D_2D_1} u_2, \hat{1}_{D_1} \rangle - \langle R^{(1)}_{D_1D_2} \hat{1}_{D_1}, \hat{1}_{D_2} \rangle \langle u, \hat{1}_{D_2} \rangle \to 0.$$

Hence, as $\rho \to 0$,

$$\tilde{\mathcal{W}}_2^{(3)} \to 0.$$

Now,

$$\begin{aligned}
\tilde{\mathcal{W}}_2^{(4)} &= \frac{1}{|D_1|\sqrt{|D_2|}} \int_{D_1} \int_{D_2} u(y)\mathrm{d}y\mathrm{d}x \int_{D_1} \int_{D_2} \log|x-y|\mathrm{d}y\mathrm{d}x + \\
&\quad + \frac{1}{|D_1|\sqrt{|D_2|}} \int_{D_1} \int_{D_2} \mathrm{d}y\mathrm{d}x \int_{D_1} \int_{D_2} \log|x-y| u(y)\mathrm{d}y\mathrm{d}x - \\
&\quad - \frac{2}{|D_1||D_2|\sqrt{|D_2|}} \int_{D_1} \int_{D_2} \mathrm{d}y\mathrm{d}x \int_{D_1} \int_{D_2} \log|x-y|\mathrm{d}y\mathrm{d}x \int_{D_2} u(y)\mathrm{d}y \\
&= \sqrt{|D_2|} \int_{D_1} \int_{D_2} \log|x-y| u(y)\mathrm{d}y\mathrm{d}x - \\
&\quad - \frac{1}{\sqrt{|D_2|}} \int_{D_1} \int_{D_2} \log|x-y|\mathrm{d}y\mathrm{d}x \int_{D_2} u(y)\mathrm{d}y.
\end{aligned}$$

Using the bounds (A.22), we have

$$|D_1|\sqrt{|D_2|}\Big(\log|\alpha_1 - 2\rho| - \log|\alpha_1 + 2\rho| \Big) \int_{D_2} u(y)\mathrm{d}y \leq \tilde{\mathcal{W}}_2^{(4)},$$

and

$$\tilde{\mathcal{W}}_2^{(4)} \leq |D_1|\sqrt{|D_2|}\Big(\log|\alpha_1+2\rho| - \log|\alpha_1-2\rho|\Big)\int_{D_2} u(y)\mathrm{d}y,$$

which gives, as $\rho \to 0$,

$$\tilde{\mathcal{W}}_2^{(4)} \to 0.$$

Then,

$$\begin{aligned}\tilde{\mathcal{W}}_2^{(5)} &= \frac{1}{|D_1|\sqrt{|D_2|}}\int_{D_1}\int_{D_2} u(y)\mathrm{d}y\mathrm{d}x\int_{D_1}\int_{D_2}\frac{1}{|x-y|}\mathrm{d}y\mathrm{d}x+\\ &+\frac{1}{|D_1|\sqrt{|D_2|}}\int_{D_1}\int_{D_2}\mathrm{d}y\mathrm{d}x\int_{D_1}\int_{D_2}\frac{1}{|x-y|}u(y)\mathrm{d}y\mathrm{d}x-\\ &-\frac{2}{|D_1||D_2|\sqrt{|D_2|}}\int_{D_1}\int_{D_2}\mathrm{d}y\mathrm{d}x\int_{D_1}\int_{D_2}\frac{1}{|x-y|}\mathrm{d}y\mathrm{d}x\int_{D_2}u(y)\mathrm{d}y\\ &=\sqrt{|D_2|}\int_{D_1}\int_{D_2}\frac{1}{|x-y|}u(y)\mathrm{d}y\mathrm{d}x-\frac{1}{\sqrt{|D_2|}}\int_{D_1}\int_{D_2}\frac{1}{|x-y|}\mathrm{d}y\mathrm{d}x\int_{D_2}u(y)\mathrm{d}y.\end{aligned}$$

Using the bounds (A.25), we have

$$|D_1|\sqrt{|D_2|}\left(\frac{1}{\alpha_1+2\rho}-\frac{1}{\alpha_1-2\rho}\right)\int_{D_2}u(y)\mathrm{d}y \leq \tilde{\mathcal{W}}_2^{(5)},$$

and

$$\tilde{\mathcal{W}}_2^{(5)} \leq |D_1|\sqrt{|D_2|}\left(\frac{1}{\alpha_1-2\rho}-\frac{1}{\alpha_1+2\rho}\right)\int_{D_2}u(y)\mathrm{d}y,$$

which gives, as $\rho \to 0$,

$$\tilde{\mathcal{W}}_2^{(5)} \to 0.$$

Finally,

$$\begin{aligned}\tilde{\mathcal{W}}_2^{(6)} &= \frac{1}{|D_1|\sqrt{|D_2|}}\int_{D_1}\int_{D_2}\log|x-y|u(y)\mathrm{d}y\mathrm{d}x\int_{D_1}\int_{D_2}\frac{1}{|x-y|}\mathrm{d}y\mathrm{d}x+\\ &+\frac{1}{|D_1|\sqrt{|D_2|}}\int_{D_1}\int_{D_2}\log|x-y|\mathrm{d}y\mathrm{d}x\int_{D_1}\int_{D_2}\frac{1}{|x-y|}u(y)\mathrm{d}y\mathrm{d}x-\\ &-\frac{2}{|D_1||D_2|\sqrt{|D_2|}}\int_{D_1}\int_{D_2}\log|x-y|\mathrm{d}y\mathrm{d}x\int_{D_1}\int_{D_2}\frac{1}{|x-y|}\mathrm{d}y\mathrm{d}x\int_{D_2}u(y)\mathrm{d}y.\end{aligned}$$

Here, we combine the bounds (A.22) and (A.25) and get

$$2|D_1|\sqrt{|D_2|}\left(\frac{\log|\alpha_1-2\rho|}{|\alpha_1+2\rho|}-\frac{\log|\alpha_1+2\rho|}{|\alpha_1-2\rho|}\right)\int_{D_2}u(y)\mathrm{d}y \leq \tilde{\mathcal{W}}_2^{(6)},$$

and

$$\tilde{\mathcal{W}}_2^{(6)} \leq 2|D_1|\sqrt{|D_2|}\left(\frac{\log|\alpha_1+2\rho|}{|\alpha_1-2\rho|}-\frac{\log|\alpha_1-2\rho|}{|\alpha_1+2\rho|}\right)\int_{D_2}u(y)\mathrm{d}y,$$

which gives, as $\rho \to 0$,

$$\tilde{\mathcal{W}}_2^{(6)} \to 0.$$

Thus, we have shown that for all $i = 1, \ldots, 6$, as $\rho \to 0$,

$$\tilde{\mathcal{W}}_2^{(i)} \to 0,$$

which shows that

$$\tilde{\mathcal{W}}_2 \to 0, \qquad \text{as } \rho \to 0.$$

Also, repeating these calculation and re-indexing, we get

$$\mathcal{W}_3 \to 0, \qquad \text{as } \rho \to 0.$$

Therefore, we have that

$$\mathcal{W} = 0, \tag{A.28}$$

and hence, (A.21) follows.

Let us now move to the last part of the proof. We observe that for each $i = 1, \ldots, N$,

$$\|u_i - p_\rho u_i\|_{L^2(D)} \leq \|u\|_{L^2(D)} + \|p_\rho u\|_{L^2(D)} = 2\|u\|_{L^2(D)},$$

where we have used (A.15), and we have that,

$$\|u_i\|_{L^2(D)} = \left(\int_{D_i}|u(y)|^2\mathrm{d}y\right) \to 0, \qquad \text{as } \rho \to 0.$$

Therefore, we obtain

$$\|u_i - p_\rho u_i\|_{L^2(D)} \to 0, \qquad \text{as } \rho \to 0,$$

and so, for each subsequence of $\rho' \in \mathbb{R}$, such that $\rho' \to 0$,

$$\lim_{\rho' \to 0}\|u_i - p_{\rho'} u_i\|_{L^2(D)} = 0. \tag{A.29}$$

Hence, since (A.15), (A.16) and (A.29) hold, we have shown that all the assumptions of Theorem 2.10 in [21] hold. Thus, we conclude that the approximation formula (5.14) holds. □

Bibliography

[1] Samuel D. M. Adams, Richard V. Craster, and Sébastien Guenneau. Bloch waves in periodic multi-layered acoustic waveguides. *Proceedings of the Royal Society A: Mathematical, Physical and Engineering Sciences*, 464(2098):2669–2692, 2008.

[2] Quinten A. Akkerman and Liberato Manna. What defines a halide perovskite? *ACS Energy Letters*, 5(2):604–610, 2020.

[3] Konstantinos Alexopoulos and Bryn Davies. Asymptotic analysis of subwavelength halide perovskite resonators. *Partial Differential Equations and Applications*, 3(4):1–28, 2022.

[4] Konstantinos Alexopoulos and Bryn Davies. The effect of singularities and damping on the spectra of photonic crystals. *arXiv preprint arXiv:2306.12254*, 2023.

[5] Konstantinos Alexopoulos and Bryn Davies. A mathematical design strategy for highly dispersive resonator systems. *Mathematical Methods in the Applied Sciences*, 46(14):15883–15908, 2023.

[6] Konstantinos Alexopoulos and Bryn Davies. Topologically protected modes in dispersive materials: the case of undamped systems. *arXiv preprint arXiv:2311.05998*, 2023.

[7] Habib Ammari, Silvio Barandun, Jinghao Cao, Bryn Davies, and Erik Orvehed Hiltunen. Mathematical foundations of the non-Hermitian skin effect. *arXiv preprint arXiv:2306.15587*, 2023.

[8] Habib Ammari, Alexander Dabrowski, Brian Fitzpatrick, Pierre Millien, and Mourad Sini. Subwavelength resonant dielectric nanoparticles with high refractive indices. *Mathematical Methods in the Applied Sciences*, 42(18):6567–6579, 2019.

[9] Habib Ammari, Bryn Davies, and Erik Orvehed Hiltunen. Functional analytic methods for discrete approximations of subwavelength resonator systems. *arXiv preprint arXiv:2106.12301*, 2021.

[10] Habib Ammari, Bryn Davies, and Erik Orvehed Hiltunen. Robust edge modes in dislocated systems of subwavelength resonators. *Journal of the London Mathematical Society*, 106(3):2075–2135, 2022.

[11] Habib Ammari, Bryn Davies, Erik Orvehed Hiltunen, Hyundae Lee, and Sanghyeon Yu. Exceptional points in parity–time-symmetric subwavelength metamaterials. *SIAM Journal on Mathematical Analysis*, 54(6):6223–6253, 2022.

[12] Habib Ammari, Bryn Davies, Erik Orvehed Hiltunen, Hyundae Lee, and Sanghyeon Yu. *Wave Interaction with Subwavelength Resonators*, pages 23–83. Springer International Publishing, Cham, 2022.

[13] Habib Ammari, Bryn Davies, Erik Orvehed Hiltunen, and Sanghyeon Yu. Topologically protected edge modes in one-dimensional chains of subwavelength resonators. *Journal de Mathématiques Pures et Appliquées*, 144:17–49, 2020.

[14] Habib Ammari, Brian Fitzpatrick, Hyeonbae Kang, Matias Ruiz, Sanghyeon Yu, and Hai Zhang. *Mathematical and computational methods in photonics and phononics*, volume 235. American Mathematical Soc., 2018.

[15] Habib Ammari, Erik Orvehed Hiltunen, and Sanghyeon Yu. A high-frequency homogenization approach near the dirac points in bubbly honeycomb crystals. *Archive for Rational Mechanics and Analysis*, 238:1559–1583, 2020.

[16] Habib Ammari, Hyeonbae Kang, and Hyundae Lee. *Layer potential techniques in spectral analysis*. Number 153. American Mathematical Soc., 2009.

[17] Habib Ammari, Bowen Li, and Jun Zou. Mathematical analysis of electromagnetic scattering by dielectric nanoparticles with high refractive indices. *Transactions of the American Mathematical Society*, 2022.

[18] Habib Ammari and Pierre Millien. Shape and size dependence of dipolar plasmonic resonance of nanoparticles. *Journal de Mathématiques Pures et Appliquées*, 129:242–265, 2019.

[19] János K. Asbóth, László Oroszlány, and András Pályi. *A Short Course on Topological Insulators*, volume 919 of *Lecture Notes in Physics*. Springer, 2016.

[20] Lorenzo Baldassari, Pierre Millien, and Alice L. Vanel. Modal approximation for plasmonic resonators in the time domain: the scalar case. *Partial Differential Equations and Applications*, 2(4):1–40, 2021.

[21] Wolf-Jürgen Beyn, Yuri Latushkin, and Jens Rottmann-Matthes. Finding eigenvalues of holomorphic Fredholm operator pencils using boundary value problems and contour integrals. *Integral Equations and Operator Theory*, 78(2):155–211, 2014.

[22] Guy Bouchitté, Christophe Bourel, and Didier Felbacq. Homogenization near resonances and artificial magnetism in three dimensional dielectric metamaterials. *Archive for Rational Mechanics and Analysis*, 225(3):1233–1277, 2017.

[23] Guy Bouchitté, Sébastien Guenneau, and Frédéric Zolla. Homogenization of dielectric photonic quasi crystals. *Multiscale Modeling & Simulation*, 8(5):1862–1881, 2010.

[24] Leon Brillouin. *Wave Propagation in Periodic Structures: Electric Filters and Crystal Lattices*, volume 2. Dover Publications, 1953.

[25] Antonin Coutant and Bruno Lombard. Surface impedance and topologically protected interface modes in one-dimensional phononic crystals. *Proceedings of the Royal Society A*, 480(2282):20230533, 2024.

[26] Richard V. Craster and Bryn Davies. Asymptotic characterization of localized defect modes: Su–Schrieffer–Heeger and related models. *Multiscale Modeling & Simulation*, 21(3):827–848, 2023.

[27] Richard V. Craster and Sébastien Guenneau. *Acoustic Metamaterials: Negative Refraction, Imaging, Lensing and Cloaking*, volume 166 of *Springer Series in Materials Science*. Springer, London, 2013.

[28] Richard V. Craster, Julius Kaplunov, and Aleksey V Pichugin. High-frequency homogenization for periodic media. *Proceedings of the Royal Society A: Mathematical, Physical and Engineering Sciences*, 466(2120):2341–2362, 2010.

[29] Alexis Drouot. The bulk-edge correspondence for continuous honeycomb lattices. *Communications in Partial Differential Equations*, 44(12):1406–1430, 2019.

[30] Charles L. Fefferman, James P. Lee-Thorp, and Michael I. Weinstein. Topologically protected states in one-dimensional continuous systems and Dirac points. *Proceedings of the National Academy of Sciences*, 111(24):8759–8763, 2014.

[31] Charles L. Fefferman, James P. Lee-Thorp, and Michael I. Weinstein. *Topologically protected states in one-dimensional systems*, volume 247. American Mathematical Society, 2017.

[32] Charles L. Fefferman and Michael I. Weinstein. Wave packets in honeycomb structures and two-dimensional Dirac equations. *Communications in Mathematical Physics*, 326:251–286, 2014.

[33] Antoine Gloria, Stefan Neukamm, and Felix Otto. Quantification of ergodicity in stochastic homogenization: optimal bounds via spectral gap on Glauber dynamics. *Inventiones Mathematicae*, 199(2):455–515, 2015.

[34] Yuliya Gorb. Singular behavior of electric field of high-contrast concentrated composites. *Multiscale Modeling & Simulation*, 13(4):1312–1326, 2015.

[35] Artur L. Gower, William J. Parnell, and I. David Abrahams. Multiple waves propagate in random particulate materials. *SIAM Journal on Applied Mathematics*, 79(6):2569–2592, 2019.

[36] Leilei Gu, Swapnadeep Poddar, Yuanjing Lin, Zhenghao Long, Daquan Zhang, Qianpeng Zhang, Lei Shu, Xiao Qiu, Matthew Kam, Ali Javey, et al. A biomimetic eye with a hemispherical perovskite nanowire array retina. *Nature*, 581(7808):278–282, 2020.

[37] Sébastien Guenneau and Frédéric Zolla. Homogenization of three-dimensional finite photonic crystals. *Progress in Electromagnetics Research*, 27:91–127, 2000.

[38] Ajay Kumar Jena, Ashish Kulkarni, and Tsutomu Miyasaka. Halide perovskite photovoltaics: background, status, and future prospects. *Chemical Reviews*, 119(5):3036–3103, 2019.

[39] Sajeev John. Strong localization of photons in certain disordered dielectric superlattices. *Phys. Rev. Lett.*, 58:2486–2489, Jun 1987.

[40] Muamer Kadic, Graeme W. Milton, Martin van Hecke, and Martin Wegener. 3d metamaterials. *Nature Reviews Physics*, 1(3):198–210, 2019.

[41] Tynysbek Sh. Kalmenov and Durvudkhan Suragan. A boundary condition and spectral problems for the newton potential. In *Modern Aspects of the Theory of Partial Differential Equations*, pages 187–210. Springer, 2011.

[42] Tosio Kato. *Perturbation Theory for Linear Operators*, volume 132. Springer Science & Business Media, 2013.

[43] Alexander B. Khanikaev, S. Hossein Mousavi, Wang-Kong Tse, Mehdi Kargarian, Allan H. MacDonald, and Gennady Shvets. Photonic topological insulators. *Nature materials*, 12(3):233–239, 2013.

[44] Klaus von Klitzing, Gerhard Dorda, and Michael Pepper. New method for high-accuracy determination of the fine-structure constant based on quantized Hall resistance. *Physical Review Letters*, 45(6):494, 1980.

[45] Ralph de Laer Kronig and William G. Penney. Quantum mechanics of electrons in crystal lattices. *Proceedings of the royal society of London: Series A*, 130(814):499–513, 1931.

[46] Peter Kuchment. An overview of periodic elliptic operators. *Bulletin of the American Mathematical Society*, 53(3):343–414, 2016.

[47] Arseniy I. Kuznetsov, Andrey E. Miroshnichenko, Mark L. Brongersma, Yuri S. Kivshar, and Boris Luk'yanchuk. Optically resonant dielectric nanostructures. *Science*, 354(6314):aag2472, 2016.

[48] Gil Ju Lee, Changsoon Choi, Dae-Hyeong Kim, and Young Min Song. Bioinspired artificial eyes: optic components, digital cameras, and visual prostheses. *Advanced Functional Materials*, 28(24):1705202, 2018.

[49] Jensen Li, Lei Zhou, Che Ting Chan, and Ping Sheng. Photonic band gap from a stack of positive and negative index materials. *Physical Review Letters*, 90(8):083901, 2003.

[50] Junshan Lin and Hai Zhang. Mathematical theory for topological photonic materials in one dimension. *Journal of Physics A: Mathematical and Theoretical*, 55(49):495203, 2022.

[51] Stefan A. Maier. *Plasmonics: Fundamentals and Applications*, volume 1. Springer, 2007.

[52] Sergey Makarov, Aleksandra Furasova, Ekaterina Tiguntseva, Andreas Hemmetter, Alexander Berestennikov, Anatoly Pushkarev, Anvar Zakhidov, and Yuri Kivshar. Halide-perovskite resonant nanophotonics. *Advanced Optical Materials*, 7(1):1800784, 2019.

[53] Gustav Mie. Beiträge zur optik trüber medien, speziell kolloidaler metallösungen. *Annalen der Physik*, 330:377–445, 1908.

[54] Graeme W. Milton and Nicolae A. Nicorovici. On the cloaking effects associated with anomalous localized resonance. *Proceedings of the Royal Society A*, 462(2074):3027–3059, 2006.

[55] Andrea Moiola and Euan A. Spence. Acoustic transmission problems: wavenumber-explicit bounds and resonance-free regions. *Mathematical Models and Methods in Applied Sciences*, 29(02):317–354, 2019.

[56] Lorenzo Morini and Massimiliano Gei. Waves in one-dimensional quasicrystalline structures: dynamical trace mapping, scaling and self-similarity of the spectrum. *Journal of the Mechanics and Physics of Solids*, 119:83–103, 2018.

[57] Alexander B. Movchan, Natasha V. Movchan, and Chris G. Poulton. *Asymptotic models of fields in dilute and densely packed composites*. World Scientific, 2002.

[58] John B. Pendry. Negative refraction makes a perfect lens. *Physical Review Letters*, 85(18):3966, 2000.

[59] Hannah Price, Yidong Chong, Alexander Khanikaev, Henning Schomerus, Lukas J Maczewsky, Mark Kremer, Matthias Heinrich, Alexander Szameit, Oded Zilberberg, Yihao Yang, Baile Zhang, Andrea Alù, Ronny Thomale, Iacopo Carusotto, Philippe St-Jean, Alberto Amo, Avik Dutt, Luqi Yuan, Shanhui Fan, Xuefan Yin, Chao Peng, Tomoki Ozawa, and Andrea Blanco-Redondo. Roadmap on topological photonics. *Journal of Physics: Photonics*, 4(3):032501, 2022.

[60] Michael Schoenberg and PN Sen. Properties of a periodically stratified acoustic half-space and its relation to a biot fluid. *The Journal of the Acoustical Society of America*, 73(1):61–67, 1983.

[61] Brian Schulkin, Laszlo Sztancsik, and John F. Federici. Analytical solution for photonic band-gap crystals using Drude conductivity. *American Journal of Physics*, 72(8):1051–1054, 2004.

[62] H. S. Sehmi, Wolfgang Langbein, and Egor A. Muljarov. Applying the resonant-state expansion to realistic materials with frequency dispersion. *Physical Review B*, 101(4):045304, 2020.

[63] Michael M. Sigalas, Che Ting Chan, KM Ho, and Costas M. Soukoulis. Metallic photonic band-gap materials. *Physical Review B*, 52(16):11744, 1995.

[64] Henry J. Snaith. Present status and future prospects of perovskite photovoltaics. *Nature Materials*, 17(5):372–376, 2018.

[65] Costas M. Soukoulis. *Photonic Band Gap Materials*, volume 315. Springer Science & Business Media, 2012.

[66] Jiyu Sun, Bharat Bhushan, and Jin Tong. Structural coloration in nature. *RSC Advances*, 3(35):14862–14889, 2013.

[67] Marie Touboul, Benjamin Vial, Raphaël Assier, Sébastien Guenneau, and Richard V. Craster. High-frequency homogenization for periodic dispersive media. *arXiv preprint arXiv:2308.08559*, 2023.

[68] Kosmas L. Tsakmakidis, Allan D. Boardman, and Ortwin Hess. 'Trapped rainbow' storage of light in metamaterials. *Nature*, 450(7168):397–401, 2007.

[69] Leung Tsang, Jin Au Kong, and Kung-Hau Ding. *Scattering of electromagnetic waves: theories and applications*. John Wiley & Sons, 2004.

[70] Tak-Goa Tsuei and Peter W. Barber. Multiple scattering by two parallel dielectric cylinders. *Applied Optics*, 27(16):3375–3381, 1988.

[71] Victor G. Veselago. The electrodynamics of substances with simultaneously negative values of ϵ and μ. *Soviet Physics Uspekhi*, 10(4):509–514, 1968.

[72] Heyong Wang, Felix Utama Kosasih, Hongling Yu, Guanhaojie Zheng, Jiangbin Zhang, Galia Pozina, Yang Liu, Chunxiong Bao, Zhangjun Hu, Xianjie Liu, et al. Perovskite-molecule composite thin films for efficient and stable light-emitting diodes. *Nature Communications*, 11(1):1–9, 2020.

[73] Zheng Wang, Yidong Chong, John D. Joannopoulos, and Marin Soljačić. Observation of unidirectional backscattering-immune topological electromagnetic states. *Nature*, 461(7265):772–775, 2009.

[74] Eli Yablonovitch. Inhibited spontaneous emission in solid-state physics and electronics. *Phys. Rev. Lett.*, 58:2059–2062, May 1987.

[75] Degang Zhao, Xincheng Chen, Pan Li, and Xue-Feng Zhu. Subwavelength acoustic energy harvesting via topological interface states in 1D Helmholtz resonator arrays. *AIP Advances*, 11(1), 2021.

[76] Qian Zhao, Ji Zhou, Fuli Zhang, and Didier Lippens. Mie resonance-based dielectric metamaterials. *Materials Today*, 12(12):60–69, 2009.

[77] Yuanjin Zhao, Zhuoying Xie, Hongcheng Gu, Cun Zhu, and Zhongze Gu. Bio-inspired variable structural color materials. *Chemical Society Reviews*, 41(8):3297–3317, 2012.

Curriculum Vitae

Contact information

Name:	Konstantinos Alexopoulos
Affiliation:	Department of Mathematics, ETH Zürich
Address:	HG J 48, Rämistrasse 101, 8092 Zürich, Switzerland
Email:	konstantinos.alexopoulos@sam.math.ethz.ch
Personal webpage:	https://people.math.ethz.ch/ kalexopoulos/

Education

2021 — Present: **ETH Zürich**, Zürich, Switzerland
Doctoral student under the supervision of Prof. Habib Ammari

2020 — 2021: **University of Cambridge**, Cambridge, United Kingdom
Master of Advanced Studies (Part III) in Pure Mathematics
Essay supervisor: Prof. Mihalis Dafermos
Essay title: *The non-linear instability of anti-de Sitter spacetime*

2017 — 2020: **École Polytechnique**, Palaiseau, France
Bachelor of Science. Double major: Mathematics and Economics
Bachelor thesis supervisor: Prof. Cécile Huneau
Bachelor thesis title: *Around the colored black holes*

Publications

K. Alexopoulos and B. Davies. Asymptotic analysis of subwavelength halide perovskite resonators. *Partial Differential Equations and Applications*, 3(4):1–28, 2022.

K. Alexopoulos and B. Davies. A mathematical design strategy for highly dispersive resonator systems. *Mathematical Methods in the Applied Sciences*, pages 1-26, 2023.

K. Alexopoulos and B. Davies. The effect of singularities and damping on the spectra of photonic crystals. arXiv:2306.12254, 2023.

K. Alexopoulos and B. Davies. Topologically protected modes in dispersive materials: the case of undamped systems. arXiv:2311.05998, 2023.

Conference talks

CNRS-Imperial Metamaterials Conference, Imperial College London, September 2022.

Zürich Graduate Colloquium of Applied Mathematics (SAMinar), ETH Zürich, November 2023.

SIAM Conference on Nonlinear Waves and Coherent Structures (NWCS24), Baltimore, June 2024.

Skills

Languages: Greek (native), English (fluent/fully working proficiency), French (fluent/fully working proficiency), German (intermediate)

Programming: Python, LateX.